

AD\_\_\_\_\_

AWARD NUMBER: W81XWH-05-2-0027

TITLE: IMPACT (Imaging and Molecular Markers for Patients with Lung Cancer: Approaches with Molecular Targets and Complementary, Innovative and Therapeutic Modalities)

PRINCIPAL INVESTIGATOR: Waun Ki Hong, M.D  
Roy Herbst, M.D.,Ph.D.

CONTRACTING ORGANIZATION: University of Texas  
M.D. Anderson Cancer Center  
Houston, Texas 77030

REPORT DATE: March 2006

TYPE OF REPORT: Annual

PREPARED FOR: U.S. Army Medical Research and Materiel Command  
Fort Detrick, Maryland 21702-5012

DISTRIBUTION STATEMENT: Approved for Public Release;  
Distribution Unlimited

The views, opinions and/or findings contained in this report are those of the author(s) and should not be construed as an official Department of the Army position, policy or decision unless so designated by other documentation.

REPORT DOCUMENTATION PAGE				Form Approved OMB No. 0704-0188	
Public reporting burden for this collection of information is estimated to average 1 hour per response, including the time for reviewing instructions, searching existing data sources, gathering and maintaining the data needed, and completing and reviewing this collection of information. Send comments regarding this burden estimate or any other aspect of this collection of information, including suggestions for reducing this burden to Department of Defense, Washington Headquarters Services, Directorate for Information Operations and Reports (0704-0188), 1215 Jefferson Davis Highway, Suite 1204, Arlington, VA 22202-4302. Respondents should be aware that notwithstanding any other provision of law, no person shall be subject to any penalty for failing to comply with a collection of information if it does not display a currently valid OMB control number. <b>PLEASE DO NOT RETURN YOUR FORM TO THE ABOVE ADDRESS.</b>					
1. REPORT DATE (DD-MM-YYYY) 01-03-2006		2. REPORT TYPE Annual		3. DATES COVERED (From - To) 1 Feb 2005 – 31 Jan 2006	
4. TITLE AND SUBTITLE  IMPACT (Imaging and Molecular Markers for Patients with Lung Cancer: Approaches with Molecular Targets and Complementary, Innovative and Therapeutic Modalities)				5a. CONTRACT NUMBER	
				5b. GRANT NUMBER W81XWH-05-2-0027	
				5c. PROGRAM ELEMENT NUMBER	
6. AUTHOR(S)  Waun Ki Hong, M.D. and Roy Herbst, M.D.,Ph.D.  E-Mail:				5d. PROJECT NUMBER	
				5e. TASK NUMBER	
				5f. WORK UNIT NUMBER	
7. PERFORMING ORGANIZATION NAME(S) AND ADDRESS(ES)  University of Texas M.D. Anderson Cancer Center Houston, Texas 77030				8. PERFORMING ORGANIZATION REPORT NUMBER	
9. SPONSORING / MONITORING AGENCY NAME(S) AND ADDRESS(ES) U.S. Army Medical Research and Materiel Command Fort Detrick, Maryland 21702-5012				10. SPONSOR/MONITOR'S ACRONYM(S)	
				11. SPONSOR/MONITOR'S REPORT NUMBER(S)	
12. DISTRIBUTION / AVAILABILITY STATEMENT Approved for Public Release; Distribution Unlimited					
13. SUPPLEMENTARY NOTES					
14. ABSTRACT  The projects in this proposal specifically target several signal transduction pathways known to be critical for NSCLC pathogenesis including the EGFR pathway and the more downstream ras/raf/Mek/ERK pathway. These projects combine targeted approaches using molecular and imaging techniques to validate activity against a target and monitor response using imaging modalities specific to the receptor using either small molecules or targeted peptide approaches.  The Developmental Research projects explore new areas including 1 ) the issue of high morbidity malignant pleural effusion thereby bringing the pulmonologists into the treatment of advanced disease with molecular therapies; and 2) prevention of lung cancer in youth through a highly interactive, entertaining CD-ROM program.					
15. SUBJECT TERMS lung cancer, molecular markers, molecular imaging					
16. SECURITY CLASSIFICATION OF:			17. LIMITATION OF ABSTRACT	18. NUMBER OF PAGES	19a. NAME OF RESPONSIBLE PERSON
a. REPORT	b. ABSTRACT	c. THIS PAGE			USAMRMC
U	U	U	UU	273	19b. TELEPHONE NUMBER (include area code)

## TABLE OF CONTENTS

<b>INTRODUCTION .....</b>	<b>2</b>
<b>BODY .....</b>	<b>2</b>
Project 1 .....	2
Project 2 .....	10
Project 3 .....	13
Project 4 .....	20
Project 5 .....	22
Project 6 .....	25
Core B Biostatistics and Data Management .....	28
Core C Pathology and Specimen Procurement .....	29
Core D Imaging .....	37
Developmental Research Project 1 .....	39
Developmental Research Project 2 .....	40
<b>KEY RESEARCH ACCOMPLISHMENTS .....</b>	<b>44</b>
<b>REPORTABLE OUTCOMES .....</b>	<b>46</b>
<b>CONCLUSION .....</b>	<b>47</b>
<b>REFERENCES .....</b>	<b>48</b>
<b>APPENDICES .....</b>	<b>50</b>
Appendix A (Project 1- Revised protocol) .....	
Appendix B (Revised Statements of Work) .....	
Appendix C (DRP-1- Revised protocol) .....	
Appendix D (TALK) .....	
Appendix E (TALK) .....	
Appendix F (TALK) .....	
Appendix G (TALK) .....	
Appendix H (TALK) .....	
Appendix I (TALK) .....	
Appendix J (Manuscripts) .....	

## **IMPACT: Imaging and Molecular Markers for Patients with lung cancer: Approaches with Molecular Targets, Complementary, Innovative and Therapeutic Modalities**

### **INTRODUCTION**

Lung cancer is the most prevalent cancer worldwide and the leading cause of cancer-related mortality in both men and women in the United States. Conventional multimodality therapies including surgery, radiation and chemotherapy have reached a therapeutic ceiling in improving a five-year survival of non-small cell lung cancer (NSCLC) patients, clinically in large part due to chemo- and radiation-resistant locoregional and metastatic spread but ultimately due to poor understanding of the disease and its resistance to the therapy.

Cancer is a heterogeneous disease resulting from accumulated genetic abnormalities over years, which thus requires a coordinated attack in a truly integrated fashion on multiple altered signal pathways. An emerging targeted therapy aims to target key molecular abnormalities in cancer and has succeeded in some tumor types such as chronic myeloid leukemia (CML) (Druker et al., 2004; Druker and Sawyers et al., 2001; Druker and Talpaz et al., 2001), gastrointestinal stromal tumor (Demetri et al., 2002), colon cancer (Hurwitz et al., 2003), and breast cancer (Howell et al., 2005). Thus, the incorporation of the targeted therapy into conventional treatments appears to be a new promising approach to treatment of lung cancer.

Project IMPACT proposes to integrate targeted therapy in the lung cancer research program when initial clinical results showed disappointing response rates and survival benefit of EGFR inhibitor Gefitinib (Iressa) for non-selected lung cancer patients (Herbst et al., 2002-2004; Kris et al., 2003; Giaccone et al., 2004). It aims to validate molecular mechanisms of targeted agents alone and in combination with chemo and/or radiation therapies from preclinical studies to clinical trials. It also aims to develop effective molecular imaging and cancer cell-targeted peptide-based delivery tools to help improve efficacy of the targeted agents. Specifically, our objectives are:

- To validate preclinically and clinically several key signaling pathways and their agents for therapeutic potentials alone or in combination with each other or with radiotherapy
- To explore applications of molecular imaging for targeted therapy and identify cancer cell-targeted peptides for systemic delivery of therapeutic and imaging agents
- To discover and evaluate new molecular abnormalities and therapeutic predictors in lung cancer
- To develop an educational program for teens and young adults for smoking risk and resultant lung cancer occurrence.

**PROGRESS REPORT (BODY):** The following is the first annual report for the IMPACT grant.

#### **Project 1: Targeting epidermal growth factor receptor signaling to enhance response of lung cancer to therapeutic radiation.**

(PI and co-PI: Raymond E. Meyn, Ph.D., Ritsuko Komaki, M.D.)

In spite of significant technical advances including IMRT and chemoradiation, locally advanced lung cancer continues to have a dismal prognosis as many patients' tumors appear to be resistant to radiation therapy. The molecular basis for radiation resistance is not fully understood, but tumor cells have an enhanced survival response that involves increased capacity for DNA repair and suppressed apoptosis. Both apoptosis propensity and DNA repair capacity are thought to be partly controlled by the upstream signal transduction pathways



triggered by EGFR activation, which is constitutively activated in many NSCLCs and its activation leads to a radiation-resistant phenotype (Ochs et al., 2004). We hypothesize that the response of NSCLC to radiation can be improved through the use of inhibitors of EGFR signaling.

**Aim 1 To test the combination of external beam radiation and the selective EGFR-tyrosine kinase inhibitor erlotinib (Tarceva) in locally advanced NSCLC.**

### Update

Originally, this aim planned to use gefitinib but has since been modified to use erlotinib instead due to better survival benefit of erlotinib. Genentech has agreed to supply the drug and will support the clinical trial entitled *A Phase I/II Study of TARCEVA (erlotinib) in Combination with Chemoradiation in Patients with Stage IIIA/B Non-Small Cell Lung Cancer (NSCLC)*. The revised protocol has been submitted to our Institutional Review Board (IRB) (see Appendix A). Once approved, it will be submitted to the DOD review board for approval. The trial will open this year.

**Aim 2 To test the hypothesis that activation of the EGFR pathway leads to radiation resistance in NSCLC cells due to an enhanced capacity for repairing DNA lesions.**

### Update

Studies conducted in this aim involved characterizing the signaling pathways downstream of EGFR activation in NSCLC cell lines and correlating radiation response and DNA repair capacity in these lines with their respective activation of EGFR. A total of 4 NSCLC cell lines have been examined; A549, H1299, H322, and H358. Important features of these lines have been compared to normal human lung fibroblasts, i.e. the CCD-16 cell line. As mentioned above, initially, the focus of these investigations was understanding the effects of gefitinib as a model EGFR inhibitor, but other agents including erlotinib have been studied in parallel. Considerable progress has been made on this aim as follows:

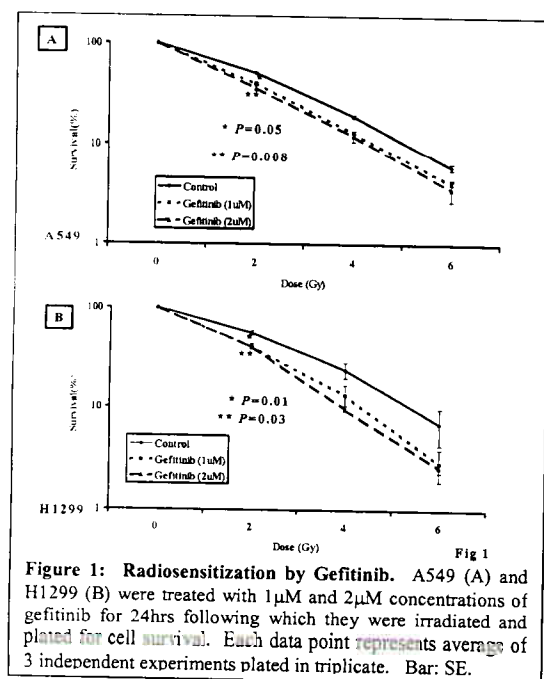
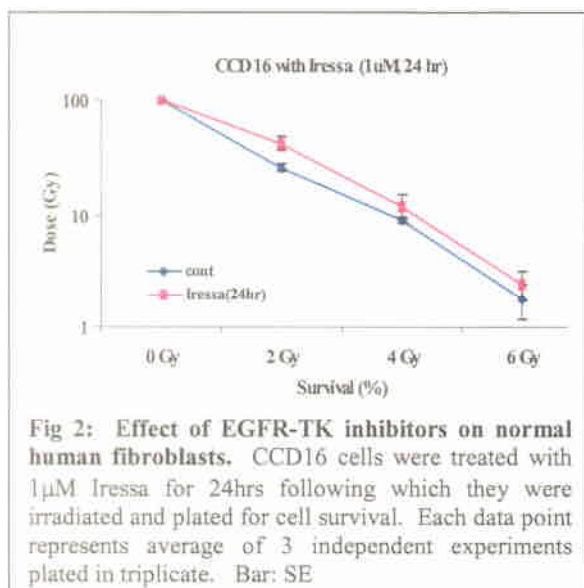


**Figure 1: Radiosensitization by Gefitinib.** A549 (A) and H1299 (B) were treated with 1 μM and 2 μM concentrations of gefitinib for 24hrs following which they were irradiated and plated for cell survival. Each data point represents average of 3 independent experiments plated in triplicate. Bar: SE.

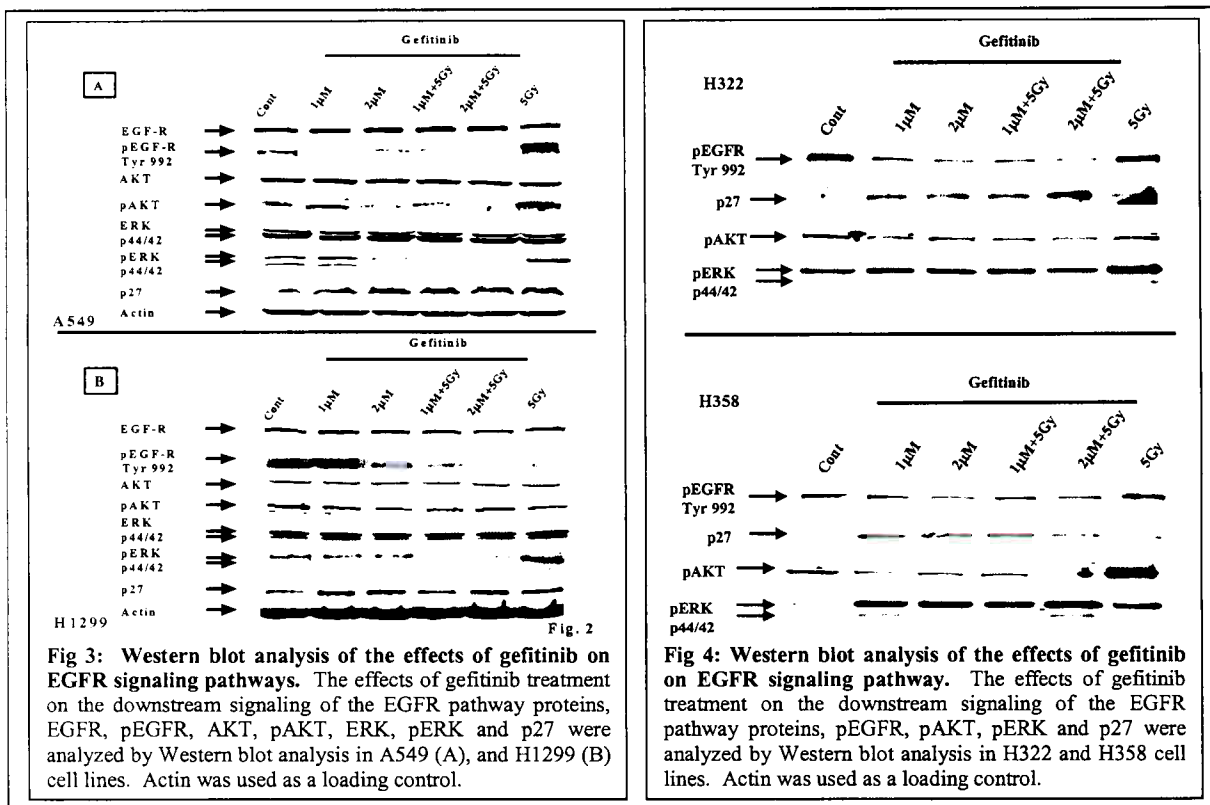
We measured the survival of human NSCLC cells exposed to combinations of gefitinib and ionizing radiation using clonogenic assays. A549 and H1299 cells were pretreated with 1 μM or 2 μM gefitinib for 24 hours and then the cells were irradiated. Pretreatment with gefitinib suppressed the clonogenic survival of both cell lines (Figure 1). In A549 cells, survival at 2 Gy (SF2) was reduced from 50.4 % ± 0.7 in the control to 39.4 % ± 0.8 ( $P=0.05$ ) in 1 μM gefitinib-treated cells and to 35.5 % ± 2.1 ( $P=0.008$ ) in 2 μM gefitinib-treated cells (Figure 1A). Similar results were obtained using the H1299 cell line: SF2 was reduced from 55.8 % ± 2.5 in the control cells to 40.9 % ± 0.06 ( $P=0.01$ ) in 1 μM gefitinib-treated cells and to 40.7 % ± 2.5 ( $P=0.03$ ) in 2 μM gefitinib-treated cells (Figure 1B). Survival enhancement ratios (SER) were calculated by dividing the radiation dose that produced 10% cell survival on the radiation-only survival curve by that for the corresponding gefitinib plus ionizing radiation curve. SER for the A549 cells was 1.1 and that for H1299 was 1.2 in 1 μM gefitinib-treated cells. The respective values were 1.2 and 1.4 in 2 μM gefitinib-treated cells. Gefitinib,

when used alone at either connection, did not significantly reduce the plating efficiency of A549 or H1299 cells compared to untreated controls. The opposite effect was observed in the H322, H358 and CCD-16 cell lines, i.e., pretreatment with 1  $\mu$ M gefitinib protected these cell lines from irradiation. An example of this effect is presented in Figure 2 for the CCD-16 cell line. Based on this pattern of sensitization and resistance induced by gefitinib in different cell lines, we have used this as a model to explore the underlying molecular mechanism that may be responsible for governing radioresponse of NSCLC cells downstream of EGFR.



As an initial investigation into the mechanism responsible for gefitinib-mediated radiosensitization, we examined the effect of gefitinib treatment on the expression of downstream targets in the EGFR signaling pathway. Dose-dependent decreases in the levels of pEGFR, pAKT, and pERK1/2 were observed in unirradiated A549 and H1299 cells following 24-hour treatment with gefitinib (Figure 3A and 3B). In addition, radiation activated pEGFR and pAKT in A549 cells but not in H1299 cells. On the other hand, radiation activated pERK1/2 in both cell lines and this activation was suppressed by gefitinib correlating with gefitinib's radiosensitizing effects (Figure 1). As has been reported previously, gefitinib enhanced the expression of p27 at both the 1  $\mu$ M and 2

$\mu$ M concentrations. A somewhat different pattern was observed in the H322 and H358 cell lines. In those lines, pretreatment with gefitinib activated pERK1/2 in unirradiated cells and did not suppress radiation-induced activation of pERK1/2 consistent with a radioprotective effect of pERK1/2 activation (Figure 4). Thus, as we predicted might be the case in our original application, the key to understanding tumor cell radioresistance due to an abnormal activation of EGFR may lie in the Ras/Raf/Mek/ERK pathway downstream of this receptor.

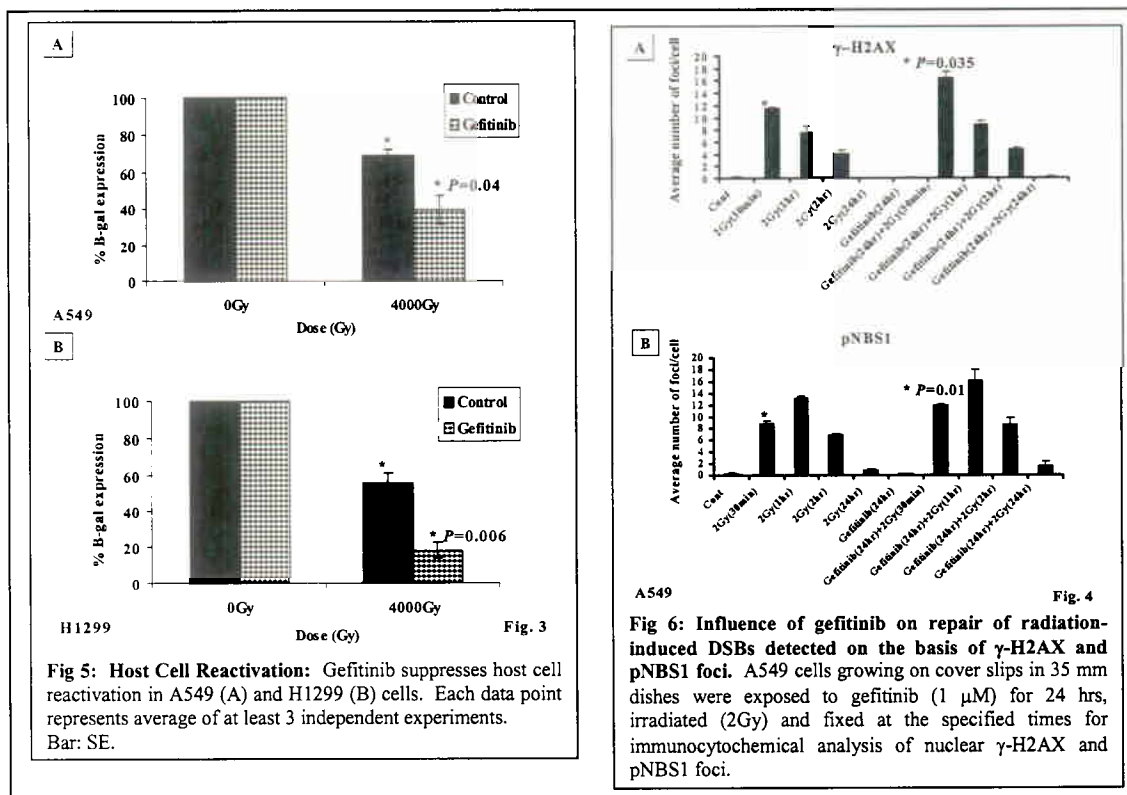


### Aim 3 Test the hypothesis that clinically useful inhibitors of EGFR signaling abrogate DNA repair capacity, restore apoptotic response and radiosensitize NSCLC cells.

As mentioned above, several clinically useful inhibitors of the EGFR pathway have already been developed and some are in clinical trials as single agents. Based on the cell models developed in aim 2 above, we proposed to test the ability of these inhibitors to suppress DNA repair in NSCLC cells using the cell models described in Specific Aim 2 above. These studies were initiated using gefitinib to follow from the observations made in Specific Aim 2.

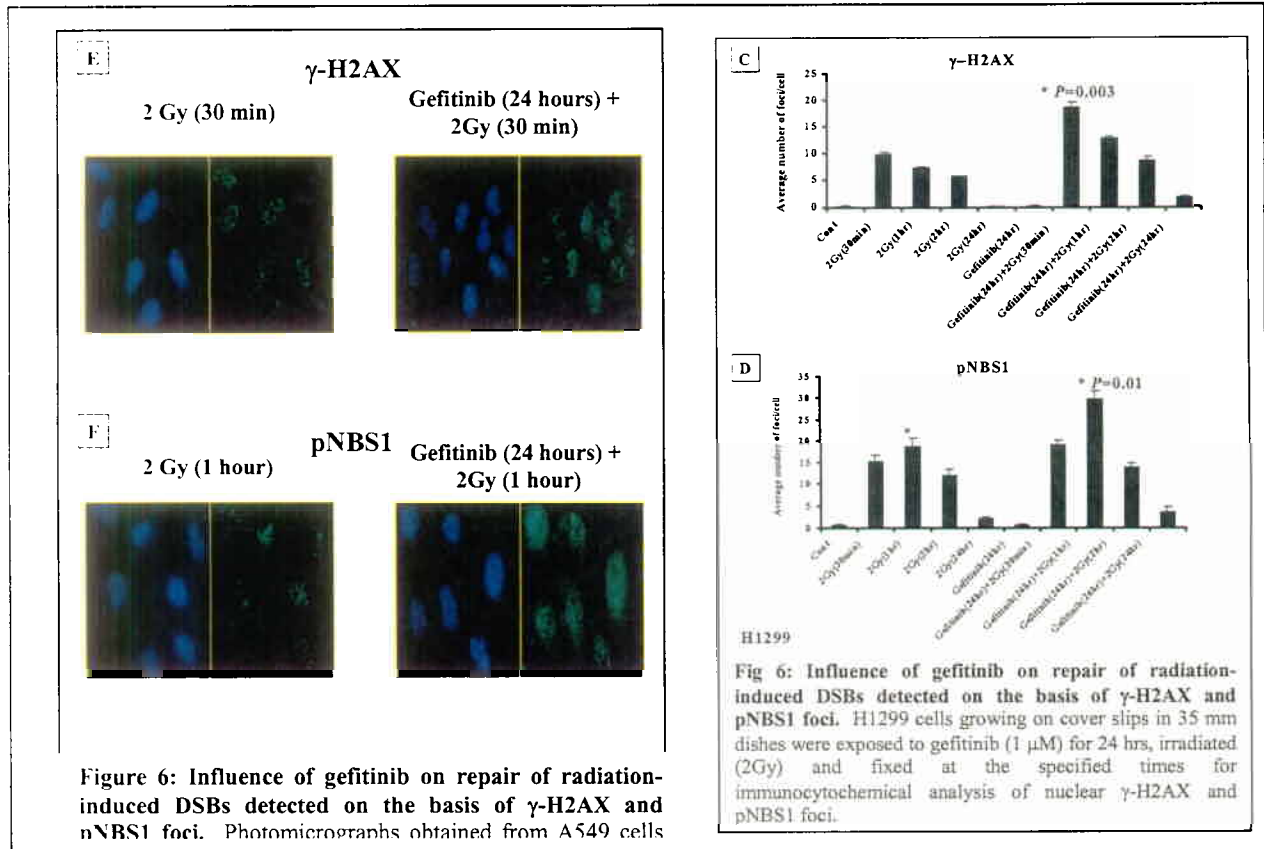
We performed a host cell reactivation (HCR) assay to determine if the radiosensitizing effect of gefitinib could be explained as a suppression of the DNA repair capacity of the NSCLC cells. The method used to assay HCR has been described in detail elsewhere (Munshi et al., 2005). For this, A549 and H1299 cells, mock treated or pretreated with gefitinib, were subsequently infected with Ad- $\beta$ -gal that had been either unirradiated or irradiated with 4000 Gy of  $\gamma$ -radiation. The ability of the NSCLC cells to reactivate the irradiated Ad- $\beta$ -gal on the basis of  $\beta$ -gal expression was assessed 24 hours later. Gefitinib-pretreated (1  $\mu$ M for 24 hours) A549 and H1299 cells had a significantly ( $P=0.04$  and  $P=0.006$ , respectively) lower capacity to reactivate irradiated Ad- $\beta$ -gal than A549 and H1299 cells that received no treatment (Figure 5).

As an additional test of our hypothesis that gefitinib impairs the repair of damaged DNA,  $\gamma$ -H2AX and pNBS1 foci were assessed as indicators of radiation-induced DSBs. Cells were grown and treated with 1  $\mu$ M gefitinib for 24 hours on coverslips placed in 35 mm dishes. Anti- $\gamma$ -H2AX (Trevigen, Gaithersburg, MD) or anti-pNBS1 antibody (Novus Biologicals, Littleton, CO) was

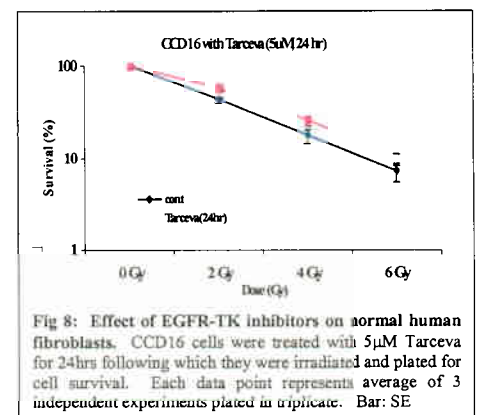
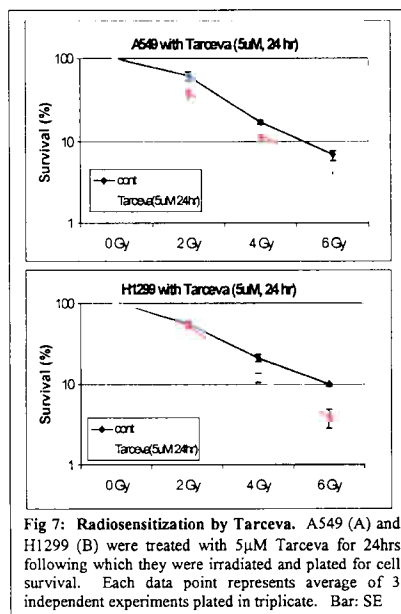
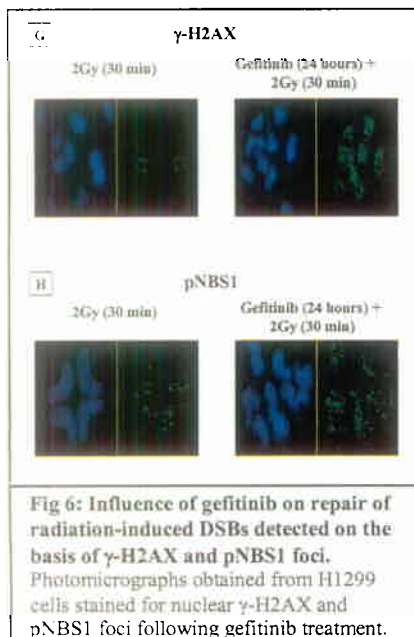


added at a dilution of 1:600 in 5% BSA in PBS and incubation continued for 2 hours at room temperature with gentle shaking. Slides were examined on a Leica fluorescence microscope, and images were captured by a CCD camera and imported into Advanced Spot Image analysis software package. For each treatment condition, the number of  $\gamma$ -H2AX or pNBS1 foci was determined in at least 50 cells.

As shown by the micrographs in Figure 6E and 6G,  $\gamma$ -H2AX foci could be clearly distinguished soon after irradiation (2 Gy) of A549 and H1299 cells. The average number of  $\gamma$ -H2AX foci per cell increased as early as 30 min after 2Gy and then decreased with time thereafter. (Fig. 6E and 6G). The average number of pNBS1 foci per cell followed a pattern similar to that seen for to  $\gamma$ -H2AX foci except that the average number of foci per cell peaked at 1 hour instead of 30 min. The average number of  $\gamma$ -H2AX foci per cell in cultures receiving the combined gefitinib/radiation treatment was significantly greater than in the radiation-only group at the 30 min time points for the A549 and H1299 cell lines,  $P=0.035$  and  $P=0.003$  respectively (Figures 6A, 6C). The average number of pNBS1 foci per cell in cells receiving the combined gefitinib/radiation treatment was significantly greater than in the radiation-only group (at 30 min  $P=0.01$  in A549 cells; at 1 hour  $P=0.01$  in H1299 cells, Figs. 6B, 6D). Treatment with gefitinib alone had no significant effect on  $\gamma$ -H2AX and pNBS1 foci. This prolongation of  $\gamma$ -H2AX and pNBS1 foci levels following the combination compared to controls suggests that gefitinib-mediated radiosensitization may involve a suppression of DSB repair pathways. We are currently extending this analysis to include additional proteins involved in the repair complex. One of these proteins, MDM2, also forms foci and we will assess the ability of gefitinib to alter radiation-induced MDM2 foci formation. An abstract describing our initial assessment of the role of MDM2 in DNA repair was submitted for the 2006 AACR annual meeting (Paternoster et al., 2006).



In addition to these results, we have begun to evaluate erlotinib (Tarceva) for its radiosensitizing effects on some of the same NSCLC cell lines evaluated above for gefitinib. Preliminary clonogenic survival curves for A549 and H1299 cells pretreated with Tarceva are presented in Figure 7. As can be seen, Tarceva is capable of radiosensitizing both of these cell lines. Again, similar to the case for gefitinib, Tarceva produces a radioprotective effect in the CCD-16 cell line (Figure 8). The next step is to see whether Tarceva suppresses pERK1/2 activation and suppresses DNA repair capacity recapitulating the findings presented above for gefitinib.





**Aim 4      Test the hypothesis that targeting both EGFR and its downstream signaling pathways will have at least an additive radiosensitizing effect on NSCLC**

As an initial approach to this aim, we have begun to evaluate molecular targeted agents that are designed to specifically target the Ras-Raf-Mek-ERK pathway downstream of EGFR. Testing of one such agent, BAY-43-9006 (Sorafenib), that targets Raf-kinase, has already been initiated. The ability of BAY-43-9006 to radiosensitize H1299 cells is presented in Figure 9. In the coming year, we will combine Sorafenib with either gefitinib or erlotinib and test whether this combination will initiate a radiosensitizing effect on those cell lines, namely H322 and H358, where gefitinib alone induced pERK1/2 activation and radioresistance. We have mocked up this treatment protocol using the combination of gefitinib and UO126, a non-clinical but highly specific Mek inhibitor. A preliminary assessment of this combination showed that UO126 downregulated gefitinib-induced pERK1/2 activation in H322 cells and radiosensitized gefitinib-pretreated cells (Fig. 10). This observation lends considerable weight to our idea of combining EGFR and Ras-Raf-Mek-ERK inhibitors to radiosensitize normally radioresistant NSCLC cells. An abstract describing a preliminary assessment of Sorafenib was submitted for the 2006 AACR annual meeting (Munshi et al, 2006).

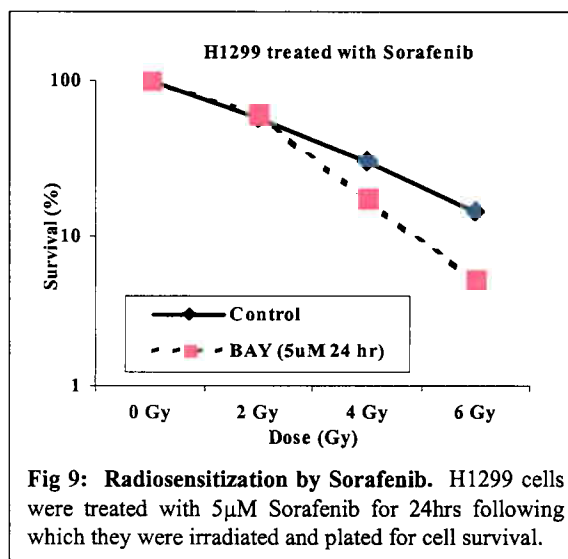


**Fig 9: Radiosensitization by Sorafenib.** H1299 cells were treated with 5 $\mu$ M Sorafenib for 24hrs following which they were irradiated and plated for cell survival.

**Aim 5      To test whether the strategies developed in Specific Aims 2-4 have efficacy in a xenograft tumor model**

**Update**

The animal study was proposed for years 3 and 4. We have submitted the animal protocols for approval through our Animal Care and Use Committee (IACUC). Initially, we proposed some simple assessment of gefitinib, erlotinib, and Sorafenib in combination with radiation in tumor xenografts growing in nude mice. Ultimately, the protocols will be modified to include the best combinations of inhibitors as revealed from the studies in Specific Aim 4.

**Conclusions**

We conclude that gefitinib and erlotinib, at clinically achievable concentrations, sensitize NSCLC cell lines to radiation. Although the degree of radiosensitization might appear to be small, the approximate 25% increase in cell kill following the dose of 2 Gy would be expected to have a substantial clinical impact if repeated over the entire course of radiotherapy, i.e., 30 or more fractions of 2 Gy, with daily administration of gefitinib or erlotinib. Gefitinib radiosensitizes NSCLC cells by suppressing the cellular capacity for repairing radiation-induced DSBs probably via a suppression of ERK activation.

**Project 2: Molecular Imaging of EGFR Expression and Activity in Targeting Therapy of Lung Cancer**

(PI and co-PI: Juri Gelovani, M.D.; Roy Herbst, M.D., Ph.D.)

During the first year, our research focused on Specific Aims 1 and 2 of the project as originally planned.

**Aim 1** To synthesize novel pharmacokinetically optimized  $^{124}\text{I}$  and  $^{18}\text{F}$ -labeled IPQA derivatives for PET imaging of EGFR kinase activity and conduct *in vitro* radiotracer accumulation studies in tumor cells expressing different levels of EGFR activity.

**Aim 1A** To synthesize novel rationally designed precursors for radiolabeling of tracers for PET imaging of EGFR expression and activity.

### Update

This part of the project was conducted by the Imaging Core. As planned, we synthesized and investigated *in vitro* a number of different morpholino-derivatives of 2-iodo-4-(phenylamino)quinazoline-6-acrylamide (IPQA) derivatives with improved water solubility, which have been selected by additional *in silico* modeling of their structure-activity relationships with active EGFR kinase. Among these compounds, we narrowed the initial library of compounds to 4 optimized lead compounds termed JGAP 1, 5, 11, and 13 (see Imaging Core D). Next, we studied the ability of these compounds to penetrate into tumor cells and inhibit their growth. For this study, we used four human NSCLC cells that express TGF $\alpha$  at different levels and express either the wild-type or mutant EGFR kinases (PC14, H441, H3255, H1975). All newly synthesized compounds demonstrated tumor growth inhibitory activities in low  $\mu\text{M}$  concentrations (Table 1), especially in H3255 expressing the L858R active mutant EGFR kinase. Based on these studies, we selected compounds JGAP-5 and JGAP-11 for further studies.

**Table 1.** IC50 of EGFR kinase inhibitors in different NSCLC cell lines *in vitro*.

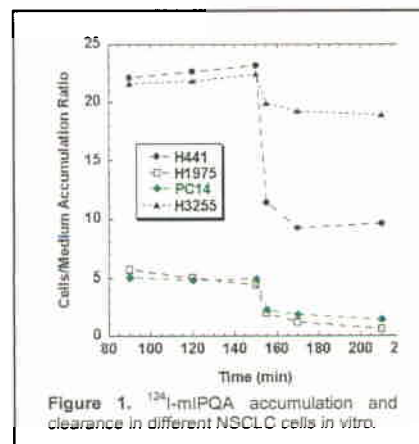
	PC14	H441	H3255	H1975
EGFR status	wild-type	wild-type	L858R mut.	L858R,T790M mut.
TGF $\alpha$ level	+	+++++	+	++
Gefitinib	12.6	40.2	2.3	> 100
JGAP-1	94.8	77.67	6.78	> 100
JGAP-5	10.74	19.75	8.82	> 100
JGAP-11	18.38	12.31	6.75	> 100
JGAP-13	60.41	28.45	7.64	> 100

Currently, we are optimizing the radiolabeling procedure for production of [ $^{124}\text{I}$ ]-JGAP-5. During the initial radiolabeling experiments, the [ $^{124}\text{I}$ ]-JGAP-5 was produced at ~60% radiochemical yield. Our goal is to improve radio-iodination yield to >80%, which should be accomplished during the next 2 months.

In addition, we evaluated the uptake and retention of our original lead candidate, the [ $^{124}\text{I}$ ]mIPQA, in the same NSCLC cells (PC14, H441, H3255, H1975). The results showed that [ $^{124}\text{I}$ ]mIPQA rapidly accumulated and was efficiently retained in the H3255 cells and in H441 cells with wild-type EGFR and high levels of TGF $\alpha$  that activates EGFR in an autocrine manner (Figure 1). The highest level of retention of [ $^{124}\text{I}$ ]mIPQA was observed in H3255 cells, which is consistent with activated EGFR kinase expressed by the cells.

In contrast, low levels of accumulation and rapid washout of [ $^{124}\text{I}$ ]mIPQA were observed in PC14 cells that express wild-type EGFR and in H1975 cells that carry both the activating L858R and resistance-inducing T790M mutations in EGFR kinase domain.

These data are consistent with sensitivity of different NSCLC cell lines to gefitinib (Table 1) and support our hypothesis that



imaging with [ $^{124}$ I]IPQA derivatives should allow for identification of tumors with increased EGFR signaling either through activating EGFR mutations or overexpression of TGF $\alpha$ .

**Aim 2** To assess the biodistribution (PK/PD) and tumor targeting by novel  $^{124}$ I and  $^{18}$ F-labeled EGFR kinase-specific IPQA derivatives using PET imaging in orthotopic mouse models of lung cancer and compare *in vivo* radiotracer uptake/retention with phospho-EGFR levels *in situ*.

### Update

We have initiated *in vivo* PET imaging studies with [ $^{124}$ I]mIPQA in mice bearing orthotopic xenografts of the four NSCLC cells (PC14, H441, H3255, H1975). These cell lines were retrovirally transduced with eGFP – Firefly luciferase fusion reporter gene (GL) to facilitate non-invasive imaging in orthotopic NSCLC model in mice. The GL reporter gene allows for fluorescence microscopic and FACS analysis of GL-expressing cells *in vitro* and bioluminescence imaging (BLI) of GL-expressing tumor xenografts in mice *in vivo*. Tumor growth was monitored by measuring the total light output from the thorax of mice implanted into their lungs with the NSCLC cells suspended in Matrigel (N=6 mice per tumor type) (Figures 2-4).

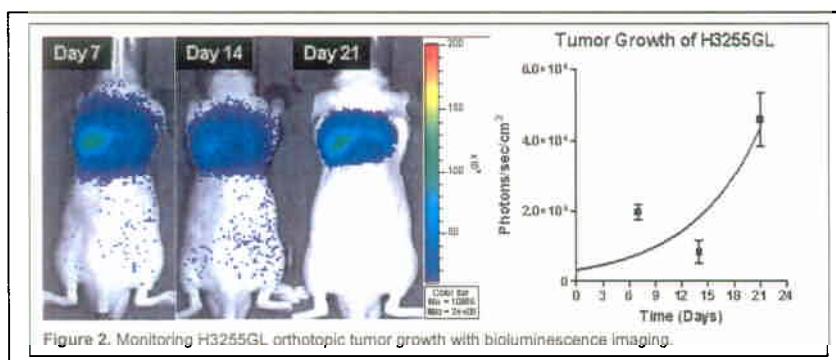


Figure 2. Monitoring H3255GL orthotopic tumor growth with bioluminescence imaging.

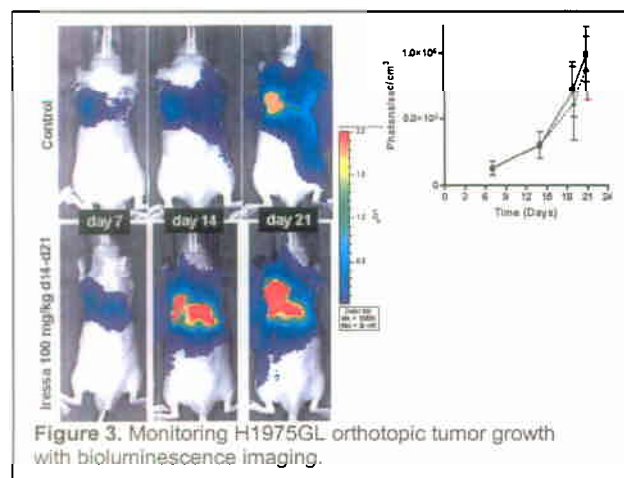


Figure 3. Monitoring H1975GL orthotopic tumor growth with bioluminescence imaging.

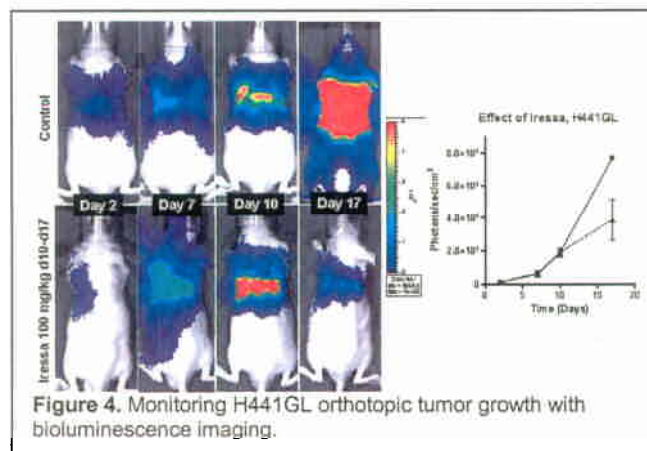
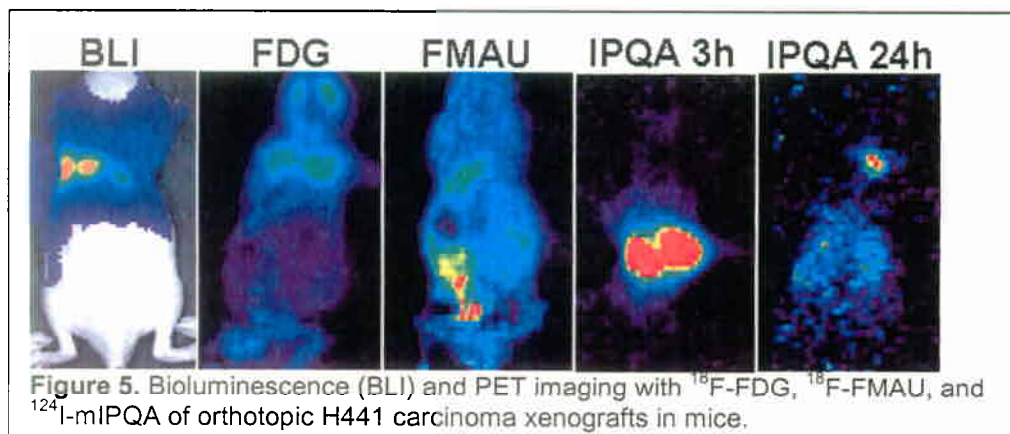


Figure 4. Monitoring H441GL orthotopic tumor growth with bioluminescence imaging.

In H441GL orthotopic carcinoma xenografts, BLI and PET imaging with [ $^{18}$ F]-FDG, [ $^{18}$ F]-FMAU, and [ $^{124}$ I]-mIPQA in the first group of 6 mice generated very promising results (Figure 5 and Table 2). [ $^{18}$ F]-FDG accumulation in H441 tumors reflected moderately increased tumor glucose metabolism and resulted in about 2.5-fold contrast between tumor and contra-lateral lung tissue.



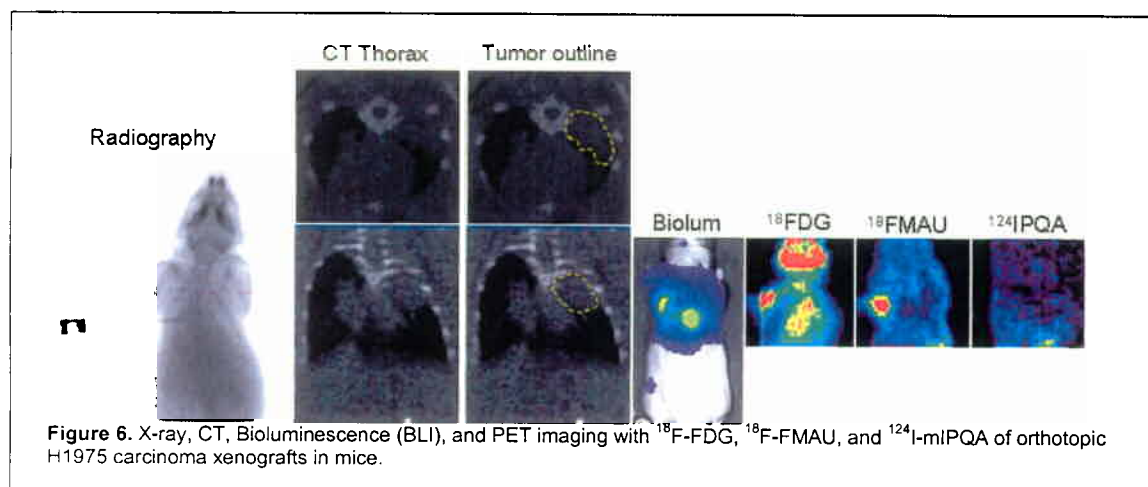
[ $^{18}\text{F}$ ]-FMAU accumulation visualized moderately proliferating tumor areas with a 3-fold tumor-to-lung accumulation ratio (contrast). PET imaging of [ $^{124}\text{I}$ ]-mIPQA performed at 3 hours after intravenous (i.v.) administration of this radiotracer did demonstrate substantial accumulation of this radiotracer in the tumor, however the high activity in the abdomen (liver and kidneys) predominates the image and makes the contrasting of the lung tumor difficult for presentation. A significantly higher tumor-to-lung accumulation ratio (~5-6-fold contrast) was observed at 24 hours after i.v. administration of [ $^{124}\text{I}$ ]-mIPQA.



**Table 2.** PET imaging with  $^{18}\text{F}$ -FDG,  $^{18}\text{F}$ -FMAU, and  $^{124}\text{I}$ -mIPQA of orthotopic H441 carcinoma xenografts in mice.

	FDG	FMAU	IPQA 3h	IPQA 24h
Tumor Accumulation (%ID/g)	6.29±1.63	7.72±2.51	4.30±2.19	2.10±1.13
Tumor-to-Lung Ratio	2.39±1.95	3.02±0.60	2.64±1.31	5.59±2.14

glucose metabolism and resulted in about 3-fold contrast between tumor and contra-lateral lung tissue. [ $^{18}\text{F}$ ]-FMAU accumulation visualized very actively proliferating tumor areas with a 12-fold tumor-to-lung accumulation ratio (contrast). PET imaging of [ $^{124}\text{I}$ ]-mIPQA performed at 3 hours after intravenous (i.v.) administration of this radiotracer demonstrated only a minimal accumulation of this radiotracer in the tumor, as compared to contralateral lung tissue. After the last PET imaging session, the animals bearing H1975GL tumors were sacrificed and whole thoraxes were cryosectioned and subjected to autoradiographic (AR), fluorescence imaging and histopathologic analysis (Figure 7).



This additional analysis confirmed the validity of bioluminescence and fluorescence imaging of this NSCLC model in mice and demonstrated that microCT imaging should be used in conjunction with microPET in future studies in this project. The latter became more obvious when CT images were co-registered with anatomical and GFP-fluorescence images of

cryosections obtained in the same plane as the CT images. Co-registration of autoradiographic images with corresponding anatomical images of the same sections that were used to produce

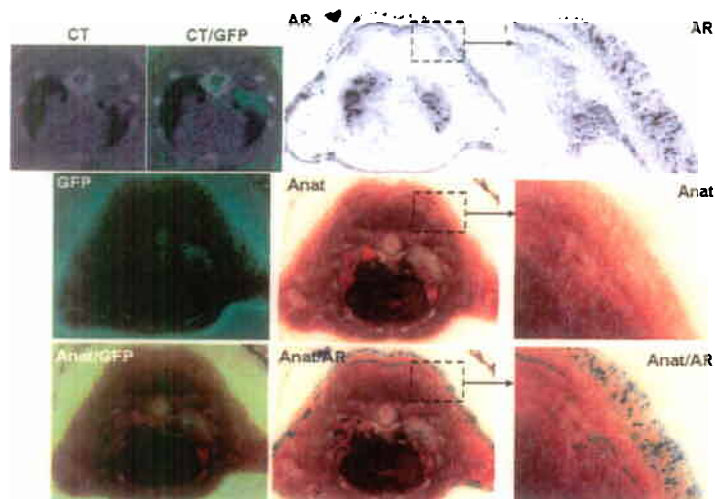


**Figure 7.** Multimodality imaging of orthotopic H1975GL carcinoma xenograft in mice. Active EGFR imaging with  $^{124}\text{I}$ -IPQA autoradiography (AR).

autoradiograms, provided high resolution images that explain the pattern of  $^{124}\text{I}$ -mIPQA distribution at 3 hours post i.v. administration.

Such pattern could not be visualized and analyzed by microPET because it has a much lower resolution and sensitivity than AR. Highly specific accumulation of  $^{124}\text{I}$ -mIPQA was observed in hair follicles, subcutaneous fat layer, and in bronchi, which is consistent with high activity of EGFR in these tissues (Figure 7). Also, a significant accumulation of  $^{124}\text{I}$ -mIPQA was observed in tumor vasculature originating from the affected lung (Figure 8). It is interesting that vascular EGFR labeling was stronger

near the affected lung tissue, but gradually decreased towards the periphery of the tumor lesion. Additional studies using  $^{124}\text{I}$ -mIPQA autoradiography and dual-munofluorescence (CD31 and phosphoEGFR) are required to investigate this phenomenon and to prove that  $^{124}\text{I}$ -mIPQA can

visualize upregulation of EGFR signaling in tumor vasculature.

The lack of  $^{124}\text{I}$ -mIPQA accumulation in H1975GL tumor cells as opposed to tumor stromal vasculature, confirms our *in vitro* observations in H1975 cells that exhibited low accumulation and retention of  $^{124}\text{I}$ -mIPQA and were resistant to growth inhibition by this class of compounds such as gefitinib due to T790M mutation in the EGFR kinase domain. Thus,  $^{124}\text{I}$ -mIPQA does not accumulate in tumors that are resistant to aminophenylquinazoline-based compounds like gefitinib.  $^{124}\text{I}$ -mIPQA autoradiography also supports what was hypothesized by Dr. Isaia Fidler (MDACC) that tumors express high levels of TGF $\alpha$ , resulting in induced expression and activation of EGFR in

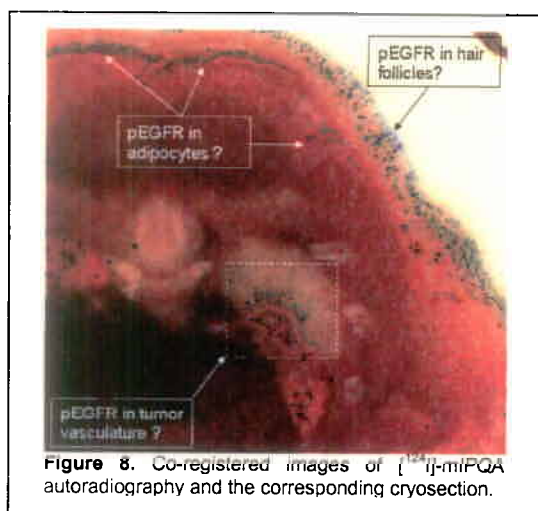


**Figure 8.** Co-registered images of  $^{124}\text{I}$ -mIPQA autoradiography and the corresponding cryosection.

tumor vasculature in a paracrine manner as well as in tumor cells in an autocrine manner, therefore such tumor lesions are sensitive to EGFR inhibitors that act predominantly via inhibition of tumor vasculature.

Currently, we are conducting similar multi-modality imaging studies in H3255GL and PC14GL xenografts in mice to further test the feasibility of non-invasive imaging of EGFR expression /activity with  $^{124}\text{I}$ -mIPQA and PET/CT.

As part of Aim 2, we assessed the efficacy of PET imaging for monitoring early changes in glucose metabolism with  $^{18}\text{F}$ -FDG and proliferative activity with  $^{18}\text{F}$ -FMAU in human NSCLC xenografts in mice in response to therapy with gefitinib. PC14, H441, H3255, and H1975 was

respectively injected s.c. ( $3 \times 10^6$  cells) in nu/nu mice. When tumors grew >5 mm in diameter, PET imaging with  $^{18}\text{F}$ -FDG and  $^{18}\text{F}$ -FMAU was performed on two consecutive days and repeated after 3 and 4 days of gefitinib (100 mg/kg) therapy, respectively. Tumor growth was monitored by calipers.

Tumor-to-muscle (T/M) ratios of  $^{18}\text{F}$ -FDG and  $^{18}\text{F}$ -FMAU accumulation for different NSCLC xenografts before and after gefitinib treatment are summarized in Table 3. Pre-treatment T/M ratios of  $^{18}\text{F}$ -FMAU were higher than those of  $^{18}\text{F}$ -FDG, especially in gefitinib-resistant NSCLCs (PC14, H1975). In these tumors, the lack of decrease in  $^{18}\text{F}$ -FMAU and  $^{18}\text{F}$ -FDG T/M ratios after 3-4 days of gefitinib therapy was predictive of tumor resistance, as evidenced by progression of tumor growth during the following 12 days of therapy with gefitinib. In gefitinib-sensitive tumors (H441 and H3255), no significant changes in  $^{18}\text{F}$ -FDG and  $^{18}\text{F}$ -FMAU T/M ratios after 3-4 days of gefitinib therapy have been observed, because of the low pre-treatment T/M ratios of both radiotracers, especially in H3255 carcinomas, which had almost complete response at 12 days of gefitinib therapy.

Table 3: Tumor-to-muscle (T/M) ratios of  $^{18}\text{F}$ -FDG and  $^{18}\text{F}$ -FMAU accumulation in xenografts before and after gefitinib

	PC14	H441	H3255	H1975
EGFR status	wild-type	wild-type	L858R mut.	L858R, T790M mut.
TGFR level	+	+++++	+	++
Gefitinib IC50 (uM)	12.6	40.2	2.3	> 100
FDG before ther.	1.86±0.98	0.87±0.30	0.82±0.24	1.46±0.41
FDG after ther.	2.41±1.19	1.12±0.48	0.74±0.15	1.41±0.93
FMAU before ther.	6.21±2.11	2.51±1.13	1.22±0.35	3.51±1.79
FMAU after ther.	7.73±2.52	2.41±0.45	0.76±0.18	2.68±1.71
Tumor growth resp.	progression	moredate resp.	complete resp.	progression

## Conclusions

We conclude that imaging with pharmacokinetically optimized more water-soluble [ $^{124}\text{I}$ ]mIPQA derivatives should allow for identification of tumors with increased EGFR signaling. PET imaging with  $^{18}\text{F}$ -FMAU demonstrated higher sensitivity for the detection of NSCLCs as compared to  $^{18}\text{F}$ -FDG. The lack of decrease in  $^{18}\text{F}$ -FDG and  $^{18}\text{F}$ -FMAU uptake early after initiation of gefitinib therapy is predictive of tumor resistance. However, in some gefitinib sensitive NSCLCs the assessment of early treatment responses by PET may not be feasible because of very low pre-treatment levels of uptake of both  $^{18}\text{F}$ -FDG and  $^{18}\text{F}$ -FMAU. Therefore, alternative imaging agents need to be developed for the detection of NSCLCs and for monitoring molecular-targeted therapies in patients.

## Project 3: Targeted Peptide-based Systemic Delivery of Therapeutic and Imaging Agents to Lung Cancer

(PI and co-PI: Renata Pasqualini, Ph.D., Wadih Arap, M.D., Ph.D.)

Two critical issues in lung cancer are the management of advanced and/or metastatic disease and the maximization of cure after surgery in localized disease. The ability to target therapies and imaging agents to malignant tumors has been a long-standing goal in medical oncology. Unfortunately, to date, there are only a few selected situations in which targeted delivery is actually feasible. Tumor targeting approaches tend to be either highly invasive or suffer from a lack of specificity and incomplete tissue penetration. Several lines of research have recently converged to explore vascular targeting by taking advantage of the differences between the newly formed vessels in tumors and the mature vessels in normal tissues. Our approach is

particularly novel because it directly selects *in vivo* for circulating probes capable of preferential homing into tumors.

We have developed an *in vivo* screening method in which peptides homing to specific vascular beds are selected after intravenous administration of a phage display random peptide library. A unique and attractive feature of this functional assay is that it detects the availability of molecular targets based on accessibility to a circulating probe, without preconceived biases or assumptions about the nature of their corresponding receptors. Our previous work has uncovered a vascular address system that allows targeting of specific tissues with diagnostic or therapeutic agents. Here, we propose to develop ligand-receptor systems for targeted peptide-based systemic delivery of therapeutic and imaging agents to lung tumors. The studies outlined in this proposal focus on the use of peptide sequences with selective lung tumor targeting properties. We will seek to validate these probes as delivery vehicles in drug and gene targeting approaches. Our strategy will be to combine homing peptides in the context of phage as gene therapy vectors. Given that many of our peptides also target angiogenic vasculature in addition to tumor cells, these studies are likely to enhance the effectiveness of therapeutic apoptosis induction and imaging technology.

**Aim 1            To select peptides targeting primary and metastatic tumors in lung cancer patients.**

### Update

#### ***Molecular Fingerprinting of Cancer Cell Lines***

First, we screened the NCI-60 cell lines including lung cancer cells using a phage-displayed combinatorial library (Weisbecker et al., 1996). By fingerprinting lung cancer cells we have confirmed the expression of a previously characterized molecular target, EGFR, in multiple cancer origins, which demonstrates the power of our approach (Kolonin et al., 2006).

Recently, we used this approach to identify a new cancer origin-selective molecular target, Ephrin A5 receptor, which we have preliminarily validated in the context of human lung cancer cell lines and tissues as described below in Specific Aim 2.

#### ***Motifs targeting NCI-60 cells in correlation with EGFR expression pattern are found within peptides similar to domains of biological EGFR ligands and bind to EGFR.***

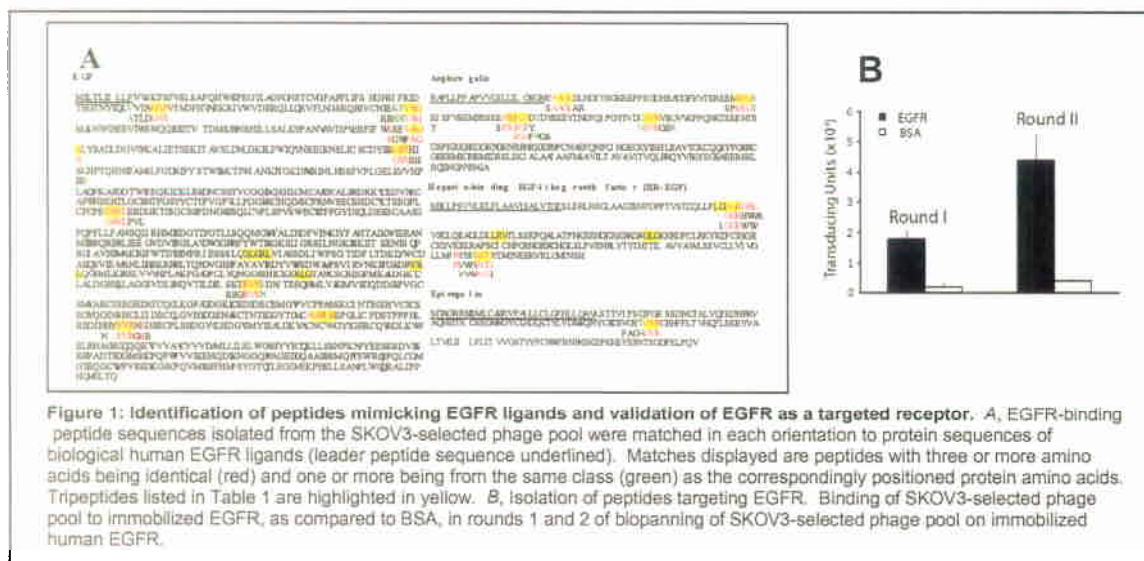
To show that the approach taken can lead to actual targetable tumor cell surface proteins, we chose to test if EGFR is bound by any of the tripeptide motifs distributed in the panel in a profile correlating with EGFR expression. Consistently, 24 out of 38 tripeptides surveyed displayed NCI-60 cell line association pattern consistent with that of EGFR expression (Kolonin et al., Table 1). Of these tripeptides, 22 were isolated in the screens on ovarian cancer cell lines SKOV3 and OVCAR4 (data not shown). Since EGFR is well known to be associated with ovarian cancer (Maihle et al., 2002; Vogelstein et al., 2004), we deemed these cell lines to be likely expressers of targetable EGFR, which would account for the selection of EGFR ligand-mimicking motifs. To validate EGFR binding by the selected motifs, we screened the SKOV3-binding phage sub-library (pooled clones recovered in rounds 2 and 3) on immobilized human EGFR. After 2 rounds of selection, we analyzed phage displaying the EGFR-binding peptides: the majority were comprised of different seven-mer peptides that contained 17 out of 22 SKOV3-selected tripeptide motifs distributed in the panel in a profile correlating with EGFR expression (Kolonin et al., 2006)(Table 1).



Motif	Mean motif count ( $\pm$ SEM) inside vs. outside cluster	P value t-test, 1-sided	P value Wilcoxon rank-sum test, 1-sided	P value Fisher exact test, 1-sided
GGS	2.2 ( $\pm$ 0.5) vs. 1.2 ( $\pm$ 0.2)	0.0422	0.0407	0.0043
GGR	1.3 ( $\pm$ 0.3) vs. 1.5 ( $\pm$ 0.2)	0.6991	0.6466	0.6739
GLG	0.7 ( $\pm$ 0.4) vs. 0.7 ( $\pm$ 0.2)	0.5375	0.6888	0.5150
GGL	1.2 ( $\pm$ 0.2) vs. 1.3 ( $\pm$ 0.2)	0.6457	0.4174	0.5485
GSS	2.2 ( $\pm$ 0.4) vs. 1.1 ( $\pm$ 0.2)	0.0422	0.0026	0.0008

**Table 1: Association of specific tripeptides with lung cancer-derived cell lines:** To determine statistical significance of association or dissociation between exemplary tripeptides and cell lines, normalized frequencies of five tripeptides predominantly associated (GGS, GGR, GLG, and GGL) or dissociated (GSS) with the cluster containing the majority of lung tumor-derived cell lines (Fig. 1, boxed) were compared for cell lines inside the cluster and outside the cluster. Selective association of tripeptide GGS with the clustered cell lines was found significant according to t-test. Fisher exact test and Wilcoxon rank-sum test (all tests one-tailed).

Phage displaying these peptides had specific affinity to EGFR, as determined by subjecting the same sub-library to immobilized bovine serum albumin (BSA) control binding (Figure 1B). Remarkably, computer-assisted analysis of sequences revealed that 12 of the seven-mer EGFR-binding peptides contained amino acid motifs similar to those present in some of the biological EGFR ligands. These peptides, containing eight of the candidate tripeptides (RVS, AGS, AGL, GVR, GGR, GGL, GSV, and GVS) were found highly similar to fragments of EGF, Amphiregulin, heparin-binding EGF-like growth factor, and Epiregulin (Figure 1A). Similarity search using the same algorithm on the same 12 seven-mers did not reveal any matches to two other EGFR ligands, TGF- $\alpha$  and betacellulin, or randomly chosen control ligands of tyrosine kinase receptors from the three other candidate families listed in Table 1 (Kolonin et al., 2006): Ephrin A, NGF- $\beta$ , and FGF6 (data not shown). Taken together, these data suggest that at least some of the peptides selected on the NCI-60 cells target EGFR, while others may bind to different tyrosine kinases possibly including those from TRK, Ephrin, or FGF receptor families.



## **Aim 2 To validate receptors for targeting human lung cancer**

### **Update**

This year, we identified and validated the receptor Ephrin A5 for targeting lung cancer as briefly mentioned above.

### ***Identification of lung cancer-targeting receptor Ephrin A5***

The peptide distribution-correlating tyrosine kinase receptors belonging to EGFR, FGFR, NGFR and Ephrin receptor families are often up-regulated in many types of cancer. On the other hand, some of the receptors, such as EphA5, presumably targeted by GGS tripeptide and its derivatives predominantly selective for lung tumor-derived cell lines appear to be at least partially specific for the progenitor cancer type. Since this approach clearly allowed identification of cell surface receptors ubiquitously upregulated in various cancers, we took a step further to attempt identification of cancer type-specific receptors.

Having chosen lung cancer for the initial procedure establishment, we identified a distinct cluster of five tripeptides associated with lung tumor-derived cell lines (Kolonin et al., 2006) (Figure 1, boxed). We compared tripeptide frequencies for the 11 cell lines within this cluster with their frequencies for the rest of NCI-60 lines by using statistical tests (Fisher exact, Wilcoxon rank-sum, and t-test). Consistently, we observed that motif GGS was isolated for the clustered lines significantly ( $P < 0.05$ ) more frequently than for the other NCI-60 cell lines (Table 1).

Based on the automated BLAST analysis (Kolonin et al., 2006) (Table 1), we identified proteins of the ephrin family candidate prototypes of the GGS-containing peptides: ephrins -B3 and A4 contain the GGS, consistent with a functional mimicry. Ephrins (A and B) and their receptors (EphA and EphB) represent a large class of cell - cell communication molecules with well-defined developmental functions. Their role in healthy adult tissues and in human disease is still largely unknown, although diverse roles in carcinogenesis have been postulated and a number of Eph receptors have been found overexpressed by various cancers (Hafner et al., 2004). Based on the COMPARE analysis of GGS distribution within NCI-60 (Kolonin et al., 2006) (Table 1), the only receptor expressed in the corresponding pattern is EphA5. The EphA5 expression has been explored using cDNA microarray analysis and reported at the DTP server (<http://dtp.nci.nih.gov/mtweb/servlet/moltidsearch?moltid=MT894>) (Figure 2); however, no studies of EphA5 function in cancer have been published. Intriguingly EphA5 is not expressed in normal lung and normally is only thought to have brain-specific functions.

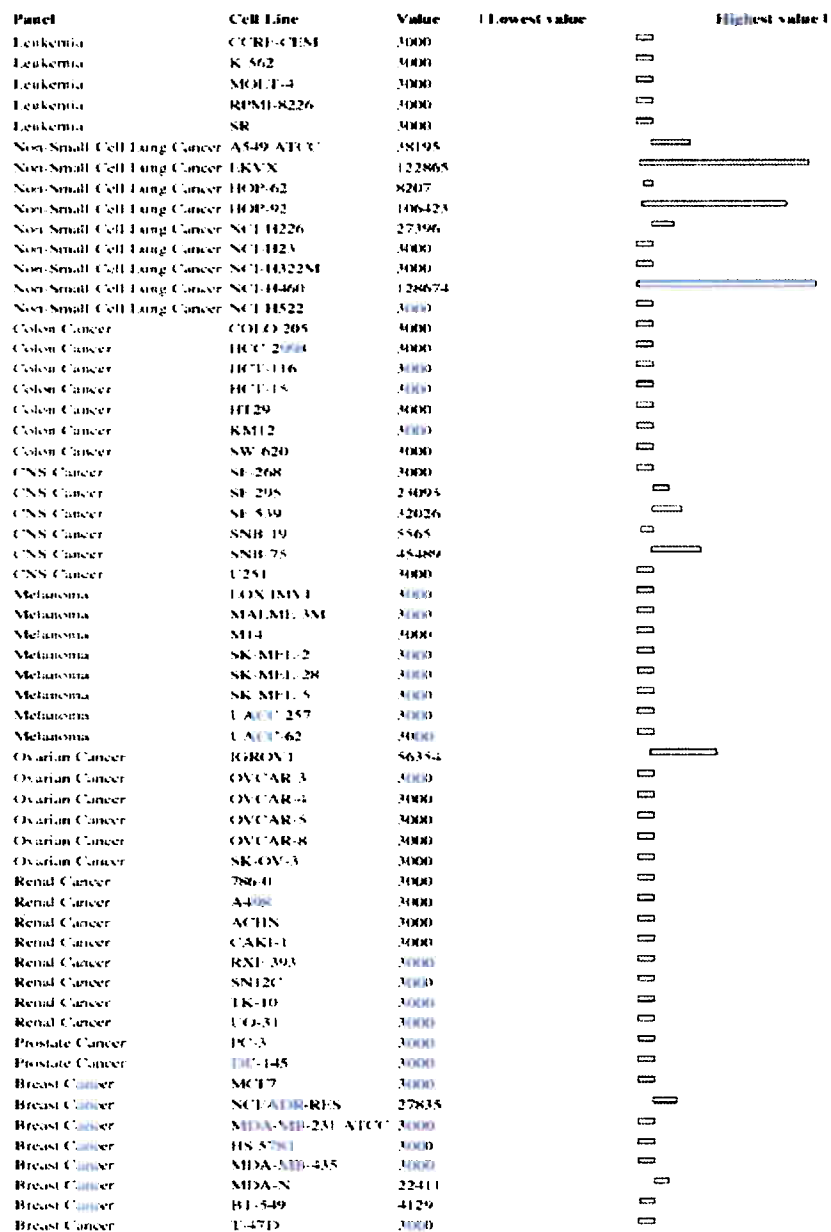
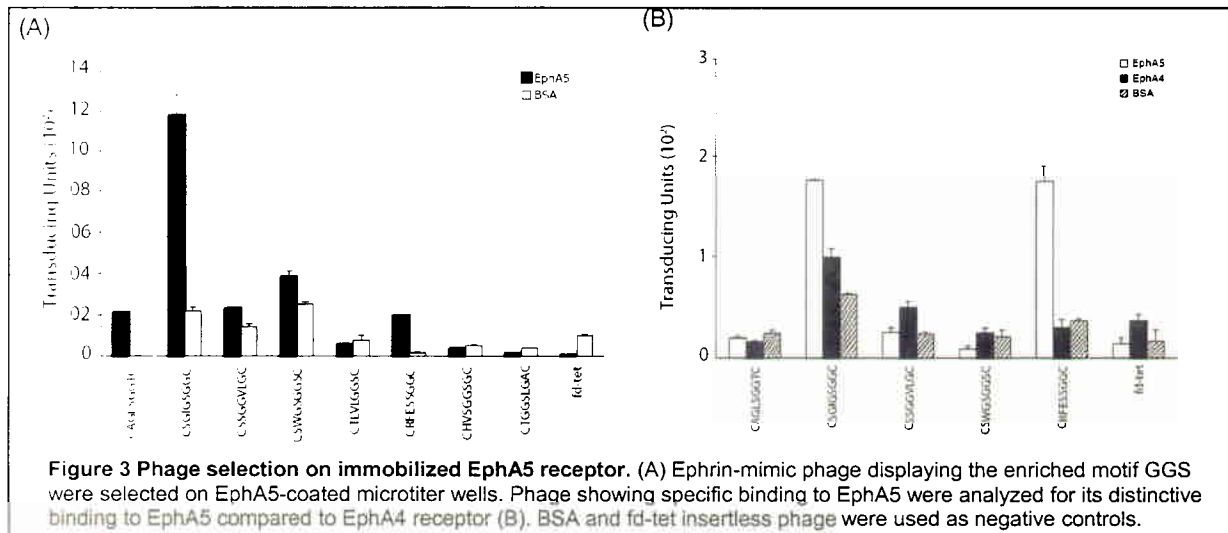


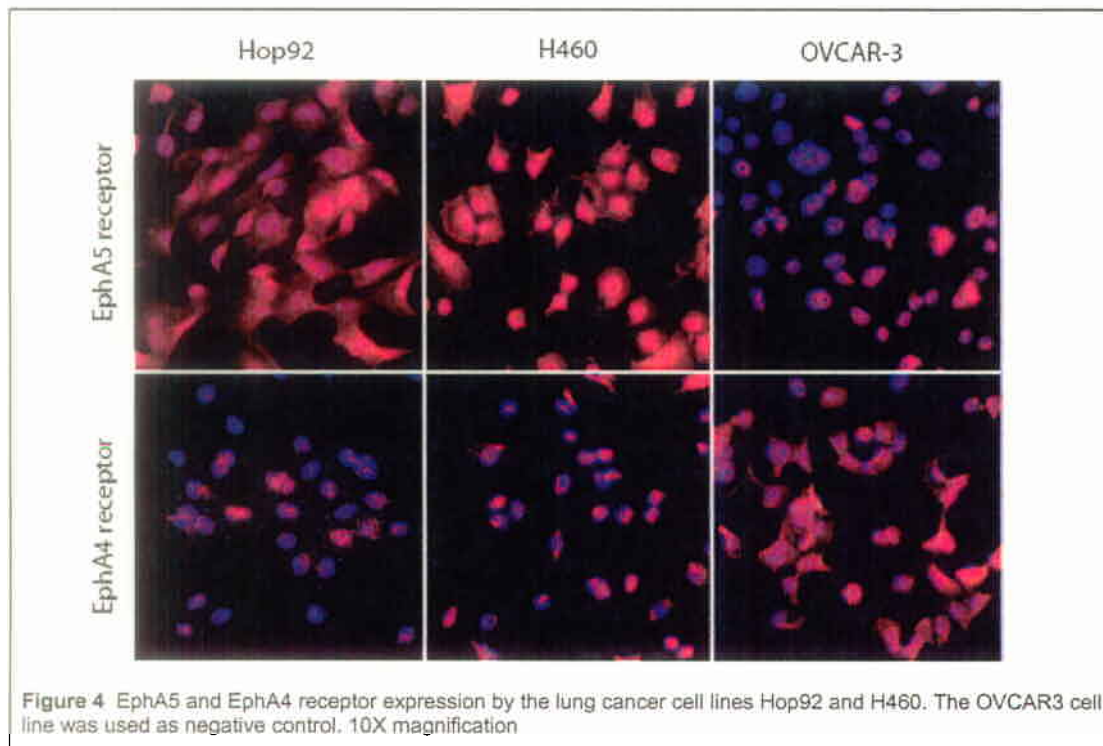
Figure 2: EphA5 receptor expression in the NCI-60. From microarray analysis reported at <http://dtp.nci.nih.gov/mtweb/servlet/multidsearch?molrid=MT894>.

### Validation of ephrin-mimic peptides in lung cancer

To validate phage containing the motif GGS as a ligand of Eph receptors, we tested phage binding to the EphA5 immobilized receptor. We started testing eight peptides (CAGLSGGTC, CSGIGSGGC, CSSGGVLGC, CSWGSGGSC, CTLVLGGSC, CRFESSGGC, CHVSGGSGC, CTGGSLGAC) containing the enriched motif GGS, all of them displayed by phage clones obtained from the screening on different cell lines known to express the EphA5 receptor (Figure 3A). From this first round of selection, 5 clones (CAGLSGGTC, CSGIGSGGC, CSSGGVLGC, CRFESSGGC and CSWGSGGSC) showed good binding to the receptor relative to the control (BSA) and were further analyzed by their ability to specifically bind to EphA5 but not to the control EphA4 receptor (Figure 3B). Phage displaying the peptide sequences CSGIGSGGC and CRFESSGGC showed binding specificity and were chosen for characterization.

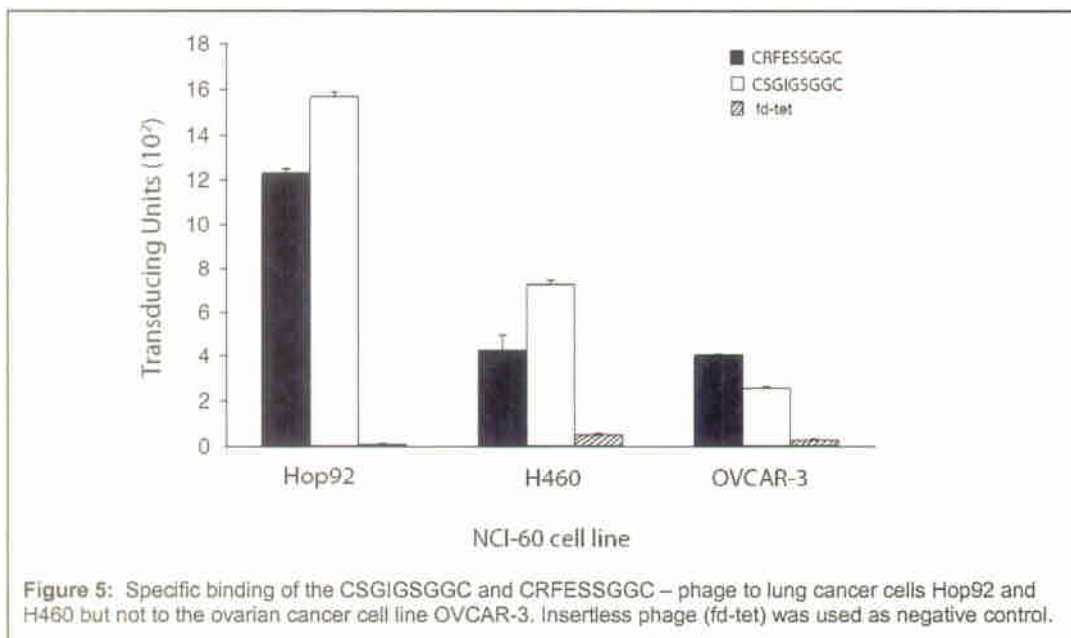


We next attempted to investigate the binding of the selected phage to the lung cancer cells Hop92 and H460. These cells are known to express EphA5 receptor on its surface, as confirmed by immunofluorescence analysis (Figure 4). The ovarian cancer cell line OVCAR-3, negative for EphA5 expression, was used as control.

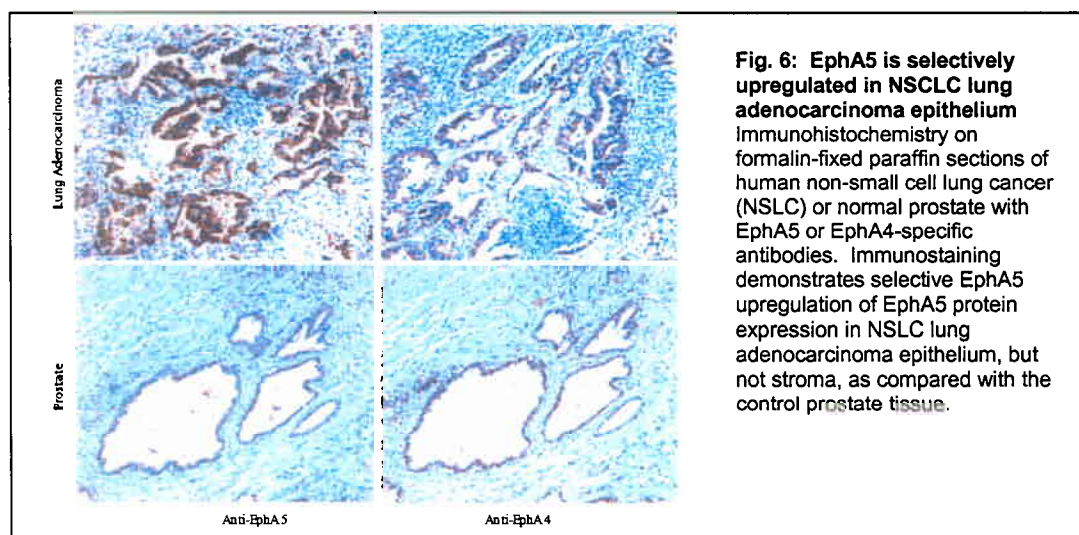


Next, we used the BRASIL method (biopanning and rapid analysis of selective interactive ligands) to analyze binding of selected phage to lung cancer cells (Giordano et al., 2001). We observed specific binding of phage displaying the sequences CSGIGSGGC and CRFESSGGC to Hop92 and H460, confirming the data obtained from the screening on the immobilized EphA5 receptor (Figure 5).





Finally, we showed that EphA5 protein is overexpressed in human lung adenocarcinoma epithelia by IHC staining patient tissues from the M. D. Anderson Cancer Center.



### Aim 3 To design tools for molecular imaging of lung cancer

We have just started the Aim. Any finding will be reported in the next round of the report.

### Conclusions

Taken together, these data suggest that the two selected phages displaying the motif GGS are ligands of EphA5 receptor. EphA5 overexpression in lung cancer cells provides original evidence for EphA5 being a lung cancer biomarker and has potential functional implications.

In the future, the cancer-associated motifs identified here can be used for the development of approaches for targeted imaging or therapy of tumors in patients. Their receptors, including EGFR, EphA5, and other yet to be identified cell surface molecules, can be further explored for their oncogenic properties and the potential to serve as universal or origin/grade-selective targets of cancer.

## Project 4: Inhibition of bFGF Signaling for Lung Cancer Therapy

(PI: Reuben Lotan, Ph.D.)

One of the reasons that the survival of lung cancer patients continues to be abysmal is that this cancer is diagnosed at advanced stages. Therefore, improvements in early detection through the identification of molecular markers for diagnosis and for intervention combined with targeted chemoprevention are urgently needed. Several growth and angiogenesis promoting signaling pathways are amplified in lung cancer. Among these, the basic fibroblast growth factor (bFGF) and its trans-membrane tyrosine kinase receptors (FGFRs) have been associated with lung cancer development and upregulated in non-small cell lung cancer (NSCLC). We hypothesize that bFGF triggers signaling pathways that contribute to malignant progression of lung cancers by stimulating tumor cell and endothelial cell proliferation and survival and augmenting angiogenesis. Therefore, agents that intervene in this pathway may be useful for lung cancer therapy either alone or in combination with cytotoxic agents. We proposed to use an inhibitor of bFGF signaling, 5, 10, 15, 20-tetrakis(methyl-4-pyridyl)-21 H, 23 H-porphine tetra- p-tosylate salt (TMPP), which blocks binding of bFGF to its receptors, for *in vitro* and *in vivo* experiments.

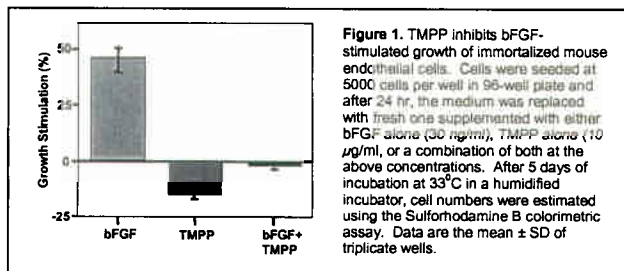
**Aim 1** To determine the effects of bFGF on *in vitro* growth, survival, motility, invasion and angiogenesis of NSCLC cells and endothelial cells.

**Aim 2** To evaluate the relative potency of several inhibitors of bFGF binding to receptor (i.e., TMPP and analogs) in inhibiting effects of bFGF detected in Specific Aim 1 and evaluate the effects of these inhibitors in combination with paclitaxel on *in vitro* growth and survival of tumor cells.

In the past year, we made some progress related to Specific Aims 1 and 2 which is reported here together.

### Update

Because bFGF is involved in angiogenesis and expected to act as a mitogen for endothelial cells, we extended our original observations of inhibitory effects of TMPP on bFGF-stimulated growth of immortalized human bronchial epithelial cells and NSCLC cells to immortalized mouse endothelial cells. The lung microvessel endothelial cells were obtained from Dr. Langley (Department of Cancer Biology at our institute), who isolated the cells from the lungs of Immortamouse, a mouse carrying a temperature sensitive mutant of Simian Virus 40 Large T antigen. At the permissive temperature of 33°C, these cells express T antigen that binds and inactivates p53 thus leading to immortalization of the cells (Langley et al., 2003). We found that bFGF could stimulate the growth of the endothelial cells by about 45% after 5 days, whereas TMPP alone can inhibit their growth by about 15%. Importantly when TMPP was added together with bFGF, it suppressed the stimulatory effect of bFGF (Figure 1).



**Aim 3** To evaluate anti-tumor activity of most effective bFGF inhibitors identified in Specific Aim 2 when used alone and in combination with paclitaxel in an orthotopic lung cancer model using luciferase-expressing NSCLC cells for *in vivo* bioluminescence imaging of tumor growth and response to treatment.

## Update

This specific aim will start upon completion of Specific Aims 1 and 2. However, we have found a commercial source for TMPP (Frontier Scientific, Logan, UT) and will not rely on the limited amounts supplied by Dr. Aviezer from Prochon company in Israel for animal experiments.

## Additional Studies

In addition to the above aims, we performed a series of experiments that we did not specify originally because we did not have access then to a sufficient number of surgical specimens from patients. However, during the previous year, Dr. Wistuba, Director of the Pathology Core with assistance from Dr. Behrens from my group, had constructed a tissue array that includes normal, premalignant and malignant lung epithelial tissues. This unique collection of specimens has enabled us to investigate the expression of bFGF and FGFR-1 and FGFR-2 by IHC staining of the tissue microarrays containing NSCLC tumors and their corresponding preneoplastic lesions. The samples examined included: 71 normal bronchial epithelia (NBE), 128 bronchial hyperplasias, 23 squamous metaplasias, 78 squamous dysplasias, 46 squamous cell carcinomas (SCC), 72 atypical adenomatous hyperplasias (AAH) and 56 adenocarcinomas (ADCA). A semi-quantitative IHC analysis of cytoplasmic and nuclear expression was performed. ADCA and SCC specimens demonstrated higher cytoplasmic expression of bFGF, FGFR-1 and FGFR-2 compared to NBE ( $P = <0.0001$ ). Nuclear expression of FGFR-2 was increased ( $P < 0.0001$ ) and FGFR-1 was reduced ( $P = 0.012$  to  $<0.0001$ ) in both tumor types compared to NBEs. However, bFGF expression was increased only in ADCA ( $P = 0.0003$ ). In the SCC development sequence, dysplasias demonstrated higher cytoplasmic expression of all markers compared to NBE ( $P = 0.003$  to  $<0.0001$ ). In the ADCA sequence, AAHs demonstrated decreased cytoplasmic expression for all markers compared to NBE ( $P = 0.01$  to  $<0.0001$ ), whereas nuclear expression of both FGFR-1 and FGFR-2 was increased ( $P < 0.0001$ ). For all tissue samples ( $N = 474$ ), correlation between cytoplasmic and nuclear expression was detected for each marker ( $P = 0.03$  to  $<0.0001$ ); cytoplasmic and nuclear expression of bFGF correlated with FGFR-1 ( $P = 0.018$ ) and cytoplasmic FGFR-2 ( $P = 0.012$ ) respectively; and cytoplasmic expression of both receptors was correlated ( $P < 0.0001$ ). These data will be presented at the 2006 annual meeting of AACR (Behrens et al., 2006). Examples of some of these findings (bFGF) are shown in Figures 2 and 3:

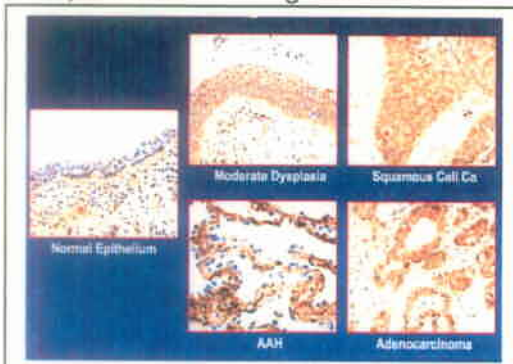


**Figure 2.** Immunohistochemical analysis of the expression of bFGF in normal epithelium and in premalignant lesions (dysplasia and atypical adenomatous hyperplasia (AAH) and their corresponding malignancies, squamous cell carcinoma and adenocarcinoma, respectively. These tissue were included in a tissue array constructed from numerous surgical specimens fixed in formalin and embedded in paraffin. Note low expression in normal epithelium and abundant expression in premalignant and malignant tissues.

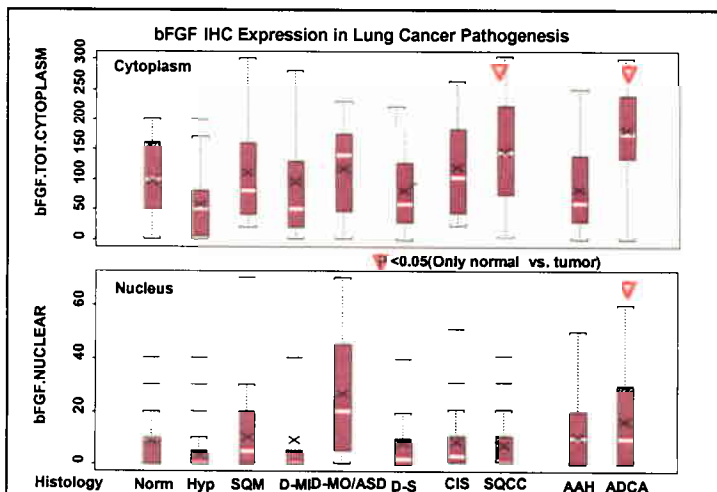


**Figure 3.** Box-plots representing immunohistochemical expression scores for cytoplasmic (upper panel) and nuclear (lower panel) bFGF in the sequential pathogenesis of lung cancer. Bars represent mean. Numbers under histology represent number of specimens (N) examined in each category. Hyp, hyperplasia; SQM, squamous metaplasia, LG-D, low-grade dysplasia; CIS =HG-D, high-grade dysplasia; SQCC, lung squamous cell carcinoma; AAH, atypical adenomatous hyperplasia; ADCA, lung adenocarcinoma.

## Conclusions

We conclude that bFGF can stimulate the growth of immortalized mouse endothelial cells that can be reversed by TMPP *in vitro* and cytoplasmic overexpression of bFGF and its receptors in NSCLC tumor specimens and dysplastic lesions in SCC sequence indicate an important role of the pathway in NSCLC pathogenesis.

## Recommended changes

Because we have access to tissue arrays that include, normal, premalignant and malignant lung tissue specimens as described above, we have an opportunity to study additional components of bFGF signaling *in vivo* including the expression of the Heparan Sulfate, Syndecan-1 and FGFR-3 in the sequential pathogenesis of lung cancer.

We also consider correlating the IHC expression of bFGF and receptors between tumor and non-malignant epithelial cells with angiogenesis (Microvascular density and VEGF/VEGFR expression).

## Project 5: Targeting mTOR and Ras signaling pathways for lung cancer therapy

(PI and co-PI: Fadlo R. Khuri, M.D., Shi-Yong Sun, Ph.D.)

The original objectives of project 5 were to study the effect of the novel mTOR inhibitor CCI-779 alone or CCI-779-based combination regimens on the growth of human NSCLC cells and their underlying mechanism, and to identify molecular determinants of cell sensitivity to CCI-779 or CCI-779-based combination treatment. Moreover, this project was to evaluate the efficacy of CCI-779 in NSCLC patients and the prognostic values of molecules identified in the preclinical studies.

Because of the difficulty in obtaining CCI-779 for our proposed clinical trial (Specific Aim 4), we have decided to substitute CCI-779 with RAD001, another mTOR inhibitor tested in many clinical trials, for our trial. Accordingly, we will work on RAD001 or rapamycin in our preclinical studies to achieve our objectives. RAD001 and CCI-779 are derivatives of rapamycin and only have minor structural modifications from rapamycin. Although RAD001 and CCI-779 have improved bioavailability, they have the same mechanism of action as rapamycin does and comparable potencies with rapamycin. Therefore, utilization of RAD001 and rapamycin in our proposed experiments will not change our overall objectives.

Due to the delay of the subcontract between M.D Anderson and Emory, our fund was only made available in October 2005. Nonetheless, we have still made some significant progress in our project as described below.

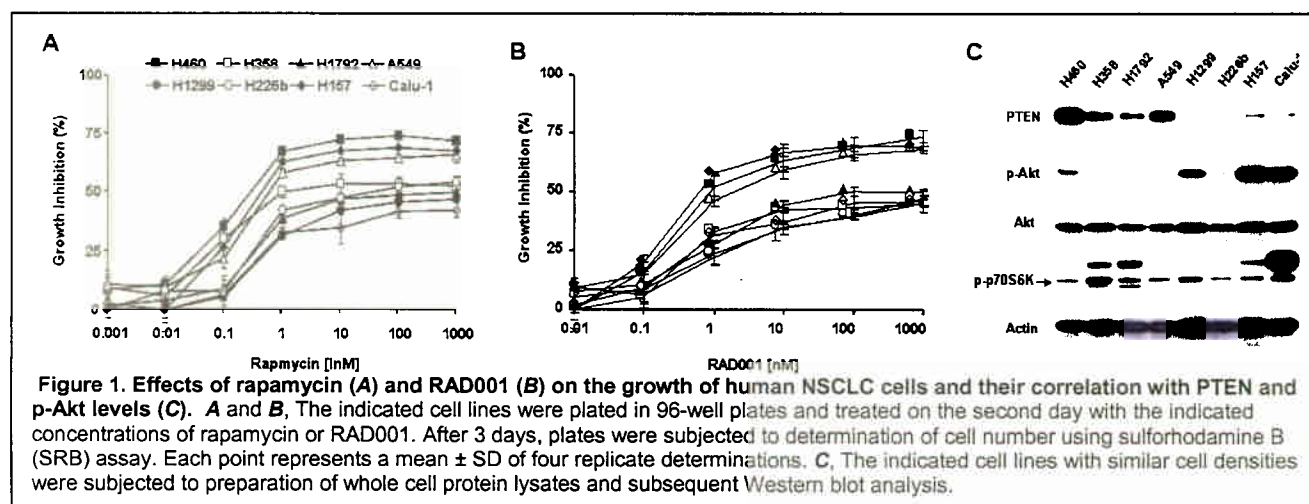
**Aim 1            To determine whether an mTOR inhibitor inhibits the growth of human NSCLC cells via G1 growth arrest or induction of apoptosis and identify the molecular determinants of mTOR inhibitor sensitivity.**

## Update

***Effects of mTOR inhibitors on the growth of human NSCLC cells and their association with levels of PTEN and p-Akt.*** We examined the effects of rapamycin and RAD001 on the growth of eight NSCLC cell lines. Both rapamycin and RAD001 at concentrations of 1 nM or greater effectively inhibited the growth of NSCLC cells. However, at concentrations ranging from 1 nM to 1000 nM, they did not appear to exhibit dose-dependent growth-inhibitory effects in these cell lines. Both drugs at concentrations ranging from 0.01 nM to 1 nM had apparent dose-dependent growth-inhibitory effects. Interestingly, even at a concentration of 1  $\mu$ M or higher, they failed to completely inhibit the growth of



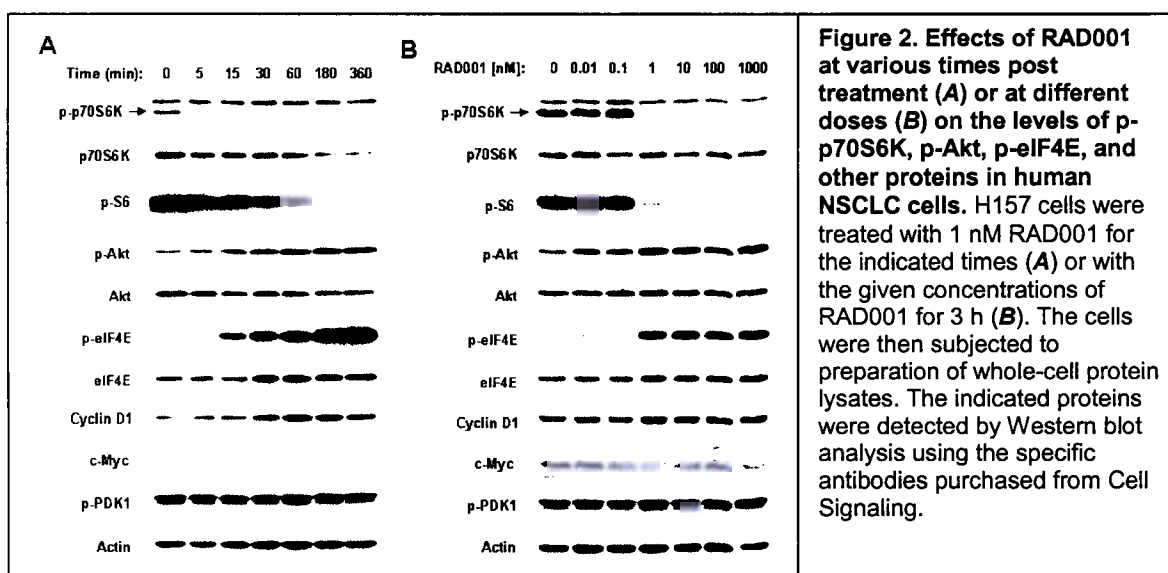
NSCLC cells, suggesting that a certain portion of the cell population is resistant to mTOR inhibitors (Figures 1A and 1B). Under the microscope, we found that cells exposed to either of the agents remained attached on dishes and had normal morphology in comparison with control cells. Sub-G1 analysis also failed to demonstrate apoptosis in rapamycin or RAD001-treated cells. Therefore, it appears that rapamycin and RAD001 inhibit the growth of human NSCLC cells without inducing cell death.



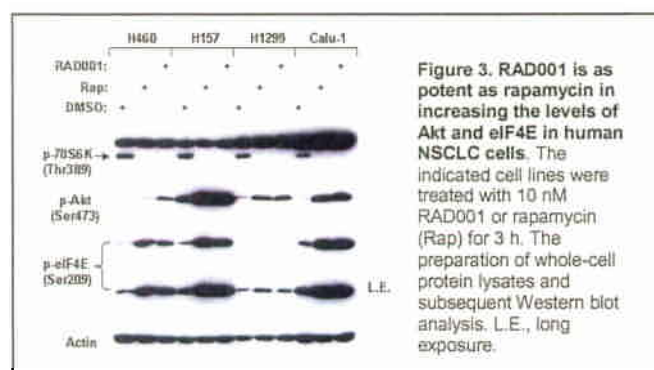
**Effects of RAD001 on mTOR signaling and phosphorylation of Akt and eIF4E.** To determine whether the mTOR pathway is constitutively activated and whether rapamycin or RAD001 exerts an inhibitory effect on mTOR signaling in human NSCLC cell lines, we examined the expression patterns of several key molecules in the mTOR axis. We detected p-mTOR, p-p70S6K, and p-4E-BP1 in all of the four NSCLC cell lines and found that mTOR signaling is constitutively active in human NSCLC cell lines. After treatment with rapamycin, p-p70S6K and p-4E-BP1 were decreased, indicating that rapamycin indeed works as an mTOR inhibitor to inhibit mTOR signaling. Rapamycin did not decrease p-mTOR levels. For details, please see Sun et al paper in *Cancer Research*, 2005.

In addition, we analyzed the levels of other molecules related to this pathway. Since p-Akt works upstream of mTOR activating mTOR axis, we speculated that rapamycin would not alter the levels of p-Akt. Unexpectedly, all the tested cell lines exposed to rapamycin exhibited increased p-Akt as well as p-GSK3 $\beta$ , a well-known molecule phosphorylated by Akt (Sun et al., 2005). These results indicate that rapamycin activates Akt survival pathway while suppressing mTOR signaling. Similarly, the phosphorylation of eIF4E, a downstream molecule of mTOR suppressed by 4E-BP1, was increased in all of the tested cell lines (Sun et al., 2005).

RAD001 effectively decreased the levels of both p-p70S6K and p-S6 (a substrate of p70S6K) with concurrent increase in both p-Akt and p-eIF4E levels only at concentrations of 1 nM or higher (Figure 2B), which are effective dose ranges for inhibiting cell growth. Within such a range, RAD001 altered the levels of these proteins in a concentration-independent manner (Figure 2B). Moreover, RAD001 decreased p-p70S6K and p-S6 levels at 5 min post treatment. Concurrently, p-Akt and p-eIF4E levels were also increased (Figure 2A). RAD001 did not alter the levels of c-Myc and p-PDK1, but actually increased cyclin D1 expression in the tested cell lines (Figure 2). Currently, we are validating the effects of RAD001 and rapamycin on the expression of c-Myc and cyclin D1 in additional lung cancer cell lines.

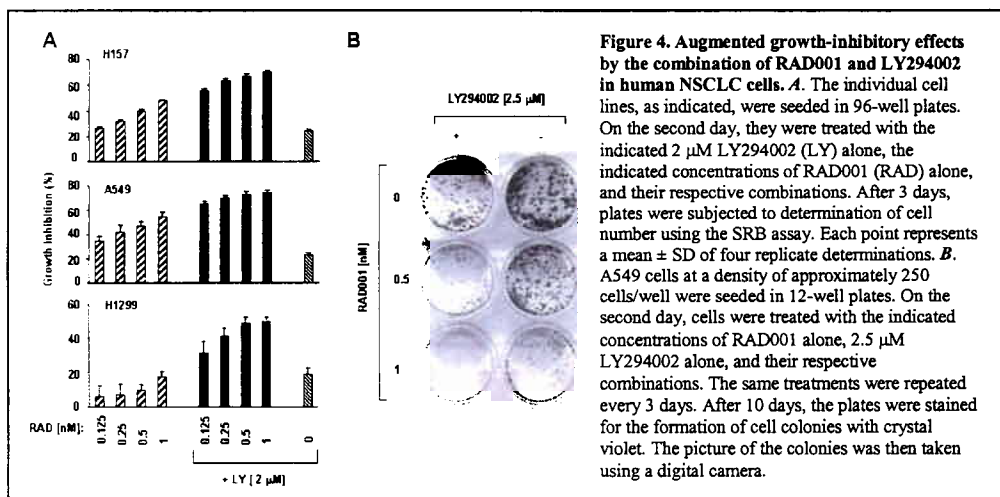


We also compared the effects of RAD001 and rapamycin on mTOR signaling and phosphorylation of Akt and eIF4E in additional lung cancer cell lines and found that they have identical modulations on p-p70S6K, p-Akt and p-eIF4E (Figure 3). Collectively, these findings demonstrate that RAD001 functions in the same fashion as rapamycin (Sun et al, 2005).



## Aim 2 To determine whether the effect of mTOR inhibitors on the growth of human NSCLC cells is enhanced in the presence of a PI3K inhibitor or a MAPK inhibitor.

We examined the effects of the mTOR inhibitors combined with a PI3K inhibitor on the growth of human NSCLC cells. In both a 3-day monolayer culture and long-term 10-day colony formation assay, the combination of rapamycin and the PI3K inhibitor LY294002 exhibited an enhanced (additive or synergistic) growth-inhibitory effect as presented in our published paper (Sun et al., 2005). We also found that the combination of RAD001 with low dose of LY294004 (i.e., 2  $\mu$ M) apparently exhibited growth-inhibitory effects that are greater than those caused by each single agent in a 3-day monolayer culture (Figure 4). In the long-term colony formation assay, we obtained similar results. The combination of the two agents appeared to work better than either single agent in decreasing colony size and number (Figure 4B). Collectively, it appears that the combination of an mTOR inhibitor and LY294002 results in an augmented growth-inhibitory effect.



**Aim 3** To determine whether restoration of the Ras-dependent death signaling pathway enhances the growth inhibitory effect of RAD001 in human NSCLC cells.

No progress has yet been made for this aim.

**Aim 4** To conduct a pilot clinical biochemical induction trial to investigate the effect of RAD001 in operable NSCLC patients and identify molecular determinants of RAD001 sensitivity and prognosis.

#### Update

We have obtained a contract with Novartis Pharmaceuticals for the conduct of the Phase IB trial utilizing RAD001 as a biochemical probe to explore mTOR signaling in lung cancer. Since the trial would be unlikely to address all of our key questions without some evaluation of the effect of RAD001 on tumor metabolism, we have revised the protocol to include serial PET scans to assess the effect of RAD001 on tumor metabolism, and submitted the revised protocol to the IRB at Emory University. We have also obtained funding from Novartis to defray the additional expenses of the PET scans. Assuming IRB approval of the revised protocol will be obtained in February 2006, we anticipate obtaining an IND and launching the study in the second quarter of 2006.

#### Conclusions

Targeting the mTOR axis appears to be a promising strategy against lung cancer. mTOR inhibitors are effective in inhibiting the growth of human lung cancer cells albeit to various degrees. Activation of Akt and eIF4E survival pathways may eventually lead to resistance to mTOR-targeted therapies. Therefore, mTOR-targeted lung cancer therapy based on a sound scientific rationale should be pursued.

#### Recommended changes

Because of the difficulty in obtaining CCI-779 for our proposed clinical trial (Specific Aim 4), we decided to substitute CCI-779 with RAD001. Accordingly, we have started to work on RAD001 or rapamycin in our preclinical studies to achieve our objectives.

#### Project 6: Identification and Evaluation of Molecular Markers in Non-Small Cell Lung Cancer (NSCLC)

(PI and co-PI: Ralf Krahe, Ph.D., Li Mao, M.D.)

A better understanding of lung cancer biology and identification of genes involved in tumor initiation, progression and metastasis are the first step leading to the development of new prognostic markers and targets for therapy. In the same context, identification of reliable predictive markers for response or resistance to therapy in NSCLC patients is also desperately desired for optimal delivery of targeted therapy and/or standard chemotherapy.

The proposed studies aim to identify the two types of markers that would eventually help develop smarter clinical trials, which will selectively recruit patients who are more likely to respond to one regimen over another and lead to improvement of overall therapeutic outcomes.

**Aim 1            To expression profile aerodigestive cancers by DNA microarray technology - with primary focus on adenocarcinoma and squamous cell carcinoma (SCC) of the lung, and head and neck squamous cell carcinoma (HNSCC) including primary tumors, normal adjacent tissues, and metastatic lesions.**

#### Update

##### ***Expression profiling of NSCLC***

To date, expression profiling has been done on 24 matched tumor/normal pairs of HNSCCs (manuscript in preparation), 8 retrospective matched tumor/normal (N/T) pairs of NSCLCs, 5 adenocarcinomas, and 3 SCCs. We had initially collected a total of 22 NSCLC N/T pairs. However, only 8 samples were good enough for expression profiling due to partial or complete degradation of RNA. Notwithstanding, DNA extracted from the same samples was of sufficient quality for Specific Aims 2 and 3. We aim to have 50 NSCLC tumor/normal pairs to be profiled. Based on limited expression profiling data currently in hand, it is too early to draw statistically meaningful conclusions.

**Aim 2            To DNA profile the same samples by complementing DNA approaches to stratify RNA expression profiles on the basis of their corresponding DNA profiles.**

#### Update

##### ***DNA profiling of corresponding NSCLC tumors***

To date, we have extracted DNA from 22 NSCLCs. Because we wish to correlate the DNA approaches with the RNA expression profiles, we are waiting until we get a more complete set of tumors for which good quality RNA is available so that these analyses can be carried out with as much overlap as possible between the two sets of tumor samples. Also, of note, whereas the original proposal suggested the idea of SNP arrays to determine regions of LOH, complemented by array CGH to look for chromosome gain/loss, there is now a DNA copy number analysis tool that has been developed by Affymetrix. This will allow analysis of chromosome copy number and LOH using the same data set (from SNP chips), making the completion of this aim less labor intensive.

**Aim 3            To evaluate the contribution of promoter hypermethylation and transcriptional inactivation of known cancer genes subject to epigenetic silencing to cancer phenotype.**

#### Update

##### ***Methylation profiling of NSCLC***

We have developed an agreement with Biotage, a Swedish/US company, to develop diagnostic tests for DNA hypermethylation. This allows us to use the PyroMethA technique developed in



our lab (Colella et al., 2003) in a high-throughput fashion with the latest analytical equipment and software. DNA from 21 NSCLCs and their matched normal samples have been collected and assays for 8 genes known or suspected to be methylated in lung cancer (*APC*, *MLH1*, *RASSF1*, *MGMT*, *CDKN2A/p14* and *p16*, *ATM*, and *GSTP1*) have been completed. Varying frequencies of methylation (0% to 37% of samples) have been observed in this initial sample set. More samples will be analyzed as they become available, and more genes will be analyzed as their methylation assays are developed. Ultimately, expression levels of the genes identified as differentially regulated (from Aim 1) will be correlated with their corresponding DNA and methylation profiles.

**Aim 4                      To determine protein signatures of Iressa (replaced with tarceva) treatment in NSCLC and identify molecular predictors of response.**

**Update**

As proposed, we first need to establish a lung heterotransplant tumor bank having implants derived from 50 primary NSCLC samples. To do this, we have established collaboration with our Lung SPORE investigators and the Pathology Core for the heterotransplant model development. We received primary tumors from 6 individual patients and implanted these tumors into nude mice. Tumors implanted into the nude mice were observed for formation of the transplants. Tumors from 3 independent primary tumors grew to 100 to 150 mm<sup>3</sup>. Unfortunately, these tumors regressed over time. To address the issue, we are now modifying our procedures including: (1) reducing the time between the tumor harvested and the tumor implantation by coordinating surgery, surgical pathology, and tumor banking process; (2) selecting male mice instead of female mice to improve the success rate based on the experience from Dr. David Sidransky's laboratory at Johns Hopkins Medical School; and (3) using matrigel with the tissue to improve the tumor intake rate. A new postdoctoral fellow has been recruited to be the person primarily responsible for the project.

**Aim 5                      To determine a clinical utility of the molecular predictors.**

Any biomarker identified must be tested in clinical trials to determine its sensitivity and specificity. In addition, the assay should be tested for its ability to use small amounts of tissues or body fluids in clinical practice. The most sensitive and reliable clinical tests are antibody-based assays.

**Update**

The assay of clinical specimens proposed in this aim has not been designed in the early year of the grant period. Also the setback of the Iressa clinical trials due to the lack of enthusiasm has negatively affected the large Phase III clinical trial with Iressa. Therefore, we may have difficulty obtaining blood samples from the Phase III trial as planned in the original proposal.

**Conclusions**

Based on the limited data currently in hand, it is premature to draw meaningful conclusions.

**Recommended Changes for Future Work**

**Aims 1- 3:** In light of the recent data on *EGFR* mutation status and response to chemotherapy in lung cancer patients (Kobayashi et al., 2005; Paez et al., 2004), we have decided to determine the *EGFR* mutation status of the NSCLC tumors from our series of patients that will be included in Specific Aims 1-3. This will enable us to stratify patients based on *EGFR* mutation status and characterize NSCLC tumors of patients (usually nonsmokers) with and without *EGFR* mutations of the same histology. To this end, we plan to enroll at least 15 patients in each group.

**Aims 4- 5:** As discussed in the progress for Aim 4, we will implement modified procedures for heterotransplant model development. If necessary, we will invite technique personnel from either Dr. Sidransky's or Dr. Pere-Solar's group for trouble shooting. Alternatively, we may send our fellow to their laboratory to master the necessary methods.

To secure blood specimens for our proposed biomarker studies (Specific Aim 5), we will discuss the possibility of obtaining samples from patients enrolled in the Tarceva trial, an agent with a mechanism similar to Iressa that has been approved by FDA for lung cancer trials, or other patients treated in our clinical service. This should make feasible testing of our panel of biomarkers.

## **Core B: Biostatistics & Data Management Core**

(Core Director: J. Jack Lee, Ph.D.)

### **Core Goals**

1. To provide statistical design, sample size/power calculations, and integrated, comprehensive analysis for each basic science, pre-clinical, and clinical study.
2. To develop a data management system that provides tracking, quality control, and integration of clinical, pathological, and basic science data.
3. To provide statistical and data management support for genomic and imaging studies including microarray, proteomics, protein antibody array, and spiral CT.
4. To develop and adapt innovative statistical methods pertinent to biomarker-integrated translational lung cancer studies.
5. To generate statistical reports for all projects.
6. To collaborate and assist all project investigators in the publication of scientific results.

### **Update**

The Biostatistics and Data Management Core has continued to work actively with all the IMPACT Projects in their research efforts, especially in the area of biostatistical support and consulting in the clinical trial design, implementation, and analysis of experimental results.

In the first year of funding, our major effort was to provide statistical support in the design and revision of the clinical trials in Project 1 and the first development project. The clinical trial to be conducted in Project 1 is: "A Phase I/II Study of TARCEVA (erlotinib) in Combination with Chemoradiation in Patients with Stage III A/B Non-Small Cell Lung Cancer" (PI: Dr. Ritsuko R. Komaki). The clinical trial to be conducted in development project is: "Treatment of Malignant Pleural Effusion with ZD6474 a Novel Vascular Endothelial Growth Factor Receptor (VEGFR) and Epidermal Growth Factor Receptor (EGFR) Tyrosine Kinase Inhibitor" (PI: Dr. Amir Onn). Biostatistical Core was involved in the protocol design, submission and revision process. We have interacted with study PI, CRC, IRB, and regulatory agencies to address critiques and provide revisions. We are in the process of meeting with investigators and research coordinators to provide assistance in designing the Case Report Forms (CRFs) for these trials.

We have also worked closely with Dr. Reuben Lotan (Project 4 PI) on synergy studies of combination drug treatment in cell lines to determine whether the effect is synergistic, additive, or antagonistic. We have generalized the currently available methods, which require strong assumptions such that drug interaction follows the same pattern at all doses, to allow different mode and magnitude of drug interaction. It is possible that the combination may produce synergistic effects in certain dose ranges but additive or antagonistic in other dose ranges. The magnitude of drug interaction can also vary from dose to dose. We have developed two new statistical methods – one parametric generalized response surface model and one semi-

parametric model, which allow more general interaction patterns for the drug interaction and they ease the restriction of the existing methods. S-PLUS codes are developed and available free for download for other researchers to use (<http://biostatistics.mdanderson.org/SoftwareDownload/>).

In addition, we assisted several investigators in the statistical data analysis and interpretation on presentations given in the DOD Science Day for Lung Cancer Research held December 5, 2005.

We also provided assistance to Dr. Sonya W Song in designing the DoD Website.

### **Core C: Pathology Core and Development of New Lung Cancer Tissue Resources**

(Director: Ignacio Wistuba, M.D.)

The IMPACT interdisciplinary research proposal for studying targeted therapy of lung cancers requires extensive histopathological, immunohistochemical and molecular studies of cell and tissues specimens, which are assisted, coordinated or performed for the Pathology Core. One of the most important roles of the Pathology Core is to coordinate and provide professional technical services for proper procurement, storage and use of human and animal tissues, as well as technical assistance for immunohistochemical analysis.

#### **Aim 1 Develop and maintain repository of tissue, cell and serum specimens from patients with lung neoplasia per request of IMPACT project PIs**

We proposed to collect two groups of samples to serve needs of IMPACT projects: one is prospectively frozen and corresponding archival tumor and normal tissues from lung cancer patients undergoing surgery in our institution and enrolled in the clinical trials; the other is retrospectively frozen and corresponding archival tumors and normal tissues from lung cancer patients already banked in the Lung Cancer SPORE/MDACC Tissue Bank in which extensive clinical data including smoking history and survival information is available.

#### **Update**

For Project 1, no specimen was requested. Clinical trial has not started yet.

For Project 2, 4 of NSCLC cell lines with *EGFR* mutation and increased gene copy number were distributed to Dr. Gelovani's lab for EGFR imaging using a mouse model proposed in his project.

For Project 3, formalin-fixed and paraffin-embedded (FFPE) specimens from 408 NSCLCs were distributed to Dr. Pasqualini's lab for immunohistochemical optimization and analysis of antibodies against GRP78, IL-11R and Eph5A biomarkers.

For Project 4, FFPE specimens from 510 NSCLCs and 372 normal bronchial epithelia and preneoplastic lesions were distributed to Dr. Lotan's lab for immunohistochemical optimization and analysis of antibodies against bFGF and receptor FGFR1 and 2.

For Project 5, no specimen was requested.

For Project 6, frozen normal and tumor tissues from 40 NSCLCs were identified and distributed to Dr. Krahe's lab for gene expression and miRNA analyses. In addition, 10 lung adenocarcinomas with known *EGFR* mutation identified by the Core were distributed to Dr. Krahe's lab.

In the first year, nearly 300 lung cancer FFPE specimens were identified from MDACC Pathology files and their histology features were reviewed. Paraffin blocks were retrieved and banked. Histopathological data were entered in a database and relevant clinical information was obtained from the MDACC Thoracic Surgery and Epidemiology Departments.

In collaboration with our Neuropathology unit, we identified 220 lung cancer brain metastasis frozen specimens and their corresponding FFPE tissues. All cases were entered in a database and the relevant clinico-pathological data are under collection. Of importance, FFPE and paraffin blocks from 68 of matched primary NSCLCs and corresponding brain metastases were identified and banked in the Core, including 50 adenocarcinoma, 11 squamous cell carcinoma, 2 adenosquamous carcinoma, 2 sarcomatoid carcinoma, and 3 other histologies. A control group of 160 NSCLC cases with similar clinico-pathological features was also identified and banked. In addition, 150 primary NSCLCs and corresponding lymph node metastases were identified and histology review and banking process are in progress.

The Core will continue to identify and collect frozen and FFPE lung cancer specimens for future study.

## **Aim 2            Develop innovative tissue and cell reagents for the investigation and validation of the molecular endpoints relevant to individual projects**

### **Update**

We focused on three methodologies:

**1) Tissue and cell pellet microarrays (TMA):** In collaboration of the UTSWMC Lung Cancer SPORE project, cell pellets from 48 of NSCLCs, 20 of SCLCs and 4 of mesothelioma cell lines were fixed in formalin, embedded in paraffin and placed in TMAs using 1 mm diameter cores in duplicate. The types of TMAs relevant to the IMPACT include 408 of NSCLCs (adenocarcinoma and squamous cell carcinoma histology), 28 of SCLCs, 60 of sarcomatoid carcinomas, and 50 of bronchioloalveolar carcinomas (BAC). Using the specimens mentioned in Specific Aim 1, we have also prepared a TMA containing 68 of matched primary NSCLCs and corresponding brain metastases (Figure 1), which will be used in immunohistochemical and fluorescent *in situ* hybridization (FISH) analysis for projects 3, 4 and Pathology Core. All TMAs containing tumor

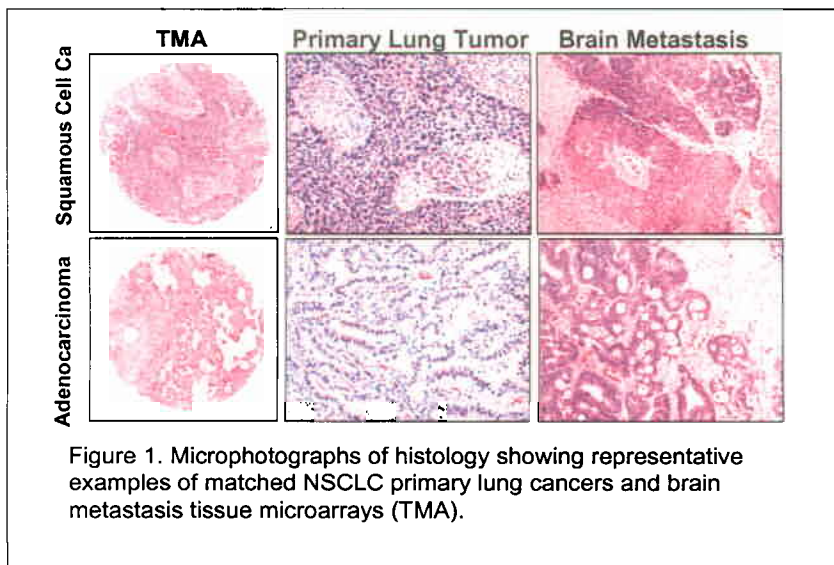


Figure 1. Microphotographs of histology showing representative examples of matched NSCLC primary lung cancers and brain metastasis tissue microarrays (TMA).

tissues were prepared in triplicates using 1 mm diameter cores obtained from central, intermediate and peripheral areas of the tumor. Histology sections of all TMAs were prepared and carefully reviewed.

**2) Establish short-term cultures and cell lines from tumor specimens.** This work has not been initiated yet because a dedicated cell culture facility is not available. The Core will move to a larger facility in March 2006 where a

dedicated cell culture room will be available for routine cell culture work.

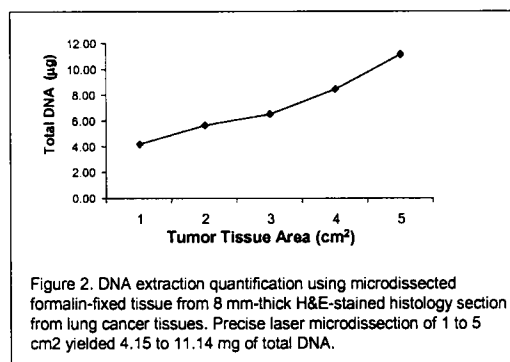
**3). Lung cancer heterotransplants using lung tumor samples.** In collaboration with Dr. Mao's lab (Project 6), we collected fresh NSCLC (adenocarcinoma and squamous cell carcinoma histology) specimens from 40 surgically resected tumors to establish tumor heterotransplant in nude mice. To increase the success rate of heterotransplants we have collected fresh tumor specimens from the operating room.

**Aim 3**            **Process human and animal cells and tissues for histopathological, immunohistochemical and molecular analyses per request of individual projects.**

#### Update

**Tissue Processing.** FFPE lung cancer tissues were processed and distributed for Projects 3 and 4. Frozen lung cancer tissues were processed and distributed for Project 6 (see Specific Aim 1). Processing (cutting and H&E staining) for histology evaluation and sectioning for immunohistochemistry were performed in about 550 paraffin-embedded blocks from lung cancer.

**Laser Capture Microdissection.** Recently, an automated laser capture microdissection equipment (Leica Microsystems, Bannockburn, IL) has been installed in the Core. Tissue microdissection for DNA extraction from FFPE was optimized and DNA was quantified. Precise laser microdissection of 8 mm-thick H&E-stained section (1 - 5 cm<sup>2</sup>) yielded 4.15 - 11.14 mg of total DNA (Figure 2).



**Aim 4**            **Perform and evaluate immunohistochemical analysis in human and animal cell and tissue specimens per request of individual projects.**

#### Update

**Immunohistochemistry (IHC).** Optimization of antibodies against 24 molecular markers of interest from individual projects were performed and summarized in Table 1 and Figures 5, 7 and 8. 22 of the markers were examined in the TMA (N=408 cases) and/or whole tissue sections (N=40 cases).

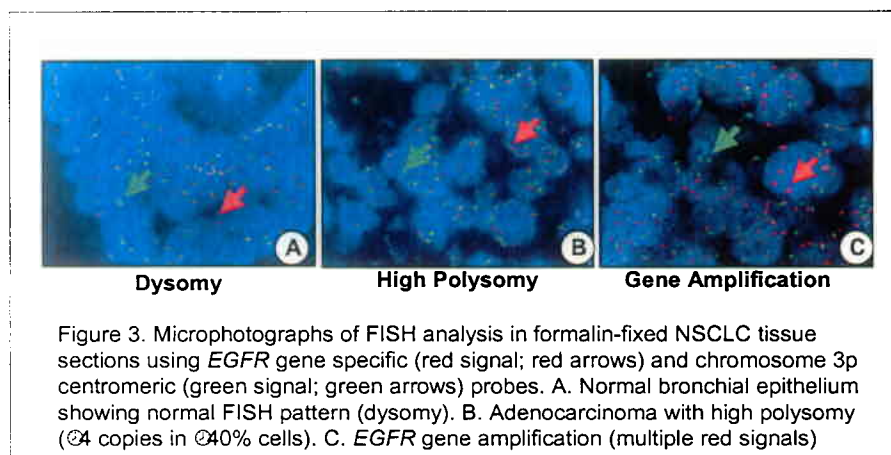


Table 1. Immunohistochemical markers optimized in the Pathology Core.

Marker	Project	Lung Cancer Specimens
EGFR	Project 2	TMA (N=408)
p-EGFR Tyr1086	Project 2	TMA (N=408)
p-EGFR Tyr1068	Project 2	TMA (N=408)
p-EGFR Tyr1173	Project 2	TMA (N=408)
p-EGFR Tyr845	Project 2	TMA (N=408)
Her2/Neu	Project 2	TMA (N=408)
Her3	Project 2	TMA (N=408)
p-Her3	Project 2	TMA (N=408)
Amphiregulin	Project 2	TMA (N=408)
Epiregulin	Project 2	TMA (N=408)
TGF- $\alpha$	Project 2	TMA (N=408)
EGF	Project 2	TMA (N=408)
VEGF	Project 2	TMA (N=408)
p-VEF	Project 2	TMA (N=408)
VEGFR	Project 2	TMA (N=408)
CD31	Project 2	Whole Sections (N=40)
CD34	Project 2	Whole Sections (N=40)
IL11-R	Project 3	TMA (N=408)/Whole Sections (N=40)
GRP78	Project 3	TMA (N=408)/Whole Sections (N=40)
bFGF	Project 4	TMA (N=408)/Preneoplasias (N=372)
FGFR1	Project 4	TMA (N=408)/Preneoplasias (N=372)
FGFR2	Project 4	TMA (N=408)/Preneoplasias (N=372)
Ki-67	Project 4	--
Cyclin D1	Project 5	--

**Image analysis evaluation of IHC.** Automated image analysis evaluation of nuclear, membrane and cytoplasmic IHC expression in tumor cells using Ariol<sup>R</sup> (Applied Imaging, San Jose, CA) instrument was optimized in the Core. Currently, validation of Ariol<sup>R</sup> (Applied Imaging, San Jose, CA) image analysis IHC reading is being conducted by 2 independent pathologists.

**Fluorescence *in situ* hybridization (FISH).** *EGFR* gene copy number analysis using FISH gene specific and chromosome 7 centromeric probes was optimized for FFPE tissue sections, including TMA specimens (Figure 3). *EGFR* gene FISH analysis of primary tumors (N=408 NSCLCs) and paired primary tumors and brain metastasis (N=68) is ongoing.



**Collaboration with research projects.** Optimization and examination of immunohistochemistry markers in collaboration with IMPACT research projects has been the most important activity of the Core during the first year. A pathologist Post-doctoral Fellow (M. Sun, M.D.) in the Core

performed this work by supervision of the Core Director (I. Wistuba, M.D.). The work is as follows:

**Project 2:** In collaboration with Dr. Herbst, co-PI, we performed a detailed analysis of the immunohistochemical expression of HER-family ligands and receptors in a large series of NSCLC using TMAs. The results will be presented at a minisymposium of the 97<sup>th</sup> Annual Meeting of AACR (Massarelli et al., 2006). A manuscript is in preparation.

We studied 359 surgically resected tumors, 219 adenocarcinoma, 20 bronchioloalveolar carcinoma (BAC) and 120 squamous cell carcinoma from patients with stage I-II-IIIa NSCLC. A semi-quantitative analysis of nuclear, cytoplasmic and membranous localization expression was performed for each marker as shown in Figure 4. We identified different patterns of correlation between ligands and receptors IHC expression (Figure 5). p-EGFR cytoplasmic and membranous overexpressions were found in cases of TGF- $\alpha$  ( $p < 0.0001$ ,  $p = 0.01$ ) or amphiregulin ( $p < 0.0001$ ,  $p = 0.008$ ) positive but not in EGF-positive cases. Lower expression of EGFR and p-EGFR nuclear was found in never smokers ( $p = 0.01$ ,  $p = 0.001$ ) and in adenocarcinoma and BAC histologies ( $p < 0.0001$ ,  $p = 0.01$ ). Her2/neu was overexpressed in adenocarcinoma and BAC ( $p = 0.0005$ ). Moderate/high levels of cytoplasmic and membranous p-EGFR were found in stage II-IIIa cases ( $p = 0.001$ ,  $p = 0.03$ ). In 14 (23.7%) of EGFR-mutated cases, high levels of Her2/neu were present ( $p = 0.02$ ) and the frequency of mutations was higher in never smokers ( $p = 0.026$ ). 10 (17.5%) of KRAS mutation –positive cases showed low levels of Her2/neu and nuclear p-EGFR ( $p = 0.02$ ,  $p = 0.03$ ; Table 2).

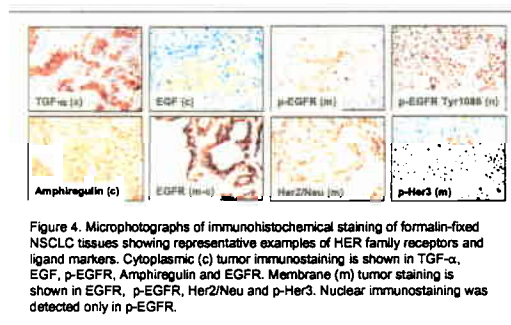


Figure 4. Microphotographs of immunohistochemical staining of formalin-fixed NSCLC tissues showing representative examples of HER family receptors and ligand markers. Cytoplasmic (c) tumor immunostaining is shown in TGF- $\alpha$ , EGF, p-EGFR, Amphiregulin and EGFR. Membrane (m) tumor staining is shown in EGFR, p-EGFR, Her2/Neu and p-Her3. Nuclear immunostaining was detected only in p-EGFR.

	AR <sup>c</sup>	TGF- $\alpha$ <sup>c</sup>	EGFR <sup>m</sup>	Her2 <sup>m</sup>	pEGFR <sup>n</sup>	pEGFR <sup>c</sup>	pEGFR <sup>m</sup>	pHer-3 <sup>m</sup>	pHer-3 <sup>c</sup>
EGF <sup>c</sup>	0.08 0.14	0.37 <0.0001	0.08 0.15	0.08 0.18	0.27 <0.0001	0.08 0.15	0.03 0.56	0.13 0.027	0.16 0.005
AR <sup>c</sup>	--	0.17 0.004	0.02 0.67	0.11 0.058	0.16 0.006	0.24 <0.0001	0.15 0.011	0.17 0.003	0.21 <0.0001
TGF- $\alpha$ <sup>c</sup>	--	--	0.11 0.061	0.02 0.75	0.1 0.099	0.24 <0.0001	0.15 0.008	0.18 0.002	0.26 <0.0001
EGFR <sup>m</sup>	--	--	--	-0.02 0.72	0.02 0.73	0.02 0.69	0.12 0.038	-0.03 0.65	0.04 0.55
Her2 <sup>m</sup>	--	--	--	--	-0.1 0.092	0.08 0.15	0.14 0.016	0.16 0.007	0.13 0.024
pEGFR <sup>n</sup>	--	--	--	--	--	0.22 <0.0001	0.00 0.94	-0.05 0.44	0.08 0.17
pEGFR <sup>c</sup>	--	--	--	--	--	--	0.76 <0.0001	0.31 <0.0001	0.574 <0.0001
pEGFR <sup>m</sup>	--	--	--	--	--	--	--	0.35 <0.0001	0.58 <0.0001
pHer-3 <sup>m</sup>	--	--	--	--	--	--	--	--	0.58 <0.0001

Figure 5. HER family pathway analysis in surgically resected NSCLCs (N=359) using TMA. The correlations between ligands and receptor markers immunohistochemical expression is shown. Red boxed indicates statistical significant correlation (c = cytoplasm; m = membrane; n = nuclear; AR = amphiregulin).

**Table 2. Correlations between biomarker IHC and KRAS and EGFR mutation for 59 adenocarcinoma cases.**

	EGF	AR	TGF- $\alpha$	EGFR	Her2/Neu	p-EGFR nuclear	PEGFR cyt	PEGFR mem	pHer3 cyt	pHer3 mem
KRAS mutation	↓ *0.74	↓ *0.74	↑ *0.92	↓ *0.44	↓ *0.02	↓ *0.03	↑ *0.59	= *0.99	↓ *0.37	↓ *0.15
EGFR mutation	↓ *0.70	↑ *0.70	↓ *0.50	↑ *0.49	↑ *0.03	↓ *0.29	↑ *0.92	↓ *0.78	↓ *0.58	↓ *0.91

AR=Amphiregulin; pEGFRcyt=pEGFRcytoplasmic; EGFRmem=pEGFRmembranous; \* Spearman rank correlation test. Arrows indicate positive (↑) and (↓) negative correlations.

With a median follow up of 3.4 years and a median recurrence-free survival of 4.7 years, independent of the age and stage, TGF- $\alpha$  overexpression demonstrated a favorable impact on recurrence-free (p=0.003, RR=0.35, 95%CI 0.17, 0.70) and overall survival (p=0.008, RR=0.32, 95%CI 0.14, 0.74). p-EGFR cytoplasmic overexpression resulted in reduced recurrence-free (p=0.005, RR=2.17, 95%CI 1.25, 3.74) and overall survival (p=0.001, RR=2.74, 95%CI 1.53, 4.94; Table 3).

**Table 3. Multivariate Cox proportional model on overall survival**

Characteristics	Parameter Estimate	*P-value	Relative risk	CI
Age ( $\geq 60$ vs. $<60$ )	1.30	$<0.0001$	3.67	1.92, 7.00
Clinical stage (II+III vs. I)	0.75	0.0004	2.12	1.40, 3.20
TGF $\alpha$ level				
Score= 1~80 vs. 0	-1.14	0.008	0.32	0.14, 0.74
Score= $>80$ vs. 0	-1.31	0.003	0.27	0.11, 0.64
pEGFR cytoplasm level				
Score= 101~200 vs. 0~100	0.48	0.05	1.61	0.99, 2.64
Score= $>200$ vs. 0~100	1.01	0.001	2.74	1.53, 4.94

\* Cox proportional hazards regression model; CI=Confidence Intervals

We have concluded that TGF- $\alpha$  and p-EGFR overexpression has a prognostic role (the first positive and the second negative) in stage I-IIIa NSCLC as indicators of recurrence-free and overall survival.

**Project 3.** In collaboration with Dr. Pasqualini, PI, we performed a semi-quantitative IHC analysis of cytoplasmic and nuclear expression of GRP78 and IL-11R markers in whole histology sections from FFPE NSCLC tissues (N=40; Table 4) and TMA specimens (N=360). For GRP78, high tumor cell cytoplasmic expression was detected in 7/20 (35%) and 3/20 (15%) adenocarcinomas and squamous cell carcinomas, respectively. Low-levels of GRP78 in tumor cell membrane were detected in 29/40 (72%) NSCLCs without differences among tumor histologies (Table 4). High-levels of IL-11R IHC expression were detected in the cytoplasm of 8/21 (20%) NSCLCs higher in squamous cell carcinoma (30%) compared to adenocarcinoma (10%; Table 4). Representative examples of GRP78 and IL-11R immunostaining in NSCLC are shown in Figure 6. Image analysis of IHC expression of both GRP78 and IL-11R in TMAs containing 408 of NSCLCs using Ariol<sup>R</sup> (Applied Imaging, San Jose, CA) instrument is ongoing.

**Table 4. Immunohistochemical expression of GRP78 and IL-11R in 40 NSCLC formalin-fixed NSCLCs.**

Tumor Histology	Number of Cases (N)	GRP78				IL11-R	
		Cytoplasm		Membrane		Cytoplasm	
		High	Intermediate-Low	Positive	Negative	High	Intermediate-Low
Adenocarcinoma	20	7 (35%)	13 (65%)	15 (75%)	5 (25%)	2 (10%)	18 (90%)
Squamous Cell Ca	20	3 (15%)	17 (85%)	14 (70%)	6 (30%)	6 (30%)	14 (70%)
Total	40	10 (25%)	30 (75%)	29 (72%)	11 (28%)	8 (20%)	32 (80%)



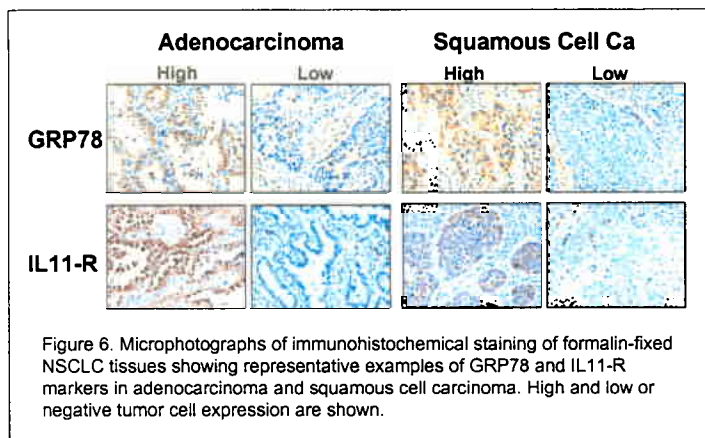


Figure 6. Microphotographs of immunohistochemical staining of formalin-fixed NSCLC tissues showing representative examples of GRP78 and IL11-R markers in adenocarcinoma and squamous cell carcinoma. High and low or negative tumor cell expression are shown.

**Project 4.** In collaboration with Drs. Reuben Lotan, PI and C. Behrens, IHC expression analysis of bFGF and receptors FGFR-1 and -2 was performed in 102 NSCLC specimens and 372 normal bronchial epithelia and lung cancer preneoplastic lesions, including 56 adenocarcinomas, 46 squamous cell carcinomas, 71 normal bronchial epithelia, 128 bronchial hyperplasias, 23 squamous metaplasias, 78 squamous dysplasias, and 72 atypical adenomatous hyperplasias (AAH). A semi-quantitative analysis of cytoplasmic and nuclear IHC expression was performed (Figure 7). Adenocarcinoma and squamous cell carcinoma specimens demonstrated higher cytoplasmic expression of bFGF, FGFR-1 and FGFR-2 compared to normal epithelia ( $P < 0.0001$ ). Comparing nuclear expression between tumor and NBE specimens we found that while FGFR-2 was increased ( $P < 0.0001$ ) and FGFR-1 was reduced ( $P = 0.012$  to  $< 0.0001$ ) in both tumor types, bFGF expression was increased only in adenocarcinoma ( $P = 0.0003$ ). The cytoplasmic overexpression of bFGF and its receptors in dysplastic squamous lesions indicates that this signaling pathway may play an important role in squamous cell carcinoma of early lung pathogenesis. In summary, we identified different

expression patterns of bFGF and receptors in cytoplasm and nuclear cell compartments in normal and premalignant lung tissues.

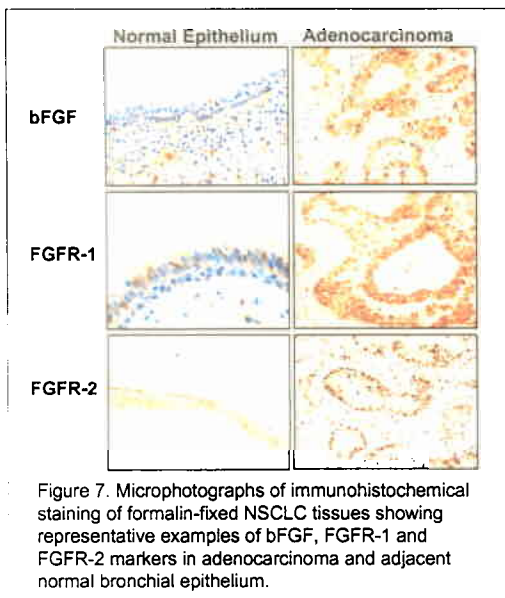


Figure 7. Microphotographs of immunohistochemical staining of formalin-fixed NSCLC tissues showing representative examples of bFGF, FGFR-1 and FGFR-2 markers in adenocarcinoma and adjacent normal bronchial epithelium.

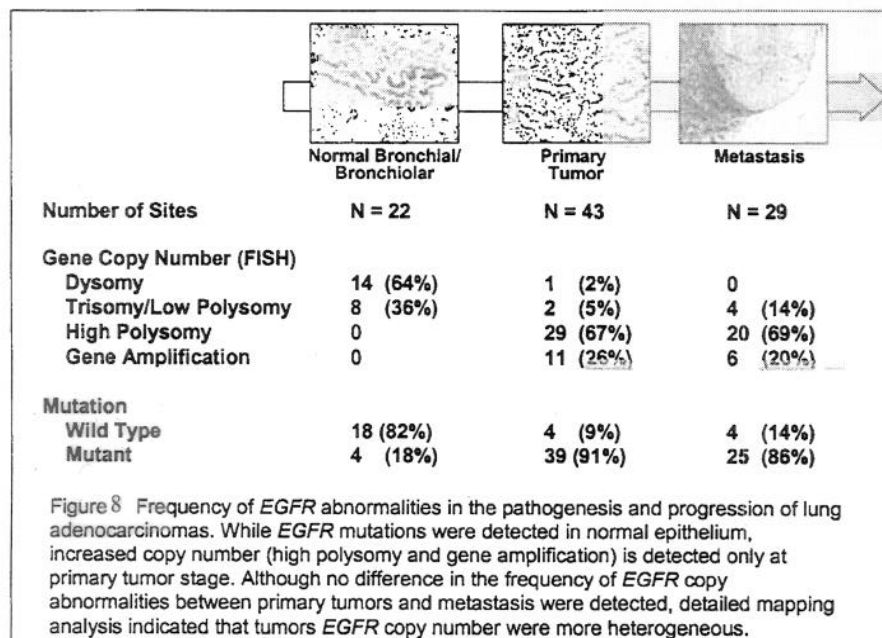
**Additional IMPACT-related research proposed based on recent findings by the Core.** The Core has performed independent research activities to better characterize the *EGFR* molecular abnormalities involved in the pathogenesis and progression of lung cancer. These results will be integrated into the ongoing research activities in Projects 1 and 2 and presented in the 97<sup>th</sup> Annual Meeting of AACR (Tang et al, 2006). A manuscript is in preparation. Part of this work has been performed in collaboration with M. Varella-Garcia, Ph.D., Colorado Cancer Center, Denver, Co.

**Aim:** In late 2004 to 2005, *EGFR* tyrosine kinase (TK) domain mutations, increased gene copy number and protein overexpression were found to be associated with lung cancer pathogenesis and correlated with response to *EGFR* TK inhibitors in lung adenocarcinoma. However, the sequence of these molecularly abnormal events in the pathogenesis and progression of lung adenocarcinoma is unknown. To elucidate this question, we performed a detailed mapping analysis correlating in the same tissue sites *EGFR* mutation, gene copy number and protein

immunohistochemistry (IHC) expression in 94 formalin-fixed tissue sites comprising normal bronchial/bronchiolar epithelium (NBE; N=22), primary tumor (PT; N=43) and metastasis (MT; N=29) histologies obtained from 9 surgically resected *EGFR* mutant (exons 19 and 21) lung adenocarcinomas.

**Methodology:** *EGFR* mutation analysis was performed by PCR and direct sequencing from DNA extracted from precisely microdissected tissues. *EGFR* gene copy number analysis was performed using FISH, and high levels of polysomy and gene amplification were considered as increased copy number. Semi-quantitative IHC expression analysis of cytoplasmic and cell membrane *EGFR* and phosphorylated *EGFR* (p-*EGFR*) was performed.

**Results:** *EGFR* mutation was found in 18% (4/22) NBE, 91% (39/43) PT and 86% (25/29) MT sites. Low genomic gain was found in 8 NBE sites (37%), but increased copy number was not detected. Of interest, 4 of *EGFR* mutant NBE sites exhibited normal gene copy number. No difference in the frequency of increased *EGFR* copy number was found comparing PT (39/43, 93%) and MT (25/29, 86%) sites. *EGFR* mutation frequency (89% vs. 41%;  $P < 0.0000$ ) and mutant to wild-type ratio mean (1.04 vs. 0.49,  $P < 0.0001$ ) in the sequencing chromatograms were significantly higher in tissue sites with increased copy number than areas with normal or low genomic gain. *EGFR* mutation heterogeneity, with two or more mutant genotypes in the same tumor case, was found in 4 of 9 (44%) PT cases, and this phenomenon was not observed in corresponding MTs. *EGFR* copy number heterogeneity was more frequent in PT than MT; however, significant copy number progression from PT to MT was not observed. Although no correlation was found between *EGFR* IHC and *EGFR* mutation or copy number status, significantly higher levels of *EGFR* and p-*EGFR* IHC expression were detected in mutant MT compared to PT sites ( $P = 0.005$  to  $< 0.0001$ ) (Figure 8).



**Summary:** Our findings indicate that *EGFR* mutation precedes genomic gain in the sequential pathogenesis of lung adenocarcinoma. In tumor specimens, there was strong correlation between *EGFR* mutation and increased copy number. The heterogeneity of *EGFR* mutation and gene copy number in primary tumor, but not in metastasis, and the increased expression of total

and p-EGFR IHC in metastasis sites are probably associated with tumor progression and could have clinical implications when these abnormalities are searched in small clinical specimens.

## Conclusion

The Core has successfully fulfilled the goals proposed for the first year. The Pathology Core has performed a number of histopathological, immunohistochemical and molecular studies in large series of lung cancer tissue specimens, assisted most IMPACT research projects, and managed to conduct additional research activities that were fully integrated with some research projects of IMPACT.

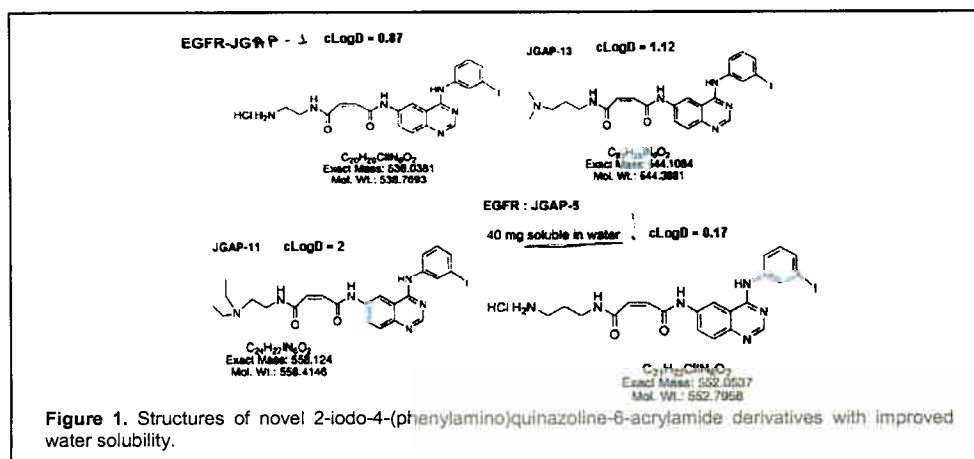
## Core D: Imaging Core: Provide Imaging Support for IMPACT Projects

(PI and co-PI: Juri Gelovani, M.D., Ph.D.; Chun Li, Ph.D.)

In the past year, the Imaging Core provided support for several IMPACT projects described below.

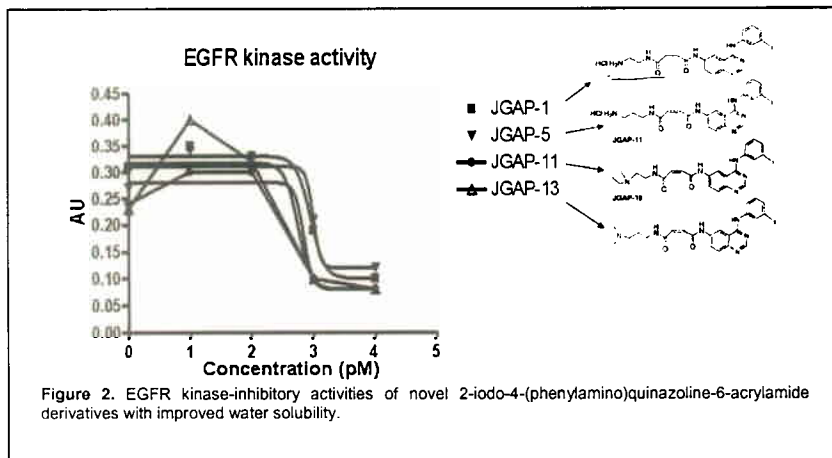
**Project 2 - Aim 1A:** To synthesize novel rationally designed precursors for radiolabeling of tracers for PET imaging of EGFR expression and activity.

As reported in Project 2, we helped synthesize and investigate *in vitro* a number of different morpholino-derivatives of 2-iodo-4-(phenylamino)quinazoline-6-acrylamide (IPQA) derivatives with improved water solubility, which have been selected by additional *in silico* modeling of their structure-activity relationships with active EGFR kinase. Among these compounds, we narrowed the initial library of compounds to 4 optimized lead compounds termed JGAP 1, 5, 11, and 13 (Figure 1). It is noteworthy that the compound JGAP-5 is soluble in water.



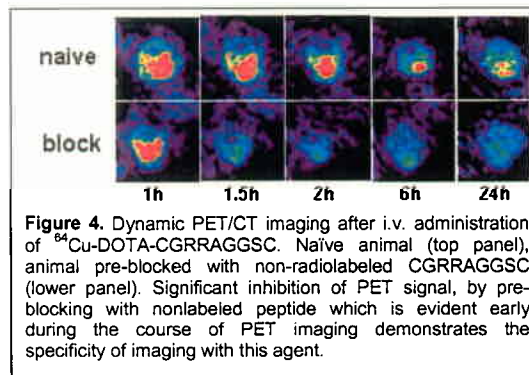
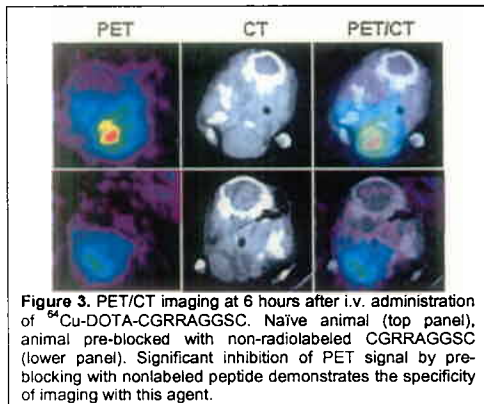
**Project 2- Aim 1C:** To assess biochemical characteristics and conduct *in vitro* radiotracer accumulation studies in tumor cells with different EGFR status

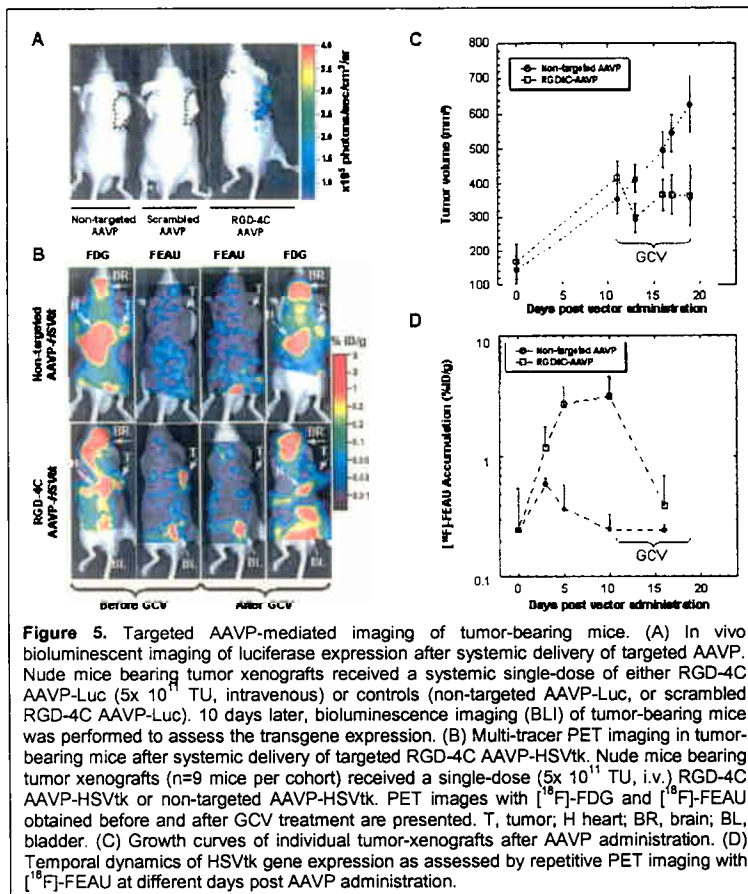
Those new compounds mentioned above were assessed *in vitro* for their ability to inhibit recombinant EGFR kinase-mediated tyrosine phosphorylation of an EGFR-specific peptide (enzyme inhibition assay). All four compounds demonstrated very low nM and sub-nM IC<sub>50</sub> for EGFR kinase (Figure 2).



### Project 3: Targeting Peptide-based systemic delivery of therapeutic and imaging agents to lung cancer

We helped establish routine synthesis of [ $^{18}\text{F}$ ]FEAU and synthesis and  $^{111}\text{In}$  and  $^{64}\text{Cu}$  radiolabeling of GRP78-specific cyclic nanopeptide CGRRAGGSC for imaging studies and performed pilot imaging studies with  $^{64}\text{Cu}$ -DOTA-CGRRAGGSC PET/CT in 6 animals (Figures 3 and 4). Also, we have conducted pilot studies with a model AAVP expressing RGD4C targeting ligands to  $\alpha\text{V}\beta\text{III}$  integrins expressed on tumor neovasculature (Figure 5).





#### Project 4: Inhibition of bFGF signaling for lung cancer therapy

The Imaging Core has generated some retrovirally transduced GFP-expressing PC14GL, H441GL, H1975, and H3255 NSCLC cells and developed several bioluminescently and fluorescently imageable orthotopic tumor models to meet the needs of Project 4

#### DRP-1: Treatment of Malignant Pleural Effusion with ZD6474, a Novel VEGFR and EGFR TK Inhibitor

(PI and co-PI: Amir Onn, M.D., Roy Herbst, M.D., Ph.D.)

- Aim 1**            **To determine clinical effects of ZD6474**
- Aim 2**            **To investigate biological correlates**
- Aim 3**            **To investigate radiographic correlates**
- Aim 4**            **To assess quality of life**

This study will examine the effect of ZD6474 therapy on malignant pleural effusion which is a common and debilitating clinical problem in our practice. It is an innovative concept for patient care and we are excited about this study.



Initially, AstraZeneca approved the study prior to submission to the DoD but later the company withdrew their support. We continued discussions with them and a couple of months ago we received a renewal of the approval. In the interim, we improved the design of the study. It is now a randomized placebo controlled trial to study the effect of ZD6474 on NSCLC-related pleural effusion. AstraZeneca has approved the revised protocol (see Appendix C) and committed to supply the drug and the placebo pills. We then submitted the protocol to our Clinical Research Committee for review and approval. Once it is approved by our IRB, we will submit the protocol to the DoD. We hope to begin patient accrual in spring 2006.

## DRP-2: TALK - Teens and Young Adults Acquiring Lung Cancer Knowledge

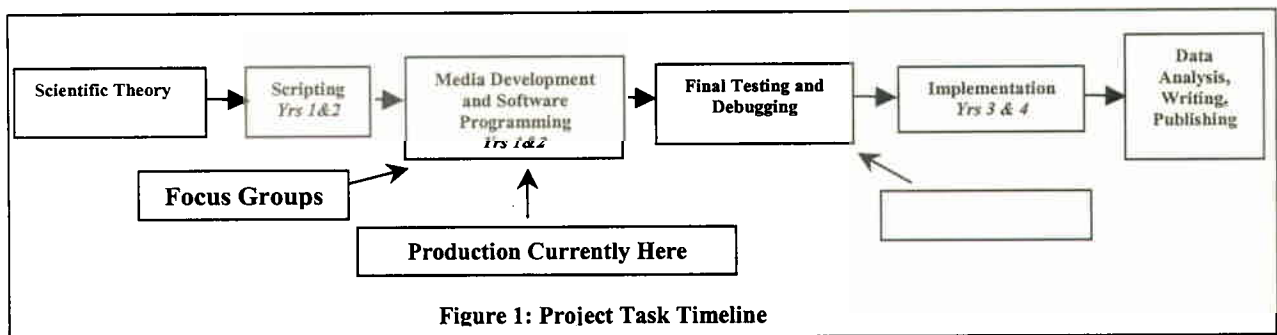
(PI: Alexander V. Prokhorov, M. D., Ph.D.)

Available health education programs often fail to adequately address the mechanisms of the causal role of cigarette smoking in development of lung cancer. They do not consistently employ state-of-the-art methods and modern computer technologies that hold a tremendous appeal to contemporary youth. Project TALK will assist in making major advances in lung cancer education and prevention among youth.

We will create an interactive, multimedia CD-ROM based on the transtheoretical model of change and knowledge pertinent to biologic and behavioral aspects of nicotine addiction and evaluate the effectiveness of the CD-ROM cigarette smoking prevention and cessation in adolescents and young adults, aged 15-24 years in Houston, Texas. The study will use a paired cohort design in which the individuals are the unit of design, allocation, and analysis. Young participants will be randomized into two conditions: (a) tobacco cessation/prevention CD-ROM intervention, or (b) the tobacco cessation/prevention pamphlet control group. Study participants will be evaluated at baseline, seven days after the intervention, and at 6 months.

### Update

In the first year, we were devoted to designing the project task timeline (Figure 1) that includes multiple time sensitive tasks ensuring a quality interactive “gaming” product. The first task was to design the development team. The Project TALK team includes Alexander V. Prokhorov, M.D., Ph.D., Ellen R. Gritz, Ph.D., Mario Luca, M.S., Nancy Stancic Luca, Ph.D, and Kentya Ford, Ph.D., in cooperation with the contracted Radiant Creative Group, is developing the overall concept. Radiant Creative Group is developing the overall platform and look/feel of the interactive program outlined in detail below. Project TALK dialog scripts, drawings, and module components may be found in Appendices D-I.



The early development period is conceptual in nature. The TALK team, based on the scientific underpinnings of the project, agreed upon the layout of the program: 1) look/feel, 2) development strategy, 3) videos to be used, 4) other media components, and 5) the user tracks as described below.

### **1) Look & Feel**

Our previous studies have shown that users in the TALK age range prefer a more realistic look and feel to the materials. Also, studies of game design show that young adult users prefer an interactive and immersive environment. Radiant Creative Group is creating the user interface to appeal to our age group, based on previous work and published literature. Since the user only has about 30 minutes per session the program must be clear and intuitive to maximize learning time. Evidence used to support the youth gaming demographics can be found in Appendix F.

### **2) Development Strategy**

To maximize our project's cost-efficiency, we will emphasize reusability of program components. A program "template" is being developed for the first user track with content that is easily switched out allowing for ease in creating the remaining tracks. One of the goals of the study is to keep programming time and costs low by making the development process more efficient. The program is being written in Flash MX and authored to run off of a CD-ROM. The introduction Staging Template can be found in Appendix G. Proposed GUIs (Graphical User Interface) are located in Appendix H.

### **3) Videos**

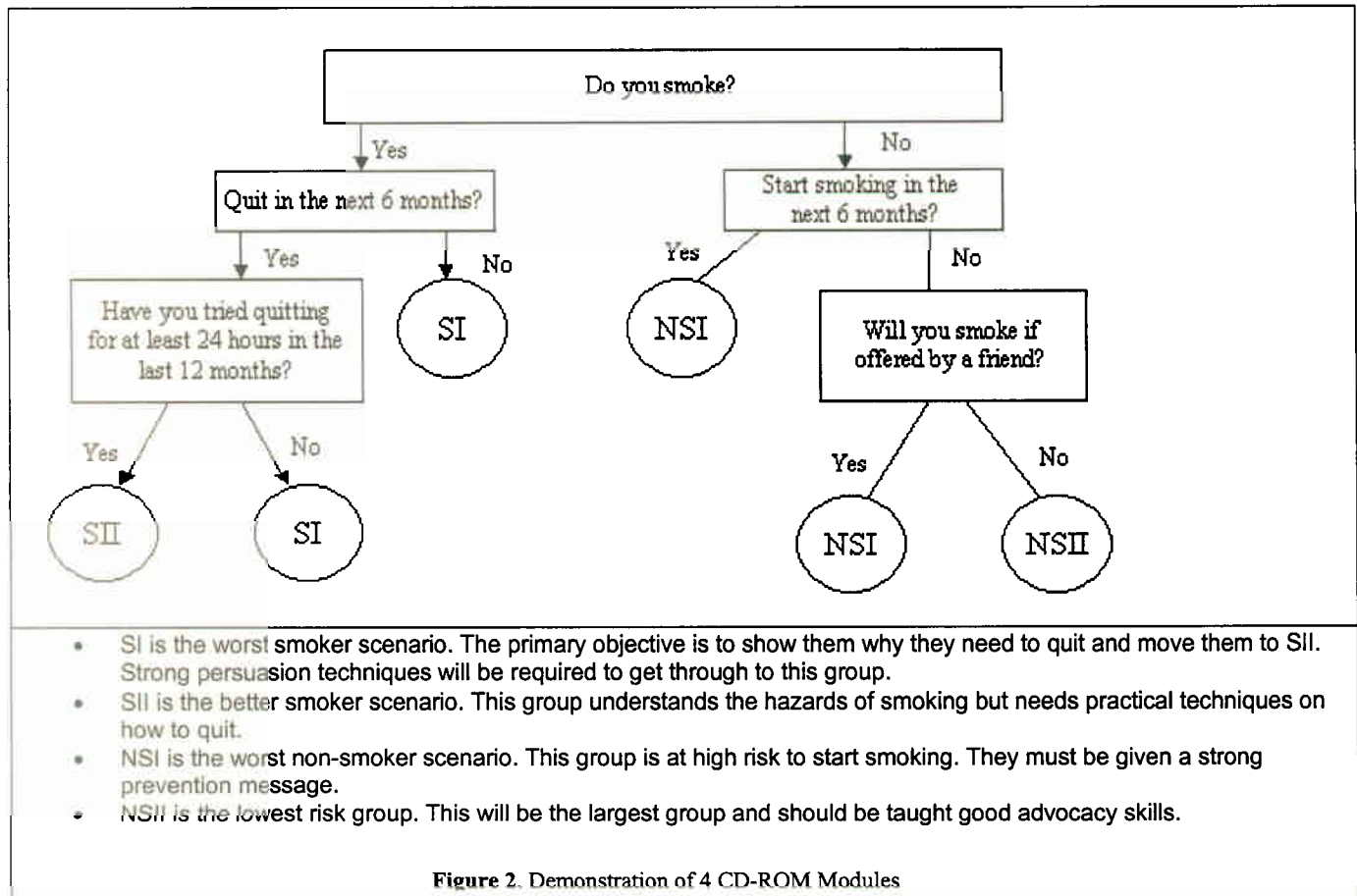
To keep video production costs within reasonable limits, videotaping and editing will be done using our in-house equipment without compromising quality. A free resource we have tapped is the **Truth®** campaigns videos created by the Legacy Foundation to which the co-investigator Dr. Ellen R. Gritz has access. We have approval to create our own version of the **Truth®** campaign, the largest national youth-focused anti-tobacco education campaign ever designed to engage teens by exposing Big Tobacco's marketing and manufacturing practices, as well as highlighting the death toll of tobacco in relevant and innovative ways. The rating of the most preferred **Truth®** ads can be found in Appendix F.

### **4) Other Media**

The Project TALK team is examining other types of media content to use in the program. Since the videos are passive, the other media components will need to be more interactive. We are creating an immersive, "other world" environment in which the user may be more responsive to the educational materials presented.

### **5) User Modules**

The CD-ROM will include 4 modules, each approximately 30 minutes in length. These modules are determined as shown in Figure 2. Each user module has three tracks: Environment, Social, and Health.



Accompanying the track grid are key learning points for both smoker and non-smoker, and gender specific points (Figure 3). Finally, other tobacco-related points are also included. These points will all be incorporated into the scripts and graphics built to support TALK.

Figure 3. TALK Key Learning Points	
<b>Smokers:</b>	<ul style="list-style-type: none"> <li>• Health Consequences – long-term and short-term</li> <li>• Tobacco addiction – Young people do not understand what addiction is all about. They believe smoking reduces their stress but actually it adds to the normal stress in their lives.</li> <li>• Financial consequences. Compute costs, etc.</li> </ul>
<b>Non-smokers:</b>	<ul style="list-style-type: none"> <li>• Strong prevention message. Emphasize that a very small percentage of people who start smoking are able to quit (3%-4%/year quit).</li> <li>• Teach advocacy skills so they can approach and encourage family and peers to stop smoking.</li> <li>• Teach that smokers are not hostile to those who want to help them and even though they may not openly acknowledge it they will still appreciate the effort.</li> </ul>
<b>Gender specific:</b>	<ul style="list-style-type: none"> <li>• Consequences of smoking during and after pregnancy.               <ul style="list-style-type: none"> <li>◦ Mental retardation</li> <li>◦ ADD</li> <li>◦ Depression</li> <li>◦ Respiratory infections</li> <li>◦ ASTHMA (growing in Houston)</li> </ul> </li> <li>• Smoking and fertility</li> <li>• Smoking and looks</li> </ul>
<b>Other:</b>	<ul style="list-style-type: none"> <li>• Depression and smoking</li> <li>• Lung Cancer – long-term consequences-that are difficult to impress on young people</li> <li>• Ethnicity – Does our small budget allow any way to make the program bilingual?</li> </ul>

### FOCUS GROUP:

During the last month of Year 1, we have organized a focus group of 10 persons, aged 18-24 in Houston, to review the concept, GUI, Staging Template, drawings and scripts for appropriateness and appeal to our targeted audience.

### Future Work for YEAR 2:

During Year 2, all four TALK modules will be completed, tested, revised and launched at agreed upon locations. As the modules are being finalized, TALK staff will be working with identified organizations that expressed interest in participating in the study. Already in Year 1, youth centers, public housing entities, and shopping centers have been mapped and will be introduced to Project TALK and recruited to participate. We anticipate the program launch date to be January 2007, the final month of Year 2 with full implementation during Years 3 and 4.

**TALK Timeline for year 2**

Due Date	Task	Details/Specifics
March 2006	Media Production	Smokers Modules: I: Smokers not willing to quit Precontemplation II: Smokers willing to quit Contemplation, Preparation, Action
April 2006	Media Production	Non-Smokers Modules: I: Non-smokers at high risk to start smoking II: Non-smokers not at risk, but advocates for others
May 2006	Complete Module Testing	Smokers Modules: I: Smokers not willing to quit Precontemplation
June 2006	Complete Module Testing	Smokers Modules: II: Smokers willing to quit Contemplation, Preparation, Action
July 2006	Complete Module Testing	Non-Smokers Modules: I: Non-smokers at high risk to start smoking
August 2006	Complete Module Testing	Non-Smokers Modules: II: Non-smokers not at risk, but advocates for others
September 2006	Completed	All Modules
October 2006	Focus Group Testing	All Modules
November 2006	Revisions based on Focus Group Testing	All Modules
December 2006	Revisions and Debugging	All Modules
January 2007 to June 2008 (Yrs. 3 and 4)	Implementation and Data Collection: N = 200 (100/condition)	Full Program and CD counterpart

### Conclusions

The project has been proceeding well as planned and on timeline.

## **KEY RESEARCH ACCOMPLISHMENTS**

### **Project 1: Targeting epidermal growth factor receptor signaling to enhance response of lung cancer to therapeutic radiation.**

- Showed that gefitinib radiosensitizes some NSCLC cell lines *in vitro* but protects others including normal cells. These lines with different EGFR status form a model for further study of the molecular mechanism of EGFR- governed radioresponse of NSCLC cells.
- Showed the ability of gefitinib to either radiosensitize or radioprotect cells correlates with pERK1/2 activation. Thus, pERK is a target for future studies.
- Showed the correlation of gefitinib-suppressed DNA repair with its radiosensitizing effects.
- Showed that erlotinib, another EGFR inhibitor, also radiosensitizes NSCLC cells *in vitro*, validating the combination trial proposed in Specific Aim 1.
- Showed that the combination of gefitinib and Mek inhibitors has an additive effect on radioresistant cells.
- Showed that a novel Raf-kinase inhibitor, Sorafinib, radiosensitizes NSCLC cells.
- Submitted a phase I/II clinical trial testing the combination of erlotinib and chemoradiation for the treatment of NSCLC.

### **Project 2: Molecular Imaging of EGFR Expression and Activity in Targeting Therapy of Lung Cancer**

- Produced novel 2-iodo-4-(phenylamino)quinazoline-6-acrylamide (IPQA) derivatives (JGAP-5 and JGAP-11) with improved water solubility.
- Showed the correlation of the uptake and retention of [ $^{124}\text{I}$ ]mIPQA with EGFR status of NSCLC cells, consistent with sensitivity of NSCLC cells to gefitinib and supporting our hypothesis that imaging with [ $^{124}\text{I}$ ]IPQA derivatives should allow for identification of tumors with increased EGFR signaling.
- Found that the accumulation of [ $^{124}\text{I}$ ]mIPQA can be observed in normal tissue structures that express highly active EGFRs (i.e., hair follicle cells) that are currently used as surrogate biomarkers of EGFR activity/inhibition and represent biological proof of the mechanisms of imaging of EGFR activity with [ $^{124}\text{I}$ ]mIPQA.
- Demonstrated that PET with  $^{18}\text{F}$ -FMAU has higher sensitivity for the detection of NSCLCs as compared to  $^{18}\text{F}$ -FDG. The lack of decrease in  $^{18}\text{F}$ -FDG and  $^{18}\text{F}$ -FMAU uptake early after initiation of gefitinib therapy is predictive of tumor resistance. However, in some gefitinib sensitive NSCLCs the assessment of early treatment responses by PET may not be feasible because of very low pre-treatment levels of uptake of both  $^{18}\text{F}$ -FDG and  $^{18}\text{F}$ -FMAU.

### **Project 3: Targeted Peptide-based Systemic Delivery of Therapeutic and Imaging Agents to Lung Cancer**

- Showed that tumor cells can be grouped by profiles of their phage display-derived peptide ligands directed to differentially expressed cell surface receptors.
- Identified and validated peptide ligands recognizing lung cancer-associated molecular targets. These ligands have been validated *in vivo* and *ex vivo* based on their ability to selectively target lung tumors.
- Validated candidate receptors (EGFR and EphA5) targeted by selected tumor-homing peptide motifs by a combination of tissue microarray-based technology and IHC.
- Linked targeting peptides homing to these receptors to proapoptotic agents to induce apoptosis following specific receptor-mediated internalization.

### **Project 4: Inhibition of bFGF Signaling for Lung Cancer Therapy**

- Found that bFGF can stimulate the growth of immortalized mouse endothelial cells that can be reversed by bFGF inhibitor TMPP *in vitro*.
- Identified different expression patterns of bFGF and receptors in cytoplasm and nuclear cell



compartments in normal and premalignant lung tissues.

- Observed that the cytoplasmic overexpression of bFGF and its receptors occurs not only in NSCLC tumor specimens but also in dysplastic squamous lesions, suggesting that the bFGF/FGFR signaling pathway(s) may play an important role already at early stages of NSCLC carcinogenesis.

#### **Project 5: Targeting mTOR and Ras signaling pathways for lung cancer therapy**

- Demonstrated that mTOR inhibitors are effective in inhibiting the growth of NSCLC cells. PTEN mutations or p-Akt levels in NSCLC cells may not predict cellular response to mTOR inhibitors.
- First showed that mTOR inhibitors activate Akt and eIF4E survival pathways while inhibiting mTOR signaling in human lung and other cancer types.
- Demonstrated that co-targeting of mTOR and PI3K/Akt signaling pathways exhibits enhanced growth-inhibitory effect of lung cancer cells.

#### **Project 6: Identification and Evaluation of Molecular Markers in Non-Small Cell Lung Cancer (NSCLC)**

- Global expression analysis of an initial group of lung adeno- and squamous cell carcinomas has been completed. Corresponding SNP (DNA) analysis will follow after additional samples are acquired.
- Methylation analysis of approximately half of the proposed samples has been completed for 8 genes. Aberrant methylation of several genes has been observed in the samples.

#### **Pathology Core:**

- Identified a large series of NSCLC primary tumors specimens and their corresponding brain and lymph node metastases and prepared NSCLC metastasis tissue microarrays (TMA) including 68 matched lung cancer primary tumors and brain metastases.
- Optimized 24 IHC markers for some IMPACT research projects, of which 22 were validated in tumor TMAs and whole histology sections.
- In collaboration with Project 1, we have demonstrated that TGF- $\alpha$  and p-EGFR IHC over-expression has a prognostic role (the first positive and the second negative) in stage I-IIIa NSCLC as indicators of recurrence-free and overall survival.
- Found that *EGFR* mutation precedes genomic gain in the sequential pathogenesis of lung adenocarcinoma.
- Found higher heterogeneity for increased *EGFR* gene copy number in primary lung adenocarcinomas compared to metastasis, which may be associated with tumor progression that can be validated using small clinical specimens.

#### **Imaging Core:**

- Produced novel 2-iodo-4-(phenylamino)quinazoline-6-acrylamide (IPQA) derivatives (JGAP-5 and JGAP-11) with improved water solubility (as described above);
- Routinely produced [ $^{124}\text{I}$ ]mIPQA for studies in Aim 2 of Project 2;
- Performed all multi-modality imaging studies described in Project 2I;
- Established routine synthesis of [ $^{18}\text{F}$ ]FEAU for Project 3;
- Established synthesis and  $^{111}\text{In}$  and  $^{64}\text{Cu}$  radiolabeling of GRP78-specific cyclic nanopetide CGRRAGGSC for imaging studies in Project III and performed pilot imaging studies with  $^{64}\text{Cu}$ -DOTA-CGRRAGGSC PET/CT in 6 animals for Project 3.
- Conducted pilot studies with a model AAVP expressing RGD4C targeting ligands to  $\alpha\text{V}\beta\text{III}$  integrins expressed on tumor neovasculature.
- Generated retrovirally transduced GFP-expressing PC14GL, H441GL, H1975, and H3255 NSCLC cells and developed several bioluminescently and fluorescently imageable orthotopic tumor models for the Project 4.

### **DRP-1: Treatment of Malignant Pleural Effusion with ZD6474**

- The project will begin in spring 2006 when all approvals have been received.

### **DRP-2: TALK**

- Designed Project TALK design team
- Developed the overall platform for the Project TALK interactive program including 1) look/feel, 2) development strategy, 3) videos to be used, 4) other media components, and 5) the user tracks
- Developed Project TALK avatar models.
- Developed Project TALK operating room artwork.
- Developed Project TALK hospital administrative room artwork (ready for Flash).
- Created Project TALK database animation and storyboards.
- Organized Project TALK focus group of 10 persons, aged 18-24 in Houston, to review the concept, GUI, Staging Template, drawings and scripts for appropriateness and appeal to our targeted audience.

## **REPORTABLE OUTCOMES**

### **Articles**

1. **Sun S-Y**, Rosenberg LM, Wang X, Zhou Z, Yue P, Fu H, **Khuri FR**. Activation of Akt and eIF4E survival pathways by rapamycin-mediated mTOR inhibition. *Cancer Res (Priority Report)*, 65:7052-8, 2005.
2. Kolonin MG, Bover L, Sun J, Zurita AJ, Do KA, Lahdenranta J, Cardo-Vila M, Giordano RJ, Jaalouk DE, Ozawa MG, Moya CA, Souza GR, Staquicini FI, Kunyiasu A, Scudiero DA, Holbeck SI, Sausville EA, Arap W, **Pasqualini Renata**. Ligand-directed surface profiling of human cancer cells with combinatorial peptide libraries. *Cancer Res (Priority Report)*, 66: 34-40, 2006.
3. Hajitou A, Trepel M, Lilly CE, Soghomonyan S, Alauddin MM, Marini III FC, Restel BH, Ozawa MG, Moya CA, Rangel R, Sun Y, Zaoui K, Schmidt M, Kalle CV, Weitzman MD, Gelovani JG, Pasqualini R, **Arap W**. A hybrid vector for ligand-directed tumor targeting and molecular imaging. *Cell* (in press), 2006.

### **Abstracts**

1. Erminia Massarelli, Xian Zhou, Natalie Ozburn, Marie Wislez, Benjamin N. Bekele, Jack A. Roth, Michael O'Reilly, Waun Ki Hong, John Kurie, Roy S. Herbst, **Ignacio I. Wistuba**. TGF- $\alpha$  and phosphorylated EGFR protein levels impact the survival of patients with stage I-III A Non Small Cell Lung Cancer. 97<sup>th</sup> AACR meeting (Oral presentation at minisymposium), 2006.
2. Ximing Tang, Marileila Varella-Garcia, Ana Carolina Xavier, Xiaoqing Bi, Natalie Ozburn, Waun Ki Hong, **Ignacio I. Wistuba**. Analysis of EGFR abnormalities in the sequential pathogenesis and progression of lung adenocarcinoma. 97<sup>th</sup> AACR Annual Meeting. 2006.
3. Laura Paternoster, Anupama Munshi, **Raymond E. Meyn**. Role of MDM2 in DNA repair. The 97<sup>th</sup> AACR annual meeting. 2006.
4. Anupama Munshi, Toshimitsu Tanaka, Marvette L. Hobbs, **Raymond E. Meyn**. Radiosensitization of human melanoma cells by sorafenib (BAY 43-9006), a multi-kinase inhibitor. The 97<sup>th</sup> AACR Annual Meeting. 2006.
5. Behrens C, Wistuba II, Feng L, Lee JJ, Hong WK, and **Lotan R**. Expression of fibroblast growth factor and its receptors in premalignant and malignant human lung tissues. AACR, 2006 (Oral presentation)
6. **Alexander V. Prokhorov**, Ellen R. Gritz, Nancy Stancic Luca, **Salma Marani**, Mario Luca, Jeff McLaughlin, Tim Maloney, Michael Stovall. Project *TALK* (Teens and Young Adults

Acquiring Lung Cancer Knowledge). Science Day for Lung Cancer Research, Dec. 2005. MD Anderson Cancer Center, Houston, TX.

### Grants

1. Lung cancer PO1 (PI: Fadlo R. Khuri) and RO1 (PI: Shi-Yong Sun).  
Data generated from Project 5 were used to successfully obtain funding for a lung cancer PO1 and for RO1 submission that has received an encouraging score.

### Project-Generated Resources

1. We are generating an extensive database for targeting ligands and vascular receptors identified in our laboratory. This database is likely to be very useful as it can be integrated with the system that is in place under the IMPACT Program to correlate clinical information and responses to therapy with the expression of selective molecular targets. Moreover, targeted therapies and imaging agents are likely to derive from this work.

### Biostatistics Tool

1. Synergy Program for Download: <http://biostatistics.mdanderson.org/SoftwareDownload/>

### CONCLUSION

For the first year of the grant period, the research projects have been progressing very well and basically as originally proposed in the grant except minor recommended changes in Projects 4, 5, and 6. These changes have been detailed in the body of the report. 2 of 4 proposed clinical trials are in process for review and approval, and should be activated to recruit patients in the second year. Preparation of the protocol for the clinical trial planned in Project 2 will begin at the end of the second year as originally planned.

In the first year, we have 3 publications, 1 in *Cell* and 2 in *Cancer Research* (priority reports), and 5 abstracts to be presented at 2006 AACR Annual meeting. We have been granted the NCI Lung Cancer PO1 and received a favorable score for the NCI R01 grant based on data generated from Project 5.

In summary, the individual projects of IMPACT can conclude as follows:

**Project 1** concludes that gefitinib and erlotinib, at clinically achievable concentrations, sensitize NSCLC cell lines to radiation. Although the degree of radiosensitization might appear to be small, 25% increase in cell death would be expected to have a substantial clinical impact if repeated over the entire course of radiotherapy (i.e., 30 or more fractions of 2 Gy) with daily administration of the agent. Gefitinib radiosensitizes NSCLC cells by suppressing repairing radiation-induced DSBs probably via an inhibition of ERK activation.

**Project 2** concludes that imaging with pharmacokinetically optimized water-soluble [ $^{124}\text{I}$ ]mIPQA derivatives should allow for identification of tumors with increased EGFR signaling. PET imaging with  $^{18}\text{F}$ -FMAU demonstrated higher sensitivity for the detection of NSCLCs as compared to  $^{18}\text{F}$ -FDG. The lack of decrease in  $^{18}\text{F}$ -FDG and  $^{18}\text{F}$ -FMAU uptake early after initiation of gefitinib therapy is predictive of tumor resistance. However, in some gefitinib sensitive NSCLCs, the assessment of early treatment responses by PET may not be feasible because of very low pre-treatment levels of uptake of both  $^{18}\text{F}$ -FDG and  $^{18}\text{F}$ -FMAU. Therefore, alternative imaging agents need to be developed for the detection of NSCLCs and for monitoring molecular-targeted therapies in patients.

**Project 3** demonstrates that two selected phages displaying the motif GGS are ligands of EphA5 receptor, and EphA5 overexpression in lung cancer cells provides original evidence of EphA5 as a lung cancer biomarker which has potential functional implications.

**Project 4** concludes that bFGF can stimulate the growth of immortalized mouse endothelial cells that can be reversed by bFGF inhibitor TMPP *in vitro* and cytoplasmic overexpression of bFGF and its receptors in NSCLC tumor specimens and dysplastic lesions in SCC sequence indicate an important role of the pathway in NSCLC pathogenesis.

**Project 5** concludes that mTOR inhibitors suppress the growth of human lung cancer cells albeit to various degrees and activation of Akt and eIF4E survival pathways may eventually lead to resistance to mTOR-targeted therapies. Targeting mTOR axis may be a promising strategy against lung cancer when combined with other agents.

**Project 6** concludes that based on the limited data currently in hand, it is premature to draw meaningful conclusions.

**Biostatistics Core** has provided biostatistical support and consulting in trial design and implementation for the trials of Tarceva plus chemoradiation and ZD6474 for MPE, and assisted in analyzing experimental results of Project 4. It has also developed two biostatistical methods available freely for download for other researchers to use (<http://biostatistics.mdanderson.org/SoftwareDownload/>). The Core also helped develop the DOD website.

**Pathology Core** has successfully fulfilled the goals proposed for the first year. It has performed a number of histopathological, immunohistochemical and molecular studies in a large number of tissue specimens, assisted most of IMPACT research projects, and managed to conduct additional research activities that were fully integrated with some research projects of IMPACT.

**DRP-1** plans to open the pleural effusion trial in spring 2006.

**DRP-2** is proceeding well as originally planned for the first year of the timeline.

## **REFERENCES**

1. Colella, S., et al., Sensitive and quantitative universal Pyrosequencing™ methylation analysis of CpG sites. *Biotechniques* 35: 146-152, 2003.
2. Demetri GD, von Mehren M, Blanke CD, et al: Efficacy and safety of imatinib mesylate in advanced gastrointestinal stromal tumors. *N Engl J Med* 347(7):472-80, 2002
3. Druker BJ, Sawyers CL, Kantarjian H, et al: Activity of a specific inhibitor of the BCR-ABL tyrosine kinase in the blast crisis of chronic myeloid leukemia and acute lymphoblastic leukemia with the Philadelphia chromosome. *N Engl J Med* 344:1038-42, 2001.
4. Druker BJ, Talpaz M, Resta DJ, et al. Efficacy and safety of a specific inhibitor of the BCR-ABL tyrosine kinase in chronic myeloid leukemia. *N Engl J Med* 344:1031-7, 2001.
5. Druker BJ. Imatinib as a paradigm of targeted therapies. *Adv Cancer Res* 91:1-30, 2004.
6. Giaccone G, Herbst RS, Manegold C, Scagliotti G, Rosell R, Miller V, Natale R, Schiller J, von Pawel J, Pluzanska A, Gatzemeier U, Grous J, Ochs J, Averbuch S, Wolf M, Rennie P, Fandi A, Johnson DH: A phase III clinical trial of gefitinib ('Iressa', ZD1839), and EGFR inhibitor, in combination with gemcitabine and cisplatin in advanced non-small-cell lung cancer (INTACT 1). *J Clin Oncol* 22(5):777-784, 2004
7. Giordano RJ, Cardo-Vila M, Lahdenranta J, Pasqualini R, Arap W. Biopanning and rapid analysis of selective interactive ligands. *Nat Med*. 7(11): 1249-53, 2001.
8. Hafner C, Schmitz G, Meyer S, Bataille F, Hau P, Langmann T, Dietmaier W, Landthaler M, Vogt T. Differential gene expression of Eph receptors and ephrins in benign human tissues and cancers. *Clin Chem*. 50(3): 490-9, 2004.

9. Herbst RS, Bunn PA, Jr.: Targeting the epidermal growth factor receptor in non-small cell lung cancer. *Clin Cancer Res* 9:5813-5824, 2003
10. Herbst RS, Giaccone G, Schiller J, Natale R, Miller V, Manegold C, Scagliotti G, Rosell R, Oliff I, Reeves J, Wolf M, Krebs A, Averbuch S, Ochs J, Grous J, Fandi A, Johnson DH: Gefitinib ('Iressa', ZD1839) in combination with paclitaxel and carboplatin in chemotherapy-naive patients with advanced non-small-cell lung cancer: Results from a phase III clinical trial (INTACT 2). *J Clin Oncol* 22(5):785-794, 2004.
11. Herbst RS, Maddox AM, Rothenberg ML, Small EJ, Rubin EH, Baselga J, Rojo F, Hong WK, Swaisland H, Averbuch SD, Ochs J, LoRusso PM: Selective oral epidermal growth factor receptor tyrosine kinase inhibitor ZD1839 is generally well-tolerated and has activity in non-small-cell lung cancer and other solid tumors: results of a phase I trial. *J Clin Oncol* 20:3815-3825, 2002
12. Howell A, Cuzick J, Baum M et al. Results of the ATAC (Arimidex, Tamoxifen, Alone or in Combination) trial after completion of 5 years' adjuvant treatment for breast cancer. *Lancet* 365:60-2, 2005.
13. Hurwitz H, Fehrenbacher L, Cartwright T, et al: Bevacizumab (a monoclonal antibody to vascular endothelial growth factor) prolongs survival in first-line colorectal cancer (CRC): Results of a phase III trial of bevacizumab in combination with bolus IFL (irinotecan, 5-fluorouracil, leucovorin) as first-line therapy in subjects with metastatic CRC. *PASCO* 21: Abs #3646, 2003.
14. Kobayashi, S., et al., EGFR mutation and resistance of non-small-cell lung cancer to gefitinib. *N Engl J Med* 352: 786-792, 2005.
15. Kris MG, Natale RB, Herbst RS, Lynch TJ, Jr., Prager D, Belani CP, Schiller JH, Kelly K, Spiridonidis H, Sandler A, Albain KS, Cella D, Wolf MK, Averbuch SD, Ochs JJ, Kay AC: Efficacy of gefitinib, an inhibitor of the epidermal growth factor receptor tyrosine kinase, in symptomatic patients with non-small cell lung cancer: a randomized trial. *JAMA* 290:2149-2158, 2003
16. Langley RR, Ramirez KM, Tsan RZ, Van Arsdall M, Nilsson MB, Fidler IJ. Tissue-specific microvascular endothelial cell lines from H-2K(b)-tsA58 mice for studies of angiogenesis and metastasis. *Cancer Res.* 2003 Jun 1;63(11):2971-6.
17. Maihle NJ, et al. EGF/ErbB receptor family in ovarian cancer. *Cancer Treat Res.* 107: 247-58, 2002.
18. Munshi, A, Kurland, JF, Nishikawa, T, et al. Histone deacetylase inhibitors radiosensitize human melanoma cells by suppressing DNA repair activity. *Clin Cancer Res* 2005;11:4912-22.
19. Ochs, JS. Rationale and clinical basis for combining gefitinib (IRESSA, ZD1839) with radiation therapy for solid tumors. *Int J Radiat Oncol Biol Phys* 58:941-9, 2004.
20. Paez, J.G., et al., EGFR mutations in lung cancer: correlation with clinical response to gefitinib therapy. *Science* 304: 1497-1500, 2004.
21. Vogelstein B, Kinzler KW. Cancer genes and the pathways they control. *Nat Med.* 10(8):789-99, 2004.
22. Weisbecker CS, Merrit MV, Whitesides GM. *Langmuir* 12: 3763-3772, 1996.



## **APPENDICES**

## **APPENDIX A**

### **Protocol 2005-1023**

A Phase I/II Study of TARCEVA (erlotinib) in Combination with Chemoradiation in Patients  
with Stage IIIA/B Non-Small Cell Lung Cancer

Study Chair: Ritsuko Komaki, M.D.

# PDOL Draft

A Phase I/II Study of TARCEVA (erlotinib) in Combination with  
Chemoradiation in Patients with Stage IIIA/B Non-Small Cell Lung Cancer  
(NSCLC)  
2005-1023

## Core Protocol Information

Short Title	Tarceva
Study Chair:	Ritsuko R. Komaki
Additional Contact:	Donna M. Reeves Toni Williams
Department:	Radiation Oncology
Phone:	713-563-2300
Unit:	97
Full Title:	A Phase I/II Study of TARCEVA (erlotinib) in Combination with Chemoradiation in Patients with Stage IIIA/B Non-Small Cell Lung Cancer (NSCLC)
Protocol Type:	Standard Protocol
Protocol Phase:	Phase I/Phase II
Version Status:	Draft
Version:	00

## Protocol Body

### 1.0 Background

#### **1.1 Non-small Cell Lung Cancer**

##### **1.1.1 Background on Non-small Cell Lung Cancer (NSCLC) Therapy**

Lung cancer is the second most common cancer diagnosed for both sexes in the United States, second to prostate cancer for men and breast cancer for women. Approximately 172,570 new cases are estimated for 2005. It is the leading cause of cancer deaths in both men and women, with approximately 163,510 deaths estimated for 2003.<sup>1</sup> Upon initial presentation, fewer than one-half of patients will have surgically resectable lung cancer with the potential for cure. Approximately one-quarter of patients will present with locally advanced disease involving either the ipsilateral mediastinal or subcarinal lymph nodes (American Joint Committee on Cancer [AJCC] T1-3 N2 MO, Stage IIIA) or contralateral mediastinal, hilar or ipsilateral or contralateral scalene or supraclavicular nodes (AJCC T1-2 N3 MO, Stage IIIB) without evidence of extrathoracic metastases. A smaller number of patients will have a centrally located primary tumor involving mediastinal structures (AJCC T4 Nx MO, Stage IIIB). These patients are generally not considered candidates for surgical resection. Until recently the standard therapeutic approach for these patients was a four to six week course of thoracic radiation therapy (RT). This approach resulted in excellent control of tumor related thoracic symptoms such as hemoptysis, airway obstruction, dyspnea, and chest pain. However, with median survival times of 9-12 months and five-year survival rates of only 5-8% reported with this approach, exploration of alternative therapeutic choices is well justified. One approach involves the delivery of chemotherapy and/or radiotherapy in an attempt to render these tumors potentially resectable followed by thoracotomy and attempted surgical resection. Several pilot studies have yielded encouraging results with such regimens; however, the majority of patients with stage III non-small cell lung cancer (NSCLC) have tumors, which will not be rendered resectable for cure with any pre-operative approach. For these patients, the current therapeutic challenge is to optimize available non-operative strategies.

Since the 1970's, a number of investigators sought to improve the survival results of stage III NSCLC patients by combining chemotherapy with thoracic RT. While early randomized trials failed to demonstrate any advantage of such regimens over thoracic RT alone, two developments led to clinical trial designs that have yielded a positive result. These developments included the availability of cisplatin-containing regimens and the recognition that patients with a more favorable performance status are more likely to benefit from aggressive therapy. There now have been four randomized trials published that demonstrate a statistically significant survival advantage of a cisplatin containing regimen with thoracic RT over thoracic RT alone.<sup>2-5</sup> Two of these trials used two cycles of

pre-RT full dose cisplatin and vinblastine,<sup>2-3</sup> one trial alternated chemotherapy with RT,<sup>4</sup> and the other delivered low dose daily and weekly single agent cisplatin during thoracic RT.<sup>5</sup> Based on somewhat incomplete analyses of patterns of tumor failure location, it appears that sequential chemoradiation reduces or delays the development of extra-thoracic metastases, while low dose concurrent cisplatin appeared to improve the control rate of intra-thoracic tumor, i.e., acted as a potentiator of the radiation effect. The goal of many investigators in recent years has been to take advantage of both the benefits of full dose chemotherapy and the sensitizing effects of concurrent chemoradiation.

The Radiation Therapy Oncology Group (RTOG) has conducted several phase II trials seeking to exploit the advantages of both full dose chemotherapy and the concurrent delivery of chemotherapy and thoracic RT. The most promising of these trials combined two cycles of cisplatin and oral etoposide concurrently with twice-daily thoracic RT. A total of 76 patients were entered, and the estimated median survival time was a remarkable 19.6 months.<sup>6</sup> This compared with a median survival time of 9.6 and 11.4 months with standard RT and 13.7 and 13.8 months with sequential chemoradiation in two previously cited randomized trials.<sup>2-3</sup> The exciting phase II result led to the phase III trial (RTOG 94-10) that compared the regimen to an established sequential chemoradiation regimen of vinblastine and cisplatin followed by once-daily RT on Day 50 and another concurrent chemoradiation regimen in which once- or twice-daily RT and the same chemotherapy were used.<sup>7</sup> Median survival times were 14.6 months for the sequential arm and 17 and 15.6 months for the concurrent arms with once-daily and twice-daily RT, respectively.

The West Japan Lung Cancer Group compared sequential to concurrent chemoradiation using Mitomycin, vindesine, and cisplatin, (MVC) chemotherapy among 320 patients with stage III NSCLC and demonstrated a survival advantage favoring the concurrent arm, with median survival times of 16.5 versus 13.3 months, respectively (P=0.047).<sup>8</sup>

#### 1.1.2 Paclitaxel, Carboplatin, and RT in NSCLC

Paclitaxel acts as a mitotic inhibitor, blocking cells in G2 and M phases of the cell cycle. The inhibition is unique in that the drug enhances the rate and yields of microtubular assembly and prevents microtubular depolymerization.<sup>9-10</sup> It is well known that cells in the G2 and M phase of the cell cycle are particularly sensitive to radiation.<sup>11</sup> Tishler et al. showed that 24-hour treatment with 10 nM paclitaxel resulted in a radiosensitivity enhancement in a radio-resistant astrocytoma cell line.<sup>12</sup> The enhanced level of cell kill was consistent with the greater radiosensitivity of G2 /M cells. A radiation sensitizing effect of paclitaxel was also observed with only one hour of treatment with 300 nM Taxol, in human leukemia cell line (HL-60) and human lung cancer cell line (Calu-3).<sup>13</sup>

Carboplatin also can be used as a radiation sensitizer. The mechanism of



radiation sensitization with carboplatin is different from that of paclitaxel. Carboplatin potentially interferes with repair of sublethal radiation injury while paclitaxel recruits cells in the radiosensitive G2/M phase. Laboratory data have suggested a possible synergistic relationship of paclitaxel and carboplatin.<sup>14</sup>

The Clinical Oncology Group of Rhode Island (COGRI) conducted a phase II study of paclitaxel and RT for non-small cell lung cancer.<sup>15</sup> Thirty-three patients with unresectable stage IIIA and IIIB NSCLC entered this phase II clinical trial. Paclitaxel (60 mg/m<sup>2</sup>) was administered as a three-hour infusion, weekly for 6 weeks. Radiation therapy was given concurrently to the primary tumor and regional lymph nodes (40.0 Gy) followed by a boost to the tumor (20.0 Gy). Esophagitis was the principal toxicity. Grade 3 or 4 esophagitis occurred in 11 patients (37%). One patient died of pneumonia following completion of therapy. Additional grade 3 toxicities included pneumonitis (3%) and neutropenia (6%). One patient had a grade 3 hypersensitivity reaction. Twenty-nine patients were evaluable for response. Two patients achieved a complete response (7%) and twenty-three (79%) achieved a partial response, for an overall response rate of 86% (95% confidence interval, 68% to 96%). The one-year survival rate was 72% and median survival was 18.4 months. This study demonstrated promising activity with weekly paclitaxel and RT for patients with unresectable stage IIIA and IIIB NSCLC.

In order to further improve local control and distant metastasis, a phase II study of concurrent weekly paclitaxel (50 mg/m<sup>2</sup>/wkly/7wks), carboplatin (AUC 2 wkly/7wks), and RT (66.0 Gy in 33 fractions) followed by two additional cycles of adjuvant paclitaxel, (200mg/m<sup>2</sup>/q3wks X 2) and carboplatin (AUC 6 q3wksX 2) was designed at the COGRI.<sup>16</sup> The goal was to determine the response rate and toxicity of the regimen. A total of 39 eligible patients with previously untreated, inoperable, locally advanced NSCLC were treated on the study. One-year and two-year survival rates were 56.3% and 38.3 % respectively, with a median overall survival of 20.5 months. One- and two year progression-free survival were 43.6% and 34.7%, respectively. Thirty-seven patients were evaluable for response with an overall response rate (CR+PR) of 75.7%. The primary toxicity observed was esophagitis (46% grade 3 and 4).

Belani et al. conducted a phase II study of weekly low dose paclitaxel at 45 mg/m<sup>2</sup> (three-hour infusion) with carboplatin, 100 mg/m<sup>2</sup>, and simultaneous standard-dose thoracic radiotherapy (total of 60.0-65.0 Gy) for patients with locally advanced NSCLC.<sup>17</sup> Thirty-eight patients were enrolled, of which 16 were stage IIIa and 22 were stage IIIB. The main toxicities included nine grade 3 leukopenia; three grade 3 mucositis and esophagitis; two grade 3 fatigue; and two grade 3 nausea/vomiting. No grade 4 toxicities were reported. Overall, the regimen was well tolerated. There were 12 instances of dose reduction and a delay in treatment duration of  $\geq 1$  week in 5 patients. Three patients died as a result of rapidly progressive disease without any evidence of dose-limiting

toxicities. The median survival had not been reached at the time of the report. The one, two and three-year actuarial survival rates for this group of patients with locally advanced NSCLC were 63% (95 CI: 44-77%); 54% (95 CI: 35-70%); and 54% (95 CI: 35-70%) respectively.

More recent multimodality studies involving paclitaxel, carboplatin, and RT were reported at the 2000 annual American Society of Clinical Oncology (ASCO) meeting.<sup>15-16, 18</sup> Choy et al. reported on three sequential studies, the first regimen being paclitaxel and RT (Trial 1),<sup>15</sup> the second study adding carboplatin to that regimen (Trial 2),<sup>16</sup> and the third study using paclitaxel, carboplatin, and hyperfractionated RT (Trial 3).<sup>18</sup> One hundred and fifteen patients were enrolled in the three studies (Trial 1, n=33; Trial 2, n=39; and Trial 3, n=43). The patients in all three trials were similar in terms of age range, disease stage (IIIA/B), performance status, and pattern of failure. Response rates for the three studies were 76% Trial 1 (weekly paclitaxel 60 mg/m<sup>2</sup> x 6 and RT 60.0 Gy); 75.7% for Trial 2 (weekly paclitaxel 50 mg/m<sup>2</sup> and carboplatin AUC 2 x 7 plus RT 66.0 Gy); and 78.6% for Trial 3 (weekly paclitaxel 50 mg/m<sup>2</sup> and carboplatin AUC 2 x 6 plus RT 69.9 Gy as 1.2 Gy BID). Median survival was 20 months in Trial 1, 20.5 months in Trial 2, and 14.3 months in Trial 3; the differences between the studies were not statistically significant. Incidence of esophagitis was similar across the three trials. The investigators concluded that the survival times obtained with the regimens were important enough to encourage further evaluation.

The Cancer and Leukemia Group B (CALGB) reported on its study of induction chemotherapy with paclitaxel and carboplatin followed by concurrent RT, paclitaxel and carboplatin.<sup>19</sup> Patients with unresectable stage III NSCLC were enrolled onto the study and received induction therapy consisting of two cycles of paclitaxel (200 mg/m<sup>2</sup>) and carboplatin (AUC 6) administered every 3 weeks. This was followed by weekly paclitaxel (50 mg/m<sup>2</sup>) and carboplatin (AUC 2) with RT (2.0 Gy/day for 66.0 Gy). Fortyone patients (61% males) were enrolled on the study, with median age 60 years and 61% performance status of 0. The primary toxicity was esophagitis, with 35% of patients experiencing grade 3 or 4. The response rate for the induction phase was 24% (all PRs) while the overall response rate (induction and concurrent therapy) was 56% (7% CRs). Median survival was 14 months and progression-free survival was 7.7 months. One and two year survival rates were estimated at 56% and 43%, respectively. The CALGB concluded that the induction and concurrent regimens could be delivered safely and is currently conducting a randomized phase III study to further evaluate the value of induction therapy prior to immediate concurrent paclitaxel, carboplatin, and RT.

## **1.2 Epidermal Growth Factor Receptor**

The epidermal growth factor receptor (EGFR) is a commonly expressed transmembrane glycoprotein of the tyrosine kinase growth factor receptor family. EGFR is expressed in many normal human tissues, and activation of this

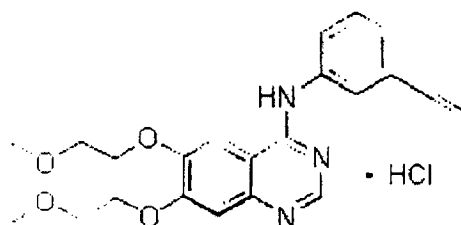
proto-oncogene results in overexpression in many types of human tumors. As a transmembrane glycoprotein, the extracellular domain of the EGFR is a ligand-binding site for transforming growth factor alpha (TGF $\alpha$ ) and epidermal growth factor (EGF). Upon ligand binding, the intracellular domain of EGFR is activated, thereby triggering cellular mechanisms that regulate cell growth.<sup>20</sup> In vitro analysis using cells that express high numbers of EGFR and produce a ligand for these receptors has shown evidence that the EGFR may be activated through an autocrine pathway, thereby leading to the proliferation of cells in culture.<sup>21</sup> In order to inhibit proliferation of EGFR-rich cells, antagonists to EGFR have been produced that block the ligand-binding site; in this capacity, monoclonal antibodies to EGFR have been shown to inhibit the proliferation of cells that produce both TGF $\alpha$  and EGF.<sup>22</sup> An antagonist directed against the ligand-binding site of EGFR offers an interesting approach to the therapy of cancers involving upregulated EGFR-dependent pathways. Among those cancers that overexpress EGFR are some of the most prevalent including: esophageal 92%, head and neck 90%, colorectal 72%<sup>23</sup>, prostate 65%, bladder 65%, ovarian 60%, cervical 60%, pancreatic 89%, renal cell 50%, and lung 50%.<sup>24-25</sup> Prognosis for many of these malignancies is poor if not diagnosed at an early stage, and therapy for advanced disease is limited.

#### 1.2.1 *EGFR Inhibition and the Cell Cycle*

The effects of EGFR blockade on cell cycle progression have been investigated in several human cell types, including DiFi colon adenocarcinoma cells, non-transformed breast epithelial MCF10A cells, A431 squamous epithelial carcinoma cells, and DU145 prostatic cancer cells. These studies suggest that blocking EGFR with monoclonal antibodies such as erlotinib leads to cell cycle arrest in G1 which is accompanied by a decrease in cyclin dependent kinase (CDK) 2 activity, and an increase in the expression of CDK inhibitor p27KIP1.<sup>26-27</sup> In addition to inducing G1-phase arrest, EGFR blockade also was shown to lead to cell death via apoptosis in DiFi colon adenocarcinoma cells.<sup>28</sup>

#### 1.2.2 TARCEVA<sup>TM</sup> (erlotinib)

Tarceva (erlotinib) is a Human Epidermal Growth Factor Receptor Type 1/Epidermal Growth Factor Receptor (HER1/EGFR) tyrosine kinase inhibitor. Erlotinib is a quinazolinamine with the chemical name N-(3-ethynylphenyl)-6,7-bis(2-methoxyethoxy)-4-quinazolinamine. TARCEVA contains erlotinib as the hydrochloride salt which has the following structural formula:



Erlotinib hydrochloride has the molecular formula  $C_{22}H_{23}N_3O_4 \cdot HCl$  and a molecular weight of 429.90. The molecule has a  $pK_a$  of 5.42 at 25°C. Erlotinib hydrochloride is very slightly soluble in water, slightly soluble in methanol and practically insoluble in acetonitrile, acetone, ethyl acetate and hexane.

Aqueous solubility of erlotinib hydrochloride is dependent on pH with increased solubility at a pH of less than 5 due to protonation of the secondary amine. Over the pH range of 1.4 to 9.6, maximal solubility of approximately 0.4 mg/mL occurs at a pH of approximately 2.

#### **1.2.2.1 Clinical Pharmacology**

##### **Mechanism of Action and Pharmacodynamics**

The mechanism of clinical antitumor action of erlotinib is not fully characterized. Erlotinib inhibits the intracellular phosphorylation of tyrosine kinase associated with the epidermal growth factor receptor (EGFR). Specificity of inhibition with regard to other tyrosine kinase receptors has not been fully characterized. EGFR is expressed on the cell surface of normal cells and cancer cells.

##### **Pharmacokinetics**

Erlotinib is about 60% absorbed after oral administration and its bioavailability is substantially increased by food to almost 100%. Its half-life is about 36 hours and it is cleared predominantly by CYP3A4 metabolism.

##### **Absorption and Distribution**

Bioavailability of erlotinib following a 150 mg oral dose of TARCEVA is about 60% and peak plasma levels occur 4 hrs after dosing. Food increases bioavailability substantially, to almost 100%.

Following absorption, erlotinib is approximately 93% protein bound to albumin and alpha-1 acid glycoprotein (AAG). Erlotinib has an apparent volume of distribution of 232 liters.

##### **Metabolism and Elimination**

In vitro assays of cytochrome P450 metabolism showed that erlotinib is metabolized primarily by CYP3A4 and to a lesser extent by CYP1A2, and the extrahepatic isoform CYP1A1. Following a 100 mg oral dose, 91% of the dose was recovered: 83% in feces (1% of the dose as intact parent) and 8% in urine (0.3% of the dose as intact parent).

A population pharmacokinetic analysis in 591 patients receiving single-agent TARCEVA showed a median half-life of 36.2 hours. Time to reach steady state plasma concentration would therefore be 7 - 8 days. No significant relationships of clearance to covariates of patient age, body weight or gender were observed.

Smokers had a 24% higher rate of erlotinib clearance.

### **Special Populations**

#### **Patients with Hepatic Impairment**

Erlotinib is cleared predominantly by the liver. No data are currently available regarding the influence of hepatic dysfunction and/or hepatic metastases on the pharmacokinetics of erlotinib (see **PRECAUTIONS- Patients with Hepatic Impairment, ADVERSE REACTIONS and DOSAGE AND ADMINISTRATION Dose Modifications** sections).

#### ***Patients with Renal Impairment***

Less than 9% of a single dose is excreted in the urine. No clinical studies have been conducted in patients with compromised renal function.

### **Interactions**

Erlotinib is metabolized predominantly by CYP3A4, and inhibitors of CYP3A4 would be expected to increase exposure. Co-treatment with the potent CYP3A4 inhibitor ketoconazole increased erlotinib AUC by 2/3 (see **PRECAUTIONS - Drug Interactions and DOSAGE and ADMINISTRATION Modifications** sections).

Pre- or co-treatment with the CYP3A4 inducer rifampicin increased erlotinib clearance by 3-fold and reduced AUC by 2/3 (see **PRECAUTIONS - Drug Interactions and DOSAGE and ADMINISTRATION Dose Modifications** sections).

## **1.3 Clinical Studies**

- 1.3.1 **TARCEVA as Monotherapy in Non-Small Cell Lung Cancer (NSCLC)**  
The efficacy and safety of single-agent TARCEVA was assessed in a randomized, double blind, placebo- controlled trial in 731 patients with locally advanced or metastatic NSCLC after failure of at least one chemotherapy regimen. Patients were randomized 2:1 to receive TARCEVA 150 mg or placebo (488 Tarceva, 243 placebo) orally once daily until disease progression or unacceptable toxicity. Study end points included overall survival, response rate, and progression-free survival (PFS). Duration of response was also examined. The primary endpoint was survival. The study was conducted in 17 countries 1/3 of the patients (238) had EGFR expression status characterized.

Table 1 summarizes the demographic and disease characteristics of the study population characteristics were well balanced between the two treatment groups. About two-thirds of the patients were male. Approximately one-fourth had a baseline ECOG performance status (PS) of 2, and 9% had a baseline ECOG PS of 3. Fifty percent of the patients had received only one prior regimen of chemotherapy. About three quarters of these patients were known to have smoked at some time.



**Table 1: Demographic and Disease Characteristics**

	TARCEVA (N = 488)		Placebo (N = 243)	
Characteristics	N	(%)	N	(%)
Gender				
Female	173	(35)	83	(34)
Male	315	(65)	160	(66)
Age (Years)				
<65	299	(61)	153	(63)
≥65	189	(39)	90	(37)
Race				
Caucasian	379	(78)	188	(77)
Black	18	(4)	12	(5)
Asian	63	(13)	28	(12)
Other	28	(6)	15	(6)
ECOG Performance Status at Baseline*				
0	64	(13)	34	(14)
1	256	(52)	132	(54)
2	126	(26)	56	(23)
3	42	(9)	21	(9)
Weight Loss in Previous 6 Months				
<5%	320	(66)	166	(68)
5 – 10%	96	(20)	36	(15)

	TARCEVA (N = 488)		Placebo (N = 243)	
Characteristics	N	(%)	N	(%)
≤ 10%	52	(11)	29	(12)
Unknown	20	(4)	12	(5)
Smoking History				
Never Smoked	104	(21)	42	(17)
Current or Ex-smoker	358	(73)	187	(77)
Unknown	26	(5)	14	(6)
Histological Classification				
Adenocarcinoma	246	(50)	119	(49)
Squamous	144	(30)	78	(32)
Undifferentiated Large Cell	41	(8)	23	(9)
Mixed Non-Small Cell	11	(2)	2	(<1)
Other	46	(9)	21	(9)
Time from Initial Diagnosis to Randomization (Months)				
≤ 6	63	(13)	34	(14)
6 – 12	157	(32)	85	(35)
> 12	268	(55)	124	(51)
Best Response to Prior Therapy at Baseline*				
CR/PR	196	(40)	96	(40)
PD	101	(21)	51	(21)
SD	191	(39)	96	(40)
Number of Prior Regimens at Baseline*				
1	243	(50)	121	(50)
2	238	(49)	119	(49)
3	7	(1)	3	(1)
Exposure to Prior Platinum at Baseline*				
Yes	454	(93)	224	(92)
No	34	(7)	19	(8)

\* Stratification factor as documented at baseline; distribution differs slightly from value randomization.

The results of the study are shown in Table 2.

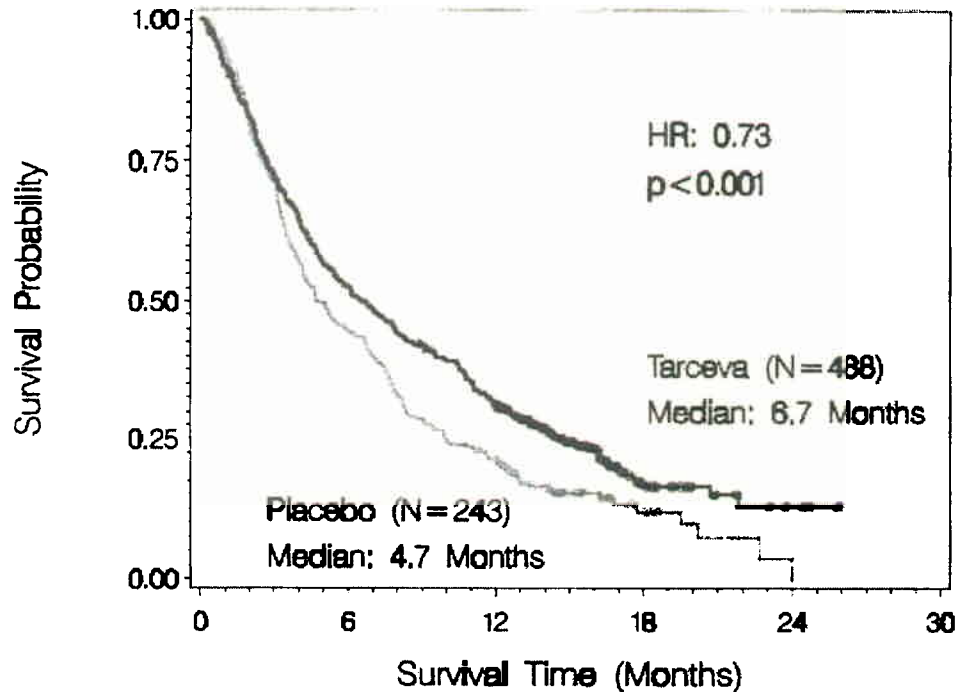
**Table 2: Efficacy Results**

	<b>Tarceva</b>	<b>Placebo</b>	<b>Hazard Ratio (1)</b>	<b>95% CI</b>	<b>p-value</b>
Survival	Median 6.7 mo	Median 4.7 mo	0.73	0.61 – 0.86	<0.001 (2)
1-year Survival	31.2%	21.5%			
Progression-Free Survival	Median 9.9 wk	Median 7.9 wk	0.59	0.50 – 0.70	<0.001 (2)
Tumor Response (CR+PR)	8.9%	0.9%			<0.001 (3)
Response Duration	Median 34.3 wk	Median 15.9 wk			

- (1) Cox regression model with the following covariates: ECOG performance status, number of prior regimens, prior platinum, best response to prior chemotherapy.
- (2) Two-sided Log-Rank test stratified by ECOG performance status, number of prior regimens, prior platinum, best response to prior chemotherapy.
- (3) Two-sided Fisher's exact test

Survival was evaluated in the intent-to-treat population. Figure 1 depicts the Kaplan-Meier curves for overall survival. The primary survival and PFS analyses were two-sided Log-Rank tests stratified by ECOG performance status, number of prior regimens, prior platinum, best response to prior chemotherapy.

**Figure 1: Kaplan-Meier Curve for Overall Survival of Patients by Treatment Group**

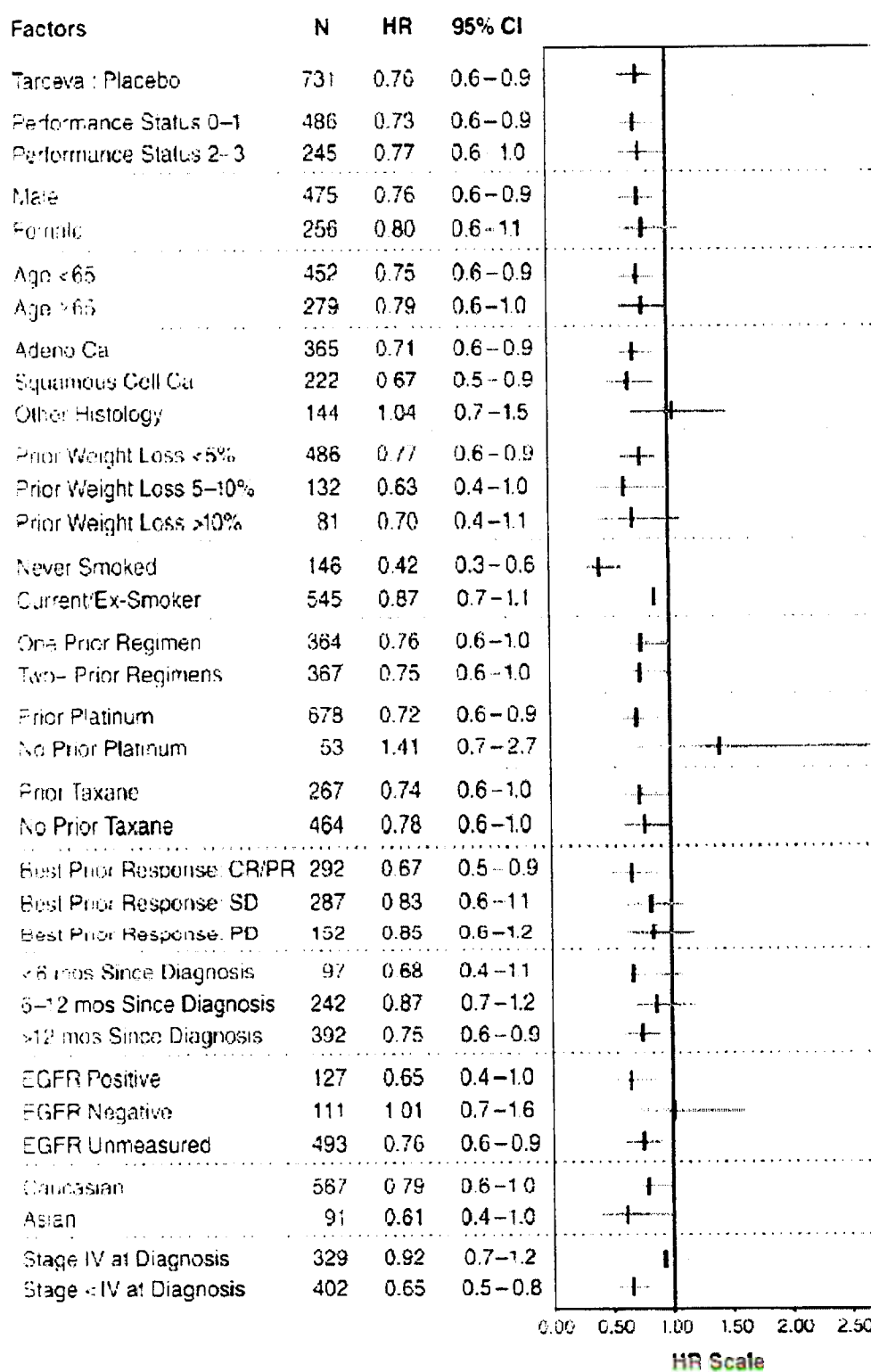


Note: HR is from Cox regression model with the following covariates: ECOG performance status, number of prior regimens, prior platinum, best response to prior chemotherapy. P-value is from two-sided Log-Rank test stratified by ECOG performance status, number of prior regimens, prior platinum, best response to prior chemotherapy.

A series of subsets of patients were examined in exploratory univariate analyses. The results of these analyses are shown in Figure 2. The effect of TARCEVA on survival was similar across most subsets. An apparently larger effect, however, was observed in two subsets: patients with EGFR positive tumors (HR = 0.65) and patients who never smoked (HR = 0.42). These subsets are considered further below.

**Figure 2: Survival Hazard Ratio (HR) (Tarceva : Placebo) in Subgroups**

# According to Pretreatment Characteristics





Note: Depicted are the univariate hazard ratio (HR) for death in the TARCEVA patients relative to the placebo patients, the 95% confidence interval (CI) for the HR, and the sample size (N) in each subgroup. The hash mark on the horizontal bar represents the HR, and the length of the horizontal bar represents the 95% confidence interval. A hash mark to the left of the vertical line corresponds to a HR that is less than 1.00, which indicates that survival is better in the TARCEVA arm compared with the placebo arm in that subgroup.

#### **Relation of Single-Agent TARCEVA Results in NSCLC to EGFR Protein Expression Status (as Determined by Immunohistochemistry)**

Analysis of the impact of EGFR expression status on the treatment effect on clinical outcome is limited because EGFR status is known for 326 NSCLC study patients (45%). EGFR status was ascertained for patients who already had tissue samples prior to study enrollment. However, the survival in the EGFR tested population and the effects of single-agent TARCEVA were almost identical to that in the entire study population, suggesting that the tested population was a representative sample. A positive EGFR expression status was defined as having at least 10% of cells staining for EGFR in contrast to the 1% cut-off specified in the EGFR pharmDx™ kit instructions. The use of the pharmDx kit has not been validated for use in non-small cell lung cancer.

Single-agent TARCEVA prolonged survival in the EGFR positive subgroup (N = 185; HR = 0.68; 95% CI = 0.49 - 0.94) (Figure 3) and the subgroup whose EGFR status was unmeasured (N = 405; HR = 0.77; 95% CI = 0.61 - 0.98) (Figure 5), but did not appear to have an effect on survival in the EGFR negative subgroup (N = 141; HR = 0.93; 95% CI = 0.63 - 1.36) (Figure 4). However, the confidence intervals for the EGFR positive, negative and unmeasured subgroups of NSCLC patients are wide and overlap, so that a survival benefit due to TARCEVA in the EGFR negative subgroup cannot be excluded.

For the subgroup of NSCLC patients who never smoked, EGFR status also appeared to be predictive of TARCEVA survival benefit. Patients who never smoked and were EGFR positive had a large TARCEVA survival benefit (N = 41; HR = 0.28; 95% CI = 0.13 - 0.61). There were too few EGFR negative patients who never smoked to reach a conclusion.

Tumor responses were observed in all EGFR subgroups: 11.6% in the EGFR positive subgroup, 9.5% in the EGFR unmeasured subgroup and 3.2% in the EGFR negative subgroup. An improvement in progression free survival was demonstrated in the EGFR positive subgroup (HR 0.49; 95% CI = 0.33 - 0.72), the EGFR unmeasured subgroup (HR 0.56; 95% CI = 0.46 - 0.70), and less certain in the EGFR negative subgroup (HR 0.91; 95% CI = 0.59 - 1.39).

**Figure 3: Survival in EGFR Positive Patients**

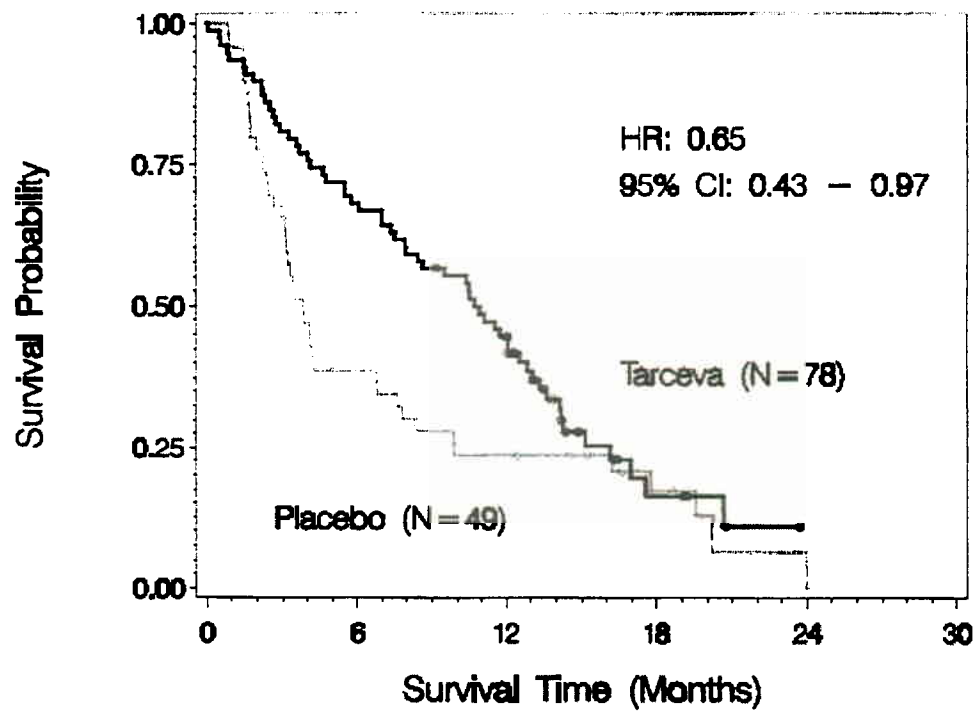


**Figure 4: Survival in EGFR Negative Patients**

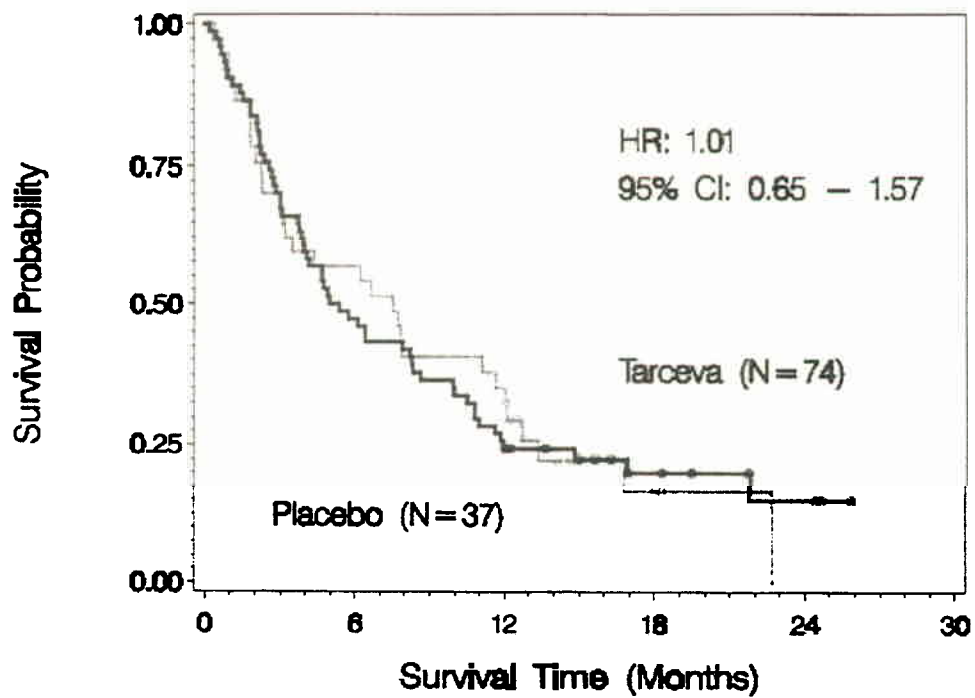
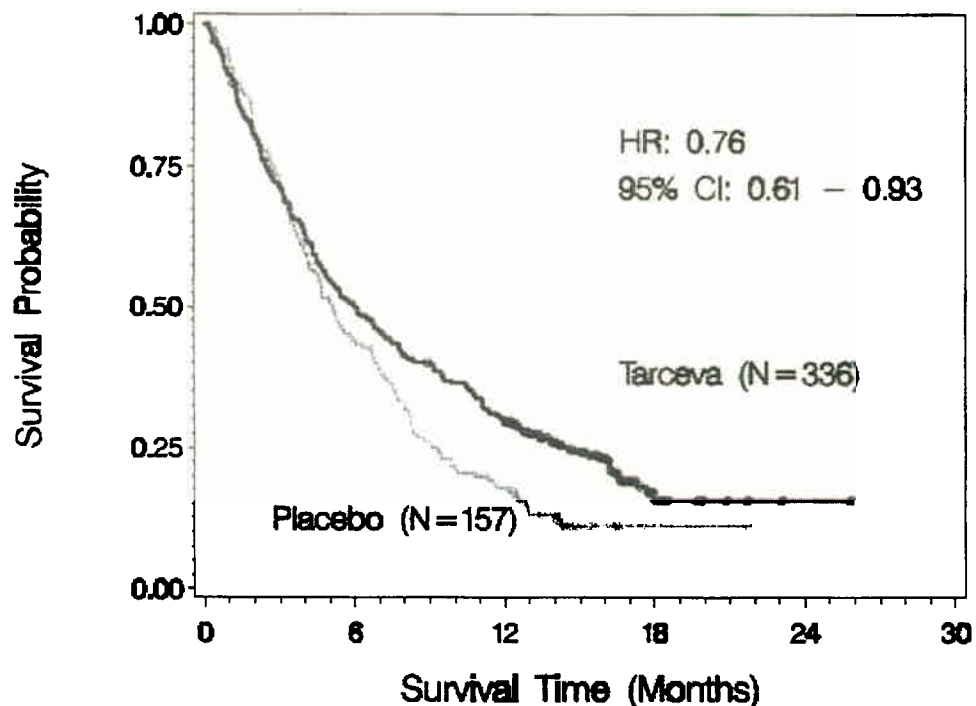


**Figure 5: Survival in EGFR Unmeasured Patients**



#### **TARCEVA Administered Concurrently with Chemotherapy**

Results from two, multicenter, placebo-controlled, randomized, trials in over 1000 patients conducted in first-line patients with locally advanced or metastatic NSCLC showed no clinical benefit with the concurrent administration of TARCEVA with platinum-based chemotherapy [carboplatin and paclitaxel (TARCEVA, N = 526) or gemcitabine and cisplatin (TARCEVA, N = 580)].

#### **1.3.2 Indications and Usage**

TARCEVA is indicated for the treatment of patients with locally advanced or metastatic non-small cell lung cancer after failure of at least one prior chemotherapy regimen.

Results from two, multicenter, placebo-controlled, randomized, Phase 3 trials conducted in first-line patients with locally advanced or metastatic NSCLC showed no clinical benefit with the concurrent administration of TARCEVA with platinum-based chemotherapy [carboplatin and paclitaxel or gemcitabine and cisplatin] and its use is not recommended in that setting.

### 1.3.3 Warnings

#### **Pulmonary Toxicity**

There have been infrequent reports of serious Interstitial Lung Disease (ILD)-like events, including fatalities, in patients receiving TARCEVA for treatment of NSCLC, pancreatic cancer or other advanced solid tumors. In the randomized single-agent NSCLC study (see CLINICAL STUDIES section), the incidence of ILD-like events (0.8%) was the same in both the placebo and TARCEVA groups. In the pancreatic cancer study - in combination with gemcitabine - (see CLINICAL STUDIES section), the incidence of ILD-like events was 2.5% in the TARCEVA plus gemcitabine group vs. 0.4% in the placebo plus gemcitabine group.

The overall incidence in approximately 4900 TARCEVA-treated patients from all studies (including uncontrolled studies and studies with concurrent chemotherapy) was approximately 0.7%. Reported diagnoses in patients suspected of having ILD-like events included pneumonitis, radiation pneumonitis, hypersensitivity pneumonitis, interstitial pneumonia, interstitial lung disease, obliterative bronchiolitis, pulmonary fibrosis, Acute Respiratory Distress Syndrome and lung infiltration. Symptoms started from 5 days to more than 9 months (median 39 days) after initiating TARCEVA therapy. Most of the cases were associated with confounding or contributing factors such as concomitant/prior chemotherapy, prior radiotherapy, pre-existing parenchymal lung disease, metastatic lung disease, or pulmonary infections.

In the event of acute onset of new or progressive, unexplained pulmonary symptoms such as dyspnea, cough, and fever, TARCEVA therapy should be interrupted pending diagnostic evaluation. If ILD is diagnosed, TARCEVA should be discontinued and appropriate treatment instituted as necessary (see ADVERSE REACTIONS and DOSAGE AND ADMINISTRATION - Dose Modifications sections).

#### **Pregnancy Category D**

Erlotinib has been shown to cause maternal toxicity with associated embryo/fetal lethality and abortion in rabbits when given at doses that result in plasma drug concentrations of approximately 3 times those in humans (AUCs at 150 mg daily dose). When given during the period of organogenesis to achieve plasma drug concentrations approximately equal to those in humans, based on AUC, there was no increased incidence of embryo/fetal lethality or abortion in rabbits or rats. However, female rats treated with 30 mg/m<sup>2</sup>/day or 60 mg/m<sup>2</sup>/day (0.3 or 0.7 times the clinical dose, on a mg/m<sup>2</sup> basis) of erlotinib prior to mating through the first week of pregnancy had an increase in early resorptions which resulted in a decrease in the number of live fetuses.

No teratogenic effects were observed in rabbits or rats.

There are no adequate and well-controlled studies in pregnant women using TARCEVA. Women of childbearing potential should be advised to avoid pregnancy while on TARCEVA. Adequate contraceptive methods should be used during therapy, and for at least 2 weeks after completing therapy. Treatment should only be continued in pregnant women if the potential benefit to the mother outweighs the risk to the fetus. If TARCEVA is used during pregnancy, the patient should be apprised of the potential hazard to the fetus or potential risk for loss of the pregnancy.

#### 1.3.4 Precautions

##### **Drug Interactions**

Co-treatment with the potent CYP3A4 inhibitor ketoconazole increases erlotinib AUC by 2/3. Caution should be used when administering or taking TARCEVA with ketoconazole and other strong CYP3A4 inhibitors such as atazanavir, clarithromycin, indinavir, itraconazole, nefazodone, nelfinavir, ritonavir, saquinavir, telithromycin, troleandomycin (TAO), and voriconazole (see DOSAGE AND ADMINISTRATION - Dose Modifications section).

Pre-treatment with the CYP3A4 inducer rifampicin decreased erlotinib AUC by about 2/3. Alternate treatments lacking CYP3A4 inducing activity should be considered. If an alternative treatment is unavailable, a TARCEVA dose greater than 150 mg should be considered for NSCLC patients, and greater than 100 mg considered for pancreatic cancer patients. If the TARCEVA dose is adjusted upward, the dose will need to be reduced upon discontinuation of rifampicin or other inducers. Other CYP3A4 inducers include, but are not limited to, rifabutin, rifapentine, phenytoin, carbamazepine, phenobarbital and St. John's Wort (see DOSAGE AND ADMINISTRATION - Dose Modifications section).

##### **Hepatotoxicity**

Asymptomatic increases in liver transaminases have been observed in TARCEVA treated patients; therefore, periodic liver function testing (transaminases, bilirubin, and alkaline phosphatase) should be considered. Dose reduction or interruption of TARCEVA should be considered if changes in liver function are severe (see ADVERSE REACTIONS section).

##### **Patients with Hepatic Impairment**

In vitro and in vivo evidence suggest that erlotinib is cleared primarily by the liver. Therefore, erlotinib exposure may be increased in patients with hepatic dysfunction (see CLINICAL PHARMACOLOGY - Special Populations - Patients with Hepatic Impairment and DOSAGE AND ADMINISTRATION - Dose Modification sections).

##### **Elevated International Normalized Ratio and Potential Bleeding**

International Normalized Ratio (INR) elevations, and infrequent reports of bleeding events including gastrointestinal bleeding have been reported in clinical studies, some associated with concomitant warfarin administration. Patients



taking warfarin or other coumarin-derivative anticoagulants should be monitored regularly for changes in prothrombin time or INR (see ADVERSE REACTIONS section).

### **Carcinogenesis, Mutagenesis, Impairment of Fertility**

Erlotinib has not been tested for carcinogenicity.

Erlotinib has been tested for genotoxicity in a series of in vitro assays (bacterial mutation, human lymphocyte chromosome aberration, and mammalian cell mutation) and an in vivo mouse bone marrow micronucleus test and did not cause genetic damage. Erlotinib did not impair fertility in either male or female rats.

### **Pregnancy**

Pregnancy Category D (see WARNINGS and PRECAUTIONS - Information for Patients sections).

### **Nursing Mothers**

It is not known whether erlotinib is excreted in human milk. Because many drugs are excreted in human milk and because the effects of TARCEVA on infants have not been studied, women should be advised against breastfeeding while receiving TARCEVA therapy.

### **Pediatric Use**

The safety and effectiveness of TARCEVA in pediatric patients have not been studied.

### **Geriatric Use**

Of the total number of patients participating in the randomized NSCLC trial, 62% were less than 65 years of age, and 38% of patients were aged 65 years or older. The survival benefit was maintained across both age groups (see CLINICAL STUDIES section). In the randomized combination pancreatic cancer study, 53% of patients were younger than 65 years of age and 47% were 65 years of age or older. No meaningful differences in safety or pharmacokinetics were observed between younger and older patients in either study. Therefore, no dosage adjustments are recommended in elderly patients.

### **Information for Patients**

If the following signs or symptoms occur, patients should seek medical advice promptly (see **WARNINGS, ADVERSE REACTIONS and DOSAGE AND ADMINISTRATION - Dose Modification sections**).

Severe or persistent diarrhea, nausea, anorexia, or vomiting

Onset or worsening of unexplained shortness of breath or cough

Eye irritation

Women of childbearing potential should be advised to avoid becoming pregnant while taking TARCEVA (see WARNINGS - Pregnancy Category D section).

### 1.3.5 Adverse Reactions

Table 3: Adverse Events Occurring in  $\geq 10\%$  of TARCEVA-treated Patients (2:1 Randomization of TARCEVA to Placebo)

	TARCEVA N = 485			Placebo N = 242		
NCI CTC Grade	Any Grade	Grade 3	Grade 4	Any Grade	Grade 3	Grade 4
MedDRA Preferred Term	%	%	%	%	%	%
Rash	75	8	<1	17	0	0
Diarrhea	54	6	<1	18	<1	0
Anorexia	52	8	1	38	5	<1
Fatigue	52	14	4	45	16	4
Dyspnea	41	17	11	35	15	11
Cough	33	4	0	29	2	0
Nausea	33	3	0	24	2	0
Infection	24	4	0	15	2	0
Vomiting	23	2	<1	19	2	0
Stomatitis	17	<1	0	3	0	0
Pruritus	13	<1	0	5	0	0
Dry skin	12	0	0	4	0	0
Conjunctivitis	12	<1	0	2	<1	0
Keratoconjunctivitis sicca	12	0	0	3	0	0
Abdominal pain	11	2	<1	7	1	<1

### 1.3.6 Overdosage

Single oral doses of TARCEVA up to 1,000 mg in healthy subjects and up to 1,600 mg in cancer patients have been tolerated. Repeated twice-daily doses of 200 mg single-agent TARCEVA in healthy subjects were poorly tolerated after only a few days of dosing. Based on the data from these studies, an unacceptable incidence of severe adverse events, such as diarrhea, rash, and liver transaminase elevation, may occur above the recommended dose (see DOSAGE AND ADMINISTRATION SECTION). In case of suspected overdose, TARCEVA should be withheld and symptomatic treatment instituted.

### 1.3.7 Dosage and Administration

#### **Dose Modifications**

In patients who develop an acute onset of new or progressive pulmonary symptoms, such as dyspnea, cough or fever, treatment with TARCEVA should be interrupted pending diagnostic evaluation. If ILD is diagnosed, TARCEVA should be discontinued and appropriate treatment instituted as necessary (see WARNINGS section).

Diarrhea can usually be managed with loperamide. Patients with severe diarrhea who are unresponsive to loperamide or who become dehydrated may require dose reduction or temporary interruption of therapy. Patients with severe skin reactions may also require dose reduction or temporary interruption of therapy.

When dose reduction is necessary, the TARCEVA dose should be reduced in 50 mg decrements.

In patients who are being concomitantly treated with a strong CYP3A4 inhibitor such as atazanavir, clarithromycin, indinavir, itraconazole, ketoconazole, nefazodone, nelfinavir, ritonavir, saquinavir, telithromycin, troleandomycin (TAO), or voriconazole, a dose reduction should be considered should severe adverse reactions occur.

Pre-treatment with the CYP3A4 inducer rifampicin decreased erlotinib AUC by about 2/3. Alternate treatments lacking CYP3A4 inducing activity should be considered. If an alternative treatment is unavailable, a TARCEVA dose greater than 150 mg should be considered. If the TARCEVA dose is adjusted upward, the dose will need to be reduced upon discontinuation of rifampicin or other inducers. Other CYP3A4 inducers include rifabutin, rifapentin, phenytoin, carbamazepine, phenobarbital and St. John's Wort. These too should be avoided if possible (see PRECAUTIONS - Drug Interactions section).

Erlotinib is eliminated by hepatic metabolism and biliary excretion. Therefore, caution should be used when administering TARCEVA to patients with hepatic impairment. Dose reduction or interruption of TARCEVA should be considered should severe adverse reactions occur (see PHARMACOKINETICS - Special Populations, PRECAUTIONS - Patients With Hepatic Impairment, and ADVERSE REACTIONS sections).

### 1.4 Rationale

At the 2002 annual meeting of the American Society of Clinical Oncology (ASCO), preliminary results from the American College of Radiology (ACR) Locally Advanced Multi-Modality Protocol (LAMP) study, ACR 427, were presented.<sup>32</sup> This study enrolled patients with unresected stage III NSCLC and randomized them to one of three arms: sequential paclitaxel/carboplatin followed

by RT (Arm 1); induction therapy with paclitaxel/carboplatin followed by concurrent paclitaxel/carboplatin/RT (Arm 2); or concurrent paclitaxel/carboplatin/RT followed by consolidation therapy with paclitaxel/carboplatin (Arm 3). The preliminary survival data led to the termination of accrual to Arm 2, but were sufficiently promising to continue accrual to Arms 1 and 3. Recently, the Southwest Oncology Group (SWOG) published updated results of a study (SWOG 9504) of concurrent therapy followed by consolidation therapy.<sup>33</sup> Patients with stage IIIB NSCLC were treated with a regimen of concurrent cisplatin/etoposide/RT followed by consolidation with docetaxel. The results presented were compared to an earlier study using the same concurrent regimen, but without consolidation therapy. Median survival and one-, two-, and three-year survival rates were substantially increased with the addition of the consolidation therapy.

Several agents designed to block the effects of the EGFR have undergone clinical testing in patients with NSCLC. At the 2001 ASCO meeting, the results of a phase II trial utilizing the oral EGFR tyrosine kinase inhibitor OSI-774 were reported.<sup>34</sup> In that trial of patients with recurrent NSCLC, 19% of patients had received > 3 prior chemotherapy regimens. Overall, 1.8% of patients achieved a CR, 10.5% PR, and 26.3% SD with OSI-774. Importantly, the duration of PR's lasted 17-36 weeks. Subsequently, the results of a phase I study with OSI-774 in combination with docetaxel were reported at the 2002 ASCO annual meeting.<sup>35</sup> This study included patients with NSCLC and, as of the time of the report, minor response and stable disease had been observed in NSCLC patients.

Also at the 2002 ASCO annual meeting, several studies of another EGFR tyrosine kinase inhibitor, ZD1839, were reported.<sup>36-38</sup> Two of the trials, designated IDEAL 1 37 (n=210) and IDEAL 2 37 (n=216), evaluated the activity of oral, single agent ZD1839 in patients with NSCLC. Patients on the IDEAL 1 trial had failed one or two prior regimens, at least one containing a platinum compound while patients on IDEAL 2 had failed two or more previous regimens containing platinum and docetaxel. Response rates for the IDEAL 1 trial were 18.4% with a dose of 250 mg/day and 19% with a dose of 500 mg/day. In terms of second and third line treatment, response rates were similar at 17.9% and 19.8%, respectively. Toxicity was milder with the 250 mg/day dose, primarily rash, diarrhea, pruritus, and dry skin. The conclusion from the IDEAL 1 trial was that ZD1839 demonstrated clinically significant antitumor activity and a favorable safety profile. Response rates obtained with the IDEAL 2 trial were 11.8% (250 mg/day) and 8.8% (500 mg/day). The duration of tumor response ranged from 3 to 7+ months, and median survival was 6.1 months for the 250 mg/day group and 6.0 months for the 500 mg/day group. As with IDEAL 1, toxicity was mild in IDEAL 2, consisting mostly of diarrhea and skin rash. The results of IDEAL 2 indicated that ZD 1839 also had clinically significant anti-tumor activity in heavily pretreated patients with NSCLC. Additional evidence for the efficacy of single agent ZD 1839 in NSCLC came from a compassionate use study, in which potential benefit (partial response + minor response + stable disease) was

observed in 26.6% of the patients enrolled.<sup>38</sup>

The question of whether overexpression of EGFR correlates with response to EGFR inhibiting therapies also has been examined. An exploratory analysis using tumour biopsies taken prior to treatment from patients enrolled in two phase II studies of gefitinib in advanced NSCLC did not reveal any evidence of a correlation between the levels of membrane EGFR expression as measured and tumour response.<sup>39</sup>

Clearly the precedent has been set for the use of anti-EGFR therapy in NSCLC with the oral tyrosine kinase inhibitor compounds OSI-74 and ZD1839, and it is a logical step to evaluate the activity of erlotinib in this disease. Baselga et al. have reported on three phase I erlotinib studies in which a total of eight patients with NSCLC were given erlotinib, two as single agent therapy and six in combination with cisplatin.<sup>40</sup> Although results were not reported by disease state, patients in all three studies experienced disease stabilization and erlotinib-associated toxicity was minimal.

At the 2003 ASCO annual meeting, the results of several phase II studies were reported regarding the combination of C225 with chemotherapy.<sup>41</sup> In a phase I/II study in untreated metastatic NSCLC combining C225 with paclitaxel and carboplatin (C225 loading dose of 400 mg/m<sup>2</sup> then weekly 250 mg/m<sup>2</sup> maintenance; paclitaxel 225 mg/m<sup>2</sup> q 3 weeks; carboplatin AUC 6), 31 patients were accrued. The overall response rate (ORR) was 29% (9 patients), time to progression was 5.4 months, and the median survival was 15.7 months. The most common toxicity was rash, with 9.7% (3 patients) having a grade 3/4 acne-like rash. The most common grade 3 toxicity was fatigue at 19.4% (6 patients).

A phase I/II study in untreated metastatic NSCLC combining C225 with gemcitabine and carboplatin accrued 35 patients and reported an ORR of 28.6% (10 patients); time to progression was 5.5 months, and median survival was 10.3 months.<sup>42</sup> The most common toxicity was rash at 80% (28 patients), with 20% (7 patients) experiencing a grade 3 acne-like rash. These studies demonstrated the feasibility of combining C225 with systemic chemotherapy in NSCLC. Both regimens had acceptable safety profiles, and encouraging clinical activity.

NCI Canada clinical trials group conducted a study of Erlotinib in previously treated NSCLC. They conducted a randomized, placebo-controlled, double-blind trial to determine whether the epidermal growth factor receptor inhibitor erlotinib prolongs survival in non-small-cell lung cancer after the failure of first-line or second-line chemotherapy. Patients had stage IIIB or IV non-small-cell lung cancer, with performance status from 0 to 3, were eligible if they had received one or two prior chemotherapy regimens. The patients were stratified according



to center, performance status, response to prior chemotherapy, number of prior regimens, and prior platinum-based therapy and were randomly assigned in a 2:1 ratio to receive oral erlotinib, at a dose of 150 mg daily, or placebo. The median age of the 731 patients who underwent randomization was 61.4 years; 49 percent had received two prior chemotherapy regimens, and 93 percent had received platinum-based chemotherapy. The response rate was 8.9 percent in the erlotinib group and less than 1 percent in the placebo group ( $P<0.001$ ); the median duration of the response was 7.9 months and 3.7 months, respectively. Progression-free survival was 2.2 months and 1.8 months, respectively (hazard ratio, 0.61, adjusted for stratification categories;  $P<0.001$ ). Overall survival was 6.7 months and 4.7 months, respectively (hazard ratio, 0.70;  $P<0.001$ ), in favor of erlotinib. Five percent of patients discontinued erlotinib because of toxic effects. They concluded that Erlotinib can prolong survival in patients with non-small-cell lung cancer after first-line or second-line chemotherapy.<sup>50</sup>

The present study is based upon a combination of the data from the studies described above. The use of concurrent chemoradiation therapy followed by consolidation therapy which is based upon Arm 3 of the LAMP study and the SWOG 9504 study. The addition of biologic therapy with erlotinib to the regimen hopefully will result in even better efficacy without increasing toxicity.

Clearly this study is a logical next step in the attempt to find the optimal regimen for the treatment of advanced NSCLC.

## **2.0 Objectives**

### **2.1 Primary Objective**

Determine the feasibility of concurrent erlotinib and chemoradiation as measured by safety and compliance. Safety is measured by the rate of grade 3 or worse nonhematological toxicities occurring prior to the beginning of consolidation therapy (including all toxicities attributed to chemoradiation occurring within 90 days of the start of radiation therapy); compliance is defined as the completion of the treatment regimen with no more than minor variations.

### **2.2 Secondary Objectives**

- 2.2.1** Estimate the treatment response rate of patients on the study regimen (complete and partial response rates)
- 2.2.2** Estimate overall survival of patients on the study regimen (one and two year rates, median survival).
- 2.2.3** Estimate the time to disease progression of patients on the study regimen (one and two year rates)
- 2.2.4** Investigate associations between EGFR expression and toxicity, response, overall survival, and progression

### 3.0 Patient Eligibility

#### 3.1 Eligibility

- 3.1.1 Histologically or cytologically documented NSCLC, including squamous cell carcinoma, adenocarcinoma (including bronchoalveolar cell), and large cell anaplastic carcinoma (including giant and clear cell carcinomas) and poorly differentiated (not otherwise specified, NOS) non-small cell lung cancer; totally resected tumors are excluded.
- Patients must be M0;
  - Patients with T1 or T2 disease with N2 or T3N1-2 disease (Stage IIIA) are eligible if they are deemed inoperable. Patients with T4 with any N or any T with N2 or N3 disease are eligible if unresectable. Radiographic evidence of mediastinal lymph nodes > 2.0 cm in the largest diameter is sufficient to stage N2 or N3 disease. If the largest mediastinal node is < 2.0 cm in diameter and this is the basis for stage III disease, then at least one of the nodes must be proven positive cytologically or histologically;
  - Measurable disease is required. See Section 11.3 for RECIST definitions of measurable disease.
- 3.1.2 Patients with tumors adjacent to a vertebral body are eligible as long as all gross disease can be encompassed in the radiation boost field. The boost volume must be limited to < 50% of the ipsilateral lung volume.
- 3.1.3 Patients must be  $\geq 18$  years of age;
- 3.1.4 Patients with Zubrod performance status 0-1 (See Appendix E);
- 3.1.5 Adequate hematologic function defined as: ANC  $\geq 1,500/\text{mm}^3$ , platelets  $\geq 100,000/\text{mm}^3$ , and hemoglobin  $\geq 9$  g/dL (prior to transfusions); adequate hepatic function defined as: total bilirubin  $\leq 1.5$  mg/dl, SGOT or SGPT  $\leq 3 \times \text{ULN}$ , adequate renal function defined as a serum creatinine level  $\leq 2.0$  mg/dl, alkaline phosphatase  $\leq 2.5 \times \text{ULN}$ , glucose  $\leq 2 \times \text{ULN}$ ;
- 3.1.6 FEV1 with  $\geq 1200$  cc;
- 3.1.7 Patients with weight loss  $\leq 5\%$  over the past 3 months;
- 3.1.8 Patients with a pleural effusion that is a transudate, cytologically negative and nonbloody are eligible if the radiation oncologists feel the tumor can still be encompassed within a reasonable field of radiotherapy (See Sections 6.4 and 6.5). If a pleural effusion can be seen on the chest CT but not on CXR and is too small to tap, the patient is eligible.
- 3.1.9 Patients who have recovered from exploratory thoracotomy;
- 3.1.10 Women of childbearing potential (A woman of child-bearing potential is a sexually mature woman who has not undergone a hysterectomy or who has not been naturally postmenopausal for at least 24 consecutive months [i.e., who has had menses at any time in the preceding 24 consecutive months]) and male participants must practice effective contraception throughout the study and for four weeks after completion of treatment.
- 3.1.11 Patients must sign a study-specific consent form prior to study entry.

#### 3.2 Conditions for Patient Ineligibility

- 3.2.1 Prior systemic chemotherapy and/or thoracic radiotherapy for any reason and/or surgical resection of present cancer;
- 3.2.2 Exudative, bloody, or cytologically malignant effusions;
- 3.2.3 Asymptomatic or symptomatic brain metastasis;
- 3.2.4 Prior therapy with any other drug that targets the EGFR pathway, or prior therapy with a chimerized monoclonal antibody;
- 3.2.5 Known allergy to murine proteins or Cremophor EL;
- 3.2.6 Active pulmonary infection not responsive to conventional antibiotics;
- 3.2.7 History of interstitial pneumonitis;
- 3.2.8 History of severe COPD requiring  $\geq 3$  hospitalizations over the past year;
- 3.2.9 Significant history of cardiac disease, i.e., uncontrolled hypertension, unstable angina, uncompensated congestive heart failure, myocardial infarction within the past year, or cardiac ventricular arrhythmias requiring medication; patients with left ventricular ejection fraction (LVEF) below the institutional range of normal on a baseline multiple gated acquisition (MUGA) scan or echocardiogram.
- 3.2.10 Patients with  $>$  grade 1 neuropathy;
- 3.2.11 Evidence of malignancy in the past 2 years except for adequately treated basal cell or squamous cell skin cancer, in situ cervical cancer, or other in situ cancers;
- 3.2.12 Women who are pregnant or breast feeding, as treatment involves unforeseeable risks to the participant, embryo, fetus, or nursing infant; women with a positive pregnancy test on enrollment or prior to study drug administration;
- 3.2.13 Women of childbearing potential and male participants who are unwilling or unable to use an acceptable method of contraception throughout the study and for four weeks after completion of treatment or those who are using a prohibited contraceptive method.
- 3.2.14 Patients who currently are participating in other clinical trials and/or who have participated in other clinical trials in the previous 30 days.
- 3.2.15 Caution should be used when administering or taking TARCEVA with ketoconazole and other strong CYP3A4 inhibitors such as atazanavir, clarithromycin, indinavir, itraconazole, nefazodone, nelfinavir, ritonavir, saquinavir, telithromycin, troleandomycin (TAO), and voriconazole

## 4.0 Pretreatment evaluation

(In addition to required evaluations in Section 3.0)

- 4.1 PET scan of chest at pretreatment and 4 weeks after completion of concurrent therapy to assess acute toxicity;
- 4.2 For all patients for whom tumor tissue is available and who have consented to participate in the tissue component of the study, specimens will be sent for immunohistochemistry assay for evidence of EGFR expression (see Section 10.0). Unavailability of tissue is not a criterion for exclusion. If tissue is unavailable, the reason(s) should be documented in the site's source documentation.

## 5.0 Radiation Therapy

**Intensity Modulated RT (IMRT) is allowed.**

### 5.1 Doses

Total dose of radiation will be as follows:

A total radiation dose of 63Gy at 1.8 Gy per fraction once a day .

All doses are to be prescribed and calculated assuming a homogeneous patient; that is, there will be no heterogeneity corrections used in the definitions in these doses.

- 5.1.1 At the center of the target area on the central ray for a single beam.
- 5.1.2 At mid-separation on the central ray for two opposed coaxial equally weighted beams.
- 5.1.3 At the center of the target area on the central ray for two opposed coaxial unequally weighted beams.
- 5.1.4 At the point of intersection of the central rays for two or more intersecting beams which are not coaxial.
- 5.1.5 At the center of the rotation in the plane of rotation containing the central axis for rotation or arc therapy.
- 5.1.6 At the center of the target area for complex treatment arrangements which are not covered above.
- 5.1.7 At the depth of the 90% isodose line for single electron beams. Select an electron beam energy which provides at least 90% dose at 3 cm depth.

Two different target volumes shall be considered, the initial large field target volume consisting of the primary tumor and mediastinum and the boost target volume consisting of the primary tumor only.

In treating the initial fields, various sets of fields may be used, which may be coplanar but not coaxial or may not even be coplanar.

### 5.2 Irradiation Portals:

The irradiated target volume must be defined by the individually shaped ports with secondary lead blocking or tailor-made blocks.

#### 5.2.1 Target volume of primary tumor:

- a) Includes complete extent of visible primary or as defined radiographically with a minimum of 1.5 cm and a maximum of 2.0 cm around the mass.
- b) Entire lung may be included for extensive lesions if complicated by atelectasis or pneumonitis, which will be modified depending on FEV1 and/or other pulmonary function tests. One endometrial brachytherapy is allowed to open up total atelectasis before definitive radiation therapy plus chemotherapy.

#### 5.2.2. Target volume of lymph nodes:

The following nodes must be included:

- a) Supraclavicular lymph nodes - if primary is in an upper lobe or there is a main stem bronchus lesion. It is acceptable to treat the ipsilateral supraclavicular nodes only.
- b) Ipsilateral hilar lymph nodes - always (1.5 cm margin).
- c) Contralateral hilar lymph nodes - always (1 cm margin).
- d) Superior mediastinal lymph nodes (above carina) - always (ipsilateral; 1.5 cm margin).
- e) Subcarinal lymph nodes (contralateral 1 cm margin to 3 cm below carina) - always.

### 5.3 Technical Factors

5.3.1 Electron Beam Energy. Megavoltage equipment is required with effective photon energies higher than 1 MeV. Electrons with at least 90% dose at 3 cm depth may be used to boost supraclavicular lymph nodes.

5.3.2 Treatment Distance. Minimal treatment distance to skin should be 80 cm for SSD technique and minimum isocenter distance should be 80 cm for SAD techniques.

#### 5.3.3 Blocking:

- a) In the case of x-ray beams, the primary collimation may be used, and blocking will be required only for shaping of the ports to exclude volumes of tissues that are not to be irradiated.
- b) With Cobalt 60, however, beam trimmers or secondary blocking must be used all the way around the ports.

#### 5.3.4 Compensating Filters or Wedges:

In the case of a large sloping contour, such as that usually encountered when treating Upper lobe tumors in large patients, compensating filters are recommended. A wedge may also be used as a 2-dimensional tissue compensator. If necessary, field size must be reduced appropriately to avoid excessive irradiation to critical structures.

#### 5.3.5 Fractionation:

- a) Each field is to be treated every day.
- b) Adherence to the fractionation schemes is required, although slight deviations in the daily dose fraction are allowed ( $\pm 5\%$ ).

#### 5.3.6 Therapy Interruptions:

- a) If interruptions of therapy up to two weeks become necessary, irradiation should be completed to the prescribed doses. Total number of fractions and elapsed days should be carefully reported.
- b) If more than two weeks, interruption is required, resumption of the treatment is at the discretion of the radiation oncologist. The patient will be considered a major protocol deviation although follow-up will be continued.



#### 5.3.7 Treatment Planning:

- a) Treatment planning should be performed in accordance with the prescribing doses to each target volume, together with restrictions in dose to normal tissues as given in Section 6.2.4.
- b) One set should be calculated without lung correction while the other should be calculated with lung correction. Sagittal dose distributions are encouraged. The lung correction reporting form must be completed, which requires both uncorrected and corrected calculations of the dose to the center of the target volume. The lung correction can be calculated by any method which the institution prefers.
- c) In addition to the isodose distributions, the following specific points of dose calculations, should be observed:
  - 1) Spinal Cord Dose: Maximal spinal cord dose should not exceed 30 Gy for patient cohort 1 and not exceed 45 Gy at any level for patient cohort 2 and 3.
  - 2) Subcarinal Nodes: Are assumed to be at mid-plane.
  - 3) Ipsilateral Normal Lung Dose: This is to be calculated at the level of the central rays of the boost fields at the point of maximum dose in the lung which lies at least 2 cm outside the projected borders of the initial treatment fields in the ipsilateral lung.
  - 4) Contralateral Normal Lung Dose: This is to be calculated at the level of the central rays of the boost field at the point of maximum dose in the lung which lies at least 2 cm outside of the projected border of the initial treatment fields in the contralateral lung.
  - 5) Maximum Normal Tissue Dose: This is to be calculated at the level of the central rays of boost fields as the maximum total dose at least 2 cm outside of the target volume.

#### 5.3.8 Localization Films:

Localization films taken on simulators and/or on the treatment machine will be necessary in all cases.

#### 5.4 Anticipated Side Effects or Toxic Effects:

##### 5.4.1 Suggested Maximum Uncorrected Doses to Critically Sensitive Normal Structures

The following maximum doses to normal structures are suggested:

<u>Organ</u>	<u>Dose Schedules</u>
Normal	
Ipsilateral	25 Gy
Contralateral (only if necessary)	20 Gy

Spinal Cord (Maximum Dose)	
Cohort 1	30 Gy
Cohort 2 and 3	45 Gy
Heart	
Entire Organ	45 Gy
Less than 50%	50 Gy
Esophagus	
50%	60 Gy
5 cm	66 Gy

5.4.2 The uncorrected dose to the spinal cord must be limited to 30 Gy for patient cohort 1 and 45 Gy for cohort 2 and 3. A posterior spinal cord shield will not be an acceptable technique. Patient must be treated with an oblique or lateral field.

5.4.3 Reversible alopecia, bone marrow toxicity, skin pigmentation and esophagitis are expected side effects of radiation therapy, while radiation-induced myocarditis or transverse myelitis rarely occur at doses lower than 50 Gy. Radiation pneumonitis and subsequent fibrosis of the lung will occur in 100% of all patients receiving 40 Gy to the lung, usually within the first six months after initiation of treatment, so it is essential to spare all normal lung possible.

## 6.0 Drug Therapy

### 6.1 TARCEVA (erlotinib)

#### 6.1.1 Formulation:

TARCEVA tablets are available in three dosage strengths containing erlotinib hydrochloride 109.3 mg and 164 mg) equivalent to 25 mg, 100 mg and 150 mg erlotinib and the following inactive ingredients: lactose monohydrate, hypromellose, hydroxypropyl cellulose, magnesium stearate, microcrystalline cellulose, sodium starch glycolate, sodium lauryl sulfate and titanium dioxide. The tablets also contain trace amounts of color additives, including FD&C Yellow #6 (25 mg only) identification.

#### 6.1.2 Indication

TARCEVA is indicated for the treatment of patients with locally advanced or metastatic non-small cell lung cancer after failure of at least one prior chemotherapy regimen.

#### 6.1.3 Dosage and Administration

The recommended daily dose of TARCEVA is 150 mg taken at least one hour before or two hours after the ingestion of food. Treatment should continue until disease progression or unacceptable toxicity occurs. There is no evidence that treatment beyond progression is beneficial.

#### 6.1.4 Storage

Store at 25°C (77°F); excursions permitted to 15° - 30°C (59° - 86°F). See USP Controlled Room Temperature.

### 6.1.5 Supply

Tarceva will be supplied by Genentech.

TARCEVATM 382 (erlotinib) Tablets, 25 mg: Round, biconvex face and straight sides, white film-coated, printed in orange with a "T" and "25" on one side and plain on the other side. Supplied in bottles of 30 tablets (NDC 50242-062-01).

TARCEVATM (erlotinib) Tablets, 100 mg: Round, biconvex face and straight sides, white film-coated, printed in gray with "T" and "100" on one side and plain on the other side. Supplied in bottles of 30 tablets (NDC 50242-063-01).

TARCEVATM (erlotinib) Tablets, 150 mg: Round, biconvex face and straight sides, white film-coated, printed in maroon with "T" and "150" on one side and plain on the other side. Supplied in bottles of 30 tablets (NDC 50242-064-01).

## 6.2 Paclitaxel

### 6.2.1 Formulation

Paclitaxel is a poorly soluble plant product from the pacific yew, *Taxus brevifolia*. Improved solubility requires a mixed solvent system with further dilutions of either 0.9% sodium chloride or 5% dextrose in water. Vials will be labeled with shelf life. All solutions of paclitaxel exhibit a slight haziness directly proportional to the concentration of drug and the time elapsed after preparation, although when prepared as described above, solutions of paclitaxel (0.3-1.2 mg/ml) are physically and chemically stable for 27 hours.

### 6.2.2 Preparation

A sterile solution concentrate, 6 mg/ml in 5 ml vials (30 mg/vial) in polyoxyethylated castor oil (Cremophor EL) 50% and dehydrated alcohol, USP, 50%. The contents of the vial must be diluted just prior to clinical use. Paclitaxel for injection must be diluted before administration with 5% dextrose USP, 0.9% sodium chloride USP, or 5% dextrose in Ringer's injection to a final concentration of 0.3 to 1.2 milligrams/milliliter. This solution is stable for 27 hours under ambient temperature (25 degrees Celsius) and room lighting (Prod Info Taxol®, 1997). Use 5% polyolefin containers due to leaching of diethylhexphthalate (DEHP) plasticizer from polyvinyl chloride (PVC) bags and intravenous tubing by the Cremophor vehicle in which paclitaxel is solubilized.

Each bag/bottle should be prepared immediately before administration.

NOTE: Formation of a small number of fibers in solution has been observed after preparation of paclitaxel (NOTE: acceptable limits established by the USP Particular Matter Test for LVP's). Therefore, in-line filtration is necessary for administration of paclitaxel solutions. In-line filtration should be accomplished by incorporating a hydrophilic, microporous filter of pore size not greater than 0.22 microns (e.g.: Millex-GV Millipore Products) into the IV fluid pathway distal to the infusion

pump. Although particulate formation does not indicate loss of drug potency, solutions exhibiting excessive particulate matter formation should not be used.

#### **6.2.3 Administration**

Paclitaxel will be administered as a 60 minute IV infusion using non-PVC tubing and connectors, such as the IV administration sets (polyethylene or polyolefin) that are used to infuse parenteral nitroglycerin and/or fat emulsion. A 22 micron filter must be placed on the distal end of the infusion line. Nothing else is to be infused through the line where paclitaxel is being administered. Patients will receive prophylactic antiallergy premedication prior to paclitaxel administration as follows:  
Dexamethasone: 20 mg IV approximately 30 minutes prior to paclitaxel  
Diphenhydramine: 50 mg IV x 1 dose 30 min prior to paclitaxel (Note: if diphenhydramine is administered prior to erlotinib, repeat administration prior to paclitaxel is not required when given on the same day.)  
Ranitidine: 50 mg IV x 1 dose 30 minutes prior to paclitaxel

The premedication schedule can be altered at the discretion of the treating physician after the first paclitaxel dose.

#### **6.2.4 Storage**

Paclitaxel vials should be stored between 2°-25°C (36°-77°F).

#### **6.2.5 Adverse Effects:**

- Hematologic: Myelosuppression
- Gastrointestinal: Nausea and vomiting; diarrhea, stomatitis, mucositis, pharyngitis, typhilitis, ischemic colitis, neutropenic enterocolitis, increased liver function tests (SGOT, SGPT, bilirubin, alkaline phosphatase); hepatic failure, hepatic necrosis
- Heart: Arrhythmias, heart block, ventricular tachycardia, myocardial infarction (MI), bradycardia, atrial arrhythmia, hypotension, hypertension, lightheadedness
- Neurological: Sensory (taste), peripheral neuropathy, seizures, mood swings, hepatic encephalopathy, encephalopathy, sensation of flashing lights; blurred vision, scintillating scotoma
- Allergy: Anaphylactoid and urticarial reactions (acute); Stevens-Johnson Syndrome; flushing, rash, pruritus
- Other: Alopecia, fatigue, arthralgia, myopathy, myalgia, infiltration (erythema, induration, tenderness, rarely ulceration); radiation recall reaction.

#### **6.2.6 Supply**

Paclitaxel is commercially available.

### **6.3 Carboplatin**

#### **6.3.1 Formulation**

Carboplatin is supplied as a sterile lyophilized powder available in a single-dose vial containing 50 mg, 150 mg, and 450 mg of carboplatin for administration by intravenous infusion. Each vial contains equal parts by weight of carboplatin and mannitol.

### 6.3.2 Preparation

Immediately before use, the content of each vial must be reconstituted with either sterile water for injection, USP, 5% dextrose in water, or 0.9% sodium chloride injection, USP, according to the following schedule:

<u>Vial Strength</u>	<u>Diluent Volume</u>
50 mg	5 ml
150 mg	15 ml
450 mg	45 ml

These dilutions all produce a carboplatin concentration of 10 mg/ml. When prepared as directed, Paraplatin solutions are stable for eight hours at room temperature; since no antibacterial preservative is contained in the formulation, it is recommended that Paraplatin solutions be discarded eight hours after dilution.

### 6.3.3 Administration

Carboplatin will be administered after paclitaxel as an IV infusion over 30 minutes. The dose will be calculated based on the patient's actual body weight at each treatment visit and the AUC (area under curve) dosing.

The dose of carboplatin is calculated (in mg, not mg/m<sup>2</sup>) as follows, using the modified Calvert formula based on creatinine clearance:

AUC dose = Target AUC\* x (Creatinine clearance + 25)

The \*Target AUC for carboplatin treatment is AUC=2 (concurrent therapy) or AUC=6 (consolidation therapy).

The creatinine clearance used to calculate the carboplatin dose will be estimated, based on serum creatinine, using the Cockcroft-Gault formula:

For males:

$$\text{CrCl (mL/min)} = \frac{(140 - \text{age}) \times (\text{weight in kg})}{72 \times \text{serum creatinine in mg/dL}}$$

For females:

$$\text{CrCl (mL/min)} = 0.85 \times \frac{(140 - \text{age}) \times (\text{weight in kg})}{72 \times \text{serum creatinine in mg/dL}}$$

### 6.3.4 Storage



Unopened vials of Paraplatin are stable for the life indicated on the package when stored at controlled room temperature and protected from light.

#### 6.3.5 Adverse Events

- Hematologic: Myelosuppression
- Gastrointestinal: Nausea and vomiting; hepatic toxicity; electrolyte imbalance; hypomagnesemia; hypercalcemia
- Neurological: Peripheral neuropathy, ocular changes
- Other: Ototoxicity, myalgia, fatigue, allergic reaction

#### 6.3.6 Supply

Carboplatin is commercially available.

### 6.4 Dose Modifications

**6.4.1** Paclitaxel and carboplatin infusions will not be concurrently withheld if erlotinib is withheld. Likewise, if paclitaxel, carboplatin, or RT are delayed or withheld, erlotinib will not be concurrently delayed or withheld.

#### 6.4.2 Dose Levels

Patients will be treated at the following dose levels:

Dose Levels of Paclitaxel, Carboplatin, and Erlotinib			
	Starting Dose	Dose Level -1	Dose Level -2
<b>Concurrent Therapy <sup>3</sup></b>			
Paclitaxel	45 mg/m <sup>2</sup>	NA	NA
Carboplatin	AUC=2	NA	NA
<b>Consolidation Therapy <sup>b</sup></b>			
Paclitaxel	200 mg/m <sup>2</sup>	150 mg/m <sup>2</sup>	NA
Carboplatin	AUC=6	AUC=4.5	NA
<b>Erlotinib Dose Levels (post loading dose)</b>			
Erlotinib	150 mg	100 mg	50 mg

<sup>3</sup> For concurrent therapy, paclitaxel and carboplatin doses will not be adjusted.

<sup>b</sup> For consolidation therapy, dose reduction of paclitaxel and carboplatin below the -1 dose level will not be allowed. Dose reductions for erlotinib will not be allowed below the -2 dose level.

#### 6.4.3 Erlotinib Dose Modifications

As stated in Section 6.5.2, erlotinib dose reductions below the -2 dose level will not be allowed. All dose reductions are permanent; that is, there will not be any reescalation of erlotinib dose. If erlotinib is omitted for more than four consecutive doses for toxicity due to erlotinib or for an intercurrent illness (e.g., infection) requiring interruption of therapy, the

patient should be discontinued from further erlotinib therapy. If toxicities prevent the administration of erlotinib, the patient may continue to receive paclitaxel, carboplatin, and RT without erlotinib.

#### **6.4.3.1 Retreatment with Erlotinib Following Allergic/Hypersensitivity or Cytokine Release Reactions**

Once a erlotinib dose has been decreased due to an allergic/hypersensitivity or cytokine release reaction, it will remain decreased for all subsequent doses. If the patient has a second allergic/hypersensitivity or cytokine release reaction with the slower dose, the drug should be stopped, and the patient should receive no further erlotinib treatment. If a patient experiences a Grade 3 or 4 allergic/hypersensitivity or cytokine release reaction at any time, the patient should receive no further erlotinib treatment. If there is any question as to whether an observed reaction is an allergic/hypersensitivity or cytokine release reaction of Grades 1 – 4, the Study Chair should be contacted immediately to discuss the reaction.

If the patient experiences recurrent isolated drug fever following pre-medication and post-dosing with an appropriate antipyretic, the subsequent dosing should be 50% of the previous rate. If fever recurs following dose changes, the Investigator should assess the patient's level of discomfort with the event and use clinical judgment to determine if the patient should receive further erlotinib therapy.

#### **6.4.3.2 Erlotinib Dose Modifications for Rash**

The erlotinib dose will be modified as follows for erlotinib-related Grade 3 acnelike rash. The severity of these events will be graded according to the criteria for the CTCAE v3.0 term "Rash: acne/acneiform." Local or generalized rash with erythema and/or desquamation other than acne/acneiform should be coded separately as "Rash/desquamation." A rash that occurs within the radiation field should be coded separately as "Rash: dermatitis associated with radiation."

The Erlotinib dose alteration scheme for skin toxicity is outlined in the following figure. The first time a patient experiences a Grade 3 acne/acneiform rash, defined as acne/acneiform rash associated with pain, disfigurement, ulceration, or desquamation, erlotinib therapy is to be held for up to four consecutive doses with no change in the dose level. The Investigator also can consider concomitant treatment with topical and/or oral antibiotics; topical corticosteroids are not recommended. If the toxicity resolves to Grade 2 or less by the following treatment

period, treatment may resume. With subsequent occurrences of a Grade 3 acne/acneiform rash, erlotinib therapy again may be omitted for up to four consecutive weeks. Treatment may resume with reduced dose of erlotinib (see figure below) if skin toxicity has resolved to Grade 2 or less. erlotinib dose reductions are permanent. Erlotinib will be discontinued if there are more than four consecutive doses held or if there is a subsequent occurrence of a fourth episode of Grade 3 acne-like rash (rash/desquamation). The patient should be followed weekly until resolution of the rash.

If erlotinib is omitted for more than four consecutive doses for toxicity due to erlotinib, patients should be discontinued from further protocol therapy.

#### 6.4.4 Dose Modifications During Concurrent Therapy

##### 6.4.4.1 Paclitaxel/Carboplatin/Erlotinib Dose Modifications for Hematologic Toxicity

Toxicity NCI CTCAE Grade (CTCAE v3.0)	Paclitaxel Dose At Start of Subsequent Cycles of Therapy	Carboplatin Dose at Start of Subsequent Cycles of Therapy <sup>3</sup>	Erlotinib Dose at Start of Subsequent Cycles of Therapy <sup>3</sup>
Neutropenia 1 (1500-199/mm <sup>3</sup> )	Maintain dose level	Maintain dose level	Maintain dose level
2 (1000-1499/mm <sup>3</sup> )	Maintain dose level	Maintain dose level	Maintain dose level
3 (500-999/mm <sup>3</sup> )	Hold therapy <sup>b</sup>	Hold therapy <sup>b</sup>	Hold therapy <sup>b</sup>
4 (<500/mm <sup>3</sup> )	Hold therapy <sup>b</sup>	Hold therapy <sup>b</sup>	Hold therapy <sup>b</sup>
Neutropenic fever	Hold therapy <sup>b</sup>	Hold therapy <sup>b</sup>	Hold therapy <sup>b</sup>
Thrombocytopenia 1 (<LLN-75,000/mm <sup>3</sup> )	Maintain dose level	Maintain dose level	Maintain dose level
2 (50,000- 74,999/mm <sup>3</sup> )	Hold therapy <sup>b</sup>	Hold therapy <sup>b</sup>	Maintain dose level
3 (25,000- 49,999/mm <sup>3</sup> )	Hold therapy <sup>b</sup>	Hold therapy <sup>b</sup>	Maintain dose level
4 (<25,000/mm <sup>3</sup> )	Hold therapy <sup>b</sup>	Hold therapy <sup>b</sup>	Hold therapy <sup>b</sup>
Other Hematologic toxicities	Dose modifications for leucopenia are based on NCI CTCAE and are the same as recommended for neutropenia above.		

<sup>3</sup>Dose levels are relative to the starting dose in the previous cycle. Dose reductions of erlotinib below the -2 dose level will not be allowed. For concurrent therapy, paclitaxel and carboplatin doses will not be adjusted.

<sup>b</sup>repeat lab work weekly and resume chemotherapy based on this table.

**6.4.4.2** If paclitaxel and/or carboplatin doses must be withheld for greater than two consecutive weeks, the drug(s) will be held permanently

for the duration of concurrent therapy.

#### 6.4.4.3 Paclitaxel/Carboplatin/erlotinib Dose Modifications for Non-Hematologic Toxicity During Concurrent Therapy

Worst Toxicity NCI CTCAE Grade (CTCAE v3.0) <sup>a,d</sup>	Paclitaxel Dose At Start of Subsequent Cycles of Therapy <sup>b</sup>	Carboplatin Dose at Start of Subsequent Cycles of Therapy <sup>b</sup>	Erlotinib Dose at Start of Subsequent Cycles of Therapy <sup>b,c</sup>
<b>Nail Changes (paronychia)</b> Grade 2	Maintain dose level	Maintain dose level	Decrease by 1 dose level
<b>Neuropathy</b> ≤ Grade 1	Maintain dose level	Maintain dose level	Maintain dose level
Grade 2	Hold therapy until Grade 1 ≤ 1; restart at full dose <sup>e</sup>	Maintain dose level	Maintain dose level
Grade 3	Discontinue therapy	Maintain dose level	Maintain dose level
<b>Other non-hematologic toxicities <sup>c</sup></b> ≥ Grade 3	Hold treatment until ≤ Grade 2	Hold treatment until ≤ Grade 2	Hold treatment until ≤ Grade 2

- a For CTCAE Grade 2 non-hematologic toxicity not described above, excluding neuropathy, maintain dose level of all study. For neuropathy, follow the guidelines listed above.
- b Dose levels are relative to the starting dose in the previous cycle. Dose reductions of erlotinib below the - 2 dose level will not be allowed. For concurrent therapy, paclitaxel and carboplatin doses will not be adjusted.
- c With the exception of allergic/hypersensitivity or cytokine release reaction (see Section 6.5.3.2), acne-like rash (rash/desquamation) [see Section 6.5.3.3], anorexia, and viral infections. See Section 6.5.4.7 for treatment modifications for in-field GI and skin toxicity management.
- d Radiation therapy should continued to be delivered for . Grade 3 non-hematologic toxicities in or outside the radiation treatment field. RT should be held for all Grade 4 non-hematologic toxicity in or outside the treatment field and resumed only when toxicity is ≤ Grade 2.
- e See Section 6.4.4.5 for further neuropathy details.

In any case of erlotinib treatment delay, there will be no reloading dose, and all subsequent treatments will be at the current dose level.

#### 6.4.4.4 Carboplatin Dose Modifications for Renal Toxicity

A > 25% change in the serum creatinine, based on weekly calculated creatinine clearance, will warrant a recalculation of the carboplatin dose.

#### 6.4.4.5 Paclitaxel for Neuropathy

If paclitaxel doses must be withheld for greater than two consecutive weeks, the drug will be held permanently for the

duration of concurrent therapy (see Section 6.4.4.2).

**6.4.4.6** If there is a decline in Zubrod performance status to  $\geq 2$  for greater than 2 weeks while under treatment, radiotherapy should be held with no further chemotherapy administered. Re-evaluate patient after one week for resumption of radiotherapy.

**6.4.4.7** Paclitaxel/Carboplatin/RT Dose Modifications for In RT Field, Non-Hematologic Toxicity During Concurrent Therapy

Treatment Modification for In-Field Non-Hematologic Toxicity					
In-field	CTAE Toxicity Grade	XRT	Paclitaxel	Carboplatin	Erlotinib
Esophagus/pharynx (on day of treatment)	4	Hold treatment until $\leq$ Grade 2	Hold treatment until $\leq$ Grade 2	Hold treatment until $\leq$ Grade 2	Hold treatment until $\leq$ Grade 2
Esophagus/pharynx (on day of chemo)	3	No change or hold $\leq 5$ days (See section 7.5.4.10)	Hold treatment until $\leq$ Grade 2	Hold treatment until $\leq$ Grade 2	Hold treatment until $\leq$ Grade 2
Esophagus/pharynx (on day of chemo)	2	No change	No change	No change	No change
Pulmonary	4	Discontinue	Hold treatment until $\leq$ Grade 2	Hold treatment until $\leq$ Grade 2	Hold treatment until $\leq$ Grade 2
Pulmonary	3	Hold treatment until $\leq$ Grade 2	Hold treatment until $\leq$ Grade 2	Hold treatment until $\leq$ Grade 2	Hold treatment until $\leq$ Grade 2
Skin	4	Hold treatment until $\leq$ Grade 2	Hold treatment until $\leq$ Grade 2	Hold treatment until $\leq$ Grade 2	Follow guidelines in Section 6.5.3.3
Skin	3	No change	No change	No change	Follow guidelines in Section 6.5.3.3

**6.4.4.8** For Grade 4 infield esophagitis, radiotherapy and chemotherapy should be interrupted as detailed in the table above. Re-evaluate patient weekly.

**6.4.4.9** For Grade  $\geq 3$  esophagitis/pharyngitis, dermatitis, or other in-field radiotherapy-related toxicity, on day of chemotherapy administration during any treatment week, omit paclitaxel and carboplatin until toxicity resolves to grade  $\leq 2$  as detailed in the table above. For erlotinib skin toxicity management, follow the guidelines in Section 6.4.3.3.

**6.4.4.10** Radiotherapy should be interrupted only for Grade 4 in-field toxicity and resumed when that toxicity has decreased to Grade  $\leq 2$  as detailed in the table above. If treatment is interrupted for  $> 2$  weeks, the patient should be removed from study treatment. If the patient experiences esophagitis so that IV fluid support is needed, insertion of a feeding tube should be considered.

**6.4.4.11** For Grade 3 esophagitis, radiotherapy can be continued with



pain management and IV support, or radiotherapy can be held for  $\leq$  5 days until symptoms are  $\leq$  Grade 3.

#### 6.5. Paclitaxel/Carboplatin/Erlotinib Dose Modifications for Non-Hematologic Toxicity During Consolidation Therapy

Worst Toxicity NCI CTCAE Grade (CTCAE v3.0) <sup>a,d</sup>	Paclitaxel Dose At Start of Subsequent Cycles of Therapy <sup>b</sup>	Carboplatin Dose at Start of Subsequent Cycles of Therapy <sup>b</sup>	Erlotinib Dose at Start of Subsequent Cycles of Therapy <sup>b,c</sup>
Nail Changes (paronychia) Grade 2	Maintain dose level	Maintain dose level	Decrease by 1 dose level
<b>Neuropathy</b>			
$\leq$ Grade 1	Maintain dose level	Maintain dose level	Maintain dose level
Grade 2	Hold therapy until Grade $\leq$ 1; restart at full dose <sup>*</sup>	Maintain dose level	Maintain dose level
Grade 3	Discontinue therapy	Maintain dose level	Maintain dose level
Other non-hematologic toxicities <sup>e</sup> Grade 3	Hold treatment until $\leq$ Grade 2	Hold treatment until $\leq$ Grade 2	Hold treatment until $\leq$ Grade 2

<sup>a</sup> For . CTCAE Grade 2 non-hematologic toxicity not described above, excluding neuropathy, maintain dose level of all study drugs. For neuropathy, follow the guidelines above.

<sup>b</sup> Dose levels are relative to the worst toxicities in the previous cycle. Dose reductions of erlotinib below the -2 dose level will not be allowed. For concurrent therapy, paclitaxel and carboplatin doses will not be adjusted.

<sup>c</sup> With the exception of allergic/hypersensitivity reaction (see Section 6.5.3.2), acne-like rash (rash/desquamation) [see Section 6.5.3.3], anorexia, and viral infections. See Section 6.5.4.7 for treatment modifications for in-field GI and skin toxicity management.

<sup>d</sup> Radiation therapy should continue to be delivered for  $\leq$  Grade 3 non-hematologic toxicities in or outside the radiation treatment field. RT should be held for all Grade 4 non-hematologic toxicity in or outside the treatment field and resumed only when toxicity is  $\leq$  Grade 2.

<sup>e</sup> See Section 6.4.5.4 for further neuropathy details.

When a chemotherapy dose reduction is required during the consolidation course of therapy, re-escalation of the chemotherapy dose will not be allowed for subsequent doses during that specific course.

In any case of erlotinib treatment delay, there will be no reloading dose, and all subsequent treatments will be at the current level.

## **6.6 Duration of Treatment**

### **6.6.1 Discontinuation from Protocol Treatment**

Study therapy **MUST** be immediately discontinued for the following reasons:

- Withdrawal of consent (patient's decision to withdraw for any reason);
- Any clinical adverse event, laboratory abnormality, or intercurrent illness that, in the opinion of the Investigator, indicates that continued treatment with all study therapy is not in the best interest of the patient;
- Pregnancy;
- Progressive disease (Further treatment will be at the discretion of the treating physician).

The reason(s) for discontinuation from protocol treatment should be documented in the patient's medical record.

### **6.6.2 Treatment Compliance**

Trained medical personnel will administer study therapy. Treatment compliance will be monitored by drug accountability, as well as recording treatment administration in the patient's medical record.

### **6.6.3 This study will utilize the Common Terminology Criteria for Adverse Events (CTCAE) version 3.0 for grading of all treatment related adverse events.**

## **6.7 Reporting Requirements**

AE's should be reported in accordance with UTMDACC's policy (see appendix A)

## **7.0 Other Therapies**

### **7.1 Prohibited Therapies**

Patients should not receive any other anti-cancer drugs while receiving paclitaxel, carboplatin, or erlotinib, including hormonal and immunotherapy agents. Treatment with hormones or other chemotherapeutic agents will result in the patient's removal from the study. Exceptions are steroids administered for acute symptom management, adrenal failure, septic shock, or as antiemetics; or hormones administered for nondisease related conditions (e.g., insulin for diabetes). Colony stimulating factors (i.e., GCSF, GM-CSF, etc.) should not be administered. In case of myelotoxicity, dose reductions will be made. In addition, treatment with amifostine is not allowed during radiation or within 3 months of completion of radiation therapy.

### **7.2 Supportive Therapy**

Patients should receive full supportive care (except for colony stimulating factors) including transfusions of blood and blood products, antibiotics, antiemetics, etc., when appropriate. The use of erythropoietin (i.e., Epogen®, Procrit®) is permitted. Sucralfate slurries may provide symptomatic relief of mucositis and esophagitis. Post-treatment pneumonitis attributed to radiation should be treated with prednisone after excluding microbial causes. It is recommended that patients wear sunscreen and hats and limit sun exposure while receiving erlotinib therapy.

## **8.0 Pathology**

All patients need to have biopsy specimen and/or unstained histological slides available for review by Dr. Wistuba at UTMDACC for EGFR expression. The EGFR represents one of the most promising biomarkers studied to date with regard to clinical outcome in cancer. The results of current studies will expand and refine investigation of EGFR relationship to clinical outcome and may lead to identification of promising similar or new biomarkers with the goals of 1) identifying factors predictive of outcome such that patients may be better stratified in future trials, and 2) developing novel treatment strategies which target the molecular abnormalities identified. In this particular trial, we will gain specific information regarding any correlation between various forms of the EGFR (along with several downstream markers, such as phosphorylated MAPK, AKT, and Stat-3) and clinical outcome in patients who receive an EGFR inhibitory agent.

## **9.0 Treatment Plan**

## SCHEMA

### Concurrent Chemoradiation and Tarceva

Weeks 1-7:

Tarceva, 150 mg p.o. daily for 7 weeks, given before chemotherapy

+

Paclitaxel, 45mg/m<sup>2</sup>, and Carboplatin, AUC=2, weekly for 7 weeks

+

RT: 63 Gy/35 fractions/7weeks (+/- 5 days)

(1.8 Gy/ fraction, a total dose of 63.0 Gy in 35 fractions over 7 weeks)

Concurrent Chemoradiation should be completed within 9 weeks

### Consolidation therapy:

Weeks 8-10

Single agent Tarceva 150 mg P.O., daily for 3 weeks followed by

Weeks 11-16 Tarceva, 150 mg daily P.O., x 6 weeks, given before chemotherapy

+

Paclitaxel, 200 mg/m<sup>2</sup>, and Carboplatin, AUC=6, every 3 weeks for two cycles

## 10.0 Statistical considerations

### 10.1 Study Endpoints

**10.1.1 Primary Endpoint:** Feasibility of concurrent erlotinib and chemoradiation as measured by safety and compliance. Safety is measured by the rate of grade 3 or worse non-hematological toxicities occurring prior to the beginning of consolidation therapy (including all toxicities attributed to chemoradiation occurring within 90 days of the start of radiation therapy); compliance is defined as the completion of the treatment regimen with no more than minor variations.

**10.1.2 Secondary endpoints:**

- 10.1.2.1 Response rate (complete and partial response rates)
- 10.1.2.2 Overall survival rates (one and two year rates, median survival)
- 10.1.2.3 Time to progression rates (one and two year rates)
- 10.1.2.4 Association between EGFR expression and toxicity, response, overall survival, and progression (exploratory analysis)

## 10.2 Sample Size

The overall grade 3 or worse non-hematological toxicity rate for patients receiving concurrent chemotherapy and radiation followed by chemotherapy on BMSO/ACR 427, a randomized trial comparing three regimens in the treatment of locally advanced non-small cell lung cancer, was observed as 60%. This rate with the addition of erlotinib to the treatment regimen is of greatest interest in this study. Using a Fleming one-sample multiple test procedure<sup>44</sup> with Type I and Type II errors each set at 10% we would require 63 analyzable cases to reject a null hypothesis that the true toxicity rate of adding erlotinib to this therapy is greater than 75% in favor of the alternative hypothesis that the true rate is no more than 60%. Adjusting that number of cases by 5% to adjust for patient ineligibility, the primary endpoint requires at least 67 cases.

In order to adequately assess the clinical endpoint of survival, the sample size necessary to detect an increase median survival time (MST) from 17 months to 24 months will be calculated. An increase in MST to 24 months is justified by the results of the SWOG S950433, which showed an MST of 26 months in a similar patient population. With accrual of 5 patients per month, 12 months of follow-up, and an alpha of 0.10, a onesided test<sup>45</sup> on 80 patients has 81% statistical power. Because the primary endpoint is supported by the larger sample size required to detect a meaningful increase in MST, the sample size for this study will be 80 patients. Adjusting the number of accrued cases by 5% to allow for patient ineligibility, the targeted sample size is 84 cases.

Compliance is defined to be completion of concurrent chemoradiation plus erlotinib with no more than minor variations as defined (See Section 6.10). BMSO/ACR 427 had a compliance rate of 84% for patients receiving at least 6 cycles. Using a 95% exact confidence interval around a binomial proportion of compliant patients, with 80 analyzable patients we will have a maximum confidence interval width of 22.8%. If the compliance rate is the same as in BMSO/ACR 427 (i.e. 71 compliant cases out of the 80 analyzable, 85.0%) the width of the confidence interval will be 16.7%. If the observed compliance rate is at or no better than 46 cases out of 80 ( 53.75% with an exact 95% confidence interval of [ 42.2%, 64.97%]) – where the upper bound of the confidence interval is less than 65% – the regimen will be considered unfeasible.

## 10.3 Patient Accrual

We expect to see accrual of 2-3 patients per month.

## 10.4 Analysis and Reporting Plans

### 10.4.1 Interim Treatment Analyses for Early Stopping Due to Severe or



Excessive Nonhematologic Toxicities Accrual to this study will be suspended if any patient experiences a fatal treatment related toxicity. In the event that a patient has a fatal treatment related toxicity at any time, the study PI, will review the data and patient information to make appropriate recommendations about continuing the study. There will be five reviews of the rate of grade 3 or worse non-hematological toxicities within 90 days of the first day of radiation therapy. They will occur after the 10th, 20th, 30th, 60th, and 80th patients have been treated and followed for at least 90 days from the end of radiation therapy. According to Fleming's method, with Type I error of 0.15018 and Type II error of 0.14247, the rules are as follows:

Number of patients	Reject $H_0$ ( $\geq 75\%$ toxicity) if number of patients with grade 3 or worse non hematological	Reject $H_A$ ( $\leq 60\%$ toxicity) if number of patients with grade 3 or worse non hematological
	toxicities is $\leq$	toxicities is $\geq$
10	2 (20%)	N/A
20	9 ( 45%)	20 100%)
40	24 ( 60%)	32 ( 80%)
60	40 ( 67%)	44 (73%)
80	55 ( 69%)	56 ( 70%)

However, even if a boundary for rejecting  $H_0$  is reached at some point in the study, the study chairs may choose not to close the study so as to get better estimates of the endpoints (compliance, toxicity, response rate, survival rate, time to progression rate).

#### 10.4.2 Interim Analyses of Accrual and Toxicity Data

Interim reports will be prepared every 6 months until the initial manuscript reporting the treatment results has been submitted. The usual components of this report are:

- The patient accrual rate with a projected completion date for the accrual phase;
- The distribution of pretreatment characteristics;
- The frequency and severity of the toxicities.

The statistician will report any problems identified to the IRBcommittee.

#### 10.4.3 Analysis for Reporting Initial Treatment Results

This analysis will be done when all the patients accrued to the study have been potentially followed for a minimum of 12 months. It will include:

- Tabulation of all cases entered into the trial; exclusions with reasons;
- Distribution of important prognostic baseline variables;

d) Observed results for the endpoints listed in Section 10.1.

Overall survival will be plotted using Kaplan-Meier estimates and the MST tested using the methods of Lawless<sup>45</sup> in a one-sided test against the null value of 17 months MST.

Estimates of overall survival (calculated using the Kaplan-Meier method<sup>46</sup>) and time to progression (calculated using the method of cumulative incidence<sup>47</sup>) at one and two years will be calculated along with their associated 95% confidence intervals. Response (determined two months after completion of consolidation chemotherapy) is taken to be complete response (CR) or partial response (PR) using the new international criteria proposed by the Response Evaluation Criteria in Solid Tumors (RECIST) Committee [JNCI 92(3): 205-216, 2000]. Point and interval estimates of the proportion of patients with either PR or CR, using an exact 95% confidence interval, will be calculated. The exploratory analysis of EGFR expression and toxicity, response, and progression will be a chi-squared test for association after dichotomizing EGFR expression for each patient. The maximum reported toxicity for each patient will be dichotomized to < Grade 3 or . Grade 3; response will be categorized to CR, PR, or other than CR/PR; and progression will be dichotomized to yes/no. Patients will be grouped according to their dichotomized EGFR expression level and survival in the two groups will be compared.

#### **10.4.4 Analysis for Reporting Long-Term Results**

This analysis, if necessary, will be done when all the patients accrued to the study have been potentially followed for a minimum of 30 months or when all patients are dead.

## **11.0 Evaluation During Study**

### **11.1 Study Parameters**

Procedure	Pre-Treatment	During Therapy	End of Concurrent Therapy	End of all Protocol Therapy	Post Treatment Follow-up (See Section 11.2)
Medical History	X <sup>a</sup>		X		X
Physical Examination, Zubrod	X <sup>a</sup>	X <sup>d</sup>	X		X
RT and Med Onc consultation	X <sup>j</sup>				
Vital Signs	X <sup>a,b</sup>	X <sup>b</sup>			
Height and Weight and BSA	X <sup>a</sup>	X <sup>d,e</sup>	X <sup>e</sup>		
FEV1	X <sup>c</sup>		X		X <sup>k</sup>
EKG	X <sup>c</sup>		X		
Toxicity Assessment/Adverse Events		X	X		X
CBC with differential and platelet count, serum creatinine	X <sup>a</sup>	X <sup>d</sup>	X		X <sup>f</sup>
Electrolytes, Mg <sup>++</sup>	X	X <sup>d</sup>			
Bilirubin, SGOT or SGPT, alk. Phos., glucose	X <sup>a</sup>		X		X <sup>f</sup>
Pregnancy Test (urine or serum)	X <sup>h</sup>				
EGFR Assessment (optional)	X <sup>l</sup>				
CT Scan or MRI of Chest	X <sup>c</sup>		X		X <sup>g</sup>
Bone Scan <sup>m</sup>	X <sup>c</sup>				X <sup>f</sup>
CT Scan or MRI of Brain	X <sup>c</sup>				X <sup>f</sup>
PET Scan of chest	X <sup>l</sup>				
MUGA (if indicated)	X <sup>n</sup>				
Coagulation Profile (PT, PTT, INR)	X <sup>o</sup>	X <sup>d,o</sup>	X <sup>o</sup>	X <sup>o</sup>	X <sup>o</sup>

- a. Within 2 weeks prior to study entry;
- b. Prior to oral erlotinib , midway through intake, at completion of intake, and at one-hour post intake;
- c. Within 4 weeks prior to study entry; perform CT scan or MRI at a minimum of 1 cm slice thickness to include the lung apices through the adrenals. It is recommended that a consistent evaluation (CT or MRI) be used throughout the study.
- d. Weekly;
- e. Assess weight only; recalculate the BSA if there has been > 10% weight loss;
- f. At relapse;
- g. Recommended every 6 months for 2 years, then annually;
- h. For women of childbearing potential; within 72 hours prior to start of protocol treatment;
- i. If tissue is available; availability must be documented in chart at time of

registration.

- j. Approval to proceed must be received prior to initiation of study treatment.
- k. At 6 months after completion of consolidation therapy, then at 1 year
- l. Optional at pretreatment and 4 weeks after completion of concurrent therapy to assess acute toxicity
- m. A pretreatment PET scan, rather than a bone scan, is permitted to rule out bone metastases.
- n. If indicated
- o. If receiving anticoagulant agents

## 11.2 Post-treatment Follow up

A follow-up evaluation will be performed approximately 30 days following completion of all protocol treatment. In addition, all patients will be followed for a minimum of 30 days after the last dose of study therapy or every 4 weeks until all study drug related toxicities have resolved, returned to baseline, or are deemed irreversible, whichever is longer. Thereafter, patients will be seen for follow up every 3 months for 2 years, then every 4 months for 2 years.

## 11.3 Response Assessment (RECIST Criteria)

### 11.3.1 Measurement of Response

Response will be evaluated in this study using the international criteria proposed by the Response Evaluation Criteria in Solid Tumors (RECIST) Committee [JNCI 92(3): 205-216, 2000] See <http://ctep.info.nih.gov/guidelines/recist.html> for further details.

Only patients with measurable disease at baseline should be included in protocols where objective tumor response is the primary endpoint.

- Measurable disease - the presence of at least one measurable lesion; If the measurable disease is restricted to a solitary lesion, its neoplastic nature should be confirmed by cytology/histology.
- Measurable lesions - lesions that can be accurately measured in at least one dimension with longest diameter = 20 mm using conventional techniques or = 10 mm with spiral CT scan.
- Non-measurable lesions - all other lesions, including small lesions (longest diameter < 20 mm with conventional techniques or < 10 mm with spiral CT scan), i.e., bone lesions, leptomeningeal disease, ascites, pleural/pericardial effusion, inflammatory breast disease, lymphangitis cutis/pulmonis, cystic lesions, and also abdominal masses that are not confirmed and followed by imaging techniques

Response Criteria: Evaluation of target lesions

*Complete Response (CR):	Disappearance of all target lesions
*Partial Response (PR):	At least a 30% decrease in the sum of the LD of target lesions, taking as reference the baseline sum LD
*Progressive Disease (PD):	At least a 20% increase in the sum of the LD of target lesions, taking as reference the smallest sum LD recorded since the treatment started or the appearance of one or more new lesions
*Stable Disease (SD):	Neither sufficient shrinkage to qualify for PR nor sufficient increase to qualify for PD, taking as reference the smallest sum LD since the treatment started

## **12.0 Investigational Centers**

### **12.0 Investigational Centers**

Patients will be seen and enrolled at the University of Texas M. D. Anderson Cancer Center, Houston, TX.

#### **12.1 Investigator Contact Information**

##### **Principal Investigator:**

Ritsuko Komaki, MD  
University of Texas M.D. Anderson Cancer Center  
1515 Holcombe Blvd., Unit 097  
Houston, TX 77030  
Phone: 713-563-2300  
Fax: 713-563-2331  
Email: [rkomaki@mdanderson.org](mailto:rkomaki@mdanderson.org)

##### **Co-Principal Investigators:**

Roy Herbst, MD, PhD  
University of Texas M.D. Anderson Cancer Center  
1515 Holcombe Blvd., Unit 432  
Houston, TX 77030  
Phone: 713-792-6363  
Fax: 713-792-1220  
e-mail: [rherbst@mdanderson.org](mailto:rherbst@mdanderson.org)

Ray Meyn, PhD  
University of Texas M.D. Anderson Cancer Center  
1515 Holcombe Blvd., Unit 066  
Houston, TX 77030  
Phone: 713-792-7328  
Fax: 713-794-5369  
e-mail: [rmeyn@mdanderson.org](mailto:rmeyn@mdanderson.org)



Ignacio Wistuba, M.D.  
University of Texas M.D. Anderson Cancer Center  
1515 Holcombe Blvd., Unit 432  
Houston, TX 77030  
Phone: 713-792-6363  
Fax: 713-792-1220  
e-mail: [iwistuba@mdanderson.org](mailto:iwistuba@mdanderson.org)

## **13.0 Adverse Events**

### **13.1 Assessment of Adverse Event Severity & Relationship to Study**

All serious adverse events (defined below), whether or not deemed study-related or expected, must be reported by the Principal Investigator or designee to the HSRRB and/or USAMRMC, Deputy for Regulatory Compliance and Quality within 24 hours (one working day) by telephone. A written report must follow as soon as possible, which includes a full description of the event and any sequelae. This includes serious adverse events that occur any time after the inclusion of the subject in the study (defined as the time when the subject signs the informed consent) up to 30 days after the subject completed or discontinued the study. The subject is considered completed either after the completion of the last visit or contact (e.g., phone contact with the Investigator or designee). Discontinuation is the date a subject and/or Investigator determines that the subject can no longer comply with the requirements for any further study visits or evaluations (e.g., the subject is prematurely discontinued from the study). An adverse event temporarily related to participation in the study should be documented whether or not considered to be related to the test article. This definition includes intercurrent illnesses and injuries and exacerbations of preexisting conditions. Include the following in all IND safety reports: Subject identification number and initials; associate investigator's name and name of MTF; subject's date of birth, gender, and ethnicity; test article and dates of administration; signs/symptoms and severity; date of onset; date of resolution or death; relationship to the study drug; action taken; concomitant medication(s) including dose, route, and duration of treatment, and date of last dose.

A serious adverse event is any event that is: fatal; life-threatening (life-threatening is defined as the patient was at immediate risk of death from the adverse event as it occurred); significantly or permanently disabling; or requires in-patient hospitalization.

Important medical events that may not result in death, be life-threatening, or require hospitalization may be considered a serious adverse drug experience when, based upon appropriate medical judgment, they may jeopardize the patient or subject and may require medical or surgical intervention to prevent one of the outcomes listed in this definition. In addition, laboratory value changes may require reporting.

Reports of all serious adverse events must be communicated to the appropriate Institutional Review Board (IRB) or ethical review committee and/or reported in

accordance with local laws and regulations.

### **13.2 Procedures for Reporting Serious Adverse Events**

Serious and/or unexpected adverse events are submitted in writing to the M.D. Anderson Cancer Center Institutional Office of Protocol Research (OPR) within 5 working days of the adverse experience. Unexpected fatal or life-threatening experiences are phoned immediately to the Office of Protocol Research (713-792-2933). A follow up written report is submitted to OPR within 10 working days. The form for communication to OPR of all serious adverse events is appended to this plan.

Reports of all serious adverse events must be communicated to the appropriate Institutional Review Board (IRB) or ethical review committee and/or reported in accordance with local laws and regulations. Adverse experiences that are both serious and unexpected will be immediately reported by telephone to the USAMRMC, Deputy for Regulatory Compliance and Quality (301-619-2165) and send information by facsimile to 301-619-7803. A written report will follow the initial telephone call within 3 working days. Address the written report to the U.S. Army Medical Research and Material Command, ATTN: MCMR-RCQ, 504 Scott Street, Fort Detrick, Maryland 21702-5012.

For all protocols conducted at M.D. Anderson Cancer Center, the Principal Investigator is responsible for submitting adverse event reports to the Institutional IRB and the HSRRB and/or USAMRMC, Deputy for Regulatory Compliance and Quality on an ongoing basis. Adverse event reports are submitted to the Institutional Office of Protocol Research (OPR), where they are entered into PDMS and forwarded to the designated IRB vice chairperson for review. Any comments, questions or changes the IRB requests to the protocol as a result of this review are conveyed to the principal investigator. The investigator response and protocol modification process is monitored by the IRB vice-chairperson and OPR support staff. The vice chairperson presents the report on adverse event review to the full committee at the next IRB meeting.

Drug toxicities will be evaluated according to CTC version 3 (Appendix B). Reporting of adverse events will be according to M.D. Anderson Guidelines for AE Reporting (Appendix A).

Serious adverse events will be delivered to Clinical Research Compliance and will be submitted to the FDA by the regulatory compliance coordinator according to 21CFR 312.32.

### **13.3 Reporting of Subject Death**

The death of any subject during the study or within 30 days of study completion (as defined above), regardless of the cause, must be reported within 24 hours by

telephone, to the principal investigator and/or study coordinator and the HSRRB and/or USAMRMC, Deputy for Regulatory Compliance and Quality. A full written report must follow as soon as possible. If an autopsy is performed, the report must be provided to the Sponsor.

Reports of all **serious adverse events, including deaths**, must be communicated to the appropriate Institutional Review Board or ethical review committee and/or reported in accordance with local law and regulations.

#### **13.4 Known Adverse Events Relating to the Underlying Clinical Condition**

These will be reported on the chart and in PDMS (Protocol Data Management System).

### **14.0 Study Administration**

#### **14.1 Institutional Review Board**

This study must have the approval of a properly constituted Hospital Ethics Committee, Regional Ethics Committee, or other Institutional Review Board (IRB).

The investigator must also report all serious and medically significant adverse events to the IRB or Ethics Committee, as well as the USAMRMC, Deputy for Regulatory Compliance and Quality (see section 12).

#### **14.2 Informed Consent**

All study participants must sign and date an informed consent form prior to study participation. The investigator will be responsible for designing the consent form using appropriate National or Regional Guidelines (equivalent to the American Federal Guidelines Federal Register July 27, 1981, or 21 CFR Part 50, or International Committee on Harmonization-Good Clinical Practice).

The informed consent form must be approved by the IRB or Ethics Committee. State and local laws, and/or institutional requirements may require the disclosure of additional information on the informed consent form.

A copy of the informed consent form will be given to the participant. The investigator will keep each participant's signed informed consent form on file for inspection by a regulatory authority at any time.

#### **14.3 Record Retention**

The investigator and other appropriate study staff will be responsible for maintaining all documentation relevant to the study. Such documentation includes:

- Copies of all Serious AE reporting forms faxed to the USAMRMC, Deputy for Regulatory Compliance and Quality.

- Participant Files—should substantiate the data entered in PDMS with regard to laboratory data, participant histories, treatment regimens, etc.
- Participant Exclusion Log—should record the reason any participant was screened for the study and found to be ineligible.
- Drug Dispensing Log—should record the total amount of study drug received and returned to sponsor, and the amount distributed and returned or destroyed. This information must agree with the information entered in PDMS.
- Informed Consent Forms—completed consent forms from each participant must be available and verified for proper documentation.
- Informed Consent Log—must identify all participants who signed an Informed Consent Form so that the participants can be identified by audit.

The Investigator must keep on file protocols, amendments, IRB approvals, all copies of Form FDA 1572, all correspondence, and any other documents pertaining to the conduct of the study for a minimum of two (2) years after notification by USAMRMC, Deputy for Regulatory Compliance and Quality of either FDA approval or discontinuation of the IND.

#### **14.4 Drug Accountability**

For the drug supplied for this study, an accountability ledger containing current and accurate inventory records covering receipt, dispensing, and the return of study drug supplies must be maintained. Drug supplies must be kept in a secure, limited-access storage area under the recommended storage conditions. During the course of the study, the following information must be noted on the accountability ledger: the identification code of the subject to whom drug is dispensed, the date(s) and quantity of drug dispensed to the subject, and the date(s) and quantity of drug returned by the subject. Patients should return empty containers to the investigator, with the return noted on the ledger. These Accountability Forms must be readily available for inspection and are open to FDA inspection at any time.

#### **14.5 Study Monitoring**

The University of Texas M.D. Anderson Cancer Center Office of Institutional Compliance will monitor the study investigators to assure satisfactory enrollment rate, data recording, and protocol adherence. The investigator and staff are expected to cooperate and provide all relevant study documentation in detail at each site visit on request for review. M.D. Anderson Cancer Center will monitor and/or audit the other participating sites to assure satisfactory protocol adherence and enrollment.

##### **14.5.1 Medical Monitoring**

The medical monitor will review all serious and unexpected adverse events associated with this protocol and provide an unbiased written report of the event within ten (10) calendar days of the initial report. At a minimum, the medical monitor will comment on

the outcomes of the adverse event (AE) and relationship of the AE to the study. The medical monitor will also indicate whether he/she concurs with the details of the report provided by the study investigator.

The medical monitor for this study will be Maurie Markman, MD:

Maurie Markman, M.D.  
University of Texas M.D. Anderson Cancer Center  
Vice President, Clinical Research  
1515 Holcombe Blvd. - 424  
Houston, Texas 77030 USA  
Phone: 713/745-7140  
Fax: 713/563-9586  
Email: [mmarkman@mdanderson.org](mailto:mmarkman@mdanderson.org)

The medical monitor will forward reports to the U.S. Army Research and Material Command, ATTN: MCMR-RCQ, 504 Scott Street, Fort Detrick, Maryland, 21702-5012.

#### **14.6 Termination of Study**

The HSRRB and/or USAMRMC, Deputy for Regulatory Compliance and Quality and M. D. Anderson will retain the right to terminate the study and remove all study materials from the study site at any time. Specific instances that may precipitate such termination are as follows:

- Unsatisfactory participant enrollment with regard to quality or quantity
- Deviation from protocol requirements, without prior approval from HSRRB and M. D. Anderson.
- Inaccurate and/or incomplete data recording on a recurrent basis
- The incidence and/or severity of adverse drug events in this or other studies indicating a potential health hazard caused by the treatment

#### **14.7 Study Amendments**

The investigator will only alter the protocol to eliminate apparent immediate hazards to the participant. If preliminary or interim statistical analysis indicated that the experimental design, dosages parameters, or selection of participants should be modified, these changes will be described in an amendment to be approved by the institution's and other appropriate review committees after consultation with the statistician and Study Chairman. Any amendments cannot be enacted unless approved by the HSRRB and/or USAMRMC, Deputy for Regulatory Compliance and Quality. All revisions made to protocols previously approved by the IRB will be submitted to the IRB for approval prior to implementation of the revision. If the IRB decides to disapprove a research activity, it shall include in its written notification a statement of the reasons for its decision and give the investigator an opportunity to respond in person or in writing. No changes to the protocol will be initiated unless also approved by the Human Subjects Research Review Board.

## **14.8 Ethical and Legal Considerations**

This study will undergo full approval in accordance with the human surveillance requirements of each institution. Blood samples will be obtained for the evaluations as described in the protocol. Tissue samples obtained at the time of prior surgeries will be reviewed before participant enrollment to confirm the participant's diagnosis. Measures will be taken to ensure confidentiality of participant information. Tissue samples will be collected prospectively during the trial. Data collected on paper forms will be stored in locked file cabinets with restricted access. Data collected on electronic media will be stored in computer files with restricted password access. All staff members in the study will be informed prior to employment and at regular intervals of the necessity for keeping all data confidential. Computers will not be accessible to the public and will be located in locked offices. Subjects will be assigned a separate study number to protect subject identification. No patient identifiers will be used in any publications of this research. Data will be maintained indefinitely. When the time comes to dispose of the data, all database files will be deleted.

### **14.9 Risks/Benefits**

Participants will not be financially responsible for any study-related tests outside of accepted standard of care follow-up.

### **14.10 Gender and Minority Inclusion**

Women and minorities will be actively recruited to participate in the trial. However, since only 42% of lung cancer participants and 22% of laryngeal cancer participants are female, we expect to have more male than female subjects on the study. We expect that the ethnic distribution of the enrolled participants will reflect the local ethnic mixture of each institution's surrounding community.

### **14.11 Subject Records**

HSRRB and/or USAMRMC, Deputy for Regulatory Compliance and Quality, M.D. Anderson or their representatives may have access to subject records.

### **14.12 Publication Statement**

Data will be reviewed by the collaborating biostatistician prior to publication. HSRRB and/or USAMRMC, Deputy for Regulatory Compliance and Quality will have 30 days to review all definitive publications, such as manuscripts and book chapters, and a minimum of 10-15 days to review all abstracts.

### **14.13 Roles and Responsibilities of Key Study Personnel**

Dr. Ritsuko Komaki will serve as the Study Chairman for this protocol at M. D.



Anderson Cancer Center. She will assume primary responsibility for the study.

**Dr. Ray Meyn** will serve as Study Co-Chairman of this protocol.

**Dr. Roy Herbst** will serve as Study Co-Chairman of this protocol.

**Research Nurses** will identify eligible patients, schedule patients for collection of tissue and/or blood samples, coordinate the activities of oncologists/technicians, and be responsible for follow-up of patients.

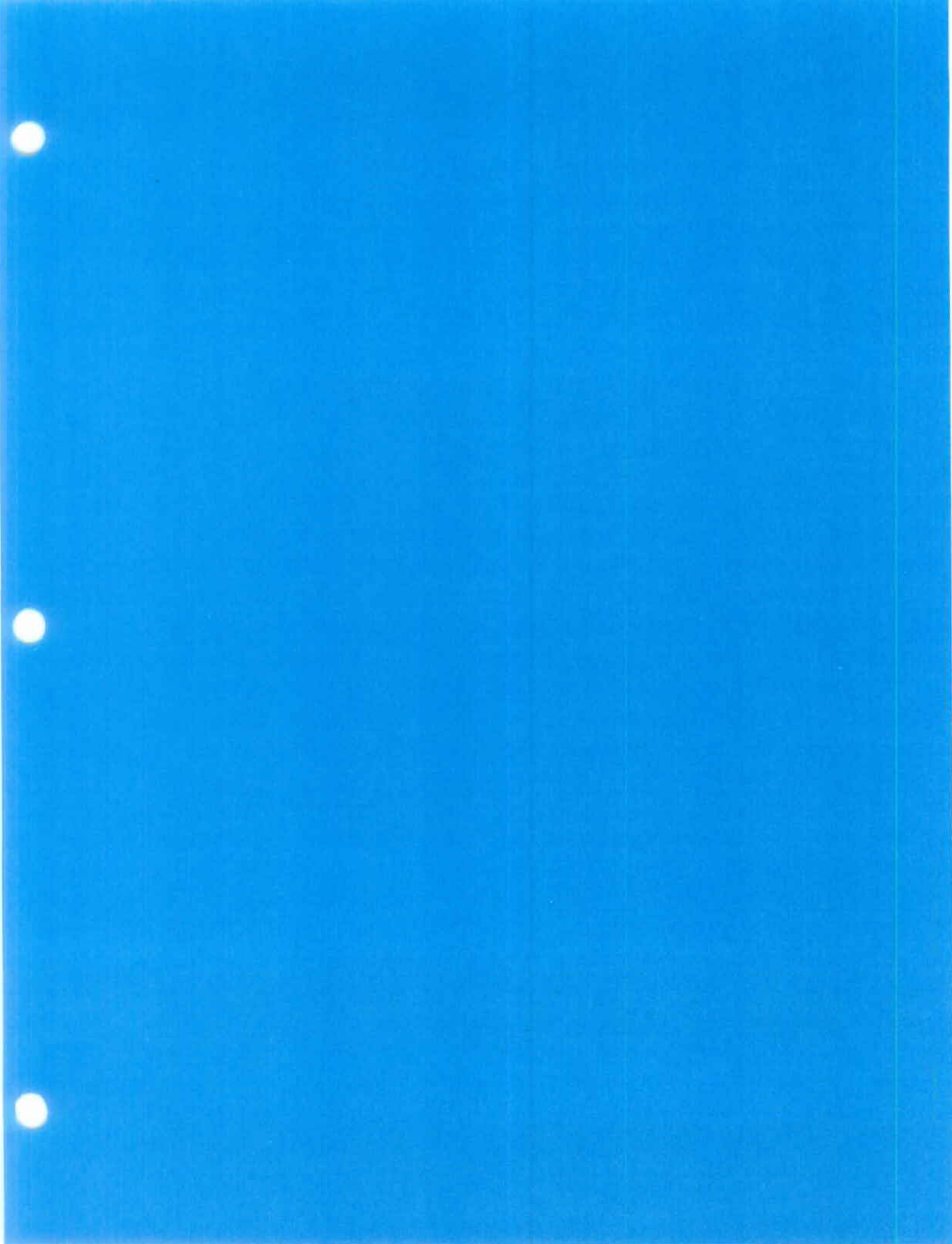
## 15.0 References

1. Cancer Facts and Figures 2002. American Cancer Society, 2003.
2. Dillman, RO, Herndon, J, Seagren, SL, et al. Improved survival in stage III non-small cell lung cancer: Seven year follow-up of Cancer and Leukemia Group B (CALGB) 8433 trial. J Natl Cancer Inst. 88:1210-1215, 1996.
3. Sause WT, Kolesar P, Taylor S, et al. Final results of phase III trial in regionally advanced unresectable non-small cell lung cancer: Radiation Therapy Oncology Group, Eastern Cooperative Oncology Group, and Southwest Oncology Group. Chest. 117(2): 358-64, 2000.
4. Le Chevalier T, Arriagada R, Tarayre M, et al. Significant effect of adjuvant chemotherapy on survival on locally advanced non-small cell lung carcinoma. J Natl Cancer Inst. 84: 58-59, 1992.
5. Schaafe-Koning, C, VanDen Bogeart W, Dalesio O, et al. Effects of concomitant cisplatin and radiotherapy on inoperable non-small cell lung cancer. NEJM. 326:524-530, 1992.
6. Lee JS, Scott CB, Komaki R, et al. Concurrent chemoradiation therapy with oral etoposide and cisplatin for locally advanced inoperable non-small lung cancer: Radiation Therapy Oncology Group protocol 91-06. J Clin Oncol. 14: 1055-1064, 1996.
7. Curran WJ, Scott C, Langer C, et al. Phase III comparison of sequential versus concurrent chemoradiation for patients with unresected stage III non-small cell lung cancer (NSCLC): Initial report of RTOG 9410. Proc Amer Soc Clin Oncol. 19:484a (abstract 1891), 2000.
8. Furuse K, Fukuoka M, Takada H, et al. A randomized phase III study of concurrent versus sequential thoracic radiotherapy in combination with mitomycin, vindesine, and cisplatin in unresectable stage III non-small cell lung cancer. Proc Amer Soc Clin Oncol. 16:459a, 1997.
9. Parness J, Horwitz SB. Taxol binds to cellular microtubules. J Cell Biol. 91: 479-487, 1981.
10. Manfredi JJ, Parness J, Horwitz SB. Paclitaxel (Taxol) binds to cellular microtubules. J Cell Biol. 94: 688-696, 1982.
11. Sinclair WK, Morton RA. X-ray sensitivity during the cell generation cycle of cultured Chinese hamster cells. Radiat Res. 29: 450-474, 1966.
12. Tishler RB, Schiff PB, Geard CR, Hall EJ. Taxol: A novel radiation sensitizer. Int J

- Radiat Oncol Biol Phys. 22: 613-617, 1992.
13. Choy H, Rodriguez FF, Koester S, Hilsenbeck S, Von Hoff DD. Investigation of Taxol, as a potential radiation sensitizer. *Cancer*. 71: 3774-3778, 1993.
  14. Choy H, Akerley W, Safran H, et al. A phase I trial of concurrent weekly paclitaxel (Taxol) administered as a 3-hr. infusion and radiation therapy for non-small cell lung cancer. *J Clin Oncol*. 12: 2682-2686, 1994.
  15. Choy H, Safran H, Akerley W, Graziano SL, Bogart JA, Cole BF. Phase II trial of weekly paclitaxel and concurrent radiation therapy for locally advanced non-small cell lung cancer (Trial 1). *Clin Cancer Res*. 4(8): 1931-6, 1998.
  16. Choy H, Akerley W, Safran H, et al. Multi-institutional trial of paclitaxel, carboplatin, and concurrent radiation therapy for locally advanced non-small cell lung cancer (Trial 2). *J Clin Oncol*. 16:3316-3322, 1998.
  17. Belani CP. Combined modality therapy for unresectable stage III non-small cell lung cancer: New chemotherapy combinations. *Chest*. 117(4 Suppl 1): 127S-132S, 2000.
  18. Choy H, Devore RF 3rd, Hande KR. A phase II study of paclitaxel, carboplatin, and hyperfractionated radiation therapy for locally advanced inoperable non-small-cell lung cancer (Trial 3) [a Vanderbilt Cancer Center Affiliate Network Study]. *Int J Radiat Oncol Biol Phys*. 47(4):931-7, 2000.
  19. Akerley W, Herndon J, Turrisi A, et al. Induction chemotherapy with paclitaxel (P) and carboplatin (C) followed by concurrent thoracic radiation and weekly PC for patients with unresectable stage III non-small cell lung cancer (NSCLC): Preliminary analysis of a phase II trial by the Cancer and Leukemia Group B. *Proc Amer Soc Clin Oncol*. 19: 490a (abstract 1915), 2000.
  20. Yarden Y, Ullrich A. Growth factor receptor tyrosine kinases. *Ann Rev Biochem*. 57:443-478, 1988.
  21. Van de Vijver MJ, Kumar R, Mendelsohn J. Ligand-induced activation of A431 cell epidermal growth factor receptors occurs primarily by an autocrine pathway that acts upon receptors on the surface rather than intracellularly. *J Biol Chem*. 266: 7503-7508, 1991.
  22. Baselga J, Norton L, Masui H, Pandiella A, Coplan K, Miller, Jr. WH, Mendelsohn J. Antitumor effects of doxorubicin in combination with anti-epidermal growth factor receptor monoclonal antibodies. *J Nat Cancer Inst*. 85:1327-1333, 1993.
  23. ImClone: Investigator Brochure. *ImClone Systems Incorporated*. erlotinib: Epidermal Growth Factor Receptor (EGFR) Antibody. Version 9.0, 2003.
  24. Al-Kasspoles M, Moore JH, Orringer MB, Beer DG. Amplification and over-expression of the EGFR and erbB-2 genes in human esophageal adenocarcinomas. *Int J. Cancer*. 54: 213-219, 1993.
  25. Grandis JR, Tweardy DJ. Elevated levels of transforming growth factor alpha and epidermal growth factor receptor messenger RNA are early markers of carcinogenesis in head and neck cancer. *Cancer Res*. 53: 3579-3584, 1993.
  26. Chou JL, Fan Z, DeBlasio T, Koff A, Rosen N, Mendelsohn J. Constitutive overexpression of cyclin D1 in human breast epithelial cells does not prevent G1 arrest induced by deprivation of epidermal growth factor. *Breast Cancer Res Treat*. 55:267-283, 1999.
  27. Fan Z, Shang BY, Lu Y, Chou JL, Mendelsohn J. Reciprocal changes in p27(Kip1) and p21(Cip1) in growth inhibition mediated by blockade or overstimulation of

- epidermal growth factor receptors. Clin Cancer Res. 3: 1943-1948, 1997.
28. Wu X, Fan Z, Masui H, Rosen N, Mendelsohn J. Apoptosis induced by an anti-epidermal growth factor receptor monoclonal antibody in a human colorectal carcinoma cell line and its delay by insulin. J Clin Invest. 95:1897-1905, 1995.
  29. Kawamoto T, Sato JD, Le A, Polikoff J, Sato GH, Mendelsohn J. Growth stimulation of A431 cell by EGF: Identification of high affinity receptors for epidermal growth factor by an anti-receptor monoclonal antibody. Proc Natl Acad Sci, USA. 80: 1337-1341, 1983.
  30. Mendelsohn J, Kawamoto T, Sato G, Sato J. Hybrid cell lines that produce monoclonal antibodies to epidermal growth factor receptor. United States Patent #4,943,533. July 24, 1990.
  31. Busam KJ, Capodieci P, Motzer R, Kiehn T, Phelan D, Halpern AC. Cutaneous side-effects in cancer patients treated with the antiepidermal growth factor receptor antibody C225. Br J Dermatol. 144(6): 1169-1176, 2001.
  32. H. Choy, WJ Curran, CB Scott, P Bonomi, et al. Preliminary report of locally advanced multimodality protocol (LAMP): ACR 427: A randomized phase II study of three chemo-radiation regimens with paclitaxel, carboplatin, and thoracic radiation (TRT) for patients with locally advanced non small cell lung cancer (LA-NSCLC). Proc Am Soc Clin Oncol. 21:291a (Abstract #1160), 2002.
  33. Gandara DR, Chansky K, Albain KS, et al. Southwest Oncology Group. Consolidation docetaxel after concurrent chemoradiotherapy in stage IIIB non-small-cell lung cancer: Phase II Southwest Oncology Group Study S9504. J Clin Oncol. 21(10): 2004-10, 2003.
  34. Perez-Soler R, Chachoua A, Huberman M, et al. A phase II trial of the epidermal growth factor receptor (EGFR) tyrosine kinase inhibitor OSI-774, following platinum-based chemotherapy, in patients with advanced, EGFR-expressing, non-small cell lung cancer (NSCLC). Proc Am Soc Clin Oncol. 20:1235 (abstract), 2001.
  35. Forouzes B, Hidalgo M, Takimoto C, et al. Phase I pharmacokinetic (PK) and biological studies of the epidermal growth factor-tyrosine kinase (EGFR-T) inhibitor OSI-774 in combination with docetaxel. Proc Am Soc Clin Oncol. 21:81(abstract), 2002.
  36. Fukuoka M, Yano S, Giaccone G, et al. Final results from a phase II trial of ZD1839 (Iressa) for patients with advanced non-small cell lung cancer (IDEAL 1). Proc Am Soc Clin Oncol. 21: 1188 (abstract), 2002.
  37. Kris MG, Natale RB, Herbst RS, et al. A phase II trial of ZD 1839 (Iressa) in advanced non-small cell lung cancer (NSCLC) patients who had failed platinum-and docetaxel-based regimens (IDEAL 2). Proc Am Soc Clin Oncol. 21: 1166 (abstract). 2002.
  38. Janne PA, Ostler PA, Lucca J, et al. ZD 1839 (Iressa) shows antitumor activity in patients with recurrent non-small cell lung cancer treated on a compassionate use protocol. Proc Am Soc Clin Oncol. 21:1274 (abstract), 2002.
  39. Bailey LR, Kris M, Wolf M, et al. Tumor EGFR membrane staining is not clinically relevant for predicting response in patients receiving gefitinib ('Iressa', ZD1839) monotherapy for pretreated advanced non-small-cell lung cancer: IDEAL 1 and 2. Proc Am Assoc Cancer Res. 44: abstract LB-170, 2003.

40. Baselga J, Pfister D, Cooper MR, et al. Phase I studies of anti-epidermal growth factor receptor chimeric antibody C225 alone and in combination with cisplatin. *J Clin Oncol.* 18:904-914, 2000.
41. Kelly N, Hanna N, Rosenberg P, Bunn PA, Needle MN. A multi-centered phase I/II study of erlotinib in combination with paclitaxel and carboplatin in untreated patients with stage IV nonsmall cell lung cancer. *Proc Amer Soc Clin Oncol.* Abstract 2592, 2003.
42. Robert F, Blumenschein K, Dicke K, Tseng J, Saleh MN, Needle MN. Phase Ib/IIa study of antiepidermal growth factor receptor (EGFR) antibody, erlotinib, in combination with gemcitabine/carboplatin in patients with advanced non-small cell lung cancer (NSCLC). *Proc Amer Soc Clin Oncol.* Abstract 2587, 2003.
43. Rischin D. 2003 ASCO Annual Meeting, and personal communication, N. Ready, M.D., PI of CALGB 30106.
44. Fleming T. One-sample multiple testing procedure for phase II clinical trials. *Biometrics.* 38:143-151, 1982.
45. Lawless JF. *Statistical Models and Methods for Lifetime Data.* New York: John Wiley and Sons;1982.
46. Kaplan EL, Meier P. Nonparametric estimation from incomplete observations. *J Amer Stat Assoc.* 53:457, 1958.
47. Kalbfleish JD, Prentice RL. *The Statistical Analysis of Failure Times Data.* New York: John Wiley and Sons; 1980.
48. Scott C, Sause W, Byhardt R, Marcial V, Pajak TF, Herskovic A, Cox JD. Recursive partitioning analysis of 1592 patients on four Radiation Therapy Oncology Group studies in inoperable nonsmall cell lung cancer. *Lung Cancer.* 17S(1): S59-S74, 1997.
49. Graham MV, Geitz LM, Byhardt R, et al. Comparison of prognostic factors and survival among black patients and white patients treated with irradiation for non-small cell lung cancer. *J Natl Cancer Inst.* 84: 1731-1735, 1992
50. Shepherd FA, Pereira JR, Ciuleanu T, Tan EH, et al. Erlotinib in Previously Treated Non-Samll-Cell Lung Cancer. *N Engl J Med* 2005;353:123-32.



## **APPENDIX B**

### **Revised Statements of Work**



## **Appendix B**

### **Revised Statements of Work**

#### **Project 4      Inhibition of bFGF Signaling for Lung Cancer Therapy**

- Task 1.      Determine the effects of bFGF on in vitro growth, survival, motility, invasion and angiogenesis of NSCLC cells and endothelial cells. (Years 1-2)
- Task 2.      Evaluate the potency of inhibitors of bFGF binding to receptor in inhibition of the effects of bFGF and evaluate the effects of these inhibitors in combination with paclitaxel on in vitro growth and survival of tumor cells. (Years 2-3)
- Task 3.      Evaluate anti-tumor activity of the most effective inhibitor identified in Specific Aim 2 when used alone and in combination with paclitaxel in an orthotopic lung cancer model using luciferase-expressing NSCLC cells for in vivo bioluminescence imaging of tumor growth and response to treatment. (Years 3-4)

**Extended Task:** To investigate the expression of bFGF and FGFR-1 and FGFR-2 by IHC staining of the tissue microarrays containing NSCLC tumors and their corresponding preneoplastic lesions.

#### **Project 5      Targeting mTOR and Ras signaling pathways for lung cancer therapy.**

- Task 1.      Conduct experiments to determine whether CCI-779 inhibits the growth of human NSCLC cells via G1 growth arrest or induction of apoptosis, and to identify the molecular determinants of CCI-779 sensitivity. (Year 1)
- Task 2.      Conduct experiments to determine whether the effect of CCI-779 on the growth of human NSCLC cells is enhanced in the presence of a PI3K inhibitor or a MAPK inhibitor. (Years 2-3)
- Task 3.      Conduct experiments to determine whether restoration of the Ras-dependent death-signaling pathway enhances the growth inhibitory effect of CCI-779 in human NSCLC cells. (Years 3-4)
- Task 4.      Conduct a pilot clinical biochemical induction trial to investigate the effect of CCI-779 in operable NSCLC patients and identify molecular determinants of CCI-779 sensitivity and prognosis. (Years 1-4)

**Modified Tasks** (replace CCI-779 in original Tasks 1-4 with RAD001):

- Task 1.      To determine whether mTOR inhibitor (RAD001) inhibits the growth of human NSCLC cells via G1 growth arrest or induction of apoptosis, and to identify the molecular determinants of mTOR inhibitor sensitivity
- Task 2.      To determine whether effects of mTOR inhibitor (RAD001) on the growth of human NSCLC cells is enhanced in the presence of a PI3K inhibitor or a MAPK inhibitor
- Task 3.      To determine whether restoration of the Ras-dependent death signaling pathway enhances the growth inhibitory effect of RAD001 in human NSCLC cells
- Task 4.      To conduct a pilot clinical biochemical induction trial to investigate the effect of RAD001 in operable NSCLC patients and identify molecular determinants of RAD001 sensitivity and prognosis.

## **Project 6 Identification of Novel Biomarkers and Therapeutic Targets in Aerodigestive Cancers**

- Task 1. Expression profile before- and after-treatment NSCLC and head and neck squamous cell carcinoma (HNSCC) patient samples and cell lines by DNA microarray technology. (Years 1-2)
- Task 2. DNA profile samples by complementing DNA approaches to stratify RNA expression profiles on the basis of their corresponding DNA profiles. (Years 1-4)
- Task 3. Evaluate the contribution of promoter hypermethylation and transcriptional inactivation of known cancer genes subject to epigenetic silencing to cancer phenotype. (Years 1-4)

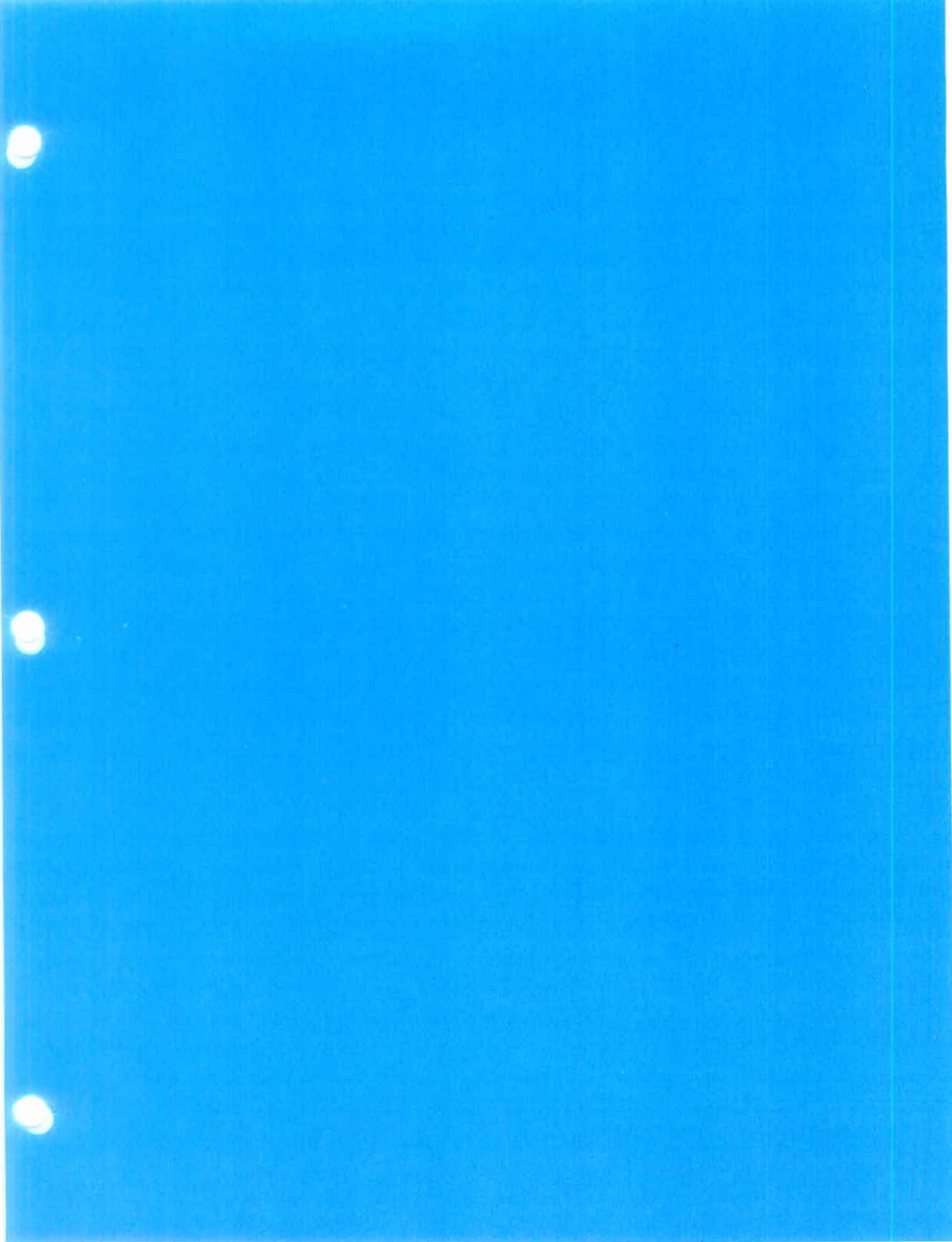
### **Extended Tasks 1- 3:**

To determine the *EGFR* mutation status of the NSCLC tumors from series of patients to stratify patients based on *EGFR* mutation status and characterize NSCLC tumors of patients (usually nonsmokers) with and without *EGFR* mutations of the same histology. To this end, we plan to enroll at least 15 patients in each group.

- Task 4. Determine protein signatures of Iressa treatment in NSCLC and to identify molecular predictors of treatment response. (Years 1-4)
- Task 5. Determine a clinical utility of the molecular predictors. (43-60 month)

### **Modified Tasks 4- 5 (replace Iressa with Tarceva):**

- Task 4:** To determine protein signatures of tarceva treatment in NSCLC and identify molecular predictors of response.
- Task 5:** To determine a clinical utility of the molecular predictors for tarceva treatment



## **Appendix C**

### **Protocol 2005-0929**

Treatment of Malignant Pleural Effusion with ZD6474, a Novel Vascular Endothelial Growth Factor Receptor (VEGFR) and Epidermal Growth Factor Receptor (EGFR) Tyrosine Kinase Inhibitor

Study Chair: Amir Onn, M.D.



## Protocol Page

Treatment of Malignant Pleural Effusion with ZD6474,  
a Novel Vascular Endothelial Growth Factor Receptor (VEGFR)  
and Epidermal Growth factor Receptor (EGFR) Tyrosine Kinase Inhibitor  
2005-0929

### Core Protocol Information

<b>Short Title</b>	ZD6474 Pleural Effusion
<b>Study Chair:</b>	Amir Onn
<b>Additional Contact:</b>	Alisha Thierry Mellanie J. Price
<b>Department:</b>	Thoracic and Head and Neck Med
<b>Phone:</b>	713-792-6363
<b>Unit:</b>	432
<b>Full Title:</b>	Treatment of Malignant Pleural Effusion with ZD6474, a Novel Vascular Endothelial Growth Factor Receptor (VEGFR) and Epidermal Growth factor Receptor (EGFR) Tyrosine Kinase Inhibitor
<b>Protocol Type:</b>	Standard Protocol
<b>Protocol Phase:</b>	Phase II
<b>Version Status:</b>	Re-Submitted 02/21/2006
<b>Version:</b>	02
<b>Submitted by:</b>	Mellanie J. Price--2/21/2006 1:03:02 PM

## 1.0 Introduction

### 1.1 Background and Significance

Recurrent malignant pleural effusion (MPE) is a debilitating condition, which is associated with a significant morbidity and worsening of quality of life (QOL). Overall median survival of patients with MPE is poor and it changes slightly by histology: breast cancer, 7.4 months; non-small cell lung cancer (NSCLC), 4.3 months; and ovarian cancer, 9.4 months. <sup>(1)</sup> Therapy of MPE is symptomatic and palliative, and consists of mechanical evacuation of the effusion to relieve pulmonary compression and dyspnea. There are no well-established methods of therapy, and the techniques used vary. They include repeated thoracentesis with small-bore catheters, tube thoracostomy, or video-assisted thoracic surgery for optimal drainage. Pleurodesis may be induced chemically by talc, tetracycline, doxycycline, bleomycin, or instillation of talc slurry. <sup>(1)</sup> Patient selection is required since these techniques may be associated with complications. <sup>(2)</sup> Several studies examined the utility of intrapleural drug administration for management of MPE. In a randomized trial, methylprednisolone did not delay reaccumulation of symptomatic pleural effusion compared to placebo. <sup>(3)</sup> Immunotherapy with OK-432 had been shown to be feasible and active for MPE in a small-randomized trial. <sup>(4)</sup> Recently a chronic indwelling pleural catheter has been introduced for the therapy of MPE. A randomized study examined its safety and efficacy versus tube thoracostomy and doxycycline sclerosis. <sup>(5)</sup> Outpatient treatment with indwelling pleural catheter was found to be safe and equivalent in efficacy to treatment with tube thoracostomy. <sup>(5)</sup> In addition, it was associated with fewer hospitalization days and was less expensive than inpatient methods. <sup>(6)</sup> Our common practice in recent years had been placement of the indwelling pleural catheter in all patients who had reaccumulation of symptomatic malignant pleural effusion.

Vascular Endothelial Growth Factor (VEGF), also known as vascular permeability factor (VPF), is considered one of the key regulators of pleural effusion pathophysiology <sup>(7)</sup> and high levels of VEGF were found in diverse exudative effusion in human patients. <sup>(8-10)</sup>

A direct relationship between VEGF production and pleural effusion formation by lung cancer tumor cells was found in an animal model. <sup>(11)</sup> Furthermore, transfection with an antisense to VEGF reduced pleural effusion formation in a highly VEGF expressing cell line, and transfection with sense VEGF to a cell line that did not produce pleural effusion, resulted in effusion formation. <sup>(11)</sup> Using the same animal model, a reduction in the formation of malignant pleural effusion was induced by inhibition of VEGF receptor tyrosine kinase phosphorylation, using PTK787 (Novartis, Switzerland). <sup>(12)</sup>

Another study demonstrated that pleural effusions and ascites from human patients activate human endothelial cell in vitro, in relation to the amount of VEGF in the fluid. Furthermore, this activation was reduced when the endothelial cells were treated with a VEGFR tyrosine kinase inhibitor. <sup>(13)</sup>



ZD6474[N-(4-bromo-2-fluorophenyl)-6-methoxy-7-[1-methylpiperidin-4-yl)methoxy]quinazolin-4-amine] is a novel tyrosine kinase developed by AstraZeneca.<sup>(14)</sup> It is a low molecular weight inhibitor of VEGFR2 (KDR) tyrosine kinase, which is also active against VEGFR3 and EGFR. This oral available compound has shown inhibition of VEGF signaling, angiogenesis and inhibited growth of human tumor cell xenografts in nude mice.<sup>(14)</sup> In addition, it has shown an anti tumor activity both in vitro and in vivo against tumor cells that expressed EGFR but not VEGFR2.<sup>(15)</sup> The results of the first phase I study of ZD6474 in patients with solid tumors were presented recently.<sup>(16)</sup> Eighteen Japanese patients with solid tumors refractory to standard therapy were recruited. Therapy at doses of  $\leq 300$  mg/day was well tolerated. Common adverse events in all groups were rash (n=14), asymptomatic QTc prolongation (n=11), diarrhea (n=10), proteinuria (n=10), and hypertension (n=7). Two patients developed dose-limiting toxicities (grade 3 SGPT elevation and grade 3 hypertension) at 400 mg/day, which was concluded to exceed the maximal tolerated dose. Cmax and AUC of ZD6474 linearly increased with dose. The t1/2 ranged from 72-196 hours, median 96 hours.

Recently Wu studied the effect of ZD6474, a dual VEGFR and EGFR tyrosine kinase inhibitor (AstraZeneca, UK), on mice bearing lung cancer tumors and pleural effusion. She demonstrated significant reduction in pleural effusion in association with VEGFR phosphorylation inhibition on tumor associated endothelial cells.<sup>(17)</sup>

## 1.2 Summary of Adverse Events (AE) in ZD6474

The most common AEs associated with ZD6474 in the phase I and other monotherapy studies included rash, diarrhea and asymptomatic QTc prolongation. In Study 6474IL/0006, patients with advanced or metastatic NSCLC were enrolled after failure of prior platinum-based chemotherapy. Patients were randomized to treatment with a standard dose of docetaxel and either placebo or 100 mg of ZD6474 or 300 mg of ZD6474. The median duration of therapy for each arm (docetaxel/placebo, docetaxel /ZD6474 100 mg, and docetaxel /ZD6474 300 mg) was 65 days, 91days, and 61.5 days, respectively. More patients discontinued therapy as a result of AEs for those who received 300 mg ZD6474 (22.7%) compared to those who received 100 mg (4.8%) or placebo (12.6%).

The AE profile was similar for all three treatment arms, although somewhat higher frequencies were observed for the 100 mg ZD6474 arm compared with placebo, and for the 300 mg ZD6474 arm compared with 100 mg ZD6474.

The most frequent AEs observed in this study were similar to those observed in prior trials for ZD6474 or reported for docetaxel in the literature. The most common AEs and their frequencies as reported in the 300 mg ZD6474, 100 mg ZD6474 and placebo arms, respectively, were diarrhea (50.0%, 38.1%, 24.4%), fatigue (45.5%, 40.5%, 26.8%), neutropenia (31.8%, 26.2%, 19.5%) and nausea (29.5%, 26.2%, 19.5%). Rash was observed in 15.9%, 16.7% and 9.8% of patients in the three arms.

Gastrointestinal events (77.3%, 59.5%, 41.5%), and skin events (72.7%, 64.3%, 41.5%) were more common in the ZD6474-containing arms. For all arms the majority of these events were common toxicity criteria (CTC) grade 1 and 2; however CTC grade 3/4 events were more prominent in the ZD6474 300 mg arm. Cardiac disorders occurred more frequently in ZD6474-containing arms (15.9%, 14.3%, 2.4%). The majority were CTC grade 1/2 and included a variety of terms, none ventricular. The frequency of respiratory events (50.0%, 57.1%, 46.3%) was similar in all arms. Neutropenia (31.8%, 26.2%, 19.5%) and related terms were more common in ZD6474-containing arms, but this did not result in an increase in infection. There was little difference in frequency of other hematologic events.

Approximately 10% of patients receiving ZD6474 developed an AE of hypertension. The majority of events were CTC grade 1 or 2, and no events were CTC grade 4. There were no serious adverse events (SAEs) of hypertension. The maximum median rise in both systolic and diastolic blood pressure was approximately 8 mm Hg in patients who received ZD6474 300 mg, and approximately 4 mm Hg in patients who received ZD6474 100 mg.

For the analysis of AEs that might have been caused by QT prolongation, AstraZeneca utilized the broad Special Medical Dictionary for Regulatory Activities (MedDRA) Query (SMQ) for QT prolongation. The terms queried included electrocardiogram (ECG) QT corrected interval prolonged, ECG QT interval abnormal, ECG QT prolonged, long QT syndrome, long QT syndrome congenital, Torsades de Pointes, ventricular tachycardia, cardiac death, sudden cardiac death, sudden death, cardiac arrest, cardiac fibrillation, cardiorespiratory arrest, ECG repolarization abnormality, ECG J wave abnormality, ECG U-wave abnormality, loss of consciousness, syncope, syncope vasovagal, ventricular arrhythmia, ventricular fibrillation, and ventricular flutter.

The only event that was actually reported in the randomized phase was ECG QT (corrected) interval prolonged, which occurred in 7, 5, and 2 patients treated with ZD6474 300 mg, ZD6474 100 mg, and placebo, respectively.

In addition, AstraZeneca reviewed the data for patients who experienced a confirmed prolongation of the ECG QTc interval, as specified in the protocol. Seven patients had confirmed QTc prolongation in this study. Five (16%) occurred on the ZD6474 300 mg/docetaxel arm, 4 of which occurred in the first 28 days and 1 at day 70. Two (12%) occurred on the ZD6474 100 mg /docetaxel arm, at days 22 and 43. No patients with confirmed QTc prolongation in study 6474IL/0006 experienced a potentially relevant AE. One patient in the run-in phase of trial 6 had received ZD6474 300 mg plus docetaxel, was hospitalized with a post-obstructive pneumonia as well as hypokalemia resulting from prednisone and fluorinef given to treat adrenal insufficiency resulting from adrenal metastases. He was noted to have a QTc interval of 626 millisecond (msec). During this hospitalization he developed a 12 beat run of ventricular tachycardia, which was asymptomatic and resolved without treatment.

### **1.3 Rationale**

On the basis of the results from the studies cited above, we hypothesize that inhibition of VEGFR activation may decrease pleural effusion production in cancer patients. To test this hypothesis, we propose to treat NSCLC patients who have an indwelling pleural catheter due to malignant pleural effusion with ZD6474. This compound inhibits VEGFR and also EGFR phosphorylation, and has shown a relatively safe profile at dose of 300 mg/day. Successful results of this study may improve the QOL of end stage cancer patients with recurrent pleural effusion, and may reduce the expenses associated with their disease.

## **2.0 Study Objectives**

### **2.1 Research Design and Methods**

Our goal is to better understand the biology of VEGF/VPF in vascular permeability and pleural effusion formation to improve therapy of malignant pleural effusion in lung cancer patients.

Based on our preclinical studies described in the background section, a clinical trial is planned to answer specific questions regarding the role of VEGF signaling and effect of its inhibition on NSCLC patients with MPE. In this study, eligible patients with recurrent symptomatic MPE who have an indwelling pleural catheter will be randomized to treatment with ZD6474, a VEGFR and EGFR inhibitor, or placebo.

The first aim is to achieve a beneficial clinical effect of ZD6474 on patients with MPE. The specific question is if ZD6474 alters pleural effusion re-accumulation following placement of an indwelling pleural catheter to the extent that it will enable significant shortening of time to removal of the catheter.

Additional aims will analyze the biology of VEGF signaling in MPE and will help to develop biomarkers of activity and noninvasive monitoring to such therapy:

The second aim is to analyze the amount of daily fluid drained with or without therapy.

The third aim is to assess radiographic correlates: Monthly chest CT to study effect on primary tumor burden, and measurement of vascular permeability using a dynamic contrast enhanced chest CT, which will be performed within 72 hours after initiation of ZD6474 therapy.

Our fourth aim is to study biological correlates. We will study the level of several factors and inflammatory cytokines in the effusion and in the serum at baseline and on a bi-weekly basis. We plan to study expression of VEGFR and EGFR on cells from effusion to demonstrate inhibitory effect of ZD6474 on receptor activation. Finally, we will study

the effect of ZD6474 therapy on level of circulating endothelial cells and circulating progenitor endothelial cells.

Our fifth aim is to assess drug effect on patient quality of life (QOL) and shortness of breath using standard questionnaires.

## **2.2 Primary Objective**

The primary objective of this study is to examine the effect of ZD6474 on the time between placement of an indwelling pleural catheter and its removal.

## **2.3 Secondary Objectives**

- 2.3.1 Measure the amount of pleural fluid drainage.
- 2.3.2 Study expression of VEGF, IL-6, IL-8, bFGF, LDH, protein, pH in serum and pleural effusion.
- 2.3.3 Study expression of VEGFR, EGFR and activated receptors on tumor cells collected from effusion.
- 2.3.4 Measure level of circulating endothelial cells and circulating endothelial progenitor cells in serum and pleural effusion.
- 2.3.5 Evaluate the effect of the study agent on tumor burden with chest CTs.
- 2.3.6 Evaluate the effect of the study agent on vascular permeability with Dynamic Contrast Enhanced Chest CTs.
- 2.3.7 Evaluate the effect of the study agent on QOL and shortness of breath using standard questionnaires.

## **3.0 Study Plan and Overview**

108 non-small cell lung cancer (NSCLC) patients with recurrent malignant pleural effusion will be recruited and treated with ZD6474 or placebo for 10 weeks.

### **3.1 Timeline**

In the first two years of the proposed project, we will conduct the clinical trial and collect samples and information. Biological correlates and data analysis will be performed in the third year.

### **3.2 Patient Recruitment**

Patients will be seen in and enrolled through the MD Anderson Thoracic Center.

### **3.3 Pretreatment Evaluations**

Unless otherwise noted, labs and physical exams are to be performed within 7 days of beginning treatment and imaging studies are to be performed within 30 days of beginning treatment.

3.3.1 Sign an informed consent.

3.3.2 Complete physical exam, including measurement of vital signs, performance status, height, weight.

3.3.3 Pretreatment laboratory tests:

- **Hematology:** CBC with differential, ANC, RBC, hematocrit, hemoglobin, and platelet count.
- **Chemistry:** Electrolytes, BUN, creatinine, glucose, albumin, alkaline phosphatase, ALT or AST, LDH, and total bilirubin.
- **Coagulation:** Prothrombin time (PT) and partial thromboplastin time (PTT).
- **Serum Pregnancy test:** Required for females of child-bearing potential. Must be obtained prior to first dose of ZD6474 and must be negative to enroll.
- **Imaging Studies:** Chest roentgenogram, chest CT of tumor burden, (optional) dynamic contrast enhanced chest CT of tumor

3.3.4 Screening 12-lead ECG

3.3.5 FACT-BRM quality of life questionnaire

3.3.6 Dyspnea visual analog scale

### 3.4 On-Study Evaluations

Eligible patients will undergo placement of an indwelling intrapleural catheter and will be randomized to ZD6474 or placebo on the day of the procedure. Patients will be treated for the whole period of 10 weeks, and clinical course of disease will be monitored throughout this time. (Note: Follow-up evaluations may be done within  $\pm$  3 days of the date specified in the protocol.)

3.4.1 Patients will document daily amount of pleural fluid drainage.

3.4.2 Patients will be evaluated every 4 weeks and at the time of removal from the study with complete interim histories and physical examinations including measurement of vital signs, performance status, and weight

3.4.3 Patients will complete a FACT-BRM quality of life questionnaire and dyspnea visual analog scale weekly for the first 4 weeks.

3.4.4 Blood samples for CBC with differential, platelet count, and PT/PTT will be collected every 4 weeks.

- 3.4.5 Tests to measure serum electrolytes, BUN, creatinine, glucose, albumin, alkaline phosphatase, AST or ALT, LDH, and total bilirubin will be performed every 4 weeks.
- 3.4.6 Chest roentgenogram and CT scan will be performed every 4 weeks or earlier, if clinically indicated, to determine amount of effusion and drug effect on tumor burden, following completion of the QOL and dyspnea tests.
- 3.4.7 Blood and pleural effusion will be collected at each clinic visit. Residual fluid collected may be used or stored for additional research studies (optional).
- 3.4.8 ECG weekly for the first 6 weeks, then every 4 weeks thereafter.
- 3.4.9 Optional: Blood will be collected every 4 weeks for biological correlates.
- 3.4.10 Optional: Drug effect on vascular permeability will be studied with dynamic contrast enhanced chest CT on patients with primary lesions > 3cm, up to 72 hours after initiation of therapy.

### **3.5 Subject Identification**

Upon enrollment, subjects will be assigned a study ID number. Patients will be consented by the treating physician and the research nurse. Witnesses will be clinic nurses or other members present during the informed consent interview process. Patients may request information and decide to enroll at a later date.

A unique master subject ID will be assigned to each individual participating in the study. A password protected secured file will be created to store the cross reference list between the master ID and confidential patient information such as name, birth date, hospital number, and social security number (if available), etc. Master ID will be used throughout the trial and in database for patient identification purpose. Confidential patient information will be used only when it is necessary such as in patient care setting.

## **4.0 Eligibility Criteria**

### **4.1 Inclusion Criteria**

- 4.1.1 Patients with pleural effusion requiring placement of an indwelling intrapleural catheter for recurrent symptomatic malignant pleural effusion.
- 4.1.2 Pathologic documentation of NSCLC.
- 4.1.3 Performance status 0 to 2 (Karnofsky scale).
- 4.1.4 No evidence of coagulopathy (INR  $\geq 1.5$  and PTT  $\geq 30$ )
- 4.1.5 Signed informed consent.
- 4.1.6 Subject must be female or male age 18 years or over

### **4.2 Exclusion Criteria**

- 4.2.1 Chemotherapy or other anticancer therapy in the 3 weeks prior to study. Radiotherapy will be allowed to extra thoracic sites 2 weeks prior to study.



- 4.2.2 No prior malignancy is allowed except for adequately treated basal cell or squamous cell skin cancer, in situ cervical cancer, or other cancer from which the patient has been disease-free for at least five years.
- 4.2.3 Laboratory results sustained at: Neutrophils less than  $1.5 \times 10^9/L$  or platelets less than  $100 \times 10^9/L$ ; Serum bilirubin greater than the upper limit of reference range (ULRR); Serum creatinine greater than  $1.5 \times$  ULRR or creatinine clearance  $\leq 50$  mL/minute (calculated by Cockcroft-Gault formula). Potassium,  $<4.0$  mmol despite supplementation; serum calcium (ionized or adjusted for albumin), or magnesium out of normal range despite supplementation; Alanine aminotransferase (ALT) or aspartate aminotransferase (AST) greater than  $1.5 \times$  ULRR or alkaline phosphatase  $>2.5 \times$  ULRR
- 4.2.4 Serious underlying medical condition that would impair the ability of the patient to receive protocol treatment, specifically cardiac diseases, uncontrolled hypertension or renal diseases.
- 4.2.5 Diagnosis of post-obstructive pneumonia or other serious infection in the 14 days prior to registration.
- 4.2.6 Any psychological, familial, sociological or geographical condition potentially hampering compliance with the study protocol and follow-up schedule.
- 4.2.7 Evidence of severe or uncontrolled systemic disease or any concurrent condition which in the Investigator's opinion makes it undesirable for the patient to participate in the trial or which would jeopardize compliance with the protocol
- 4.2.8 Clinically significant cardiac event such as Myocardial infarction; New York Heart Association (NYHA) classification of heart disease  $\geq 2$  (See Appendix C) within 3 months before entry; or presence of cardiac disease that in the opinion of the Investigator increases the risk of ventricular arrhythmia.
- 4.2.9 History of arrhythmia (multifocal premature ventricular contractions (PVCs), bigeminy, trigeminy, ventricular tachycardia, or uncontrolled atrial fibrillation) which is symptomatic or requires treatment (CTCAE grade 3) or asymptomatic sustained ventricular tachycardia. Atrial fibrillation, controlled on medication is not excluded.
- 4.2.10 Previous history of QTc prolongation with other medication that required discontinuation of that medication
- 4.2.11 Congenital long QT syndrome or 1<sup>st</sup> degree relative with unexplained sudden death under 40 years of age.
- 4.2.12 QTc with Bazett's correction that is unmeasurable, or  $\geq 480$  msec on screening ECG. If a patient has QTc  $\geq 480$  msec on screening ECG, the screen ECG may be repeated twice (at least 24 hours apart). The average QTc from the three screening ECGs must be  $<480$  msec in order for the patient to be eligible for the study).
- 4.2.13 Any concomitant medication that may cause QTc prolongation or induce Torsades de Pointes (See Appendix A) or induce CYP3A4 function (Refer to section 5.1.7)
- 4.2.14 Hypertension not controlled by medical therapy (systolic blood pressure greater than 160 mm Hg or diastolic blood pressure greater than 100 mm Hg)
- 4.2.15 Currently active diarrhea that may affect the ability of the patient to absorb the ZD6474.

- 4.2.16 Women who are currently pregnant or breast feeding
- 4.2.17 Participation in a clinical trial of any investigational agents within 30 days prior to commencing study treatment
- 4.2.18 In 2<sup>nd</sup> line or later, the last dose of prior chemotherapy is discontinued less than 3 weeks before the start of study therapy
- 4.2.19 In 2<sup>nd</sup> line or later, the last radiation therapy discontinued less than 2 weeks before the start of study therapy except palliative radiotherapy.
- 4.2.20 In 2<sup>nd</sup> line or later, any unresolved toxicity greater than CTC grade 1 from previous anti-cancer therapy
- 4.2.21 Previous enrollment or randomization of treatment in the present study.

### **4.3 Restrictions**

Because of the experimental nature of ZD6474, female patients must be one year post-menopausal, surgically sterile, or using an acceptable method of contraception (oral contraceptives, barrier methods, approved contraceptive implant, long-term injectable contraception, intrauterine device or tubal ligation). Male patients must be surgically sterile or using an acceptable method of contraception during their participation in this study.

Patients who are blood donors should not donate blood during the trial and for 3 months following their last dose of study medication.

## **5.0 Treatment Plan**

Patients will receive daily oral ZD6474 (300mg/day) or placebo. Patients will be instructed to take the ZD6474 at approximately the same time each morning.

We anticipate this study will be activated in March, 2006 and will be completed in August, 2008.

### **5.1 Study Drug**

#### **5.1.1 Accountability**

FDA regulations require investigators to establish a record of the receipt, use and disposition of all investigational agents. Investigators may delegate responsibility for drug ordering, storage, accountability and preparation to his/her designee. The Investigator, or the responsible party designated by the investigator, must maintain a careful record of the inventory and disposition of all agents dispensed as part of this study.

#### **5.1.2 Storage**

ZD6474 tablets have been shown to be chemically and physically stable to elevated temperature and humidity but exhibit slight photosensitivity when directly exposed to light. The supplied packaging provides the required level of protection from light, and normal handling in daylight should not present a problem. A storage life has been assigned to ZD6474 tablets when stored at controlled room temperature (20 to 25C; 68 to 77F) and protected from light. This shelf life will be reviewed periodically as more data become available.

The tablets should be stored in the original pack until use. For further information investigators should refer to the investigational product label.

### **5.1.3 Labeling**

AstraZeneca will pack tablets into high-density polyethylene (HDPE) bottles with child-resistant tamper-evident closures. Each bottle will be labeled with the statement: "Caution: New Drug - Limited by Federal (or USA) Law to Investigational Use". Instructions stating that the tablets are to be taken orally "as directed by your doctor" will be included. Information on the label will indicate the identity and quantity of tablets and storage conditions. There will be blank lines for trial number, patient number, center number, and date dispensed; this information should be recorded by the investigator at the time the bottle is dispensed.

### **5.1.4 Mechanism of Drug Destruction**

ZD6474 must be dispensed only from the study site by authorized personnel according to local regulations. It should be stored in a secure area according to local regulations. It is the responsibility of the Investigator to ensure that study drug is only dispensed to study patients. Unless otherwise instructed by AstraZeneca in writing, the Institution will destroy any supplies of ZD6474 that expire during this study. The Institution will destroy these materials in accordance with all applicable regulations and governmental guidelines and institutional policies.

Documentation indicating study drug was destroyed will be sent to AstraZeneca.

### **5.1.5 Possible Adverse Effects**

Data from rat and dog toxicology studies indicate that the principal toxicities of ZD6474 are associated with the liver (elevated transaminase levels, hepatocellular necrosis, and acute cholangitis), the gastrointestinal tract (emesis and diarrhea), the kidneys (papillary necrosis), and the skin (acute folliculitis). The gastrointestinal and skin effects are probably related to the EGFR activity of ZD6474.

Data from the first clinical trial also indicate a potential for rash and diarrhea with ZD6474; these effects appear to be dose related.

Please refer to section 1.2 for summary of Adverse events in ZD6474.

#### **5.1.6 Precautions for Treatment**

ZD6474 should not be administered to pregnant women. A negative pregnancy test should be confirmed before administration of ZD6474.

There is no known antidote for ZD6474, and treatment of adverse events associated with its use should be for the underlying adverse symptoms.

#### **5.1.7 Concomitant Treatment**

ZD6474 should not be administered in patients receiving drugs known to prolong QT interval or cause Torsades-de-Pointes. (See Appendix A for list of drugs known to prolong QT interval or cause Torsades-de-Pointes.)

Nausea, vomiting, or both may be controlled with antiemetic therapy. 5HT-3 antagonists may prolong QTc interval risk with use of Ondansetron. Increased monitoring is suggested and discussed below.

Concomitant use of the known potent inducers of CYP3A4: rifampicin, phenytoin, carbamazepine, barbiturates and St John's Wort are not allowed within 2 weeks of study or during the study.

Concomitant use of medications generally accepted as having a risk of causing Torsades de Pointes (see Appendix A) are not allowed within 2 weeks of study or during study.

The following medications can be taken by patients, but require additional monitoring:

- Co-administration of drugs that by some reports might be associated with Torsades de Pointes but at this time lack substantial evidence of Torsades de Pointes (see Appendix A, Table 2) should be avoided if possible. However, these drugs will be allowed, at the discretion of the Investigator, if considered absolutely necessary. In such cases, the patient must be closely monitored including regular checks of QTc and electrolytes. The ECG must be checked within 24 hours of commencing the concomitant medication and then at least once per week while the patient remains on the medication. The frequency of ECG monitoring could revert to the standard schedule if no ECG prolongation has been noted during 4 weeks of co-administration of a drug from Appendix A Table 2. The electrolytes

should be maintained within the normal range using supplements if necessary.

- Warfarin is allowed in therapeutic and low-doses and these patients should be monitored regularly for changes in their International Normalized Ratio (INR), at the discretion of the Investigator.

## 5.2 Dose Modification

See section 5.3.1 for guidance on dose reduction for QTc prolongation, skin toxicity, or gastrointestinal toxicity. For all other toxicity, the dose of study drug will be withheld for up to 3 weeks until the toxicity has resolved to CTCAE grade 1 or better, and then study treatment may be restarted. Dose reduction/re-challenge for each toxicity criterion will be managed as discussed in the sections that follow.

Patients will be withdrawn from the study if toxicity does not resolve to  $\leq$  CTCAE grade 1 within 3 weeks. If toxicity recurs during the study either at the same dose or reduced dose, the patient should be withdrawn from study treatment. The withdrawal visit should be performed as soon as possible after the last dose of ZD6474. The patient will continue to be followed for resolution of toxicity and disease progression, or for 12 months, whichever comes first.

## 5.3 Guidance on the management of toxicity

Guidelines are provided below for all cases where the dose of study drug has been reduced/modified or the patient has been withdrawn due to unusual or unusually severe toxicity considered related to the study treatment. For guidance on the management of QTc prolongation, see Figure 1 below.

For all other toxicity, the dose of study drug will be withheld for up to 3 weeks until the toxicity has resolved to CTCAE grade 1 or better, and then study drug may be restarted. Dose reduction/re-challenge for each toxicity criterion will be managed as discussed in the sections that follow.

Patients will be withdrawn from the study if toxicity does not resolve to  $\leq$  CTCAE grade 1 within 3 weeks. If toxicity recurs during the study either at the same dose or reduced dose, the patient should be withdrawn from study drug.

Dose reduction will be dependent on the original dose. A guideline for dose reduction is shown in the table below.

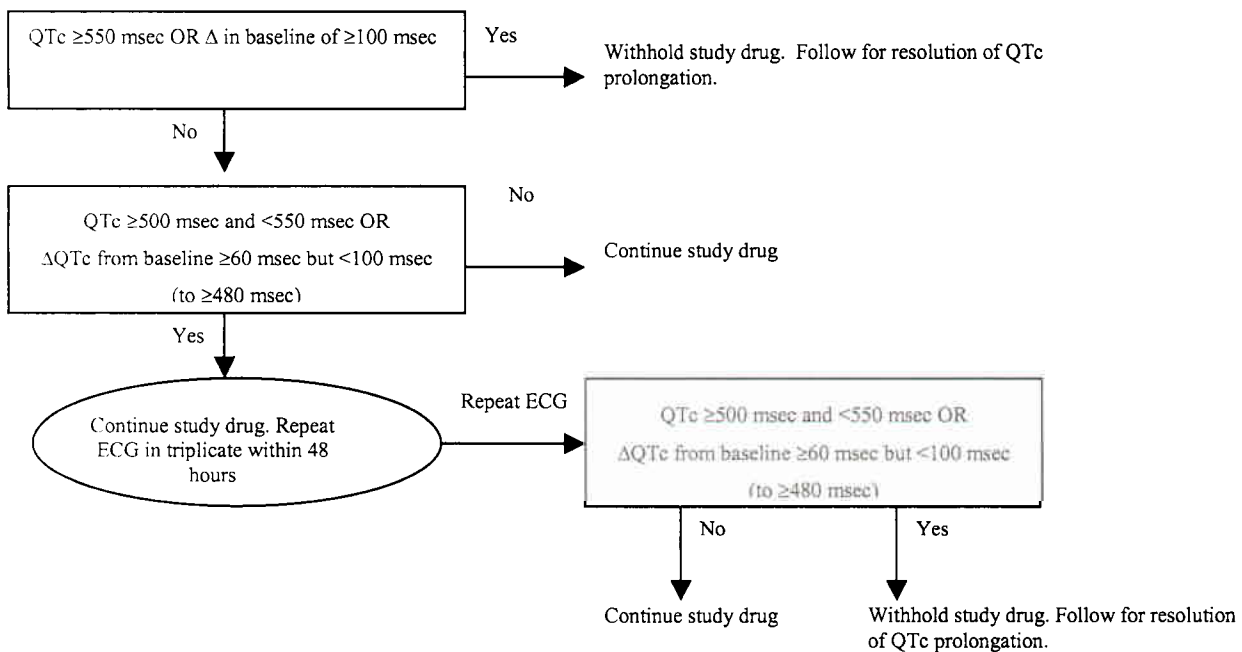
Original dose	Reduced dose	ZD6474 dispensed for reduced dose	Tablets per daily dose
300 mg	200 mg	100-mg ZD6474 tablets	2
200 mg	100 mg	100-mg ZD6474 tablets	1
100 mg	100 mg	50-mg ZD6474 tablets	1 every other day

### 5.3.1 QTc prolongation

Patients will have ECGs performed to monitor QTc interval (using Bazett's correction) as outlined in the study plan.



Figure 1 Flowchart detailing management of QTc prolongation



For this study QTc prolongation is defined as:

- A single QTc value of  $\geq 550$  msec or an increase of  $\geq 100$  msec from baseline;
- OR**
- Two consecutive ECG measurements, within 48 hours of one another, in which either of the following criteria is met:
    - A QTc interval  $\geq 500$  msec but  $< 550$  msec or
    - An increase of  $\geq 60$  msec, but  $< 100$  msec, from baseline QTc to a QTc value  $\geq 460$  msec.

The baseline will be the average of the screening and Day 1 pre-dose QTc values.

### Management of patients with QTc prolongation

For a single QTc value of  $\geq 550$  msec or an increase of  $\geq 100$  msec from baseline, ZD6474 must be withheld. ECGs and electrolytes should be followed 3 times a week until QTc falls below 480 msec or baseline, whichever is higher. ZD6474 treatment may be resumed at a lower dose after the QTc recovers to  $< 480$  msec or baseline.

For a QTc interval  $\geq 500$  msec, but  $< 550$  msec, or an increase of  $\geq 60$  msec but  $< 100$  msec from baseline QTc to a QTc value  $\geq 480$  msec, ZD6474 may be continued but a repeat ECG (in triplicate) must be obtained within 48 hours. If QTc prolongation is confirmed, ZD6474 should be withheld. ECGs and electrolytes should be checked 3 times a week until QTc falls below 480 msec or baseline, whichever is higher. ZD6474 treatment may be resumed at a lower dose, as outlined in section 3.3.5, after the QTc recovers to  $< 480$  msec or baseline. If the patient does not meet the criteria for QTc

prolongation at the repeat ECG then the patient should continue treatment and resume the ECG schedule as outlined in the Study Plan.

If ZD6474 is restarted after the QTc prolongation has resolved, ECGs should be performed 1, 2, 4, 7, 13 weeks and then every 3 months after treatment is restarted. If ZD6474 must be withheld for >3 weeks to allow for QTc prolongation to recover to <480 msec or baseline, the patient will not be restarted on study medication. If QTc prolongation recurs after the dose reduction as detailed, the patient must permanently discontinue treatment with study medication.

### **5.3.2 Management of skin toxicity**

It is strongly recommended that all patients follow a program of sun protective measures while receiving study therapy and for 3-4 weeks after discontinuing study therapy. The aim is to reduce the risk of development of skin rash, or minimize the severity of skin rash, and to minimize the requirement for dose reduction of study therapy.

If a patient develops a skin rash, the following actions are recommended to the Investigator for the management of this reaction:

- A variety of agents can be used to manage skin rashes. These include mild to moderate strength steroid creams, either topical or systemic antibiotics, topical or systemic antihistamines, and occasionally retinoid creams.
- The rash should be graded as soon as possible according to the CTCAE cutaneous toxicity criteria.
- If a rash of CTCAE grade 2 or higher is detected, immediate symptomatic treatment should be provided.
- If a rash of CTCAE grade 3 or higher is detected, ZD6474 should be withheld until recovery to grade 1 or below. The following actions should be instituted:
- ZD6474 should be dose reduced as per section 5.3.

If severe cutaneous toxicity recurs at reduced dose of ZD6474, the patient will permanently discontinue study treatment of ZD6474. If ZD6474 must be withheld for >3 weeks due to cutaneous toxicity, the patient will discontinue treatment.

### **5.3.3 Management of gastrointestinal (GI) toxicity**

Nausea, vomiting, or both may be controlled with antiemetic therapy. Diarrhea should be treated with standard medications to avoid dose modification or interruption, if possible. Electrolyte supplementation with regular laboratory monitoring should be used, when appropriate, to maintain electrolytes within normal limits and prevent an increased risk of QTc prolongation. No dose modifications will be made because of grade 1 or 2 diarrhea. If grade 3 diarrhea develops, ZD6474 should be withheld until

diarrhea resolves to grade 1 or below. Patients who are clinically unstable because of diarrhea or other intercurrent medical illness must be admitted and evaluated using telemetry, until clinically stable. Upon recovery, treatment may resume at a permanently reduced dose (refer to section 5.3). If ZD6474 must be withheld for more than 3 weeks for resolution of diarrhea, the patient will not restart treatment with study medication. If grade 3 or 4 diarrhea recurs after this dose reduction, the patient must permanently discontinue study treatment.

#### 5.3.4 Other Toxicity

If any other grade 3 or 4 toxicity that is not outlined in Sections 5.3.1 to 5.3.3 develops and is attributable to ZD6474, ZD6474 should be withheld until the toxicity resolves to grade 1 or below. Upon recovery, treatment may resume at a permanently reduced dose (refer to section 5.3). If ZD6474 must be withheld for more than 3 weeks for resolution of toxicity, the patient will not restart treatment with study medication. If grade 3 or 4 toxicity recurs after dose reduction, the patient must permanently discontinue study treatment. Patients who develop CTCAE grade 3 hypertension may continue on therapy if blood pressure is controlled on antihypertensive medication. If blood pressure cannot be stabilized with increased antihypertensive medication, study treatment must be discontinued and cannot be resumed until blood pressure is controlled to baseline level. Patients with CTCAE grade 4 hypertension should discontinue study treatment and cannot resume therapy until blood pressure is controlled to baseline level. If study treatment must be interrupted for more than 3 weeks to allow for toxicity to resolve, the patient's participation in the part of the study will be discontinued.

**Table 1**                      **Summary of guidance on the management of toxicity for ZD6474**

<b>Toxicity</b>	<b>ZD6474</b>
QTc value $\geq 550$ msec or prolonged $\geq 100$ msec from baseline	Withhold dose; if QTc recovers to $< 480$ msec or baseline, then reduce dose as per section 5.3.1. If QTc does not recover to $< 480$ msec or baseline within 3 weeks, patient will permanently discontinue ZD6474.
QTc value $\geq 500$ msec or prolonged $\geq 60$ msec from baseline	Continue dosing; repeat ECG (in triplicate) within 48 hours; if repeat ECG meets criteria, withhold dose; then if QTc recovers to $< 480$ msec or baseline, reduce dose as per section 5.3.1. If QTc does not recover to $< 480$ msec or baseline within 3 weeks, patient must permanently discontinue treatment with study medication. Or, if the repeat ECG does not meet criteria, patient should continue study medication.
Hematological toxicity as specified in section 5.3	No change
Platelets $< 100 \times 10^9/L$	No change
Grade 3 or 4 cutaneous	Withhold dose until toxicity has resolved to CTCAE grade 1 or less, then reduce dose as per section 5.3.2.

Toxicity	ZD6474
Grade 3 or 4 Peripheral neuropathy	No change
Grade 3 or 4 allergic reaction/hypersensitivity that is clearly attributable to docetaxel	No change
Severe fluid retention (grade 3 or 4 edema)	No change
Other grade 3 or 4 toxicity related to ZD6474	Withhold dose until toxicity has resolved to CTCAE grade 1 or less, then reduce dose as per section 5.3.4.

## 6.0 Statistical Considerations

This is a double-blind study to evaluate the effect of ZD6474 on the management of pleural effusion in NSCLC patients. The primary endpoint is the time from randomization, i.e., time of inserting Denver catheter, to the removal of Denver catheter. We plan to enroll 108 patients and randomize them with equal probability into either the ZD6474 arm or the placebo arm. A random permuted block design with a block size of 2 or 4 will be used. We assumed that the time to catheter removal follows an exponential distribution. It is estimated that the median time to removal for the placebo arm is 50 days while it decreases to 25 days in the ZD6474 treatment arm. A common dropout rate of 15% is assumed in both groups. Dropouts are due to complications produced by the catheter procedure and are not related to ZD6474 (non informative censoring). We assume that the time to drop out also follows an exponential distribution. All patients will be followed for up to 70 days; if the removal has not occurred by day 70, the observation will be treated as censored at day 70. With 108 patients randomized, the log rank test will have 80% power in detecting the difference in time to catheter removal between the two groups with a two-sided 5% significance level. We expect an accrual of 4 patients per month. This implies that it is required a 27-month accrual period and approximately 30 months for duration of the study (27 months plus 70 days of follow up for the last patient accrued). Sample size calculations were performed using nQuery and verified by our own simulation program. This was done by assuming instantaneous accrual rate, which is a reasonable assumption given that all patients will be followed for up to 70 days, regardless of the date of accrual.

For the primary analysis, patients who died before removal occurs will be censored at the time of death. Patients who withdraw from the study due to toxicity prior to the completion of the study will be treated as treatment failure at the time of withdraw. Competing risk models will be appropriate for this kind of data. In addition to the primary analysis stated above, we will also apply methods

for competing risk analysis (for example, the cmprsk package by Bob Gray) to estimate the subdistribution for each type of failure.

Based on the observations produced by the trial, we are interested in finding factors that may have influence on the time to catheter removal. Cox model analysis will be applied to examine the effect of covariates on the time to catheter removal. The effect of possible covariates including patient characteristics at baseline such as age, gender, histology and stage of disease, performance status, etc. will be evaluated. Univariate analysis will be performed first, followed with multi-covariate model by including significant covariates found in the univariate analysis ( $p < 0.05$ ). Best model can be determined by a forward stepwise regression with backward elimination procedure.

## **7.0 Investigational Centers**

Patients will be seen and enrolled at the University of Texas M. D. Anderson Cancer Center, Thoracic Center, Houston, TX.

### **7.1 Investigator Contact Information**

#### **Principal Investigator:**

Amir Onn, MD  
University of Texas M.D. Anderson Cancer Center  
1515 Holcombe Blvd., Unit 403  
Houston, TX 77030  
Phone: 713-563-6707  
Fax: 713-794-4922  
Email: [amironn@mdanderson.org](mailto:amironn@mdanderson.org)

#### **Co-Principal Investigators:**

Roy Herbst, MD, PhD  
University of Texas M.D. Anderson Cancer Center  
1515 Holcombe Blvd., Unit 432  
Houston, TX 77030  
Phone: 713-792-6363  
Fax: 713-796-8655  
e-mail: [rherbst@mdanderson.org](mailto:rherbst@mdanderson.org)

David J. Stewart, M.D.  
University of Texas M.D. Anderson Cancer Center  
1515 Holcombe Blvd., Unit 432  
Houston, TX 77030  
Phone: 713-792-6363  
Fax: 713-796-8655  
e-mail: [dstewart@mdanderson.org](mailto:dstewart@mdanderson.org)

Carlos A. Jimenez, M.D.  
University of Texas M.D. Anderson Cancer Center  
1515 Holcombe Blvd., Unit 403  
Houston, TX 77030  
Phone: 713-563-4255  
Fax: 713-794-4922  
e-mail: [cjimenez@mdanderson.org](mailto:cjimenez@mdanderson.org)

**Statistician:**

J. Jack Lee, PhD  
University of Texas M.D. Anderson Cancer Center  
1515 Holcombe Blvd., Unit 447  
Houston, TX 77030  
Phone: 713-794-4158  
Fax: 713-563-4242  
e-mail: [jjlee@mdanderson.org](mailto:jjlee@mdanderson.org)

**8.0 Criteria for Discontinuation on Study**

Patients will be removed from the study for any of the following reasons:

1. Patient requests to withdraw
2. Unwilling or unable to comply with study requirements
3. Unrelated intercurrent illness that will affect assessment of clinical status to a significant degree as determined by the principal investigator or the treating physician
4. The treating physician or investigator must discontinue study if he/she thinks that the patient's health or well-being is threatened by continuation on study.

Appropriate safety monitoring will continue until the patient is discharged from the study. Patients withdrawn from the study will be followed for survival. The reason for and date of the discontinuation will be obtained.

If a patient is non-compliant or lost to follow-up, the research nurse or his/her designee will make three attempts to call the patient over the period of one month. These attempts will be documented. If the research nurse or his/her designee is unable to make contact with either the patient or a family member after three phone calls, then a letter will be sent to the patient's last known address.

**9.0 Adverse Events**



## **9.1 Assessment of Adverse Event Severity & Relationship to Study**

All serious adverse events (defined below), whether or not deemed study-related or expected, must be reported by the Principal Investigator or designee to the HSRRB (Human Subjects Research Review Board) and/or USAMRMC (U.S. Army Medical Research and Materiel Command), Deputy for Regulatory Compliance and Quality within 24 hours (one working day) by telephone. A written report must follow as soon as possible, which includes a full description of the event and any sequelae. This includes serious adverse events that occur any time after the inclusion of the subject in the study (defined as the time when the subject signs the informed consent) up to 30 days after the subject completed or discontinued the study. The subject is considered completed either after the completion of the last visit or contact (e.g., phone contact with the Investigator or designee). Discontinuation is the date a subject and/or Investigator determines that the subject can no longer comply with the requirements for any further study visits or evaluations (e.g., the subject is prematurely discontinued from the study). An adverse event temporarily related to participation in the study should be documented whether or not considered to be related to the test article. This definition includes intercurrent illnesses and injuries and exacerbations of preexisting conditions. Include the following in all IND safety reports: Subject identification number and initials; associate investigator's name and name of MTF; subject's date of birth, gender, and ethnicity; test article and dates of administration; signs/symptoms and severity; date of onset; date of resolution or death; relationship to the study drug; action taken; concomitant medication(s) including dose, route, and duration of treatment, and date of last dose.

A serious adverse event is any event that is: fatal; life-threatening (life-threatening is defined as the patient was at immediate risk of death from the adverse event as it occurred); significantly or permanently disabling; or requires in-patient hospitalization.

Important medical events that may not result in death, be life-threatening, or require hospitalization may be considered a serious adverse drug experience when, based upon appropriate medical judgment, they may jeopardize the patient or subject and may require medical or surgical intervention to prevent one of the outcomes listed in this definition. In addition, laboratory value changes may require reporting.

Reports of all serious adverse events must be communicated to the appropriate Institutional Review Board (IRB) or ethical review committee and/or reported in accordance with local laws and regulations.

## **9.2 Procedures for Reporting Serious Adverse Events**

Serious and/or unexpected adverse events are submitted in writing to the M.D. Anderson Cancer Center Institutional Office of Protocol Research (OPR) within five working days of the adverse experience. Unexpected fatal or life-threatening experiences are phoned immediately to the Office of Protocol Research (713-792-

2933). A follow up written report is submitted to OPR within 10 working days. The form for communication to OPR of all serious adverse events is appended to this plan.

Reports of all serious adverse events must be communicated to the appropriate Institutional Review Board (IRB) or ethical review committee and/or reported in accordance with local laws and regulations. Adverse experiences that are both serious and unexpected will be immediately reported by telephone to the USAMRMC, Deputy for Regulatory Compliance and Quality (301-619-2165) and send information by facsimile to 301-619-7803. A written report will follow the initial telephone call within 3 working days. Address the written report to the U.S. Army Medical Research and Material Command, ATTN: MCMR-RCQ, 504 Scott Street, Fort Detrick, Maryland 21702-5012.

For all protocols conducted at M.D. Anderson Cancer Center, the Principal Investigator is responsible for submitting adverse event reports to the Institutional IRB and the HSRRB and/or USAMRMC, Deputy for Regulatory Compliance and Quality on an ongoing basis. Adverse event reports are submitted to the Institutional Office of Protocol Research (OPR), where they are entered into PDMS and forwarded to the designated IRB vice chairperson for review. Any comments, questions or changes the IRB requests to the protocol as a result of this review are conveyed to the principal investigator. The investigator response and protocol modification process is monitored by the IRB vice-chairperson and OPR support staff. The vice chairperson presents the report on adverse event review to the full committee at the next IRB meeting.

Drug toxicities will be evaluated according to CTC version 3 (Appendix B). Reporting of adverse events will be according to M.D. Anderson Guidelines for AE Reporting (Appendix J).

Serious adverse events will be delivered to Clinical Research Compliance and will be submitted to the FDA by the regulatory compliance coordinator according to 21CFR 312.32.

Investigators and other site personnel must inform the FDA of any serious or unexpected adverse event that occurs in accordance with the reporting obligations of 21 CFR 312.32, and will concurrently forward all such reports to AstraZeneca. A copy of the MDA safety report will be faxed to AstraZeneca at the time the event is reported to the FDA. It is the responsibility of the investigator to compile all necessary information and ensure that the FDA receives a report according to the FDA reporting requirement timelines and to ensure that these reports are also submitted to AstraZeneca at the same time.

A cover page should accompany the safety report form indicating the following:

- ZD6474 Investigator Sponsored Study (ISS)
- The investigator IND number assigned by the FDA
- The investigator's name and address
- The trial name and AstraZeneca Reference number

Send by way of fax to: (302) 886-1528, Attention ZD6474 ISS Safety Representative

If a non-serious AE becomes serious, this and other relevant follow-up information must also be provided to AstraZeneca and the FDA.

Serious adverse events that do not require expedited reporting to the FDA need to be reported to AstraZeneca preferably on a monthly basis and under no circumstance less frequently than quarterly.

In the case of blinded trials, AstraZeneca will request that the Sponsor either provide a copy of the randomization code or unblind those SAEs which require expedited reporting.

Nonserious adverse events should be reported to AstraZeneca quarterly, preferably using the MedDRA coding language for adverse events, serious and nonserious.

All SAEs have to be reported to AstraZeneca, whether or not considered causally related to the investigational product. All SAEs will be documented. The investigator is responsible for informing the IRB and/or the Regulatory Authority of the SAE as per local requirements.

### **9.3 Reporting of Subject Death**

The death of any subject during the study or within 30 days of study completion (as defined above), regardless of the cause, must be reported within 24 hours by telephone, to the principal investigator and/or study coordinator and the HSRRB and/or USAMRMC, Deputy for Regulatory Compliance and Quality. A full written report must follow as soon as possible. If an autopsy is performed, the report must be provided to the Sponsor.

Reports of all **serious adverse events, including deaths**, must be communicated to the appropriate Institutional Review Board or ethical review committee and/or reported in accordance with local law and regulations.

### **9.4 Known Adverse Events Relating to the Underlying Clinical Condition**

These will be reported on the chart and in PDMS (Protocol Data Management System).

## **10.0 Study Administration and Investigator Obligations**

### **10.1 Replacement of Subjects**

Participants who withdraw from the study prior to completion of the study treatments for reasons other than serious adverse events, unacceptable toxicity or progressive

disease will be defined as dropouts and will be replaced. Replacement participants will be assigned the next sequential number.

## **10.2 Institutional Review Board**

This study must have the approval of a properly constituted Hospital Ethics Committee, Regional Ethics Committee, or other Institutional Review Board (IRB).

The investigator must also report all serious and medically significant adverse events to the IRB or Ethics Committee, as well as the USAMRMC, Deputy for Regulatory Compliance and Quality (see section 9).

## **10.3 Informed Consent**

All study participants must sign and date an informed consent form prior to study participation. The investigator will be responsible for designing the consent form using appropriate National or Regional Guidelines (equivalent to the American Federal Guidelines Federal Register July 27, 1981, or 21 CFR Part 50, or International Committee on Harmonization-Good Clinical Practice).

The informed consent form must be approved by the IRB or Ethics Committee. State and local laws, and/or institutional requirements may require the disclosure of additional information on the informed consent form.

A copy of the informed consent form will be given to the participant. The investigator will keep each participant's signed informed consent form on file for inspection by a regulatory authority at any time.

## **10.4 Record Retention**

The investigator and other appropriate study staff will be responsible for maintaining all documentation relevant to the study. Such documentation includes:

- Case Report Forms—must be accurate and up-to-date.
- Copies of all Serious AE reporting forms faxed to the USAMRMC, Deputy for Regulatory Compliance and Quality.
- Participant Files—should substantiate the data entered in PDMS with regard to laboratory data, participant histories, treatment regimens, etc.
- Participant Exclusion Log—should record the reason any participant was screened for the study and found to be ineligible.
- Drug Dispensing Log—should record the total amount of study drug received and returned to sponsor, and the amount distributed and returned or destroyed. This information must agree with the information entered in PDMS.
- Informed Consent Forms—completed consent forms from each participant must be available and verified for proper documentation.
- Informed Consent Log—must identify all participants who signed an Informed Consent Form so that the participants can be identified by audit.

The Investigator must keep on file protocols, amendments, IRB approvals, all copies of Form FDA 1572, all correspondence, and any other documents pertaining to the conduct of the study for a minimum of two (2) years after notification by USAMRMC, Deputy for Regulatory Compliance and Quality of either FDA approval or discontinuation of the IND.

## **105 Study Monitoring**

The University of Texas M.D. Anderson Cancer Center Office of Institutional Compliance will monitor the study investigators to assure satisfactory enrollment rate, data recording, and protocol adherence. The investigator and staff are expected to cooperate and provide all relevant study documentation in detail at each site visit on request for review. M.D. Anderson Cancer Center will monitor and/or audit to assure satisfactory protocol adherence and enrollment.

Authorized representatives of AstraZeneca, a regulatory authority, an Independent Ethics Committee (IEC) or an Institutional Review Board (IRB) may visit the centre to perform audits or inspections, including source data verification. The purpose of an AstraZeneca audit or inspection is to systematically and independently examine all study-related activities and documents to determine whether these activities were conducted, and data were recorded, analyzed, and accurately reported according to the protocol, Good Clinical Practice (GCP), guidelines of the International Conference on Harmonization (ICH), and any applicable regulatory requirements. The investigator should contact AstraZeneca immediately if contacted by a regulatory agency about an inspection at his or her center.

### **10.5.1 Medical Monitoring**

The medical monitor will review all serious and unexpected adverse events associated with this protocol and provide an unbiased written report of the event within ten (10) calendar days of the initial report. At a minimum, the medical monitor will comment on the outcomes of the adverse event (AE) and relationship of the AE to the study. The medical monitor will also indicate whether he/she concurs with the details of the report provided by the study investigator.

The medical monitor for this study will be Maurie Markman, MD:

Maurie Markman, M.D.  
University of Texas M.D. Anderson Cancer Center  
Vice President, Clinical Research  
1515 Holcombe Blvd. - 424  
Houston, Texas 77030 USA  
Phone: 713/745-7140  
Fax: 713/563-9586  
Email: [mmarkman@mdanderson.org](mailto:mmarkman@mdanderson.org)

The medical monitor will forward reports to the U.S. Army Research and Material Command, ATTN: MCMR-RCQ, 504 Scott Street, Fort Detrick, Maryland, 21702-5012.

## **10.6 Termination of Study**

The HSRRB and/or USAMRMC, Deputy for Regulatory Compliance and Quality and M. D. Anderson will retain the right to terminate the study and remove all study materials from the study site at any time. Specific instances that may precipitate such termination are as follows:

- Unsatisfactory participant enrollment with regard to quality or quantity
- Deviation from protocol requirements, without prior approval from HSRRB and M. D. Anderson.
- Inaccurate and/or incomplete data recording on a recurrent basis
- The incidence and/or severity of adverse drug events in this or other studies indicating a potential health hazard caused by the treatment

## **10.7 Study Amendments**

The investigator will only alter the protocol to eliminate apparent immediate hazards to the participant. If preliminary or interim statistical analysis indicated that the experimental design, dosages parameters, or selection of participants should be modified, these changes will be described in an amendment to be approved by the institution's and other appropriate review committees after consultation with the statistician and Study Chairman. Any amendments cannot be enacted unless approved by the HSRRB and/or USAMRMC, Deputy for Regulatory Compliance and Quality. All revisions made to protocols previously approved by the IRB will be submitted to the IRB for approval prior to implementation of the revision. If the IRB decides to disapprove a research activity, it shall include in its written notification a statement of the reasons for its decision and give the investigator an opportunity to respond in person or in writing. No changes to the protocol will be initiated unless also approved by the Human Subjects Research Review Board.

## **10.8 Ethical and Legal Considerations**

This study will undergo full approval in accordance with the human surveillance requirements of each institution. Blood samples will be obtained for the evaluations as described in the protocol. Tissue samples obtained at the time of prior surgeries will be reviewed before participant enrollment to confirm the participant's diagnosis. Measures will be taken to ensure confidentiality of participant information. Tissue samples will be collected prospectively during the trial. Data collected on paper forms will be stored in locked file cabinets with restricted access. Data collected on electronic media will be stored in computer files with restricted password access. All staff members in the study will be informed prior to employment and at regular intervals of the necessity for keeping all data confidential. Computers will not be accessible to the public and will be located in locked offices. Subjects will be assigned a separate study number to protect subject



identification. No patient identifiers will be used in any publications of this research. Data will be maintained indefinitely. When the time comes to dispose of the data, all database files will be deleted.

### **10.9 Risks/Benefits**

Participants may benefit from ZD6474 therapy, which is a VEGFR tyrosine kinase inhibitor (TKI). Therapy with VEGFR TKI may result in decrease in pleural effusion accumulation and improvement in patient palliation.

The risks are the adverse event mentioned above – namely fatigue, nausea, vomiting, diarrhea, or QTc prolongation.

Participants will not be financially responsible for any study-related tests outside of accepted standard of care follow-up.

### **10.10 Gender and Minority Inclusion**

Women and minorities will be actively recruited to participate in the trial. However, since only 42% of lung cancer participants and 22% of laryngeal cancer participants are female, we expect to have more male than female subjects on the study. We expect that the ethnic distribution of the enrolled participants will reflect the local ethnic mixture of each institution's surrounding community.

### **10.11 Subject Records**

HSRRB and/or USAMRMC, Deputy for Regulatory Compliance and Quality, M.D. Anderson or their representatives may have access to subject records.

### **10.12 Publication Statement**

Data will be reviewed by the collaborating biostatistician prior to publication. HSRRB and/or USAMRMC, Deputy for Regulatory Compliance and Quality will have 30 days to review all definitive publications, such as manuscripts and book chapters, and a minimum of 10-15 days to review all abstracts.

### **10.13 Roles and Responsibilities of Key Study Personnel**

**Dr. Amir Onn** will serve as the Study Chairman for this protocol at M. D. Anderson Cancer Center. He will assume primary responsibility for the study.

**Dr. Roy Herbst** will serve as Study Co-Chairman of this protocol at M. D. Anderson Cancer Center. He will coordinate and supervise all aspects of the clinical trial,

supervise the biological correlate studies, and the preparation of results for presentations and publication.

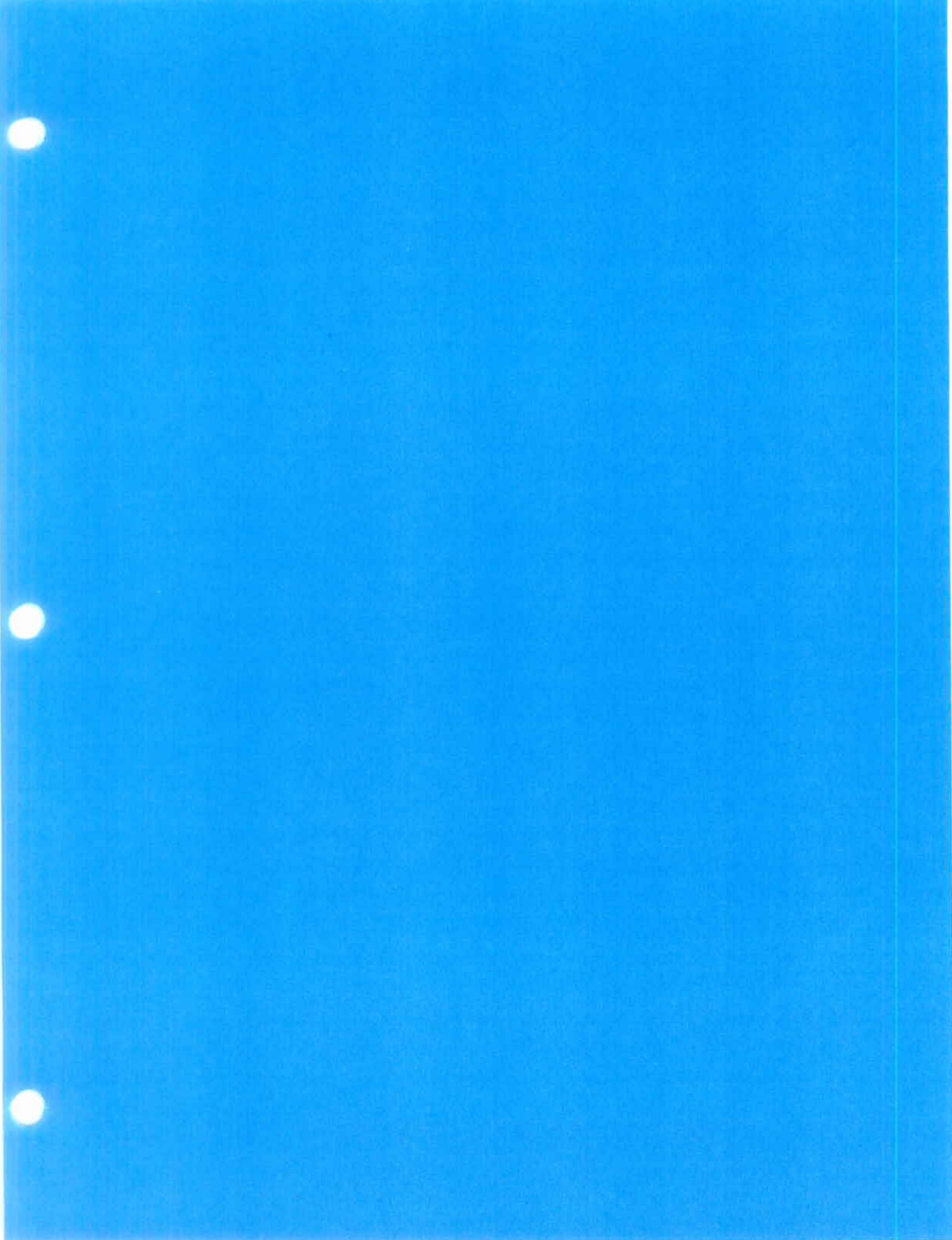
**Dr. David Stewart** will serve as a Study Co-Chairman of this protocol at M. D. Anderson Cancer Center. He will coordinate and supervise all aspects of the clinical trial, and preparation of results for presentations and publication.

**Dr. Carlos Jimenez** will assist with pleural procedures for patients enrolled in the clinical trial at M. D. Anderson Cancer Center.

## 11.0 References

1. Putnam JB. Malignant pleural effusions. *Surg Clin North Am* 82:867-83, 2002.
2. Bernard A. Early and late mortality after Pleurodesis for malignant pleural effusion. *Ann Thoracic Surg* 74:213-7, 2002.
3. North SA. A randomized, phase III, double-blind, placebo-controlled trial of intrapleural instillation of methylprednisolone acetate in the management of malignant pleural effusion. *Chest* 123:822-7, 2003.
4. Shibata K. Randomized phase II trial of OK-432 for malignant pleural effusion due to non-small cell lung cancer. *Proc ASCO*, abstract 2595, 2003.
5. Putnam JB. A randomized comparison of indwelling pleural catheter and doxycycline pleurodesis in the management of malignant pleural effusions. *Cancer* 86:1992-9, 1999.
6. Putnam JB. Outpatient management of malignant pleural effusion by chronic indwelling catheter. *Ann Thoracic Surg* 69:369-75, 2000.
7. Dvorak HF. VPF/VEGF: a critical cytokine in tumor angiogenesis and a potential target for diagnosis and therapy. *JCO* 20:4368-80, 2002.
8. Cheng DS. VEGF in pleural effusion. *Chest* 116:760-5, 1999.
9. Zebrowski BK. VEGF levels and induction of permeability in malignant pleural effusion. *CCR* 5:3364-8, 1999.
10. Thickett DR. VEGF in inflammatory and malignant pleural effusion. *Thorax* 54:707-10, 1999.
11. Yano S. Production of experimental malignant pleural effusions is dependent on invasion of the pleura and expression of VEGF/VPF by human lung cancer cells. *Am J Pathol* 157:1893-1903, 2000.
12. Yano S. Treatment of malignant pleural effusion of human lung adenocarcinoma by inhibition of VEGFR tyrosine kinase phosphorylation. *CCR* 6:957-65, 2000.
13. Verheul HMW. Targeting VEGF blockade: Ascites and pleural effusion formation. *The Oncologist* 5:45-50, 2000.
14. Wedge SR. ZD6474 inhibits VEGF signaling, angiogenesis, and tumor growth following oral administration. *Cancer Res* 62:4645-55, 2002.
15. Ciardiello F. Antitumor effects of ZD6474, a small molecule VEGFR tyrosine kinase inhibitor, with additional activity against EGFR tyrosine kinase. *CCR* 9:1546-56, 2003.
16. Minami H. A phase I study of an oral VEGF receptor tyrosine kinase inhibitor ZD6+474, in Japanese patients with solid tumors. *ASCO abstract #778*, 2003.
17. Wu W, Isobe T, Itasaka S, et al: ZD6474, a small molecule targeting VEGF and EGF receptor signaling, inhibits lung angiogenesis and metastasis and improves survival in an orthotopic model of non-small cell lung cancer. *Proc AACR* 4551, 2004.





## **APPENDIX D**

### **Project TALK**



## **APPENDIX D**

### **Stages of Interactive Multimedia CD-ROM Production**

#### **Intro**

The development of an interactive multimedia CD-ROM is a lengthy process that requires the efforts of various people with different skill sets to be carefully coordinated into the production of a well thought out and technically reliable end product. The production moves through various stages.

#### **Scientific Theory**

The early development period is more conceptual in nature. Very general questions like “What is the purpose of this study?” or “What scientific principles can be best applied to cause an effect?” must be answered by theorists that are involved in the project. All of the scientific underpinnings of the project must be agreed upon and noted for future reference. The materials that are subsequently developed must all refer back to and agree with the original theoretical concepts that were laid out at the beginning of the project. The length of this stage of development varies according to the complexity and scope of the project.

#### **Scripting**

In the next stage of development a writer specializing in multimedia development is brought in to translate the scientific concepts that have been agreed upon into a user-friendly form. The writer must first start by creating a large, all-encompassing framework for the project. Unlike traditional media, multimedia is interactive and tailors itself according to the user’s responses. Every user’s experience in the program will be unique. The framework the writer conceives must take into account all of the possible branch points the user navigates through as they progress through the program. The greater the amount of tailoring that is deemed necessary, the more complex this framework becomes. In this framework the writer must also account for the amount and type of media that can be produced in accordance with the media and programming budget for the project. The writer must also consult with the software programmer to ascertain the technical feasibility of the proposed ideas and the amount of production time needed. Once a framework has been laid out that meets budget and technical constraints the writer can progress to writing scripts for the necessary media pieces described in the framework.

These multimedia pieces can be of various forms like animations, videos, quizzes, games and texts. The writer creates scripts for these media pieces. The scripts are reviewed by the theorists for scientific relevance and the software programmer for technical feasibility. This is an iterative process that requires many cycles of writing and revision. Once the framework and scripts are given the green light the project can go into “production”. The importance of a clear and well-thought out framework cannot be emphasized enough. Poorly thought out software projects that go into hurried production usually incur great losses of time and money (See references).

#### **Production: Media development and Software Programming**

The production phase of the project requires the coordinated efforts of media artists with the software developer. The media artists create the components necessary for the program. They create the graphics, animations and videos that are described in the scripts. The software

developer integrates these components into a programming framework that adheres to the writer's conceptualizations as closely as possible.

In a large, complex project, the software developer will usually complete a small section of the program that is representative of the entire program and have it tested before continuing with the entire project. Sometimes what "looks good on paper" does not always translate into the imagined outcome so having the theorists, the writer and a sampling of typical users evaluate a small section of the program is a good money and time saving idea and assures some quality control. Once approval for the small section is agreed upon the software developer will complete the programming for the entire project.

Ideally, it's a good idea to once again have the theorists, writer and some typical users evaluate the completed product and give it one last review. The developer will then incorporate this last batch of "tweaks" into the program.

### **Final Testing and Debugging**

The programmer will then proceed to thoroughly test and de-bug the program. Considering the complexity of multimedia programs this is a lengthy process. The programmer will also test the program across various computing platforms for operating system and hardware compatibility.

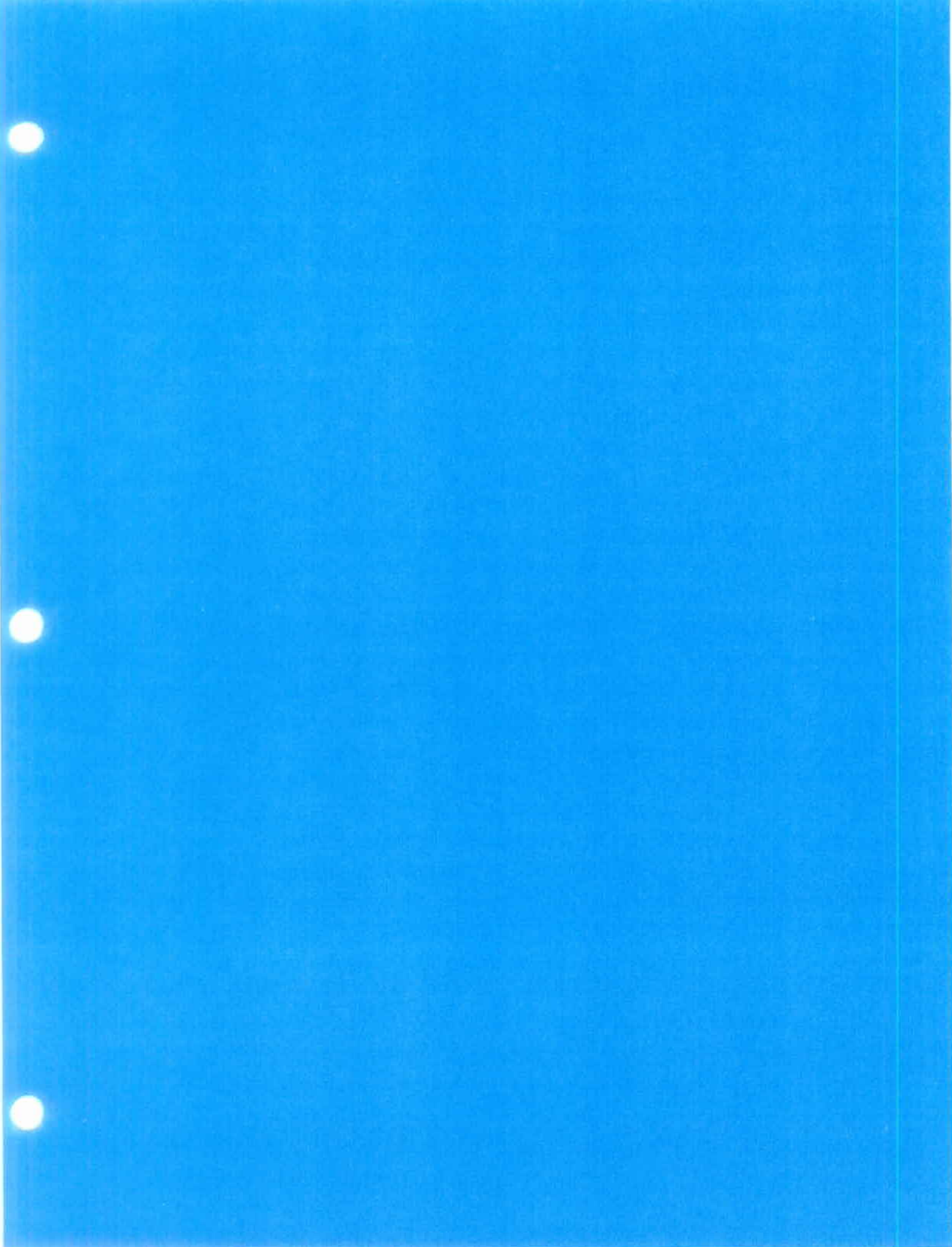
### **Conclusion**

Producing a large, interactive multimedia CD-ROM project is a time consuming process. To be successful it requires the close collaboration of people with differing scientific, artistic and technical backgrounds. With careful and patient management these talents can be coordinated together to produce a successful end product.

### **References:**

Code Complete by Steve McConnell (1993)

The Pragmatic Programmer by Andrew Hunt and David Thomas (2000)



## **APPENDIX E**

### **PROJECT TALK**

## **APPENDIX E**

### **Module Scripts Module Graphics (Working Documents)**

1. SI Module Scripts
2. SII Module Scripts
3. Avitar Builder
4. Initial User Interface Screen
5. Operating Room Screen
6. Health Administration Room Screen

## **SI Module Scripts: Smokers Not Willing to Quit Module**

### **S1\_1 Stage Intro**

Visual: Dark, shadowy, ugly hospital admissions room. The waiting room chairs are filled with an assortment of shady characters.

Guide: Welcome to <<cough, cough>> Nicotiana, a place some never escape. You're in the admitting room. It looks like you've already filled out your forms. Now we just need them in triplicate. Just kidding, <<coughing, choking, laugh>>.

Guide: It looks like you've diagnosed yourself as a smoker who doesn't want to quit. Now that's scary...but see for yourself. Right through that door you'll learn about the physical and health consequences of smoking.

Guide: Think you can handle it? I'm following you.

Visual: Door at end of room opens. Player and guide move through.

### **S1\_1 Administration Room – Short and Medium -Term Health Consequences** *Health Track*

Visual: Player and guide find themselves in menacing, dark administration room. At the far wall is an exit door, locked.

Guide: I don't like this place. It looks like the only way out is that door down there. Figure out a way to get us out of here.

Visual: Player moves around room, looking for clues. When he walks up to workstation, it trips an infrared beam, triggering a pop-up interactive screen. It's hazy and green. A face appears. This is the mission director.

Mission Director (in flat, computer-generated voice): Prepare for security analysis.

Visual: Scan of player's eyes or body.

Mission Director: Identity verified. Welcome (player's name). There is critical information found in the following intelligence reports that you'll need if you want to get out of this room. Our surveillance cameras have been monitoring people just like you as they go about their daily routines. Here is Veronica at the mall.

Visual: Girl talking to guy at the mall. Guy is dressed like Kevin Federline.

Brian: Hey Veronica, you're looking fine. Want to hear me rap?

Veronica: (cringing) No thanks Brian. I've got to get going.

Brian: (rapping) Me too, yeah it's true, do you... <<cough, cough, cough>>. Want to go outside and smoke?



Visual: He smiles, showing yellow teeth and gum disease.

Veronica: That's hot. Not. How long have you been smoking? And already, you've got yellow teeth, filthy gums and a nasty cough. And that breath! No thanks.

Brian: That's cold.

Visual: Tape stops. Code at bottom of screen is the letter "L".

Mission Director: This next segment is pretty eye-opening, too.

Visual: Jeff, a young guy, is looking in the mirror, fixing his hair, humming, smoking a cigarette, thinking he's pretty hot. He's dressed like a typical teenager. His friend Jon walks up and joins him.

Jon: What are you doing?

Jeff: (distracted). Um, what? I'm just checking to see if I've still got it...

Jon: Yeah, you've got it alright. You've got grey hair and you're starting to get wrinkles, dude. Maybe it's time to lay off the smokes.

Visual: You see his face. Jeff is much older than his years.

Jeff: You're crazy, brah. Why you got to be a playa-hater?

Visual: Tape stops. Code at bottom of screen is the letter "O."

Mission Director: Let's continue. Check this out.

Visual: Two girls, Erica and Sarah, are sitting at a Starbucks-type place.

Erica: I love your new bag. I saw Nicole Richie carrying one just like it in US Weekly. Let me see it.

Visual: Sarah hands over bag. Erica stares at Sarah's fingers, which are yellow and stained.

Erica: A little sloppy with the self-tanner?

Sarah: What are you talking about? I don't do that.

Erica: Oh gross, Sarah, You're fingers are stained yellow. From smoking!

Visual: Sarah sits on her hands.

Erica: How are you ever going to hook up with Trent Rockmore like that? And another thing...it can make you infertile. Don't you want beautiful Rockmore babies some day? Good thing he doesn't smoke, or he could end up impotent.

Sarah: I wonder where my triple decaf non-fat light whip extra hot latte is?

Visual: Tape stops. Code at the bottom of the screen is the letter “S.”

Mission Director. (Laughing, then stops). Yes, this is serious stuff. And it gets worse. Take a look.

Visual: Alex, a guy in his mid-twenties, talking to Carla, his girlfriend. They’re sitting on a couch watching TV.

Alex: Have you seen my smokes?

Carla: (Sighs) I threw them out.

Alex: You did what? I want a cigarette. I need one. I deserve one!

Carla: You’re an addict, you know that?

Alex: Yeah, I know. I will quit. Someday. But not right now. I can’t.

Carla: Well, then don’t do it around me.

Alex: OK, that’s cool....(pauses for a few seconds, watching TV, then gets up quickly and leaves.) Later!

Visual: Carla shaking her head.

Visual: Tape stops. Letter “E” slides into code.

Mission Director: This is the last segment. Pay close attention.

Visual: Two guys, Mike and Adam, doing homework. One is studying while the other is playing the guitar and smoking a cigarette.

Mike: Could you put that out please? It’s gross and it’s stinking up the room.

Adam: I’m a sensitive artist, a tortured soul. Cigarettes help my creative process.

Mike: They’re not helping you, fool. Don’t you ever think about lung cancer or emphysema or heart disease? Tobacco kills more people than alcohol, murder, cocaine, heroin and AIDS combined.

Adam: That’s really sad. Maybe I’ll write a song about that.

Mike: Just put it out. Please.

Adam: (singing) “Tobacco, so beautiful, so dangerous, a puff of pleasure, the kiss of death...”

Visual: Tape stops. Final letter, “R”, slides into code, spelling “LOSER.”

Mission Director: Congratulations. You’ve cracked the code. Enter it into the door alarm and get ready for the next part of your journey.

Visual: Player enters code and door unlocks. Player and guide move through.

## **S1\_2 Operating room – Long Term Health Consequences**

### *Health Track*

Guide: I don't know how this could get any worse, what with...what the?

Visual: Operating room, with surgery in progress on operating table.

Guide: Oh sick, I think they cut that guy wide open. I can't look. But you have to if we're ever going to get out of this place.

Visual: Player moves toward operating table, which triggers a pop-up screen of surgery video.

Guide: And don't try to chicken out! You have to watch the whole thing. I'll just be over here if you're looking for me.

Visual: Player watching explicit surgery video.

Visual: When video finishes, sound of exit door unlocking.

Guide: OK, show's over. Let's move it along. Buh-bye.

## **S1\_3 Recap**

### *Health Track*

Visual: Character and guide are now in parking lot.

Guide: Still thinking about not quitting smoking? That's OK. There's lots more to see. But think about the short and long term effects that smoking has on you and your body – Grey hair? Impotence? Lung cancer? And don't forget about that poor fool getting split open. I told you it wouldn't be pretty. So let's have some fun. Maybe a trip to the carnival might lighten things up.

Visual: Taxi pulls up, they get in and speed off to next section.

## **S2\_1 Ticket Booth – Orientation**

### *Social Track*

Visual: Amusement park/carnival exterior with entrances to three areas. A ticket booth is in the center. Player needs tickets to unlock the entrances (aka get on rides/attractions). After unlocking and completing one area, player must move through remaining two areas.

Barker: Step right up folks! Step right up! Inside you'll find thrills and excitement, romance, mystery and even magic! Get your tickets here!

Guide: This sounds a lot better than that last place. Why don't you get us some tickets?

Visual: Player approaches booth, gets tickets. Guide looks at map of park. Perspective changes to view of people milling around on the plaza.

## **S2\_2 Find a Mate**

### *Social Track*

Guide: Look, it's up to you, but what do you say we make the Tunnel of Love our first stop? Don't look at me like that!...I meant that maybe you could find someone you'd like to go with you.

Visual: Player approaches other avatars to seek out suitable mate, based on smoking status. Pop up dialogue bubbles contain text. Player can check off "yes" or "no" to make choice.

Sample interactions:

Player: Hey, want to go through the Tunnel of Love with me?

Avatar: I don't think so. You smell like smoke and I don't think you respect yourself.

Player: Hey, want to go through the Tunnel of Love with me?

Avatar: Maybe. Do you have an extra cigarette?

Player: Hey, want to go through the Tunnel of Love with me?

Avatar: I guess so. Even though you smoke, my therapist tells me I have low self esteem and need a date.

Player: Hey, want to go through the Tunnel of Love with me?

Avatar: I might. Just don't smoke around me. I don't want to smell like an ashtray.

Player: Hey, want to go through the Tunnel of Love with me?

Avatar: No thanks, I'm trying to quit smoking and I think you're a bad influence.

Player: Hey, want to go through the Tunnel of Love with me?

Avatar: Well yeah! All the cool kids smoke, don't they? I mean, they do, right? .

Visual: This continues until the player finds a suitable mate. Player makes choice.

Guide: What are you waiting for? It's time to get busy....oh you know what I mean.

### **S2\_3 Tunnel of Love**

#### *Social Track*

Visual: Player and friend travel through ornate, romantic, baroque Tunnel of Love. Short peer videos play as overlay.

Variety of peer videos about social attitudes toward smoking.

Visual: Guide is waiting on other side.

### **S3\_1 Plaza**

#### *Environment Track*

Visual: Deserted city street, trash piled everywhere, burned out buildings, graffiti, abandoned cars. There is a pawn shop on one side of the street, with a TV in the window playing static. The items the user collected along the way (but lost due to behaviors) are also displayed in the window.

Guide: I guess a lot can change in 30 years. I mean, I still look good...but you have lost it. Hey, go find yo sh<<BLEEP>>, yo.

### **S3\_2 Pawn Shop**

#### *Environment Track*

Visual: Player moves toward pawn shop, and TV screen comes to life. It's an investigative newsmagazine show.

Annrcr: Tonight on 60 Seconds, we take a look at the real story of tobacco. Cigarettes are fun, right? Smoking doesn't hurt anyone...or does it? I want to warn you, folks, this is some pretty gruesome stuff. We go now to Ron Burgundy, in the field.

Visual: Field reporter beside a river.

Reporter: Thanks, Dan. I'm standing here at the river, which as you can see is polluted with cigarette butts (Visual: dead ducks and plants). Smoking kills again! They say they're even too toxic for landfills! Alice?

Visual: Field reporter leaving a bar restaurant, with a big cloud of smoke rolling out behind her.

Reporter: Cough cough Thanks, Ron. We tried to have a nice dinner in the NON-smoking section of this popular downtown restaurant, but when anyone is smoking, we all feel the effects of second-hand smoke. The employees have it worse. Night after night, breathing in other people's smoke. A dangerous situation indeed! Clint?

Visual: Field reporter outside a burning house.

Reporter: Good evening everyone. Yes, it's yet another preventable housefire, again caused by someone smoking in bed...Fires due to careless smoking kill thousands of people every year and...

Visual: Cuts back to anchor

ANNCR: Sorry, Clint. This just in. We must pause now for a special network report.

Cue Truth Ad.

ANNCR: The truth indeed. Until next time, I'm Dan Wallace. From all of us here at 60 Seconds, good night, and good health.



## SII Module Scripts: Smokers Willing to Quit Module

### A1\_1 Library (orientation)

Visual: Comfortable, sunny school library. Books, posters, computers, etc.

Guide: Congratulations on wanting to quit smoking and welcome to Academia, a place where you'll learn how to quit and how to begin living as a non-smoker. You'll see how social pressure, your mood, and even your level of addiction can affect your success.

Don't be fooled by this serious-looking library. Beyond that door is some pretty crazy stuff, but I think you'll like it. Hey, it's better than being stuck in a library all day, right?

You're looking healthier already. So let's go. You lead the way.

Visual: Door at end of room opens. Player and guide move through.

### A1\_1 Laboratory *Social Track*

Visual: This is your stereotypical "mad-scientist's" laboratory, with test tubes and beakers fizzing, buzzing monitors, random jars, etc. There is a monitor in the room with the words "secret formula" on the screen. At the far wall is a locked exit door.

Guide: Now this is more like it! I wonder what they're making here. Why don't you go see?

Visual: Player moves around lab, equipment fizzes and pops. When he walks up to monitor, it triggers a pop-up screen. "Secret Formula" becomes "Secret Formula for Quitting Smoking."

Mad Scientist face appears on screen.

Scientist: Sorry, I've stepped away from my lab for a second. Please leave a message after the tone. Bwaaahaaahaaahhaahaaa, just kidding. I don't know how you got in here, but I've been looking for a new patient...I mean, assistant. I've been working on this secret formula for a while. Actually, it's really pretty simple – how to recognize, remember and react to social pressures about smoking. I surgically extracted it...I mean borrowed it... from the brains of various smart people around town. You could call me a "social scientist." Get it?

Visual: The words "recognize, remember and react" appear on screen.

Visual: Quick cuts of people in situations where you might be exposed to smoking

VO: First, **recognize** situations where you might be tempted.

- 1) At a party – guy offering a cigarette. "Hey, have a smoke."
- 2) Group of people at bowling alley – girl offers. "Everybody's smoking. Come on!"
- 3) Behind the school – girl offers. "Hey, have a smoke and hang out."

VO: Then **remember why** you want to quit.

- 1) A guy with a bat. "I want a sneaker contract."
- 2) A goth girl. "I'm tired of being unhealthy. So, so tired."
- 3) A nerd guy. "It never made me popular anyway."
- 4) A cheerleader. "I don't want to – mess up my – B-O-D-Y!."

Scientist: Now, this part is up to you. You have to choose how you're going to **react**. If you get the answers right, you'll get the exit code, and I'll let you go. If not, I might turn you into a zombie. No, I'm not kidding, I really will. It's fun.

Visual: Good Choice/Bad Choice or Matching Game Exercise

Text: **Choosing to Ignore** is a good avoidance strategy.

Player chooses correctly, and inset screen has a guy in headphones yelling, "I'm sorry, did you say something?!?" Letter "C" slides into place.

Text: **Humor** is a solid approach

Player chooses correctly, and inset screen has an extremely tall girl saying "Nah, I don't want to stunt my growth" Letter "H" slides into place.

Text: **Ask for Support** when trying to quit.

Player chooses correctly, and inset screen has a woman saying "Hey, I'm trying to quit, OK? Whose side are you on?" Letter "A" slides into place.

Text: **Now Make Positive Plans** and you're on your way.

Player chooses correctly, and inset screen has a gang kid saying, embarrassed "Sorry, I, uh, I have ballroom dancing practice." Letter "N" slides into place.

Text: **Get Smart** about the dangers of smoking.

Player chooses correctly, and inset screen has a nerd saying "I don't think I'll be more popular with the ladies if I stink, I can't breathe and I'm impotent. Just a theory." Letter "G" slides into place.

Text: **Every time you're offered a cigarette, change the subject**

Player chooses correctly, and inset screen has a jock saying "You see that game last night? Wanna arm wrestle?" Letter "E" slides into place.

Completed code **CHANGE** appears.

Scientist: Oh great, outsmarted again. Well, I may be mad, but I'm a man of honor. You're free to go.

Guide: You did it! Now you know how to recognize, remember and react to the social pressures about smoking. Put the code in the door lock and let's jet.

Player moves to door, enters code, and door opens. Player and guide move through.

## **A\_2 Sanitarium**

### *Social Track*

Visual: Player and guide are in sanitarium or psych ward, where the scientist's zombies/creations are milling about.

Guide: Uh oh...looks like these guys weren't as lucky as you. I wonder why they failed the test. They look pretty harmless. Go talk to them.

Timed activity (:60)

Visual: Player moves around room and interacts with zombies, many of whom are holding cigarettes. As player approaches each, he asks, "why are you still smoking?"

Player: "Why are you still smoking?"

Zombie 1: "I'm feeling down and stressed out. I'm crazed for a cigarette!"

Player: Why are you still smoking?

Zombie 2: I suck at sports. I always get picked last. I know I'm a zombie and all, but still."

Player: Why are you still smoking?

Zombie 3: I guess nobody really understands me. Not even these other zombies."

Player: Why are you still smoking?

Zombie 4: I thought this girl zombie wanted to go out with me, but she really just wanted to eat my brain."

Player: Why are you still smoking?

Zombie 5: Man, my parents won't get off my back about that whole body-snatching thing. I mean it was years ago."

Guide: For a bunch of zombies they're not too brain-dead. Like they said, there are a lot of mood triggers out there. So it's important to remember why you don't want to smoke – and react to the temptations by finding something else to do. Hey, there's a good show coming on in the nurses lounge. Let's go.

Visual: Player and guide enter nurses lounge, where a bunch of them are sitting around watching TV. A TV screen pops up, featuring a game show like Family Feud.

SFX: Loud game show music.

Announcer: It's time to play CHILL, CHAT AND CHANGE!!!! Here's your host...Chuck Charleston.

Chuck: Good evening teams, and welcome to the show. As you know, it's Smoking Week on the program, so tonight you're going to be asked questions about temptations. Not THE Temptations, that was Motown Week. So let's get started. We asked 100 people the following questions and you've got to guess their answers. Top five answers are on the board.

Visual: Players face off at podium.

Chuck: Chilling out is one way to react to temptations. Instead of smoking, what are the most popular ways to chill out?

Visual: Player 1 buzzes in.

Player 1: Umm....Meditation?

Chuck: Meditation...survey says!

Visual: Top line on game board flips over: MEDITATION 50

Chuck: Correct. You have control of the board. What's another way to chill out?

Player one: Oh, I'm so nervous....how about exercise?

Visual: Third line on game board flips over: EXERCISE 15

Chuck: Great answer!! Want to keep playing?

Player one: OK...how about journal writing?

Chuck: Survey says!

Visual: Second line on game board flips over: JOURNAL WRITING 20

Chuck: Two answers left. Let's make it interesting...how about you try to guess both?

Player one: Gee, I don't know...I guess I'll go with music and deep breathing?

Visual: Lines four and five flip over, with MUSIC AND DEEP BREATHING as answers.

Chuck: Amazing.. a clean sweep. This is a first on our show! Congratulations!!! Player Two, the pressure's on. Are you ready for a challenge?

Player Two: Bring it, Chuck!

Chuck: Here's how the second round goes. You have five seconds to write down who you would chat with when you want to resist temptation. And.....go!

Visual: Players, heads down, write their lists.

Chuck: Time's up, please turn over your cards.

Visual: Close up on two lists. One has:

Parents

Friends

Teachers

Pastor

Psychic Friends Network

The other has:

My mom  
A counselor  
That smart old man at the gas station  
My friends  
A doctor

Chuck: It's close...but I don't think we can count Psychic Friends! Sorry, player one. You've both got the right idea. Just pick a good person, set a time and then ask questions. Always be open and honest.

Chuck: Final round. And this is about changing your thinking. Maybe negativity is holding you back. Buzz in to fill in the blanks:

Chuck: If you want to succeed, set realistic...

Player One: Expectations?

Chuck: Correct! Just do your...

Player Two: Best?

Chuck: Right! Don't be too "blank" on yourself.

Player Two: Hard!

Chuck: Great answer: Maybe you have to "blank" your thinking.

Player one: Change!

Chuck: Yes!!!! Last one, and this is for the game. Always turn a negative into a...

Player Two: A positive!

Chuck: You win! We all win when we use these strategies! Good night everyone, and thanks for joining us on CHILL, CHAT AND CHANGE!

Guide: I love that show. Were you paying attention? Let me ask you a few questions.

Visual: A multiple choice quiz appears. Player checks off correct answers.

- 1) What are some ways to chill:
  - a. Exercise
  - b. Meditation
  - c. Worrying
  - d. Journal Writing
  - e. Binge eating
  - f. Listening to music

- 2) Who's a good person to chat with?
  - a. Parent
  - b. Zombie
  - c. Friend
  - d. Teacher
  - e. Complete stranger
  - f. Counselor
  
- 3) What are some ways to change your thinking?
  - a. Turn negative thoughts into positive ones
  - b. Ignore problems and hope they'll go away
  - c. Stop being so hard on yourself.
  - d. Set realistic expectations
  - e. Give up before you even try.
  - f. Just do your best.

Guide: So you were paying attention. I knew you weren't like the rest of these zombies. Oh, look, I think Jerry Springer's coming on. Ahhh, I'm TiVo ing it anyway. Let's get moving.

Visual: Player and guide exit psych ward, and enter outside maze.

## **A2\_2 Nurses Lounge**

*Social*

Visual: Player and guide enter nurses lounge, where a bunch of them are sitting around watching TV. A TV screen pops up, featuring a game show like Family Feud.

SFX: Loud game show music.

Announcer: It's time to play CHILL, CHAT AND CHANGE!!!! Here's your host...Chuck Charleston.

Chuck: Good evening teams, and welcome to the show. As you know, it's Smoking Week on the program, so tonight you're going to be asked questions about temptations. Not THE Temptations, that was Motown Week. So let's get started. We asked 100 people the following questions and you've got to guess their answers. Top five answers are on the board.

Visual: Players face off at podium.

Chuck: Chilling out is one way to react to temptations. Instead of smoking, what are the most popular ways to chill out?

Visual: Player 1 buzzes in.

Player 1: Umm....Meditation?

Chuck: Meditation...survey says!

Visual: Top line on game board flips over: MEDITATION 50



Chuck: Correct. You have control of the board. What's another way to chill out?

Player one: Oh, I'm so nervous....how about exercise?

Visual: Third line on game board flips over: EXERCISE 15

Chuck: Great answer!! Want to keep playing?

Player one: OK...how about journal writing?

Chuck: Survey says!

Visual: Second line on game board flips over: JOURNAL WRITING 20

Chuck: Two answers left. Let's make it interesting...how about you try to guess both?

Player one: Gee, I don't know...I guess I'll go with music and deep breathing?

Visual: Lines four and five flip over, with MUSIC AND DEEP BREATHING as answers.

Chuck: Amazing.. a clean sweep. This is a first on our show! Congratulations!!! Player Two, the pressure's on. Are you ready for a challenge?

Player Two: Bring it, Chuck!

Chuck: Here's how the second round goes. You have five seconds to write down who you would chat with when you want to resist temptation. And.....go!

Visual: Players, heads down, write their lists.

Chuck: Time's up, please turn over your cards.

Visual: Close up on two lists. One has:

- Parents
- Friends
- Teachers
- Pastor
- Psychic Friends Network

The other has:

- My mom
- A counselor
- That smart old man at the gas station
- My friends
- A doctor

Chuck: It's close...but I don't think we can count Psychic Friends! Sorry, player one. You've both got the right idea. Just pick a good person, set a time and then ask questions. Always be open and honest.

Chuck: Final round. And this is about changing your thinking. Maybe negativity is holding you back. Buzz in to fill in the blanks:

Chuck: If you want to succeed, set realistic...

Player One: Expectations?

Chuck: Correct! Just do your...

Player Two: Best?

Chuck: Right! Don't be too "blank" on yourself.

Player Two: Hard!

Chuck: Great answer: Maybe you have to "blank" your thinking.

Player one: Change!

Chuck: Yes!!!! Last one, and this is for the game. Always turn a negative into a...

Player Two: A positive!

Chuck: You win! We all win when we use these strategies! Good night everyone, and thanks for joining us on CHILL, CHAT AND CHANGE!

Guide: I love that show. Were you paying attention? Let me ask you a few questions.

Visual: A multiple choice quiz appears. Player checks off correct answers.

- 4) What are some ways to chill:
  - a. Exercise
  - b. Meditation
  - c. Worrying
  - d. Journal Writing
  - e. Binge eating
  - f. Listening to music
- 5) Who's a good person to chat with?
  - a. Parent
  - b. Zombie
  - c. Friend
  - d. Teacher
  - e. Complete stranger
  - f. Counselor
- 6) What are some ways to change your thinking?
  - a. Turn negative thoughts into positive ones
  - b. Ignore problems and hope they'll go away
  - c. Stop being so hard on yourself.

- d. Set realistic expectations
- e. Give up before you even try.
- f. Just do your best.

Guide: So you were paying attention. I knew you weren't like the rest of these zombies. Oh, look, I think Jerry Springer's coming on. Ahhh, I'm TiVo ing it anyway. Let's get moving.

Visual: Player and guide exit psych ward, and enter outside maze.

### Avitar Builder

**Tell us all about YOURSELF**

AGE  
Under 35

GENDER  
☒ MALE  
☐ FEMALE

ETHNICITY  
Caucasian

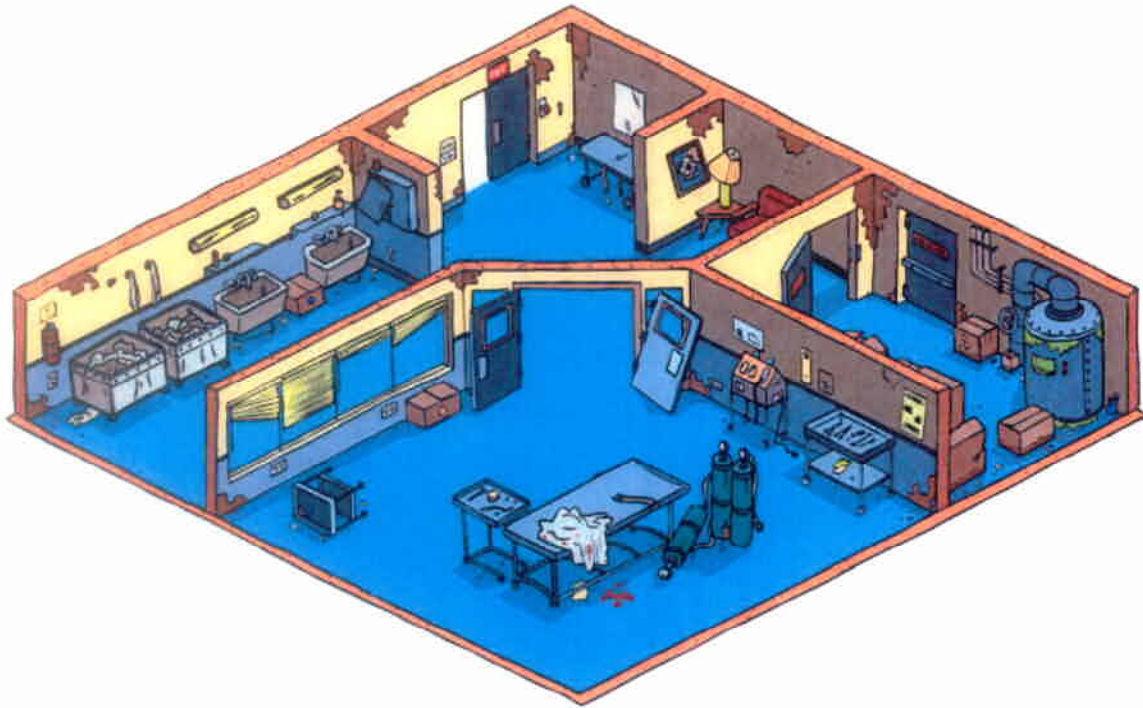
**Build your AVATAR**  
USE THE YELLOW ARROWS TO SELECT

OK!

## User Interface Screen



### Operating Room Screen



### Health Administration Room Screen





## **Video Gaming Demographics**

Radiant Creative Group has been engaged by UT-Health Science Center to develop Project TALK, a smoking education/cessation intervention program targeted at 15-24 year olds who are outside of education environments. They may be high school drop outs, immigrants whose first language is not English, or high school graduates who have not gone on to college. The goal is to reach them with an interactive education curriculum that is fun, easy, informative and effective – combining games and activities with traditional facts and figures.

To ensure that we reach this audience most effectively when developing the overall concept for Project Talk, Radiant researched a variety of topics, including gaming demographics – who responds to what and why. The following is a summary of that research.

### **Overview**

Today, both males and females are dedicated gamers. While about the same number of men and women are playing, there are distinct differences in preference about the media format, game content and structure.

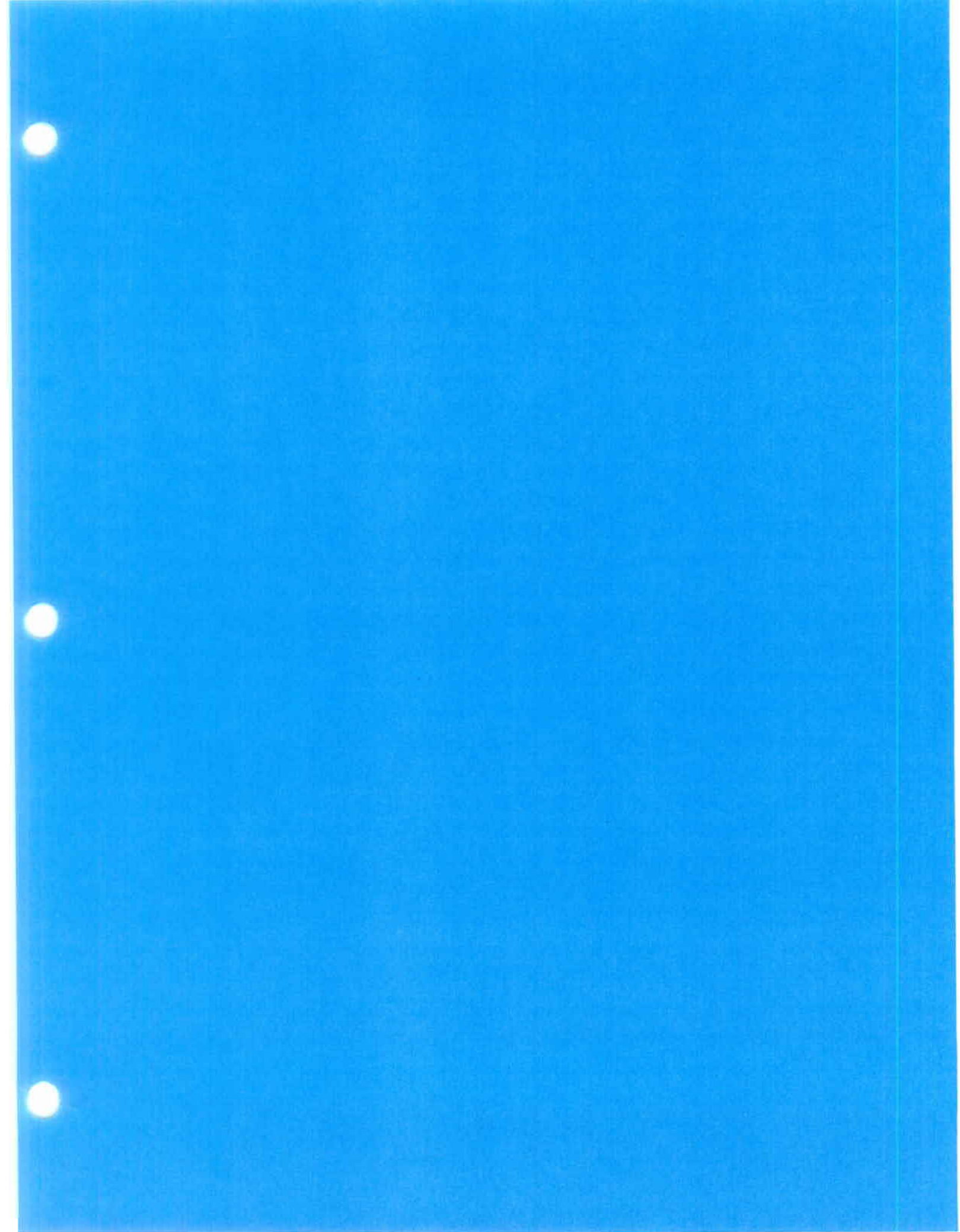
- According to the IDSA's (Interactive Digital Software Association) fourth annual Video and PC Game Industry Trends Survey (2004), more women are playing games than ever. Thirty five percent of console game players and more than 43 percent of PC gamers are women, a slight increase over last year.
- Women are purchasing just as much video/PC entertainment software as men. In 1999, 49 percent of PC entertainment software buyers were women, while 51 percent of console software purchasers were women.
- What people are playing:
  - Americans are most likely to purchase the following types of PC games: 1) Puzzle/Board/Card/Learning games  
2) Action Games and Strategy  
3) Driving/Racing and Adventure/Role Play games.
  - As for console games, the popularity order is  
1) Action games  
2) Puzzle/Board/Card and Driving/Racing games  
3) Adventure/Role Play games.

### **Male Vs. Female**

Source: *American Demographics*, Oct. 1, 2003:

- While about the same number of male and female students report playing video games, more women than men (60 percent versus 40 percent) play computer games (solitaire, etc.) and online games (Internet-based games against other remote players).





## **APPENDIX F**

### **PROJECT TALK**

## **APPENDIX F**

### **Preparation Documents**

Video Gaming Demographics  
Legacy Truth® Ads Ranking

- Researchers say that part of the reason the gals aren't as keen on video games as the boys may be because many of these games tend to be violent in nature.
- Some women may be put off by video game characters that often exaggerate and stereotype gender roles, whereas computer games generally don't require players to choose a character and online games offer more options to disguise and manipulate their identities.

### *Games Women Play*

Source: The Hollywood Reporter, June 17, 2004:

According to a study conducted for AOL:

- Female gamers over 40 spend the most hours per week playing online games -- 9.1 hours or 41% of their online time vs. 6.1 hours or 26% for men.
- Women seem to enjoy the word and puzzle games that are common on casual game sites (compared to the sports and shooting games that men prefer).
- They play to relieve stress and to chat with other online gamers, "much the same way that people sit around a card table and play and talk, when they are there primarily just to talk," says Matthew Bromberg, general manager of games at AOL.

Source: ELSPA (Entertainment and Leisure Software Publishers Association) white paper on women in gaming.

In addition to fast, simple puzzle and card games (the theory is that women are more pressed for time, and therefore can't undertake elaborate games at the same rate that men do), the following titles are most popular among women gamers.

- Role-playing games - Final Fantasy
- Narrative adventures - Legend of Zelda
- Easy to pick up driving sims - Colin MacRae Rally
- Puzzle adventures - Prince of Persia: The Sands of Time
- Quick-fire arcade puzzlers - Tetris
- Life simulations - The Sims

### Trends:

Source: *Christian Science Monitor*, June 11, 2004:

Industry pundits cite the growing number of women in games as evidence that the industry itself is coming of age.

- Ten years ago, "the core gaming market was teenage boys," says Douglas Lowenstein, president of the Entertainment Software Association. Today, he says, "the average age of

gamers is 29, the core demographic is 18 to 35, and a third of game players are women."

- This shift reflects major changes in the videogame landscape.
  - Primary among them: a generation of computer-literate players has now come of age.
  - Many of these are women who have never played the violent, complex, time-consuming, and expensive games that have evolved primarily for the three major consoles: Playstation, GameCube, and Xbox. But they understand computers and traditional games.
  - As broadband connections have made games faster and easier to play, researchers say these often free, simple, online versions of traditional card and board games appeal to women with limited time but a desire to socialize. They are to the current generation what the phone was to women of the past.

**Ranking of Truth® Ads by Receptivity\* among 12 to 17 Year Old Youth**

Ranking	Ad Title	Ad Description
1	Body Bags	Truth kids pile 1200 body bags outside of a major tobacco company.
2	Ratman	A man, dressed as a rat, emerges from the subway and crawls onto the sidewalk to "die." A sign is placed by him saying that cyanide, a component of rat poison, is in cigarettes.
3	Memorial	The truth kids create their own Washington Memorial out of body bags.
4	Ammoniade	At a tobacco industry conference, two truth kids try to sell "Ammoniade," alluding to the fact that tobacco companies add ammonia to their cigarettes for flavor.
5	Smaller Babies	Women are surveyed on the street whether they would prefer a healthy baby or a small unhealthy one. It is noted that cigarettes can cause birth defects such as reduced birth weight and a tobacco executive is quoted saying that some women would prefer smaller babies.
6	Box of Poison	Truth kids walk into a shipping center and ask about shipping hazardous chemicals. After a surprised reaction from the employees, it is revealed that the chemicals are simply cigarettes.
7	Dog Walker	Truth kids place signs in dog feces reading, "Ammonia is found in dog poo. Tobacco companies add it to cigarettes."
8	1200 Kids	Outside a major tobacco company, 1200 kids gather and simultaneously drop to the ground. It is then stated that 1200 people die each day from tobacco related illness.
9	Urinal	Signs are placed in urinals noting that, like urine, cigarettes contain urea.
10	Beach	Three kids bring body bags out onto the beach and play with them. One holds up a sign that reads: "What if cigarette ads told the truth?"
11	Grapes	Millions of cases of fruit were discarded after 2 grapes were found to have cyanide. There is more cyanide in a single cigarette than was found in both of those grapes.
12	Mineral Water	A voluntary recall was issued for mineral water that contained benzene. Cigarettes contain benzene and they have yet to be recalled.
13	Roadside Memorial	People gather around a makeshift sidewalk memorial with a sign that states that there are 1070 more deaths each day from cigarettes than auto accidents.
14	Baby Invasion	Dozens of robotic crawling babies are released onto the street/sidewalk. On their shirts it reads: "How do infants avoid second-hand smoke? 'At some point, the begin to crawl.' -Tobacco Executive, 1996."

*\*The Receptivity Score is composed of three Legacy Media Tracking Survey (LMTS) items: 1) ad is convincing, 2) ad grabbed my attention and, 3) ad gave me good reasons not to smoke. These questions are asked only of youth who have confirmed awareness of an ad. This list includes all of the truth® ads for which American Legacy Foundation has collected LMTS data over the years, from 1999 through the present. Receptivity scores and ranking differ somewhat for 18-24 year old youth.*  
2/20/2006



15	Low Rider	A car with smoke coming from it drives along a busy street. The side of the car reads: "Carbon Monoxide: 1 of the 4,000 chemicals in cigarette smoke."
16	Baby Stroller	A woman appears to leave a baby in a stroller on a street corner. As onlookers move in, it is revealed that the baby is a doll and a sign states that every year tobacco leaves 12,000 kids motherless.
17	Making Blacks History	Series about the absurd number of African American deaths from smoking related illness.
18	Daily Dose	This series of spots contain teenagers holding electronic signs that display the numeric value for the statistics that are overlaid. They include: "Every 8 seconds tobacco loses a customer;" "Smoke contains 101 poisons;" "Every year tobacco leaves 400,000 dead;" etc.
19	Lie Detector	Truth kids attempt to drop off a lie detector at a major tobacco company.
20	Western	Three kids place body bags onto three horses and send them running across the plains. After one of the kids holds up a sign reading "What is cigarette ads told the truth?", one of the body bags falls off.
21	\$5 Billion Stack	A dump truck dumps \$5 billion onto the street, the amount of money that the largest tobacco company would lose if the 7 out of 10 smokers that want to quit did.
22	Orange Curtain	This series of spots features truth kids reading incriminating "highlights" from tobacco documents.
23	Web Letters	In this series truth kids respond to posts from the truth message board.
24	Squadron	Flying over a crowded beach, planes with banners trailing list the contents of cigarette smoke.
25	Product Labels	Through a contest, onlookers learn that cigarettes are a product that isn't required to list ingredients.
26	H-bomm	Three basketball players wearing H-Bomm sneakers go for the basket. After the third's sneakers explode, the screen reads: "Only one product actually kills a third of the people who use it. Tobacco."
27	Night Club	Two guys with a body bag are hanging out at a night club. A sign is held up reading "What if cigarette ads told the truth?"
28	Door Hanger	At night, truth kids go around a hotel placing hanging cards on the doorknobs, like typical "Do Not Disturb" cards, only these read: "DISTURBING: Everyday tobacco kills enough people to fill this hotel."
29	Ice Cream Truck	Truth kids in an ice cream truck explain how a tobacco company considered using such trucks to promote a new cigarette. It is implied that by doing so they were targeting children.
30	Convenience Store Comparison	Three Truth teens drive past a convenient store in a "bad" neighborhood, noticing the windows are covered with tobacco ads. The store in the "good" neighborhood has only one tobacco ad.

*\*The Receptivity Score is composed of three Legacy Media Tracking Survey (LMTS) items: 1) ad is convincing, 2) ad grabbed my attention and, 3) ad gave me good reasons not to smoke. These questions are asked only of youth who have confirmed awareness of an ad. This list includes all of the truth® ads for which American Legacy Foundation has collected LMTS data over the years, from 1999 through the present. Receptivity scores and ranking differ somewhat for 18-24 year old youth.*

31	50% More	This series of spots focus on how African American men get 50% more lung cancer than white men. Truth kids then offer them 50% more of stuff that doesn't give them cancer.
32	Port-a-potty	Truth kids replace port-a-potty toilet paper with cigarette ads.
33	Splode	Three people are bungee jumping off a bridge, grabbing cans of "Splode" from the bottom. After the third jumper's can explodes, the screen reads: "Only one product actually kills a third of the people who use it. Tobacco."
34	Parachute	Body bags with parachutes are thrown out of an airplane. A sign is held up reading "What if cigarette ads told the truth?"
35	Name Tags	Truth kids fill out nametags according to tobacco companies' stereotypical descriptions. The kids put on nametags that read, "sales spike," "profit margin," etc.
36	Shredder 2000	Truth kids advertise a giant document shredder outside a major tobacco company
37	Product Recall	An April Fools announcement from a tobacco executive issuing a recall for cigarettes.
38	Kids Eye View	Truth kids attach a camera to a child's head and send him into a convenient store. Cigarette ads are placed on the same level as gum ball machines, "kids eye view."
39	Figment	An April Fools spot announcing the first 100% safe cigarette: "Figment."
40	Operation Hypnosis	Kids in a truck are driving through Tobacco Suburbia with a prerecorded message telling the resident tobacco executives to find other jobs.
41	Voice	Standing in front of a Virginia Slims poster that reads "Find Your Own Voice," a woman stands up with a voice box and asks, "Is this the voice you expected me to find?"
42	Bodega	Truth kids enter a convenient store and ask the cashier why there are so many cigarette ads, why the ads are hung near candy machines, and who put the signs up?
43	Rid-a-Zit	Three girls are standing around a mirror using a pimple medication called "Rid-a-Zit." After one of the girls bursts into flames, the screen reads: "Only one product actually kills a third of the people who use it. Tobacco."
44	Tru Ride	Three people are dropped off at their rental cars. After the third's car explodes, the screen reads: "Only one product actually kills a third of the people who use it. Tobacco."
45	Record Store	A man in a record store is listening to something he is clearly enjoying. After removing the headphones and leaving the store, another man picks up the headphones and follows in the previous man's enjoyment.

*\*The Receptivity Score is composed of three Legacy Media Tracking Survey (LMTS) items: 1) ad is convincing, 2) ad grabbed my attention and, 3) ad gave me good reasons not to smoke. These questions are asked only of youth who have confirmed awareness of an ad. This list includes all of the truth® ads for which American Legacy Foundation has collected LMTS data over the years, from 1999 through the present. Receptivity scores and ranking differ somewhat for 18-24 year old youth.*  
 2/20/2006



## **APPENDIX G**

### **PROJECT TALK**

## **APPENDIX G**

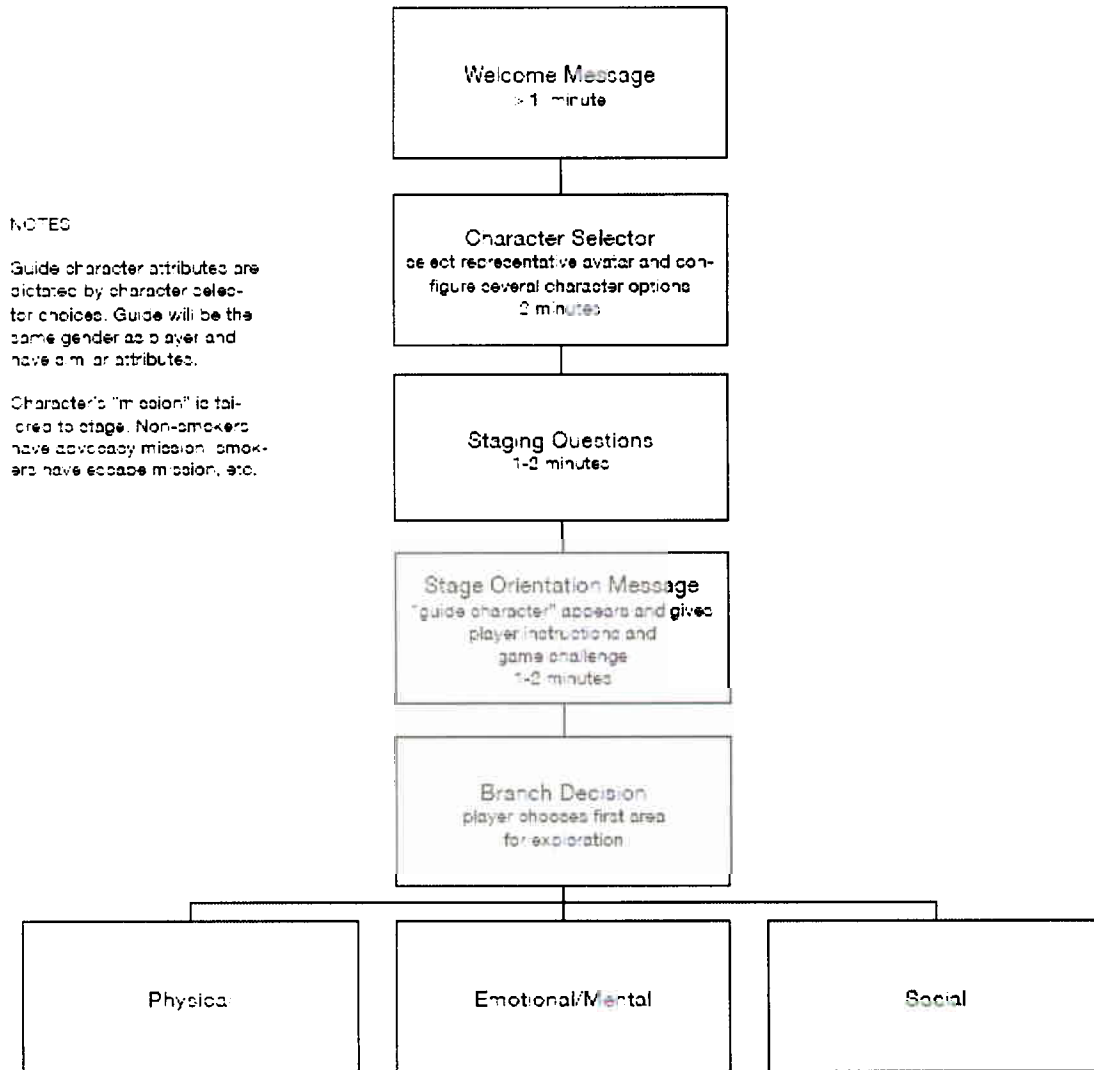
### **Module Templates**

SI Module Template

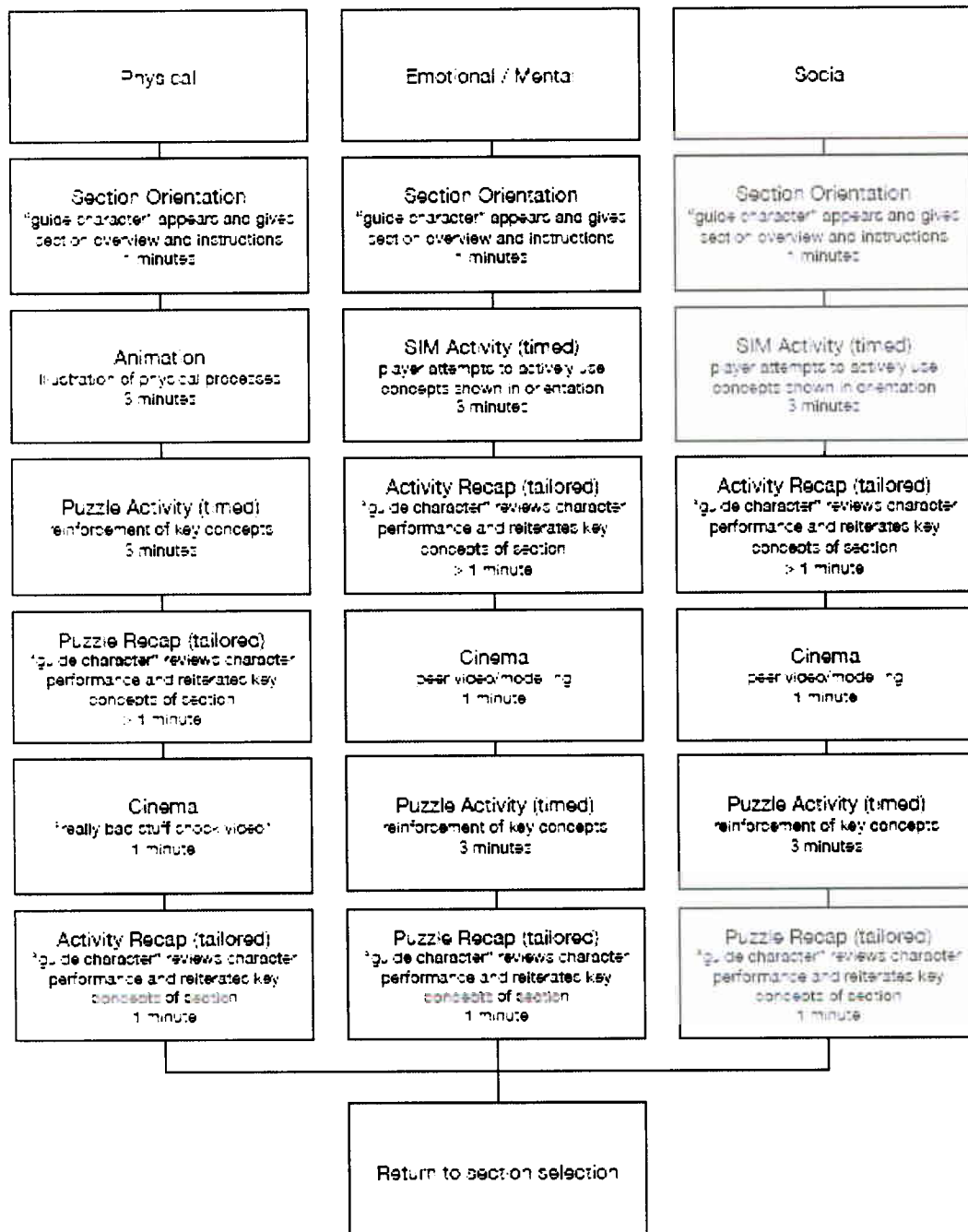
SI Module World

\*SI = Smokers Not Willing to Quit

### SI Module Template (pg. 1)



### SI Module Template (pg. 2)

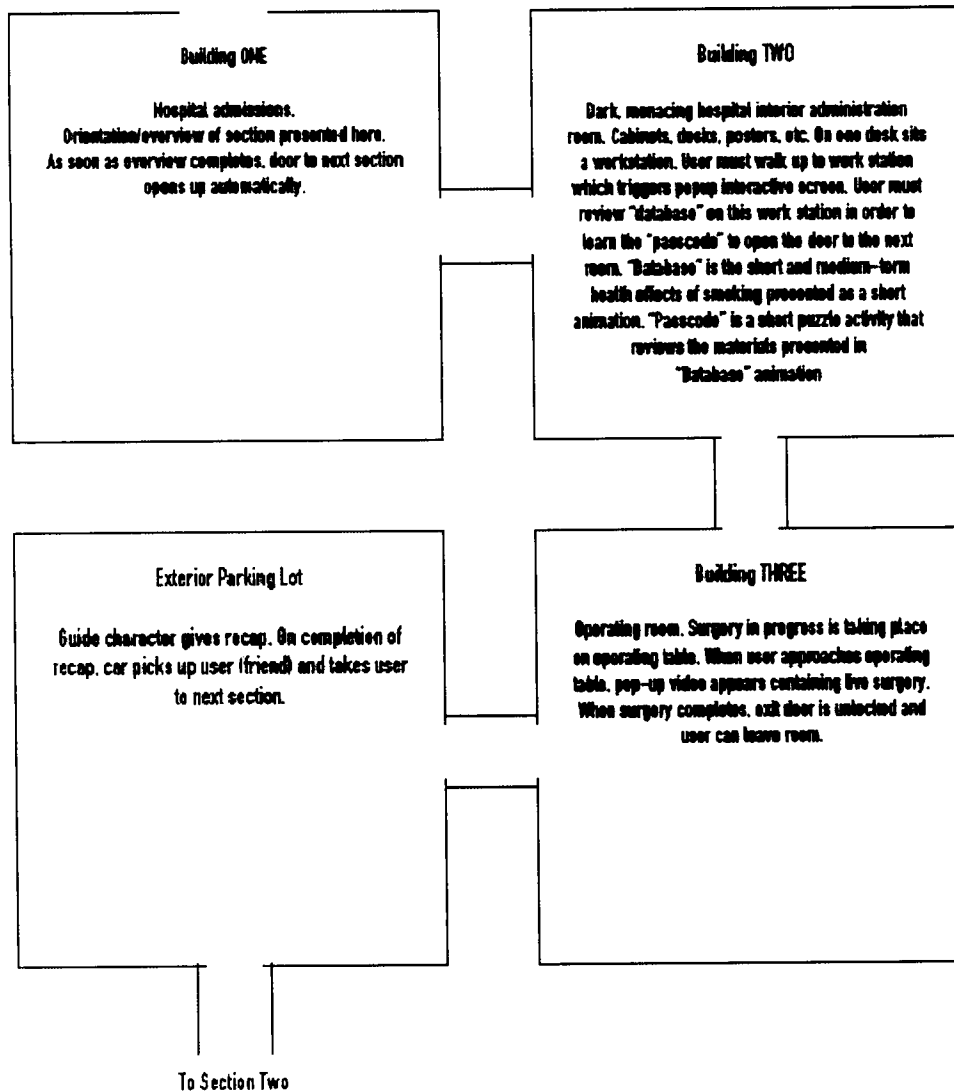




## SI Module World (pg. 1)

### PC Section ONE - Health

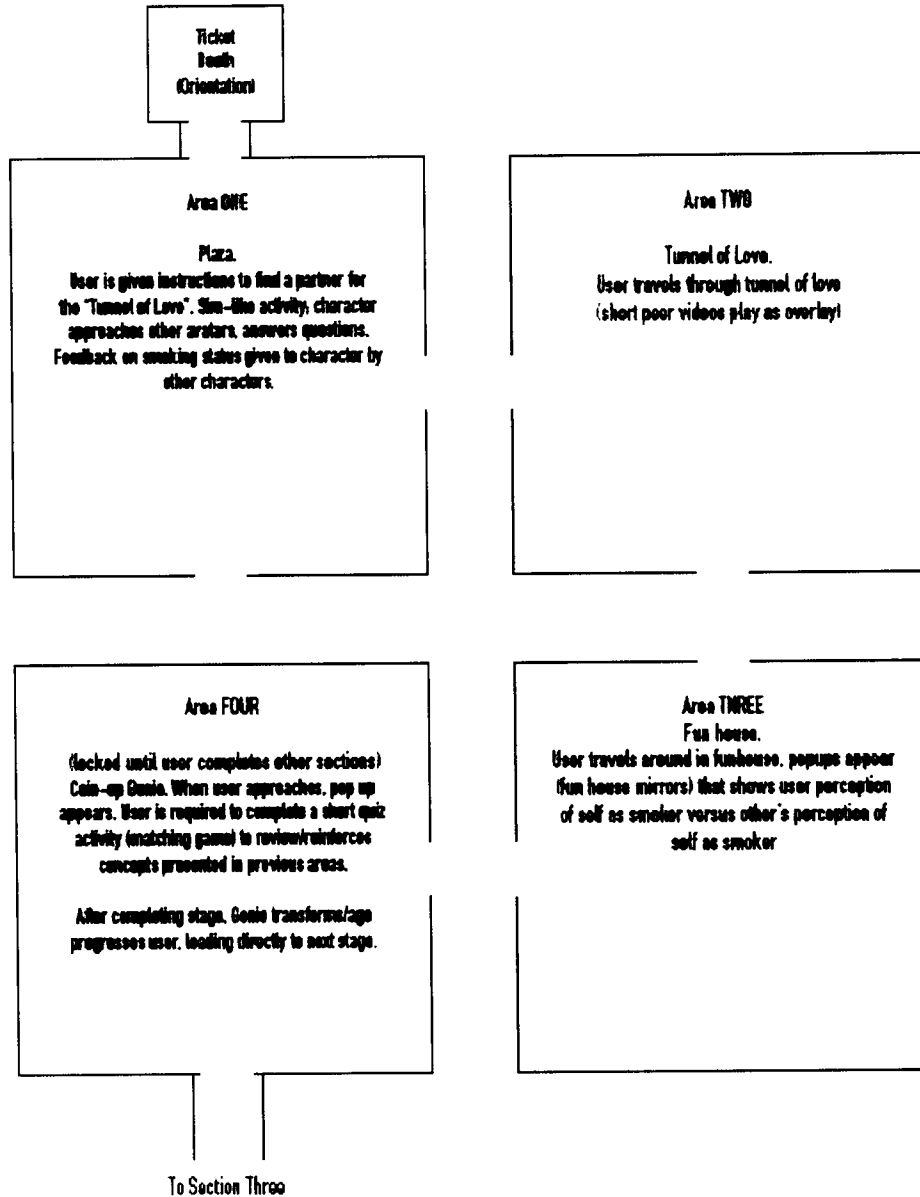
Creepy hospital interior. user must complete each "room" before moving to the next.



## SI Module World (pg. 2)

### PC Section TWO - Social

Amusement park/Hiway exterior with entrances to three areas.  
One area is locked, and becomes unlocked only when user completes first two areas



## SI Module World (pg. 3)

### PC Section THREE - Environment

Same basic exterior as previous section, but completely dilapidated and age-progressed 30 years. Empty parking lot, pawn shop, broken down fun house. User starts in an alley.

#### Area ONE

##### Plaza.

Area is covered with smoking billboards and strewn with other avatars. When user approaches another avatar, user sees billboard behind character and character delivers message. Character = reality, billboard = Illusion.

#### Area TWO

##### Pawn Shop.

Items user collected (but lost in transition) are displayed in window. TV playing static in window. When user approaches, popup appears and TV plays news story. News story is enviro effects of smoking. In the middle of news story, Truth commercial airs.

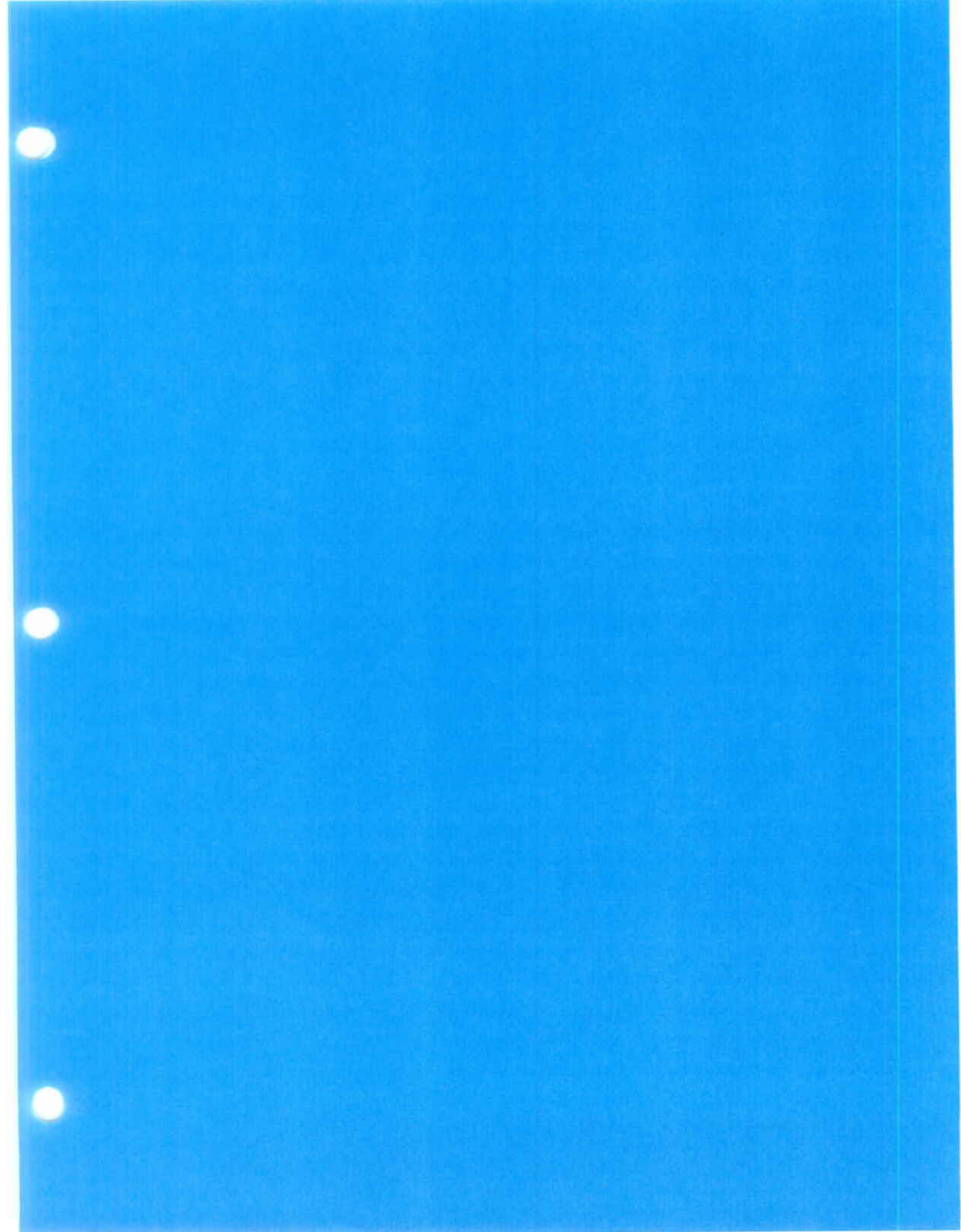
#### Area FOUR

Coin-op Genie from previous section. When user approaches Genie in this section, user gets track review. Genie asks if user would consider quitting. If user responds yes, user is transported back to program start and given option to continue program on contemplation track.

#### Area THREE

##### Fun house, now crumbling.

User travels around in funhouse, popups appear (fun house mirrors) that show long term physical effects of smoking.



## **APPENDIX H**

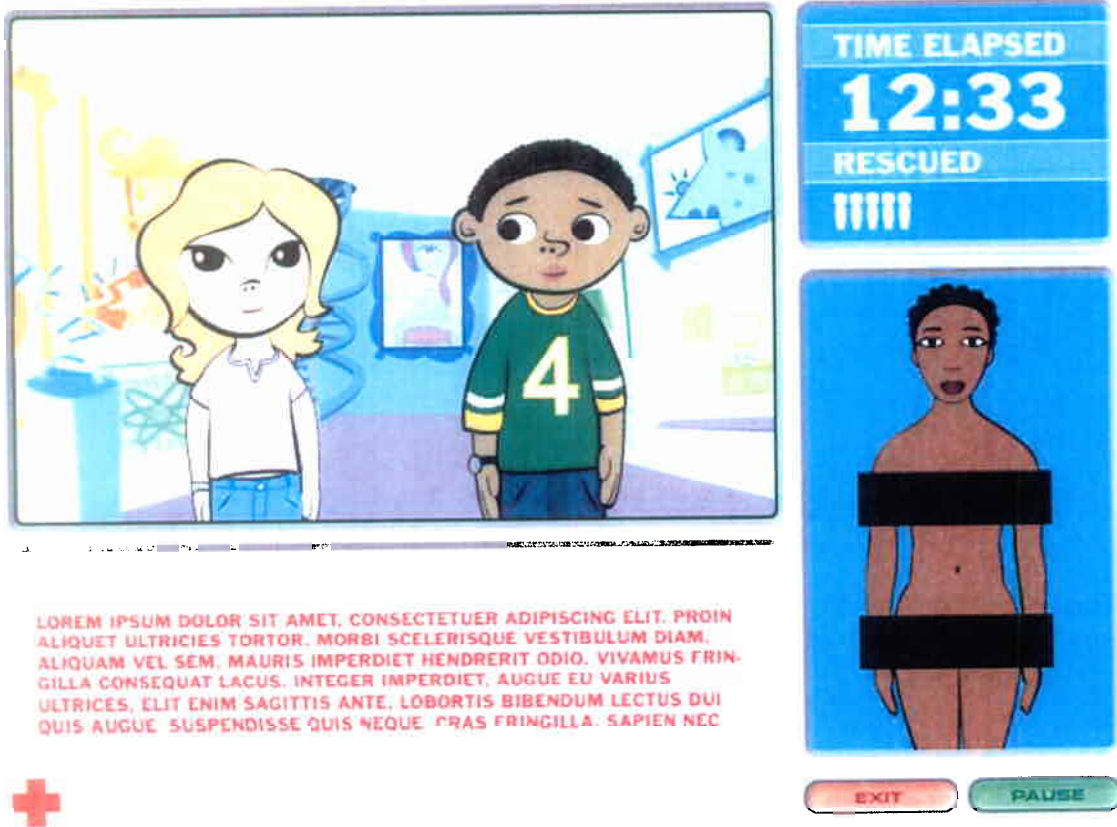
### **PROJECT TALK**

## **APPENDIX H**

### Graphic User Interface (GUI) Prototypes

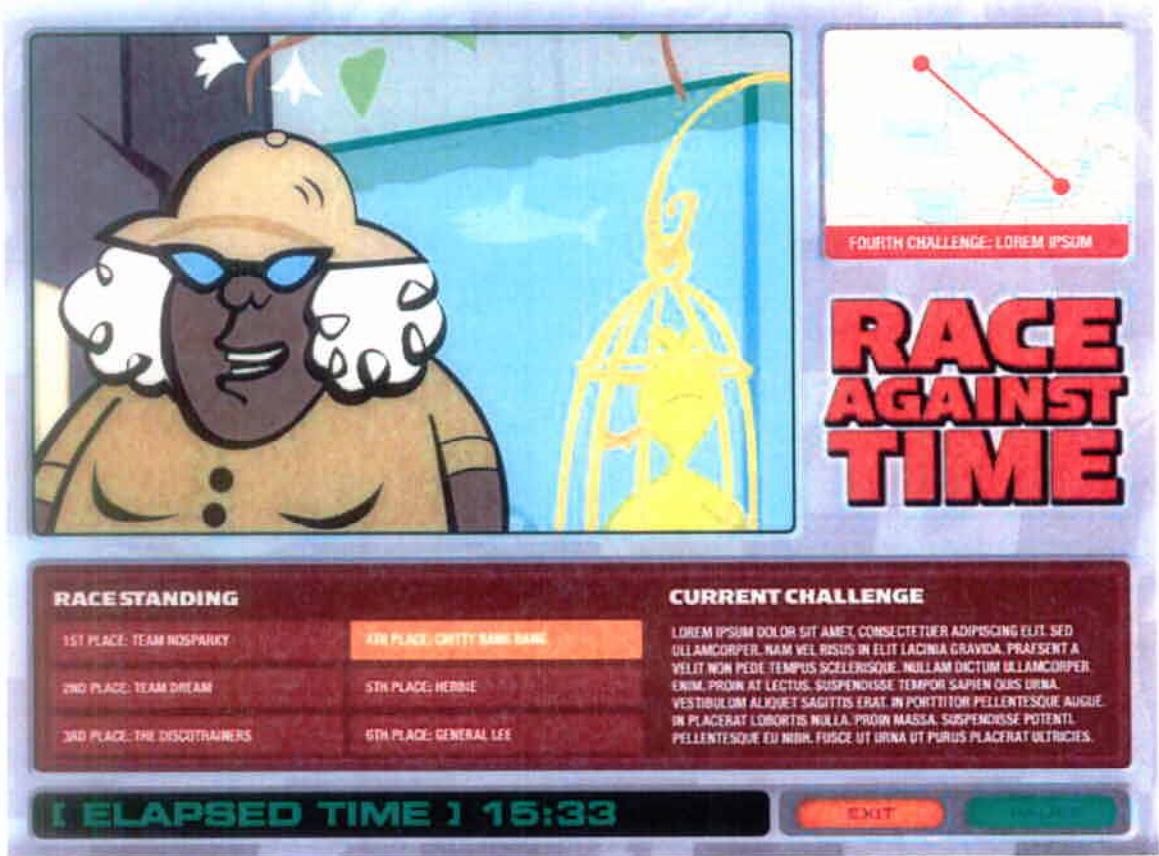
1. Extreme
2. Amazing Race
3. Psy-ops 2

## Extreme GUI





Amazing Race GUI



## Psy-Ops 2 GUI

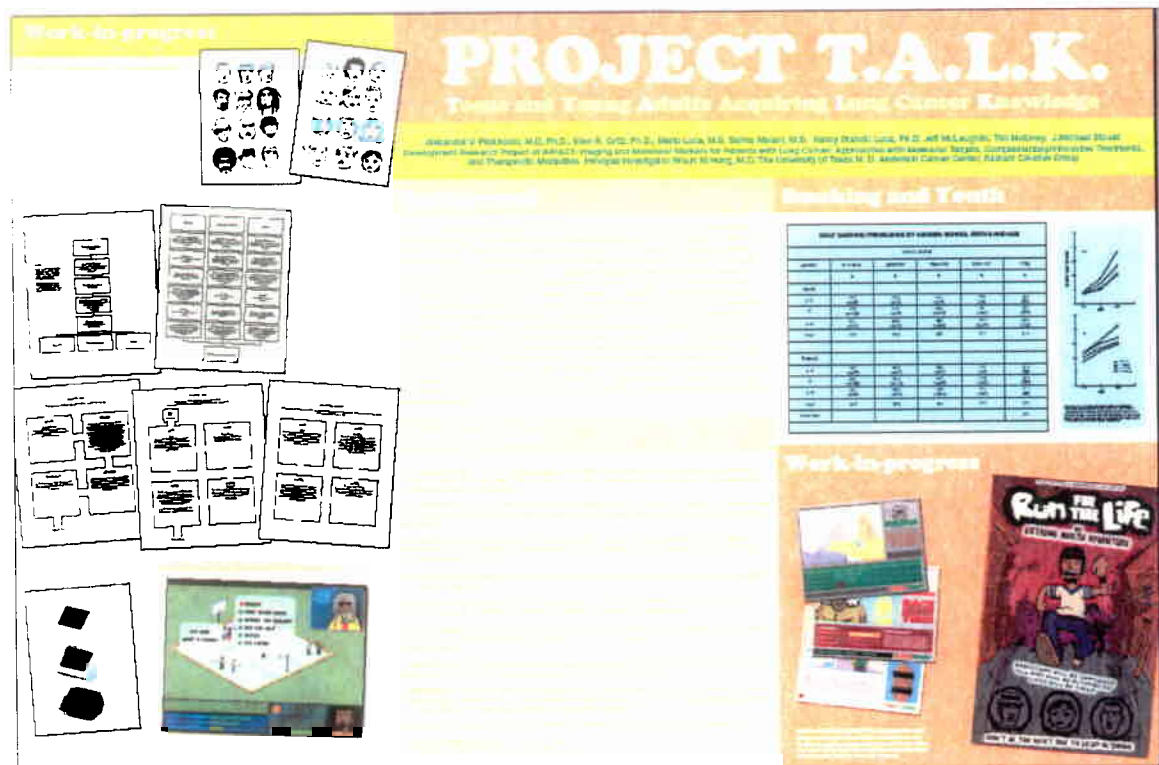




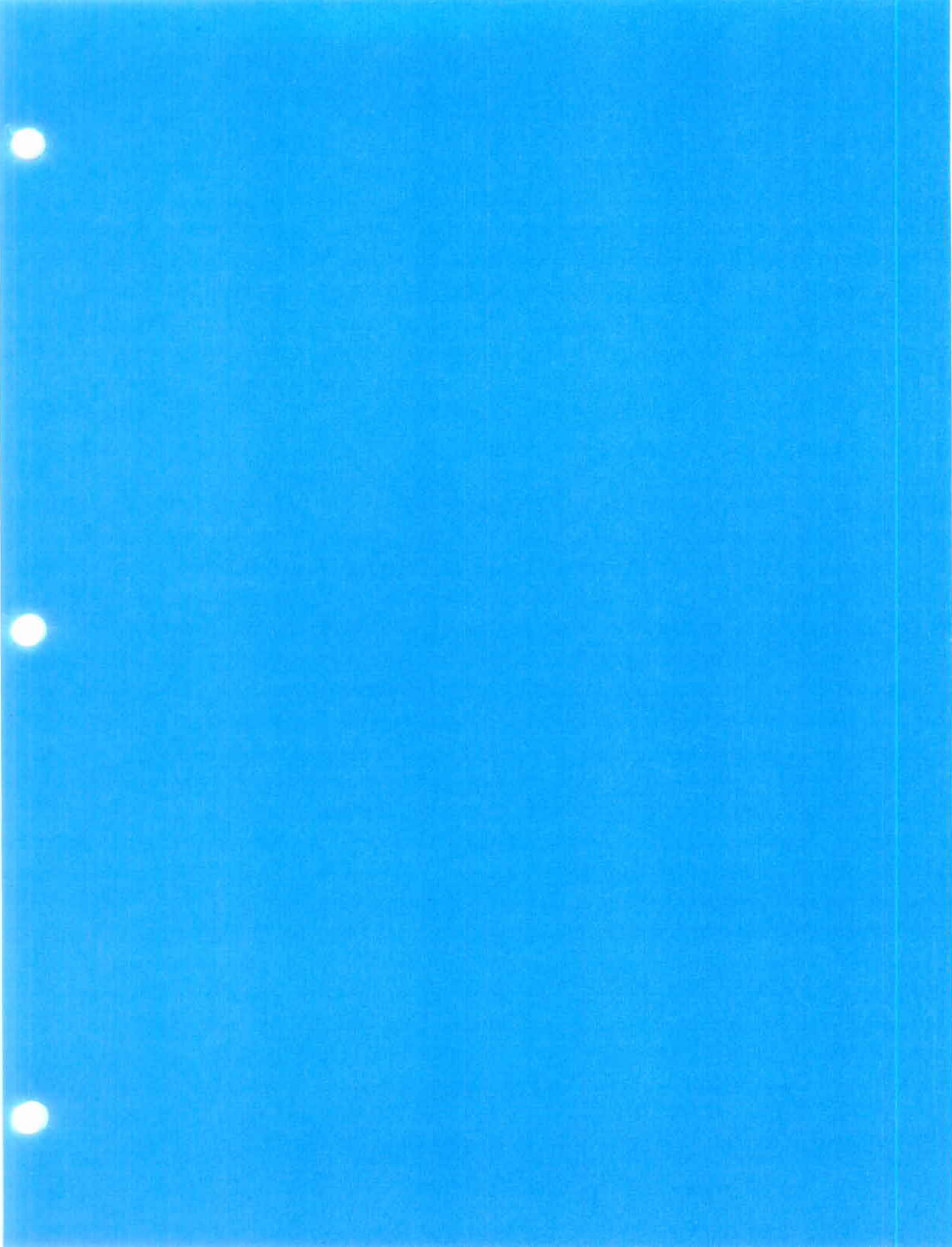
## **APPENDIX I PROJECT TALK**

## APPENDIX I

TALK Science Day Poster: December 5, 2005







## **APPENDIX J**

### **Manuscripts**



**Podoplanin is overexpressed in head and neck squamous cell carcinomas (HNSCC) and is associated with poor clinical outcome**

Ping Yuan, Stephane Temam, Adel El-Naggar, Xian Zhou, Jack Lee, and Li Mao.

*Department of Thoracic/ Head & Neck Medical Oncology, University of Texas M.D. Anderson Cancer Center, Houston, TX*

Podoplanin is a mucin-like glycoprotein that is important in lymphangiogenesis. Recent studies have shown that podoplanin may be also expressed in certain tumor cells, including squamous cell carcinomas. We first determined the expression of podoplanin in 35 patients with HNSCC including 16 with oral tumors and 19 with hypopharyngeal tumors by immunohistochemical analysis, and evaluated the association between podoplanin expression status and patients' clinical and pathologic characteristics. Podoplanin was not expressed in normal oral epithelial cells but was detected in some hyperplastic and dysplastic lesions. High podoplanin expression was found in 20 of the test cases (57%) and was associated with lymph node metastasis. We further validated the findings in an independent set of 33 patients with tongue cancer and assessed the association of podoplanin expression and survival. Twenty-three tumors in the validation set (70%) expressed high-levels of podoplanin. Patients whose tumors expressed high-levels of podoplanin had a statistically significantly higher rate of lymph node metastasis ( $P = 0.002$ ) and shorter survival durations ( $P = 0.04$  and  $P = 0.03$  for overall survival and cancer-specific survival, respectively) than did those with low podoplanin expression. Our data suggest that podoplanin is involved in oral tumorigenesis and may be useful as a marker to predict clinical outcome in patients with HNSCC. (Supported in part by National Cancer Institute grants CA106451 and CA16672; Department of Defense grant W81XWH-05-2-0027)

# **A Hybrid Vector for Ligand-directed Tumor Targeting and Molecular Imaging**

**Amin Hajitou<sup>1</sup>, Martin Trepel<sup>5,6</sup>, Caroline E. Lilley<sup>7</sup>, Suren Soghomonyan<sup>2</sup>,  
Mian M. Alauddin<sup>2</sup>, Frank C. Marini III<sup>3</sup>, Bradley H. Restel<sup>1</sup>, Michael G. Ozawa<sup>1</sup>,  
Catherine A. Moya<sup>1</sup>, Roberto Rangel<sup>1</sup>, Yan Sun<sup>1</sup>, Karim Zaoui<sup>5,6</sup>, Manfred Schmidt<sup>5,6</sup>,  
Christof von Kalle<sup>5,6</sup>, Matthew D. Weitzman<sup>7</sup>, Juri G. Gelovani<sup>2</sup>, Renata Pasqualini<sup>1,4\*</sup> and  
Wadih Arap<sup>1,4\*</sup>**

*Departments of <sup>1</sup>Genitourinary Medical Oncology, <sup>2</sup>Experimental Diagnostic Imaging, <sup>3</sup>Bone Marrow Transplantation, and <sup>4</sup>Cancer Biology, The University of Texas M. D. Anderson Cancer Center, 1515 Holcombe Boulevard, Houston, TX 77030*

*<sup>5</sup>Department of Hematology and Oncology and <sup>6</sup>Institute for Molecular Medicine and Cell Research, University of Freiburg Medical Center, Hugstetter Strasse 55, D-79106 Freiburg, Germany*

*<sup>7</sup>The Salk Institute, 10010 North Torrey Pines Road, La Jolla, CA 92037*

*\*Correspondence: (rpasqual@mdanderson.org) and/or (warap@mdanderson.org)*

## **Summary**

Merging tumor targeting and molecular-genetic imaging into an integrated platform is limited by lack of strategies to enable systemic yet ligand-directed delivery and image of specific transgenes. Many eukaryotic viruses serve for transgene delivery but require elimination of native tropism for mammalian cells; in contrast, prokaryotic viruses can be adapted to bind to mammalian receptors but are otherwise poor vehicles. Here we introduce a system containing cis-elements from adeno-associated virus (AAV) and single-stranded bacteriophage. Our AAV/phage (AAVP) prototype targets an integrin. We show that AAVP provides superior tumor transduction over phage and that incorporation of inverted terminal repeats is associated with improved fate of the delivered transgene. Moreover, we show that the temporal dynamics and spatial heterogeneity of gene expression mediated by targeted AAVP can be monitored by positron emission tomography. This new class of targeted hybrid viral particles will enable a wide range of applications in biology and medicine.

## **Introduction**

Integration of tumor targeting and imaging technologies into a single discipline has the potential to improve the practice of medicine. Non-invasive molecular-genetic imaging of temporal dynamics and spatial heterogeneity of transgene expression can provide the means for the assessment of specificity of targeting and for monitoring the efficacy of genetic transfer (Blasberg and Tjuvajev, 2003; Gross and Piwnica-Worms, 2005a; Medintz et al., 2005; Tai and Laforest, 2005). However, this emerging field depends on development of ligand-directed particles to enable systemic targeted delivery and molecular imaging of reporter transgenes.

Currently, eukaryotic viruses unquestionably provide superior transgene delivery and transduction (Kootstra and Verma, 2003) but ligand-directed targeting of such vectors requires ablation of their native tropism for mammalian cell membrane receptors (Müller et al., 2003; Mizuguchi and Hayakawa, 2004). In contrast, prokaryotic viruses such as bacteriophage (phage) are considered poor vehicles for mammalian cell transduction. However, despite their inherent shortcomings as “eukaryotic” viruses, phage particles have no tropism for mammalian cells (Barrow and Soothill, 1997; Barbas et al., 2001) and have even been adapted to transduce such cells (Ivanenkov et al., 1999; Larocca et al., 1999; Poul and Marks, 1999; Piersanti et al., 2004) albeit at low efficiency. Phage display-based technology allows direct ligand-directed selection of homing peptides to corresponding receptors selectively expressed in normal or tumor tissues (Hajitou et al., 2006). We hypothesized that combining the favorable biological attributes of eukaryotic viruses to those of prokaryotic viruses might yield chimeric particles with potential as targeted delivery tools for molecular imaging. Since the genomes of recombinant adeno-associated virus (AAV) and single-stranded phage consist of compatible DNA, we generated

novel chimeras between AAV and fd-tet (Zacher et al., 1980), an M13-derived filamentous phage, displaying short peptides (Smith and Scott, 1993) and evaluated them for tumor targeting and molecular imaging of *Herpes simplex virus thymidine kinase (HSVtk)* gene expression with [<sup>18</sup>F]-FEAU and positron emission tomography (PET) in preclinical tumor models.

## Results and Discussion

### Ligand-directed Particles Are Functional in Mammalian Cells

As a proof-of-concept, we constructed a targeted chimeric virus comprising of recombinant AAV and an fd-tet phage clone displaying the double-cyclic peptide CDCRGDCFC (termed RGD-4C) phage (Pasqualini et al., 1997; Arap et al., 1998; Ellerby et al., 1999). The RGD-4C peptide binds to  $\alpha_v$  integrins, a cell surface receptor over-expressed in both tumor and endothelial cells (Arap et al., 1998; Hood et al., 2002). To obtain chimeric viruses (further referred to as AAV/phage; AAVP), we inserted an eukaryotic gene cassette from AAV in an intergenomic region of RGD-4C phage (RGD-4C AAVP), insertless phage (non-targeted AAVP), or phage displaying control peptides, such as scrambled RGD-4C AAVP or D→E mutant (termed RGE-4C) AAVP, and packaged it with the phage DNA into the phage capsid (**Figure S1**). In order to show that the cis-elements of the resulting targeted chimeric virus remain functional, we evaluated the ligand properties of the RGD-4C peptide and the rescuing properties of the inverted terminal repeats (ITRs) in the context of AAVP. First, to evaluate peptide specificity, we show that RGD-4C AAVP binds to mammalian cells expressing  $\alpha_v$  integrins, in contrast to the non-targeted AAVP or AAVP displaying negative control peptides such as RGE-4C or various scrambled versions of the RGD-4C sequence (**Figure 1A**), which neither bind to nor infect mammalian cells. We also demonstrate that RGD-4C AAVP carrying

reporter genes can mediate ligand-directed internalization (**Figure 1B**) and transduction of mammalian cells (**Figure 1C**) relative to controls. For cell internalization experiments, negative controls included non-targeted AAVP, various RGD-4C scrambled AAVP, or RGE-4C AAVP (**Figure 1B**); for cell transduction experiments, non-targeted AAVP (**Figure 1C**), scrambled RGD-4C AAVP, or RGE-4C AAVP (data not shown) served as negative controls. Consistent with these results, we have previously demonstrated that the synthetic RGD-4C peptide specifically inhibits cell binding and internalization of various targeted RGD-4C phage-based constructs (Giordano et al., 2001; Chen et al., 2004 and unpublished results). Finally, we show that mammalian cell transduction can also be specifically competed by the synthetic RGD-4C peptide relative to negative controls such as non-targeted AAVP (**Figure 1D**), scrambled RGD-4C, or RGE-4C (data not shown). To rule out the possibility that some of these results (**Figures 1A and 1B**) could represent an artifact resulting from selective failure of the glycine (low pH) wash step to remove AAVP from cell membranes, we performed ice-cold control experiments (Giordano et al., 2001) in which we observed cell binding but not internalization mediated by RGD-4C AAVP (data not shown), thus supporting our interpretation.

Next, to evaluate whether the ITRs are still functional in the AAVP particle we performed rescue experiments. We show that functional recombinant AAV particles are generated from mammalian cells transduced with the RGD-4C AAVP only, but not from the cells transduced with negative control constructs (**Figure 1E**). These data establish that the genetic chimerization resulting in an RGD-4C AAVP particle does not fundamentally alter (i) the peptide targeting properties of the ligand-directed RGD-4C phage or (ii) the ability to rescue recombinant AAV particles from mammalian cells transduced by RGD-4C AAVP. A side-by-side time course of a reporter transgene expression revealed that RGD-4C AAVP transduction was detectable for much longer compared to that of the RGD-4C phage (**Table S1**).

### Molecular Mechanisms of Transgene Expression

To gain an insight into the molecular mechanisms of transgene expression mediated by AAVP, we investigated the fate of the transduced genome in mammalian cells. First, we generated stably transduced cell lines by using *GFPneo*-expressing AAVP to allow for the selection of individual transduced cell clones. Either RGD-4C AAVP-*GFPneo* or RGD-4C phage-*GFPneo* lacking AAV ITRs were used to transduce  $\alpha v$  integrin-expressing 293 cells and clones were isolated under G418 selection. Rescue experiments showed functional recombinant AAV-*GFPneo* generated from all the RGD-4C AAVP-*GFPneo* 293 cell clones, but none generated from the RGD-4C phage-*GFPneo* clones (data not shown), thus confirming that the chimeric individual clones contain functional ITRs. Although cells transduced with the non-chimeric RGD-4C phage-*GFPneo* retained G418-resistance, GFP expression was generally weaker than that of the RGD-4C AAVP-*GFPneo* clones (**Figure 2A**). We then set out to determine the fate of the *GFPneo* transgene cassette in stably transduced clones by a comprehensive restriction enzyme digestion of genomic DNA followed by Southern blotting and PCR analysis (**Figure 2, Figure S2 and Table S2**). To prove persistence of the transgene cassette, genomic DNA was digested with *AflIII* and *XhoI* to detect the release of full-length transgene cassettes prior to the analysis. We observed such release in 100% of the clones transduced by RGD-4C AAVP (n=9 of 9 clones), compared to only in 33% of the clones (n=3 of 9 clones) transduced by the non-chimeric RGD-4C phage construct (**Figure 2B**). We next designed another restriction digest of genomic DNA to detect potential concatemeric forms of the transgene cassette (Lieber et al., 1999; Hsiao et al., 2001). We detected the presence of head-to-tail concatemers of the transgene cassette in 67% of the clones transduced by RGD-4C AAVP (n=6 of 9 clones) while no such concatemers were detected in clones transduced by the non-chimeric RGD-4C phage construct (**Figure 2C**). To identify possible additional concatemeric forms of the transgene cassette, we



performed a multiplex PCR by using primers flanking the 5' and 3' ends of the constructs. Again, we found no concatemers in clones transduced by non-chimeric RGD-4C phage construct, whereas 100% of clones transduced by RGD-4C AAVP contained concatemeric forms (n=9 of 9 clones), all of them found in head-to-tail orientation (**Figure S2B**). Moreover, topo cloning of smaller PCR products revealed the head-to-tail orientation of the transgene cassette with ITR deletions (**Figure S2C**) (Yang et al., 1997). Finally, although the large PCR products could not be sequenced, their sizes suggest the presence of concatemers with intact ITRs at the junction site. An individual analysis of DNA for each single clone is also detailed (**Table S2**). These data suggest that AAVP may bestow an advantage in gene expression by means of an altered fate of the transgene cassette through maintenance of the entire mammalian transgene cassette, better persistence of episomal DNA, formation of concatemers of the transgene cassette, or perhaps by a combination of these non-mutually exclusive mechanisms. These observations are consistent with recent developments in the understanding of AAV (McCarty et al., 2004).

### **Tumor Targeting In Vivo and Molecular-genetic Imaging**

After demonstrating that the central elements of the targeted chimeric viral particle (i.e., the RGD-4C peptide and the AAV ITRs) are intact and functional and after elucidating the molecular mechanisms of AAVP-mediate gene expression in mammalian cells, we evaluated the specificity and efficacy of gene delivery into tumors after systemic administration of AAVP. As an initial preclinical model, we used nude mice bearing subcutaneous tumor xenografts derived from human Kaposi sarcoma KS1767 cells (Arap et al., 1998; Ellerby et al., 1999). First, to verify that the viral construct targets to KS1767-derived xenografts in mice, we administered intravenously either RGD-4C AAVP or one of several negative controls (non-targeted AAVP, scrambled RGD-4C AAVP, or RGE-4C AAVP). After a 3-5 m circulation time, a strong anti-AAVP staining in tumor vasculature was observed in mice that received RGD-4C AAVP but not

in control mice (**Figure 3A**). We next used an RGD-4C AAVP variant encoding the *GFP* gene as a reporter to determine, by using *in situ* immunofluorescence microscopic imaging, whether this vector (RGD-4C AAVP-*GFP*) can transduce KS1767-derived xenografts. We performed immunostaining against GFP in tumors and in different organs seven days after systemic administration of either RGD-4C AAVP-*GFP* or negative control constructs into tumor-bearing mice. Immunofluorescence revealed GFP expression largely in tumor blood vessels and surrounding tumor cells in mice that received RGD-4C AAVP-*GFP*. In contrast, no GFP staining was detected in tumors from control mice that received non-targeted, scrambled, or mutant AAVP-*GFP* (**Figure 3B**). This staining pattern suggests that ligand-directed transduction is mediated by targeting of  $\alpha_v$  integrins in the vascular endothelium of tumors. Consistently, several non-target control organs (brain, liver, pancreas and kidney) lacked tissue expression of GFP (**Figure S3**). These results indicate that RGD-4C AAVP particles can specifically target tumor xenografts by a ligand-directed mechanism and transduce them after systemic administration *in vivo*.

Next, we assessed the efficacy of preclinical bioluminescence imaging (BLI) and clinically applicable molecular-genetic PET imaging with [ $^{18}\text{F}$ ]-FEAU for non-invasive monitoring of temporal dynamics and spatial heterogeneity of the firefly *luciferase* (*Luc*) and of the *HSVtk* reporter gene expression, respectively, in living tumor-bearing mice following systemic administration of the RGD-4C AAVP. These molecular-genetic imaging studies were conducted in a preclinical model of human prostate cancer since this particularly prevalent tumor remains a challenge to properly image in patients. We first used a standard experimental setup for *in vivo* imaging of the *Luciferase* (*Luc*) transgene reporters in tumor-bearing mice (**Figure 4A**). We selected BLI of *Luc* expression, because it is a very sensitive method for reporter gene imaging in mice and has virtually no non-specific background activity in the images (Gross and Piwnicka-

Worms, 2005a; Gelovani and Blasberg, 2003). Tumor-specific expression of *Luc* was observed in DU145 tumors in mice receiving RGD-4C AAVP-*Luc*. In contrast, tumor-associated bioluminescence signals could not be observed in control mice receiving the non-targeted AAVP-*Luc* or scrambled RGD-4C AAVP-*Luc*. No bioluminescence was observed in normal organs with any AAVP tested. These data confirm the tumor-specificity of RGD-4C AAVP-mediated targeting and transgene expression observed with immunofluorescence microscopy imaging studies with RGD-4C AAVP-*GFP*. Consistently with previous results presented here (Figure S3), the kinetics of distribution suggests that despite the non-specific hepatic clearance of phage particles (Geier et al., 1973), such phenomenon does not result in an undesirable gene transduction of the liver. These observations are in sharp contrast with the well-documented non-specific transduction of normal organs (such as liver) by the mammalian viral gene delivery vectors. By using BLI in vivo, *Luc* reporter transgene expression within tumors was clearly detectable at day 3 after AAVP administration and increased gradually to reach maximal levels by day 10. Repetitive 2-dimensional BLI of *Luc* reporter gene expression was performed every other day and provided an initial cost-effective strategy to study the specificity, temporal dynamics, and spatial heterogeneity of reporter transgene expression mediated by AAVP. However, because BLI of *Luc* reporter gene expression is not clinically applicable, we next introduced into the AAVP vector the *HSVtk* gene, which can serve both as a “suicide” gene (when combined with gancyclovir; GCV) and as a reporter transgene for clinically applicable PET imaging with *HSVtk*-specific radiolabeled nucleoside analogues [<sup>124</sup>I]-FAIU, [<sup>18</sup>F]-FHBG, [<sup>18</sup>F]-FEAU). Previous studies established that PET imaging of *HSVtk* expression provides the ability to define the location, magnitude, and duration of transgene expression (Tjuvajev et al., 1998; Tjuvajev et al., 1999; Ray et al., 2001; Massoud and Gambhir, 2003). It has also been previously determined that the magnitude of accumulated radiolabeled tracers in *HSVtk*-transduced cell lines and tumors in vivo correlates with the level of *HSVtk* expression (Blasberg

and Tjuvajev, 2003; Gross and Piwnica-Worms, 2005a; Tai and Laforest, 2005). In the studies presented here, we selected, synthesized and used the radiolabeled nucleoside analogue 2'-[ $^{18}\text{F}$ ]-fluoro-2'-deoxy-1- $\beta$ -D-arabino-furanosyl-5-ethyl-uracil ([ $^{18}\text{F}$ ]-FEAU), which is a better radiolabeled substrate for the HSVtk enzyme than other nucleoside analogues, especially from pharmacokinetic considerations (a very low background activity in all normal organs and tissues) (Kang et al., 2005). By using repetitive PET imaging with [ $^{18}\text{F}$ ]-FEAU (on days 0, 3, 5, 10, and 16), we have visualized and quantitated the temporal dynamics and spatial heterogeneity of *HSVtk* gene expression after a single systemic administration of RGD-4C AAVP-*HSVtk* or non-targeted AAVP-*HSVtk* in DU145-derived tumor xenografts and other organs and tissues in nude mice (**Figure 4B**). Tumor xenograft sizes ( $\sim 150 \text{ mm}^3$ ) before, as well as tumor growth rates after administration of either RGD4C AAVP-*HSVtk* or non-targeted AAVP-*HSVtk* were similar in both cohorts of mice (**Figure 4C**). PET imaging with [ $^{18}\text{F}$ ]-FEAU revealed a gradual increase in the level of *HSVtk* transgene expression in tumors (increase in % administered intravenous dose per gram) during the initial five days after administration of RGD-4C AAVP-*HSVtk*, followed by gradual stabilization of *HSVtk* expression levels towards day 10 post vector administration. In contrast, in control tumor-bearing mice receiving non-targeted AAVP-*HSVtk*, only a minor increase in tumor accumulation of [ $^{18}\text{F}$ ]-FEAU was observed at day 3, which rapidly decreased to background level (**Figure 4D**). Consistent with preceding BLI experiments, no [ $^{18}\text{F}$ ]-FEAU PET-detectable *HSVtk* expression was observed in non-target organs or tissues (**Figure 4B**). Indeed, low-level heterogeneous activity in the PET images (blue color) represents normal background activity, which was intentionally intensified in the images presented to demonstrate that no truncation of low levels of radioactivity was made to artificially “improve” the specificity of *HSVtk* expression in tumors versus non-target tissues. When tumors grew to reliably palpable sizes ( $\sim 350\text{-}400 \text{ mm}^3$ ), and a plateau of *HSVtk* expression was achieved in tumors, treatment with GCV was initiated in all cohorts of animals (**Figure 4C**). PET imaging

with [ $^{18}\text{F}$ ]-fluorodeoxyglucose ([ $^{18}\text{F}$ ]-FDG) served to monitor glucose metabolism and GCV-induced changes in tumor viability. Two days before initiation of GCV therapy (day 9 post vector administration), the DU145 tumors in both groups of mice were viable and actively accumulated [ $^{18}\text{F}$ ]-FDG (**Figure 4E**). After GCV therapy, the volume of tumors in mice that received RGD-4C AAVP-*HSVtk* was significantly smaller than in mice that received non-targeted AAVP-*HSVtk* ( $p < 0.05$ ; **Figure 4C**). Moreover, tumor xenografts were also metabolically suppressed as evidenced by a decrease in accumulation of [ $^{18}\text{F}$ ]-FDG (**Figure 4E**). The levels of *HSVtk* expression in tumors of mice administered with RGD-4C AAVP-*HSVtk* were also significantly decreased after GCV therapy, as evidenced by a sharp decrease in [ $^{18}\text{F}$ ]-FEAU accumulation in PET images (**Figure 4D**), which were obtained 24 h after the last GCV dose (to avoid competition with FEAU). These studies confirm the specificity of tumor targeting by RGD-4C AAVP and demonstrate that the level of *HSVtk* transgene expression is adequately high for effective prodrug activation of GCV.

In order to evaluate efficacy horizontally in other preclinical models, we assembled a panel of tumor cell lines from different species and histological origins and generated tumors in immunosuppressed or immunocompetent mice. Cohorts of Kaposi sarcoma (KS1767)-derived tumor-bearing mice received systemically a single intravenous dose of either the RGD-4C AAVP-*HSVtk* or non-targeted AAVP-*HSVtk* (control), followed by GCV treatment in all groups. Marked tumor growth suppression was observed in tumor-bearing mice receiving RGD-4C AAVP-*HSVtk*, as compared to mice treated with vehicle or mice that received non-targeted AAVP (**Figure 5A**). Similar tumor growth suppressive effects were observed in UC3-derived bladder carcinomas (**Figure 5B**) and DU145-derived prostate carcinomas (**Figure 5C**) in nude mice, even if larger tumor xenografts were treated (**Figure 5D**) and consistent with the imaging results presented (**Figure 4**). To rule out the possibility that the observed anti-tumor effects were either species-specific or xenograft-specific, we sought to analyze the efficacy of the RGD-4C

AAVP-*HSVtk* on a standard mouse tumor model. We chose an isogenic tumor in which EF43-*FGF4* mouse mammary cells are administered subcutaneously to induce rapid growth of highly vascularized tumors in immunocompetent mice (Hajitou et al., 2001). First, we show ligand-directed homing of RGD-4C AAVP to EF43-*FGF4*-derived tumors by anti-phage immunostaining (**Figure S4**). Either RGD-4C AAVP-*GFP* or non-targeted AAVP-*GFP* was administered intravenously to mice bearing isogenic mammary tumors for a 3-5 m circulation time. Unlike the non-targeted AAVP-*GFP*, RGD-4C AAVP-*GFP* produced a strong anti-phage staining in tumors (**Figure S4A**). Next, we performed immunofluorescence with an anti-GFP antibody at seven days after intravenous administration to reveal strong GFP expression in the tumors in mice that received RGD-4C AAVP-*GFP*; in contrast, no GFP staining was detected in tumors from mice that received non-targeted AAVP-*GFP*; consistently, an anti- $\alpha v$  integrin antibody detected strong expression in EF43-*FGF4* tumors (**Figure S4B**). Again, a single systemic dose of RGD-4C AAVP-*HSVtk* followed by GCV markedly inhibited the growth of EF43-*FGF4* tumors (**Figures 5E-G** and **Figure 6**). Moreover, when tumors grew back after termination of therapy, repeated administrations of RGD-4C AAVP-*HSVtk* again inhibited EF43-*FGF4* tumor growth and improved survival of tumor-bearing mice (**Figure 5F**). Phage-based particles are known to be immunogenic but this feature can be modulated through targeting itself (Trepel et al., 2001). In fact, RGD-4C AAVP-*HSVtk* plus GCV remained surprisingly effective on phage-vaccinated immunocompetent mice despite very high titers of circulating anti-phage IgG (**Figure 5G**). In selective experiments, a comprehensive panel of negative experimental controls including vehicle alone, vehicle plus GCV, non-targeted AAVP, non-targeted AAVP plus GCV, targeted RGD-4C AAVP, targeted RGD-4C AAVP-*GFP*, and targeted RGD-4C AAVP-*GFP* plus GCV (mock transduction) were used (**Figure 6A** and data not shown).

To check for post-treatment effects, we obtained detailed histopathological analysis of EF43-*FGF4* tumors recovered seven days after therapy. We noted extensive tumor destruction caused by the single systemic dose of RGD-4C AAVP-*HSVtk* plus GCV. Specifically, hematoxylin and eosin (H&E) staining revealed uniform destruction of the central area of the tumor and only a small viable outer rim; in contrast, non-targeted AAVP-*HSVtk* had no such effect (**Figure 6B**). Staining with an anti-CD31 antibody confirmed both disrupted tumor blood vessels within the tumor central region and preserved vasculature towards the outer rim, whereas no damage was observed in the tumors treated with non-targeted AAVP-*HSVtk* (**Figure 6B**). We also evaluated the tumors for terminal deoxynucleotidyl transferase-mediated dUTP-biotin nick end-labeling (TUNEL) staining, which marks apoptotic cells, because the *HSVtk*/GCV strategy is associated with apoptotic death of cells. In tumors treated with RGD-4C AAVP-*HSVtk* and GCV, TUNEL staining detected apoptosis in the tumor central region but not within the outer rim while no apoptosis was observed in tumors from mice that received non-targeted AAVP-*HSVtk* chimera (**Figure 6B**). Control organs removed from tumor-bearing mice treated by the same experimental protocol revealed no histopathologic abnormalities (**Figure S5**). Together, these results show that a single systemic dose of RGD-4C AAVP-*HSVtk* plus GCV maintenance can suppress tumor growth.

Some of our results merit further discussion. First, the relative contribution of targeting each tumor compartment (i.e., tumor cells versus tumor vascular endothelium and/or stroma) will depend on the ligand-receptor system and on the experimental model(s) used. For instance, the expression of the membrane target (i.e.,  $\alpha_v$  integrins) in tumor cells will vary from low (EF43-*FGF4*) to strong (KS1767). Moreover, aside from the specific optimal dose for transduction of each model (and application) used, there is also an optimal time to examine transgene expression. In other words, the stoichiometry of reporter gene expression depends not only from



levels and patterns of reporter expression in individual cells, but also from the relative number of proliferating transgene-expressing cells versus dying transgene-expressing cells. Thus, while we used fixed parameters for the experiments presented here, further determination of targeted AAVP optimal doses and timeframes on a case-by-case basis still apply. Future translational studies will need to be conducted to determine what doses are clinically meaningful and how an AAVP-based system can be optimized for therapy of patients by using clinically applicable molecular-genetic imaging with PET.

Finally, one might speculate that a broad range of currently intractable biological questions well beyond molecular oncology will be addressed by using targeted AAVP, especially in combination with different pre-clinical and in clinical molecular-genetic imaging settings. For example, the systemic ligand-directed delivery of constructs with tissue- and/or disease-specific promoters (instead of a CMV promoter) to target sites will allow monitoring expression of their corresponding native genes *in vivo*; such promoter-driven transcription of reporter activity will allow the study of cell trafficking and engraftment. Several non-invasive imaging applications such as experimental monitoring of substrate-specific degradation, protein-protein interactions and other molecular events via reporter trans-activation, complementation, or reconstitution strategies in cells and in whole animals (Luker et al., 2004; De and Gambhir, 2005; Gross and Piwnicka-Worms 2005b) will likely follow. In fact, we have recently described networks of gold nanoparticles and bacteriophage as biological sensors and cell targeting agents (Souza et al., 2006), such technology can be combined with ligand-directed AAVP to further improve molecular-genetic imaging. On another note, AAVP itself may provide suitable reagents to study the mechanistic role of ITR structures in transgene persistence and chromosomal integration since (in contrast to AAV vectors) phage-based constructs with no ITRs can serve as negative experimental controls. In translational terms, the results presented here bodes well

with an existing framework leading to direct AAVP-based random peptide library screening in patients (Arap et al., 2002; Pentz et al., 2005) and may form the basis for the discovery of new or unrecognized human ligand-receptors. Thus, many other systemic targeting and imaging applications in tandem will become possible in a relatively short timeframe.

## **Conclusions**

Ligand-directed AAVP combines desirable properties from two unrelated genetic systems to yield a targeted particle for molecular imaging. Attractive features include a cheap and high-yield of production in host bacteria and no requirements for helper viruses or trans-acting factors. Moreover, the native tropism of AAV for mammalian cells is eliminated since there is no AAV capsid formation and the displayed ligand peptides allow homing to tissue-specific receptors. In the prototype presented here, the ligand-directed AAVP sustains no loss of systemic phage targeting properties and even acquires some post-targeting patterns associated with AAV. We have previously proposed that molecular imaging of marker genes would have the potential to assess therapeutic levels of expression and markedly improve our ability to predict response to therapies in which target genes are known. The introduction of ligand-directed AAVP for systemic targeting and molecular-genetic imaging, rationally designed along the lines described here, is a major step in that direction. Finally, one might speculate (i) that in addition to ligand-directed targeting, further platform refinements such as transcriptional targeting will certainly be possible by incorporation of specific promoters, and (ii) that other hybrid viruses containing prokaryotic and eukaryotic elements (such as, for instance, chimeras between adenovirus and double-stranded lambda phage) may also be envisioned for systemically targeted imaging of reporters. Based on this comprehensive analysis, it seems that the translation of our prototype particle may lead to realistic imaging of gene expression in

cancer patients. On a larger context, given the favorable tissue-targeting and molecular imaging profiles, ligand-directed AAVP is likely to be a useful tool in dissecting other relevant biological questions.

## Experimental Procedures

### Design, Construction, and Generation of Targeted AAVP Particles

RGD-4C phage and RGD-4C AAVP were engineered in a two-step process: generation of an intermediate (RGD-4C fUSE5-MCS) and subsequent production of RGD-4C phage construct and RGD-4C AAVP. RGD-4C fUSE5-MCS contained the oligonucleotide insert encoding the specific targeting peptide RGD-4C and a fragment of the fMCS plasmid that had a multicloning site (MCS) for insertion of the eukaryotic expression cassette. RGD-4C phage-derived fUSE5 DNA and phage-derived fMCS DNA were purified from lysates of *E. coli* (MC1061). We obtained the intermediate RGD-4C fUSE5-MCS by ligating a 5.4 kb *Bam*HI/*Sac*II fragment of the RGD-4C fUSE5 plasmid to the 4.1 kb *Bam*HI/*Sac*II fragment of the fMCS plasmid. Next, we created a targeted AAVP-GFP by cloning the *Pac*I fragment (2.8 kb) of pAAV-*eGFP* plasmid (enhanced GFP; Stratagene) from ITR to ITR into the *Pst*I site of RGD-4C fUSE5-MSC. Briefly, pAAV was digested with *Pac*I to release a 2.8 kb fragment, which was blunted with DNA polymerase and cloned into the blunted *Pst*I site of RGD-4C fUSE5-MSC. To generate the targeted phage constructs without ITRs, a 2.3 kb fragment located between the ITRs of pAAV-*eGFP* and containing pCMV-GFP and SV40 poly A was released by *Eco*RI digestion, blunted, and cloned into the MCS of RGD-4C fUSE5-MSC. To select cells expressing GFP, the *Bam*HI-*Sac*I fragment of the pQBI phosphoglycerate kinase-1 (QBIOgene) promoter and containing a *GFPneo* fusion sequence was cloned in the *Not*I site of AAVP or control phage constructs to ensure that cells expressing GFP were G418- resistant. The *GFPneo* fragment of pQBI PGK was released by *Bam*HI and *Sac*I digestion, and blunted with DNA polymerase; then phosphorylated linkers to *Not*I were added. After *Not*I digestion, the 1.57 kb *GFPneo* fragment was cloned into the *Not*I site of AAVP or non-chimeric phage construct. Finally, to generate a targeted AAVP particle carrying

the gene for *HSVtk* or *Luc* the *BamHI*-*NotI* fragment containing *HSVtk* or *Luc* was subcloned into *BamHI*-*NotI* site of pAAV plasmid to replace *GFP*. The ITR-*HSVtk*-ITR or ITR-*Luc*-ITR fragments were removed from pAAV-*HSVtk* and pAAV-*Luc* then inserted into RGD-4C fUSE5-MCS. Constructs were verified by DNA sequencing and restriction analysis, purified from the culture supernatant of host *E. coli* (MC1061), re-suspended in PBS and re-centrifuged. Resulting supernatants were titrated in *E. Coli* (k91Kan). Serial dilutions were plated on Luria-Bertani (LB) agar plates containing tetracycline and kanamycin and transducing units (TU) were determined by colony counting.

### **Mammalian Cell Surface Binding and Internalization Assays**

We used the biopanning and rapid analysis of selective interactive ligands (termed BRASIL) method (Giordano et al., 2001) to evaluate phage binding to intact cells. In brief, KS1767 cells were detached by EDTA and re-suspended in Dulbecco's modified Eagle's medium (DMEM) containing 1% BSA at  $4 \times 10^6$  cells per ml. The cell suspension (50  $\mu$ l) was incubated with  $10^9$  TU of either RGD-4C AAVP or AAVP clones displaying scrambled versions of RGD-4C (CDCFGDCRC, CDCGFDCRC, CRCDGFCDRC), mutant RGE-4C peptide, or non-targeted control. After 2 h, the AAVP/cell mixture (aqueous phase) was transferred to the top of a non-miscible organic phase (200  $\mu$ l solution in a 400  $\mu$ l Eppendorf tube) consisting of dibutyl phthalate: cyclohexane (9:1 [v:v], D = 1.03 g ml<sup>-1</sup>) and centrifuged at 10,000 g for 10 min at 4°C. The tube was snap-frozen in liquid nitrogen, the bottom of the tube was sliced off, the pellet was isolated and membrane-bound AAVP recovered.

For cell internalization, KS1767 cells were grown in tissue chamber slides, washed with PBS, incubated with  $10^9$  TU of RGD-4C AAVP or control AAVP displaying scrambled versions of RGD-4C or RGE-4C in DMEM containing 1% BSA at 37°C, and washed with PBS to remove

unbound AAVP after 4 h incubation. Cell membrane-bound clones to cell were eluted by 20 mM glycine. Next, cells were washed three times with PBS, fixed with PBS containing 4% PFA at RT for 15 min, washed with PBS, permeabilized with 0.2% Triton X-100, washed with PBS, and blocked with PBS containing 1% BSA. Cells were then incubated with a 1:200 dilution of the primary anti-M13 phage antibody (Amersham) in PBS containing 1% BSA at RT for 2 h, washed with PBS, and incubated with a 1:200 dilution of a Cy3-conjugated anti-rabbit secondary antibody in PBS containing 1% BSA for 1 h at RT. Finally, cells were washed with PBS, fixed with PBS containing 4% PFA, mounted, and visualized in an optical fluorescence microscope.

### **Recombinant AAV Rescue Assay**

Human 293 cells were infected with AAVP or phage. Four days after infection, cells were transfected with pXX2, an AAV *rep*- and *cap*-expressing plasmid (Xiao et al., 1998) and superinfected with adenovirus type 5. Cells were harvested 72 h post-adenoviral infection and supernatants were used to infect new 293 cells. GFP expression was FACS analyzed 48 h later.

### **Generation of Clonal Cell Lines**

Human 293 cells were infected with RGD-4C AAVP-*GFPneo* or RGD-4C phage-*GFPneo* (at  $10^6$  TU per cell in each case). Single-clones (n=9 per group) were isolated under G418 selection and FACS analyzed for GFP expression at 12 weeks after selection. Stable clones were termed phage clones #1-9 for phage-*GFPneo* and AAVP clones #1-9 for AAVP-*GFPneo*.

### **Tumor Models**

Tumor-bearing mice were established and tumor volumes calculated as described (Hajitou et al., 2001; Arap et al., 2004; Marchiò et al., 2004). Mice were anesthetized by intraperitoneal administration of Avertin® or by gas (2% isoflurane and 98% oxygen) inhalation. Tumor cells

were trypsinized, counted, centrifuged, and re-suspended in serum-free medium. A total of  $10^6$  cells from Kaposi sarcoma (KS1767), bladder carcinoma (UC3) or prostate carcinoma (DU145) lines were implanted subcutaneously into 6 week-old immunodeficient nude mice. The EF43-*FGF4* mouse mammary tumor cells ( $5 \times 10^4$ ) were implanted subcutaneously into 6 week-old female BALB/c immunocompetent mice. When tumors reached a volume of  $\sim 50 \text{ mm}^3$  (deemed small) or  $\sim 150 \text{ mm}^3$  (deemed large) DU145-derived xenografts (day 0), tumor-bearing mice received a single intravenous dose of RGD-4C AAVP-*HSVtk* or controls. GVC (80 mg/kg per day, intraperitoneal) was started two days later in cohorts of size-matched tumor-bearing mice.

### **Molecular-genetic Imaging in Tumor-bearing Mice**

For non-invasive molecular imaging, we used a model of prostate cancer based on the human cell line DU145 in which male nude mice bearing tumor xenografts in the subcutaneous area of the right shoulder were used. To image the *Luc* gene expression, tumor-bearing mice received a single-dose (150 mg/kg, intraperitoneal) of the substrate D-luciferin (Xenogen). Photonic emission was imaged with the In Vivo Imaging System 200 (IVIS200; Xenogen) after tail vein administration of targeted RGD-4C AAVP carrying the *Luc* gene or controls (non-targeted AAVP-*Luc*, or scrambled RGD-4C AAVP-*Luc*). Imaging parameters: image acquisition time, 1 min; binning, 2; no filter; f/stop, 1; field of view, 10 cm. Regions of interest (ROI) were defined manually over the tumors for measuring signal intensities, expressed as photons/sec/cm<sup>2</sup>/sr.

While BLI can assess transgene-expressing cell viability in experimental systems, it is not clinically applicable. Thus, to assess the viability of the established tumor xenografts, mice were imaged with a microPET scanner (Concorde Microsystems) at 2 h post intravenous administration of [<sup>18</sup>F]-FDG 100  $\mu\text{Ci}$ /mouse. [<sup>18</sup>F]-FDG was obtained commercially (PETNet). To image *HSVtk* gene expression, PET imaging was performed at 1-2 h after intravenous



administration of the radiolabeled nucleoside analogue [ $^{18}\text{F}$ ]-FEAU. PET imaging was performed on a microPET R4 (Concorde Microsystems), equipped with a computer-controlled positioning bed, has a 10.8-cm transaxial and 8-cm axial field of view (FOV), it has no septa and operates exclusively in 3-dimensional list mode. Fully 3-dimensional list mode data were collected using an energy window of 350–750 keV and a time window of 6 ns. All raw data were first sorted into 3-dimensional sinograms, followed by Fourier rebinning and OSEM image reconstruction using ASIPRO VM software (Concord Microsystems). Image pixel size was ~1 mm transaxially with a 1.2 mm slice thickness.

Radiolabeled [ $^{18}\text{F}$ ]-FEAU was synthesized to radiochemical purity greater than 99% by using 5-ethyluracil-2,5-bis-trimethylsilyl ether as the pyrimidine base for condensation with 1-bromo-2-deoxy-2-[ $^{18}\text{F}$ ]fluoro-3,5-di-O-benzoyl- $\alpha$ -D-arabinofuranose (Alauddin et al., 2003). To quantitate the [ $^{18}\text{F}$ ]-FEAU or [ $^{18}\text{F}$ ]-FDG-derived radioactivity concentration in tumors and other organs and tissues, regions of interest were drawn on images and the measured values converted from nCi/mm<sup>3</sup> into % injected dose per gram (%ID/g; Tjuvajev et al., 1998). Repetitive [ $^{18}\text{F}$ ]-FEAU PET imaging was performed at days 3, 5, 10, and 16 post administration of targeted AAVP carrying the *HSVtk* gene or control non-targeted AAVP; GCV treatment was administered between days 11 and 19. Of note, PET imaging at day 16 was performed at 24 h after GCV dosing to allow for sufficient elimination of GCV, which would otherwise compete with FEAU for phosphorylation by the HSVtk enzyme. PET imaging with [ $^{18}\text{F}$ ]-FDG was repeated at day 17 after AAVP administration to assess the viability of residual tumor, if any.

### **Immunohistochemistry**

Anesthetized mice were killed and perfused with PBS containing 4% PFA. Tumor vascularization was assessed on frozen sections by using a rat anti-mouse CD31 antibody (BD

Biosciences). Apoptosis analysis was performed on paraffin-embedded sections with a TUNEL kit (Promega). For phage immunodetection, paraffin sections were incubated with a rabbit anti-phage antibody (Sigma) followed by a peroxidase-conjugated anti-rabbit secondary antibody (Dako). For GFP immunostaining, tissues were fixed for 2 h in PBS containing 2% PFA and equilibrated for 48 h in PBS containing 15% sucrose. Cryosections were post-fixed in PBS containing 4% PFA for 20 min and blocked with 5% goat serum in PBS containing 1% BSA and 0.1% Triton X-100. Tissue sections were incubated with a rabbit affinity-purified GFP antibody (Molecular Probes) in 2% goat serum and 1% BSA. Sections were then stained with the secondary antibody AlexaFluor 488 conjugated goat anti-rabbit (Molecular Probes).  $\alpha$ v integrin immunostainings were performed on acetone fixed frozen sections of tumors removed from PBS-perfused animals. Sections were incubated for 1 h with a rat anti-integrin  $\alpha$ v monoclonal antibody (Chemicon), followed by a secondary Cy3 conjugated goat anti-rat antibody (Jackson ImmunoResearch).

## **Acknowledgments**

We thank Michael Andreeff, Marco Arap, Carlotta Cavazos, Toni Cathomen, Erkki Koivunen, Johanna Lahdenranta, Darwin Lee, Steven Libutti, Jude Samulski, Karen Schmidt, Richard Sidman, and Claudia Zompetta for advice, technical assistance, and reagents. Funded by grants from the NIH (including the SPORE) and DOD (including the IMPACT) and by awards from the Gillson-Longenbaugh, the Keck Foundation, and the Prostate Cancer Foundation (to RP and WA).

## Figure Legends

Figure 1. Ligand-directed RGD-4C AAVP Transduction of  $\alpha_v$  Integrin-expressing Cells and Rescue of Recombinant AAV

(A and B) Phage binding and internalization in KS1767 cells were performed with RGD-4C AAVP or negative AAVP controls (non-targeted, scrambled, or mutated) as indicated.

(C) Targeted gene transfer mediated by RGD-4C AAVP- $\beta$ -gal to KS1767 cells.

(D) Inhibition of transduction by the synthetic RGD-4C peptide, but not by an unrelated control peptide; nonspecific transduction levels were determined by using non-targeted AAVP. An anti- $\beta$ -gal antibody was used for staining and gene expression was detected by immunofluorescence.

(E) Rescue of recombinant AAV from cells infected with RGD-4C AAVP. Human 293 cells were incubated with targeted RGD-4C AAVP-GFP ( $10^6$  TU/cell) or negative controls (targeted non-chimera RGD-4C phage-GFP, non-targeted AAVP-GFP). Four days post-infection, cells were transfected with an AAV *rep*- and *cap*-expressing plasmid (pXX2; Xiao et al., 1998) and superinfected with wild-type adenovirus type 5 (Ad). Cells were harvested 72 h post-adenoviral infection and supernatants were then used to infect new 293 cells. GFP expression was FACS analyzed 48 h later. Shown are mean increases in recombinant AAV-GFP produced over background after rescue from each construct.

Figure 2. Analysis of the Fate of Genomes from RGD-4C AAVP-*GFPneo* or from RGD-4C phage-*GFPneo* Upon Transduction

We generated 293 stable clonal cell lines (n=9 per each group) that were then analyzed.

Individual clones were termed AAVP #1-9 or phage #1-9. Non-transduced 293 parental cells served as a negative control.

(A) Histogram shows a summary of flow cytometric analyses of 293 clones stably transduced with either AAVP-*GFPneo* (n=9) or phage-*GFPneo* (n=9). Open triangles indicate percentages of GFP-positive cells; black bars represent GFP expression levels (mean fluorescent intensity; MFI).

(B) Southern blot analysis of the persistence of transgene cassette in clonal cell lines transduced with RGD-4C AAVP-*GFPneo* or RGD-4C phage-*GFPneo*. Total cellular DNA from non-transduced 293 parental cells or each of the transduced cell clones (#1-9 for each group) was double-digested with *AflIII*-*XhoI* (one restriction site per enzyme within the construct DNA flanking the transgene cassette).

(C) Analysis of potential head-to-tail concatemers of the transgene cassette by Southern blot. Total cellular DNA was digested with *Xho-I* (single restriction site within the transgene cassette next to the 3' ITR) prior to Southern blotting.

Figure 3. RGD-4C AAVP-mediated Specific Gene Delivery to Tumors

(A) Immunohistochemical staining against phage in KS1767-derived xenografts after intravenous administration of RGD-4C AAVP ( $5 \times 10^{10}$  TU) or negative controls (non-targeted AAVP, scrambled RGD-4C AAVP, or RGE-4C AAVP) into nude mice bearing KS1767-derived tumor xenografts. AAVP constructs were allowed to circulate for 5 m, followed by perfusion and surgical removal of tumors. Arrows point to phage staining in tumor blood vessels.

(B) Immunofluorescence analysis of GFP expression in KS1767-derived xenografts at day 7 after systemic administration of either RGD-4C AAVP-GFP or negative controls (non-targeted, scrambled or mutant) as indicated.

Figure 4. Targeted AAVP-mediated Molecular Imaging of Tumor-bearing Mice

(A) In vivo bioluminescent imaging (BLI) of luciferase expression after systemic AAVP delivery. Nude mice bearing DU145-derived tumor xenografts received an intravenous single-dose of either RGD-4C AAVP-Luc ( $5 \times 10^{11}$  TU) or controls (non-targeted AAVP-Luc, or scrambled RGD-4C AAVP-Luc). Ten days later, BLI of tumor-bearing mice was performed.

(B) Multi-tracer PET imaging in tumor-bearing mice after systemic delivery of RGD-4C AAVP-*HSVtk*. Nude mice bearing DU145-derived tumor xenografts (n=9 tumor-bearing mice per each cohort) received an intravenous single-dose ( $5 \times 10^{11}$  TU) RGD-4C AAVP-*HSVtk* or non-targeted AAVP-*HSVtk*. PET images with [ $^{18}\text{F}$ ]-FDG and [ $^{18}\text{F}$ ]-FEAU obtained before and after GCV treatment are presented. T, tumor; H, heart; BR, brain; BL, bladder. Calibration scales are provided in panels (A) and (B). Overimposition of PET to photographic images of representative tumor-bearing mice was performed to simplify the interpretation of [ $^{18}\text{F}$ ]-FDG and [ $^{18}\text{F}$ ]-FEAU biodistribution.

(C) Growth curves of individual tumor-xenografts after AAVP administration.

(D) Temporal dynamics of *HSVtk* gene expression as assessed by repetitive PET imaging with [ $^{18}\text{F}$ ]-FEAU at different days post AAVP administration.

(E) Changes in tumor viability before and after GCV therapy as assessed with [ $^{18}\text{F}$ ]-FDG PET.

Figure 5. Tumor Growth Suppression by RGD-4C AAVP-*HSVtk* Transduction plus Gancyclovir

(A-C) Cohorts of immunodeficient nude mice with established human xenografts ( $\sim 50 \text{ mm}^3$ ) derived from KS1767 cells (A), bladder UC3 carcinoma cells (B), or prostate DU145 carcinoma

cells (C), received a single intravenous administration ( $5 \times 10^{10}$  TU) of RGD-4C AAVP-*HSVtk* or controls (non-targeted AAVP-*HSVtk*, RGD-4C AAVP-*GFP*, or vehicle alone). GCV was administered to mice from post-treatment day 2 until the end of the experiments. All mice received GCV except for a control group treated with RGD-4C AAVP-*HSVtk* and no GCV afterwards. Shown are the mean tumor volumes  $\pm$  standard deviations (SD).

(D) Growth inhibition of large DU145-derived xenografts (at  $\sim 150 \text{ mm}^3$ ) by a single intravenous dose ( $5 \times 10^{10}$  TU) of RGD-4C AAVP-*HSVtk*.

(E) Inhibition of tumor growth of EF43-*FGF4* mouse mammary carcinoma ( $\sim 50 \text{ mm}^3$ ) in immunocompetent BALB/c mice by a single intravenous dose ( $5 \times 10^{10}$  TU) of RGD-4C AAVP-*HSVtk*.

(F) Long-term efficiency of RGD-4C AAVP-*HSVtk* and GCV by repeated intravenous doses of AAVP ( $5 \times 10^{10}$  TU per dose) to immunocompetent BALB/c mice bearing isogenic EF43-*FGF4* tumors. Therapy results were consistently observed in independent experiments with tumor-bearing mice cohorts ( $n=10$  mice per treatment group). Arrows indicate times of AAVP administration. (G) Effect of humoral immune response against phage on therapy with RGD-4C AAVP-*HSVtk*. BALB/c immunocompetent mice ( $n=7$  mice per group) were first “vaccinated” with RGD-4C AAVP-*GFP* ( $10^{10}$  TU per week for three weeks, intravenous) and then implanted with EF43-*FGF4* cells. Tumor-bearing mice received a single systemic dose of RGD-4C AAVP-*HSVtk* or non-targeted AAVP-*HSVtk* followed by GCV maintenance (started at day 2 post AAVP administration). Vaccination did not affect the anti-tumor effects, despite high anti-phage antibody titers (up to  $\sim 1:10,000$ ).



Figure 6. Histological analysis of representative experiments

(A) Tumor-bearing mice (upper panel) and corresponding surgically removed tumors (lower panel) from all the experimental groups of therapy (EF43-*FGF4* mammary tumors in BALB/c immunocompetent mice).

(B) Histopathologic analysis of EF43-*FGF4* treated tumors. Non-targeted AAVP-*HSVtk*-treated tumors (left panels), the border between the outer rims and central tumor areas (middle panels), and central tumor areas of RGD-4C AAVP-*HSVtk*-treated tumors (right panels) are shown as high-magnification views from the low-magnification inserts of serial tumor sections.

Hematoxylin and eosin (H&E) staining, CD31 immunostaining (arrows, tumor blood vessels) and TUNEL staining (arrows, apoptotic cells) are shown.

## References

- Alauddin, M.M., Fissekis, J.D., and Conti, P.S. (2003). A general synthesis of 2'-deoxy-2'-([<sup>18</sup>F]fluoro-5-methyl-1-β-D-arabinofuranosyluracil and its 5-substituted nucleosides. *J. Labelled Compds. Radiopharm.* 46, 285-289.
- Arap, W., Pasqualini, R., and Ruoslahti, E. (1998). Cancer treatment by targeted drug delivery to tumor vasculature in a mouse model. *Science* 279, 377-380.
- Arap, W., Kolonin, M.G., Trepel, M., Lahdenranta, J., Cardó-Vila, M., Giordano, R.J., Mintz, P.J., Ardelt, P.U., Yao, V.J., Vidal, C.I., et al. (2002). Steps toward mapping the human vasculature by phage display. *Nature Med.* 8, 121-127.
- Arap, M.A., Lahdenranta, J., Mintz, P.J., Hajitou, A., Sarkis, A.S., Arap, W., and Pasqualini, R. (2004). Cell surface expression of the stress response chaperone GRP78 enables tumor targeting by circulating ligands. *Cancer Cell* 6, 275-284.
- Barbas III, C.F., Burton, D.R., Scott, J.K., and Silverman, G.J. (2001). *Phage Display: A Laboratory Manual* (New York: Cold Spring Harbor Press).
- Barrow, P.A., and Soothill, J. S. (1997). Bacteriophage therapy and prophylaxis: rediscovery and renewed assessment of potential. *Trends Microbiol.* 5, 268-271.

Blasberg, R.G., and Tjuvavej, J.G. (2003). Molecular-genetic imaging: current and future perspectives. J. Clin. Invest. 111, 1620-1629.

Chen, L., Zurita, A.J., Ardelt, P.U., Giordano, R.J., Arap, W., and Pasqualini, R. (2004). Design and validation of a bifunctional ligand display system for receptor targeting. Chem. Biol. 11, 1081-1091.

De, A., and Gambhir, S.S. (2005). Noninvasive imaging of protein-protein interactions from live cells and living subjects using bioluminescence resonance energy transfer. FASEB J. 19, 2017-2019.

Ellerby, H.M., Arap, W., Ellerby, L.M., Kain, R., Andrusiak, R., Rio, G.D., Krajewski, S., Lombardo, C.R., Rao, R., Ruoslahti, E., et al. (1999). Anti-cancer activity of targeted pro-apoptotic peptides. Nature Med. 5, 1032-1038.

Geier, M.R., Trigg, M.E., and Merrill, C.R. (1973). Fate of bacteriophage lambda in non-immune germ free mice. Nature 246, 221-223.

Gelovani Tjuvavej, J., and Blasberg, R.G. (2003). *In vivo* imaging of molecular-genetic targets for cancer therapy. Cancer Cell 3, 327-332.

Giordano, R.J., Cardó-Vila, M., Lahdenranta, J., Pasqualini, R., and Arap, W. (2001). Biopanning and rapid analysis of selective interactive ligands. Nature Med. 11, 1249-1253.

Gross, S., and Piwnica-Worms, D. (2005a). Spying on cancer: molecular imaging in vivo with genetically encoded reporters. *Cancer Cell* 7, 5-15.

Gross, S., and Piwnica-Worms, D. (2005b). Monitoring proteasome activity in cellulo and in living animals by bioluminescent imaging: technical considerations for design and use of genetically encoded reporters. *Methods Enzymol.* 399, 512-530.

Hajitou, A., Sounni, N.E., Devy, L., Grignet-Debrus, C., Lewalle, J.M., Li, H., Deroanne, C.F., Lu, H., Colige, A., Nusgens, B.V., Frankenke, F., et al. (2001). Down-regulation of vascular endothelial growth factor by tissue inhibitor of metalloproteinase-2: effect on in vivo mammary tumor growth and angiogenesis. *Cancer Res.* 61, 3450-3457.

Hajitou, A., Pasqualini, R., and Arap, W. (2006). Vascular targeting: recent advances and therapeutic perspectives. *Trends Cardiovasc. Med.* *In press*.

Hood, J.D., Bednarski, M., Frausto, R., Guccione, S., Reisfeld, R.A., Xiang, R., and Cheresch, D.A. (2002). Tumor regression by targeted gene delivery to the neovasculature. *Science* 296, 2404-2407.

Hsiao, C.D., Hsieh, F.J., and Tsai, H.J. (2001). Enhanced expression and stable transmission of transgenes flanked by inverted terminal repeats from adeno-associated virus in zebrafish. *Dev. Dyn.* 220, 323-336.

Ivanenkov, V.V., Felici, F., and Menon, A.G. (1999). Targeted delivery of multivalent phage display vectors into mammalian cells. *Biochim. Biophys. Acta* 1448, 463-472.

Kang, K.W., Min, J.J., Chen, X., and Gambhir, S.S. (2005). Comparison of [ $^{14}\text{C}$ ]FMAU, [ $^3\text{H}$ ]FEAU, [ $^{14}\text{C}$ ]FIAU, and [ $^3\text{H}$ ]PCV for monitoring reporter gene expression of wild type and mutant *Herpes simplex* virus type 1 thymidine kinase in cell culture. Mol. Imaging Biol. E-publication online July 23.

Kootstra, N.A., and Verma, I. M. (2003). Gene therapy with viral vectors. Annu. Rev. Pharmacol. Toxicol. 43, 413-439.

Larocca, D., Kassner, P.D., Witte, A., Ladner, R.C., Pierce, G.F., and Baird, A. (1999). Gene transfer to mammalian cells using genetically targeted filamentous bacteriophage. FASEB J. 13, 727-734.

Lieber, A., Steinwaerder, D.S., Carlson, C.A., and Kay, M.A. (1999). Integrating adenovirus- adeno-associated virus hybrid vectors devoid of all viral genes. J. Virol. 73, 9314-9324.

Luker, K.E., Smith, M.C., Luker, G.D., Gammon, S.T., Piwnica-Worms, H., and Piwnica-Worms D. (2004). Kinetics of regulated protein-protein interactions revealed with firefly luciferase complementation imaging in cells and living animals. PNAS 101, 12288-12293.

Marchiò, S., Lahdenranta, J., Schlingemann, R.O., Valdembri, D., Wesseling, P., Arap, M.A., Hajitou, A., Ozawa, M.G., Trepel, M., Giordano, R.J., et al. (2004). Aminopeptidase A is a functional target in angiogenic blood vessels. Cancer Cell 5, 151-162.

- Massoud, T.F., and Gambhir, S.S. (2003). Molecular imaging in living subjects: seeing fundamental biological processes in a new light. *Genes Dev.* 17, 545-580.
- McCarty, D.M., Young Jr., S.M., and Samulski, R.J. (2004). Integration of adeno-associated virus (AAV) and recombinant AAV vectors. *Annu. Rev. Genet.* 38, 819-845.
- Medintz, I.L., Uyeda, H.T., Goldman, E.R., and Mattoussi, H. (2005). Quantum dot bioconjugates for imaging, labelling and sensing. *Nature Mater.* 6, 435-446.
- Mizuguchi, H., and Hayakawa, T. (2004). Targeted adenovirus vectors. *Hum. Gene Ther.* 15, 1034-1044.
- Müller, O.J., Kaul, F., Weitzman, M.D., Pasqualini, R., Arap, W., Kleinschmidt, J.A., and Trepel, M. (2003). Random peptide libraries displayed on adeno-associated virus to select for targeted gene therapy vectors. *Nature Biotechnol.* 21, 1040-1046.
- Pasqualini, R., Koivunen, E., and Ruoslahti, E. (1997). Alpha v integrins as receptors for tumor targeting by circulating ligands. *Nature Biotechnol.* 15, 542-546.
- Pentz, R.D., Cohen, C.B., Wicclair, M., Devita, M.A., Flamm, A.L., Youngner, S.J., Hamric, A.B., McCabe, M.S., Glover, J.J., Kittiko, W.J., et al. (2005). Ethics guidelines for research with the recently dead. *Nature Med.* 11, 1145-1149.

Piersanti, S., Cherubini, G., Martina, Y., Salone, B., Avitabile, D., Grosso, F., Cundari, E., Di Zenzo, G., and Saggio, I. (2004). Mammalian cell transduction and internalization properties of lambda phages displaying the full-length adenoviral penton base or its central domain. *J. Mol. Med.* 82, 467-476.

Poul, M.A., and Marks, J.D. (1999). Targeted gene delivery to mammalian cells by filamentous bacteriophage. *J. Mol. Biol.* 288, 203-211.

Ray, P., Bauer, E., Iyer, M., Barrio, J.R., Satyamurthy, N., Phelps, M.E., Herschman, H.R., and Gambhir, S.S. (2001). Monitoring gene therapy with reporter gene imaging. *Semin. Nucl. Med.* 31, 312-320.

Smith, G.P., and Scott, J.K. (1993). Libraries of peptides and proteins displayed on filamentous phage. *Methods Enzymol.* 217, 228-257.

Souza, G.R., Christianson, D.R., Staquicini, F.I., Ozawa, M.G., Snyder, E.Y., Sidman, R.L., Miller, H.L., Arap, W., and Pasqualini, R. (2006). Networks of gold nanoparticles and bacteriophage as biological sensors and cell targeting agents. *PNAS* 103, 1215-1220, 2006.

Tai, Y.C., and Laforest, R. (2005). Instrumentation aspects of animal PET. *Annu. Rev. Biomed. Eng.* 7, 255-285.

Tjuvajev, J.G., Avril, N., Oku, T., Sasajima, T., Miyagawa, T., Joshi, R., Safer, M., Beattie, B., DiResta, G., Daghighian, F., et al. (1998). Imaging herpes virus thymidine kinase gene transfer and expression by positron emission tomography. *Cancer Res.* 58, 4333-4341.



- Tjuvajev, J.G., Chen, S.H., Joshi, A., Joshi, R., Guo, Z.S., Balatoni, J., Ballon, D., Koutcher, J., Finn, R., Woo, S.L., et al. (1999). Imaging adenoviral-mediated herpes virus thymidine kinase gene transfer and expression in vivo. *Cancer Res.* 59, 5186-5193.
- Trepel, M., Arap, W., and Pasqualini, R. (2001). Modulation of the immune response by systemic targeting of antigens to lymph nodes. *Cancer Res.* 61, 8110-8112.
- Xiao, X., Li, J., and Samulski, R.J. (1998). Production of high-titer recombinant adeno-associated virus vectors in the absence of helper adenovirus. *J. Virol.* 72, 2224-2232.
- Yang, C.C., Xiao, X., Zhu, X., Ansardi, D.C., Epstein, N.D., Frey, M.R., Matera, A.G., and Samulski, R.J. (1997). Cellular recombination pathways and viral terminal repeat hairpin structures are sufficient for adeno-associated virus integration in vivo and in vitro. *J. Virol.* 71, 9231-9247.
- Zacher III, A.N., Stock, C.A., Golden II, J.W., and Smith, G.P. (1980). A new filamentous phage cloning vector: fd-tet. *Gene* 9, 127-140.

Figure 1

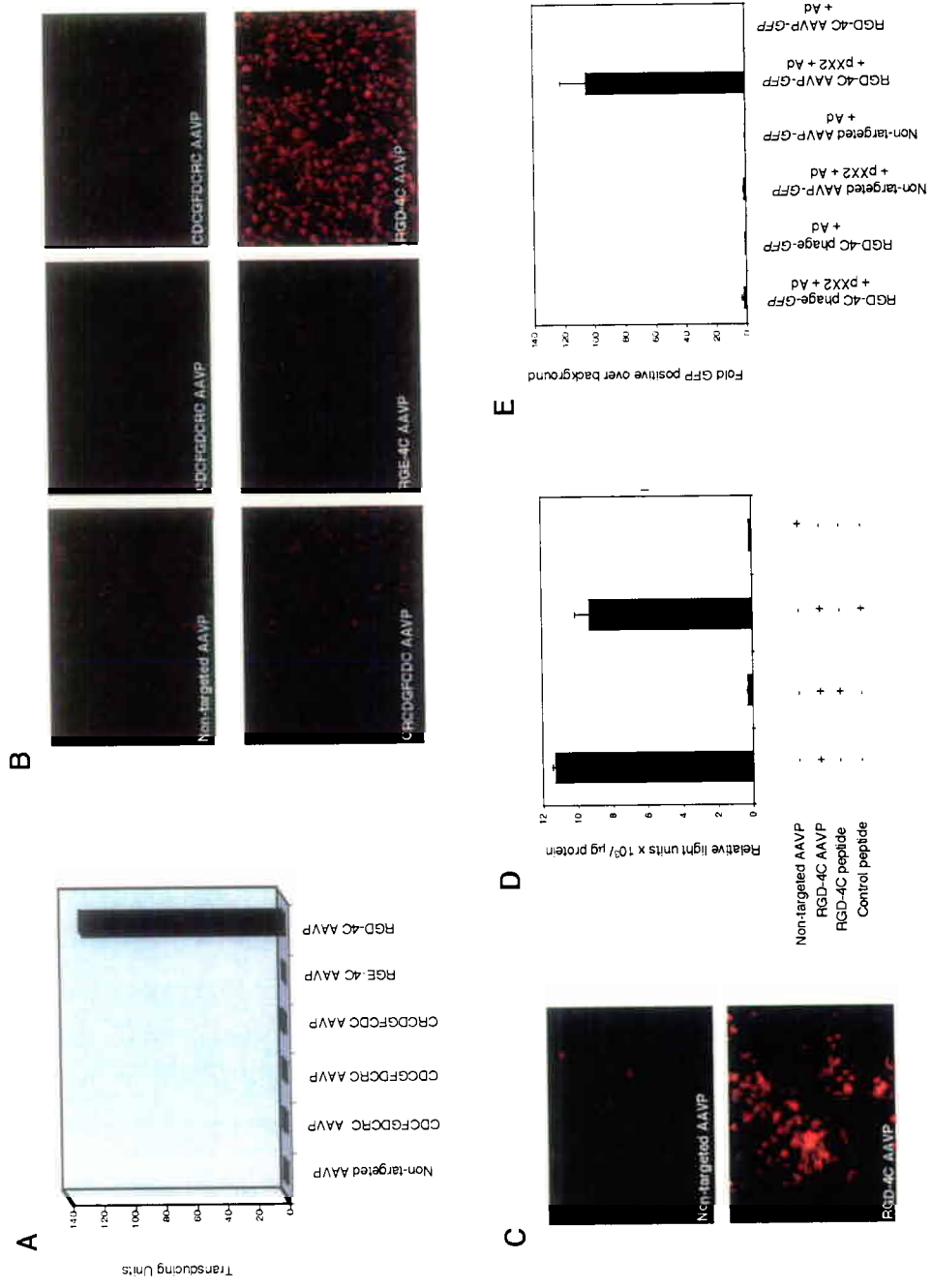
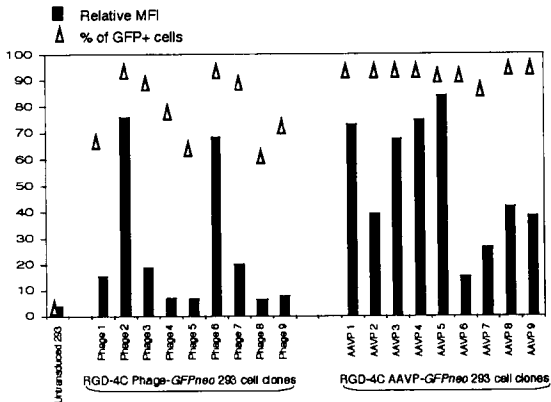
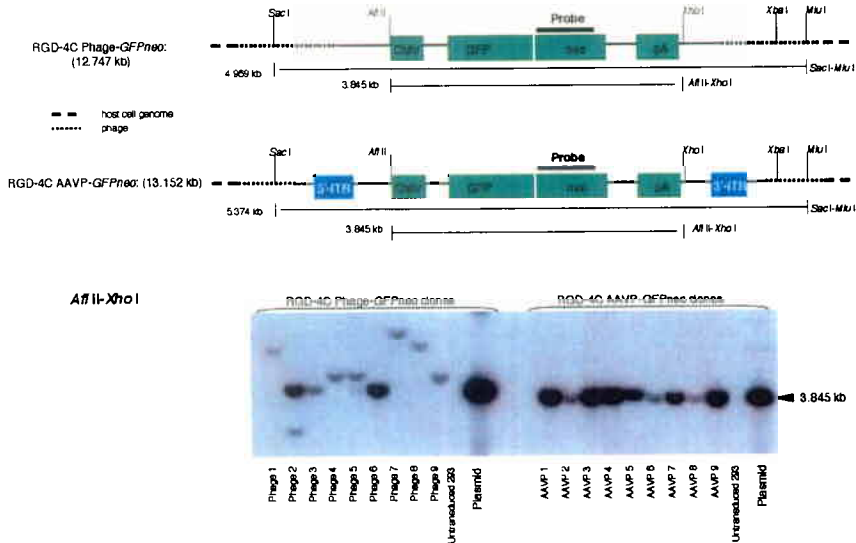


Figure 2

A



B



C

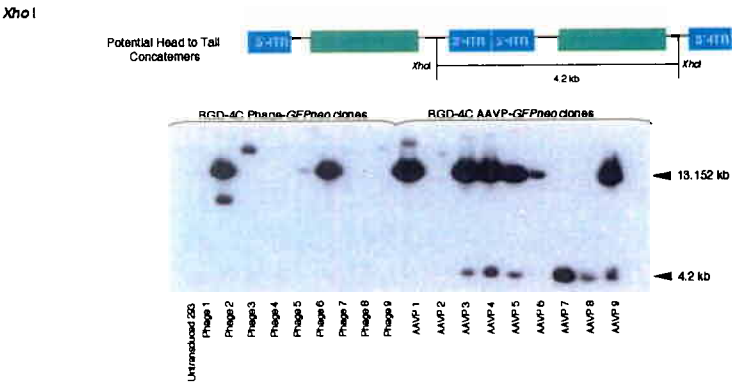


Figure 3

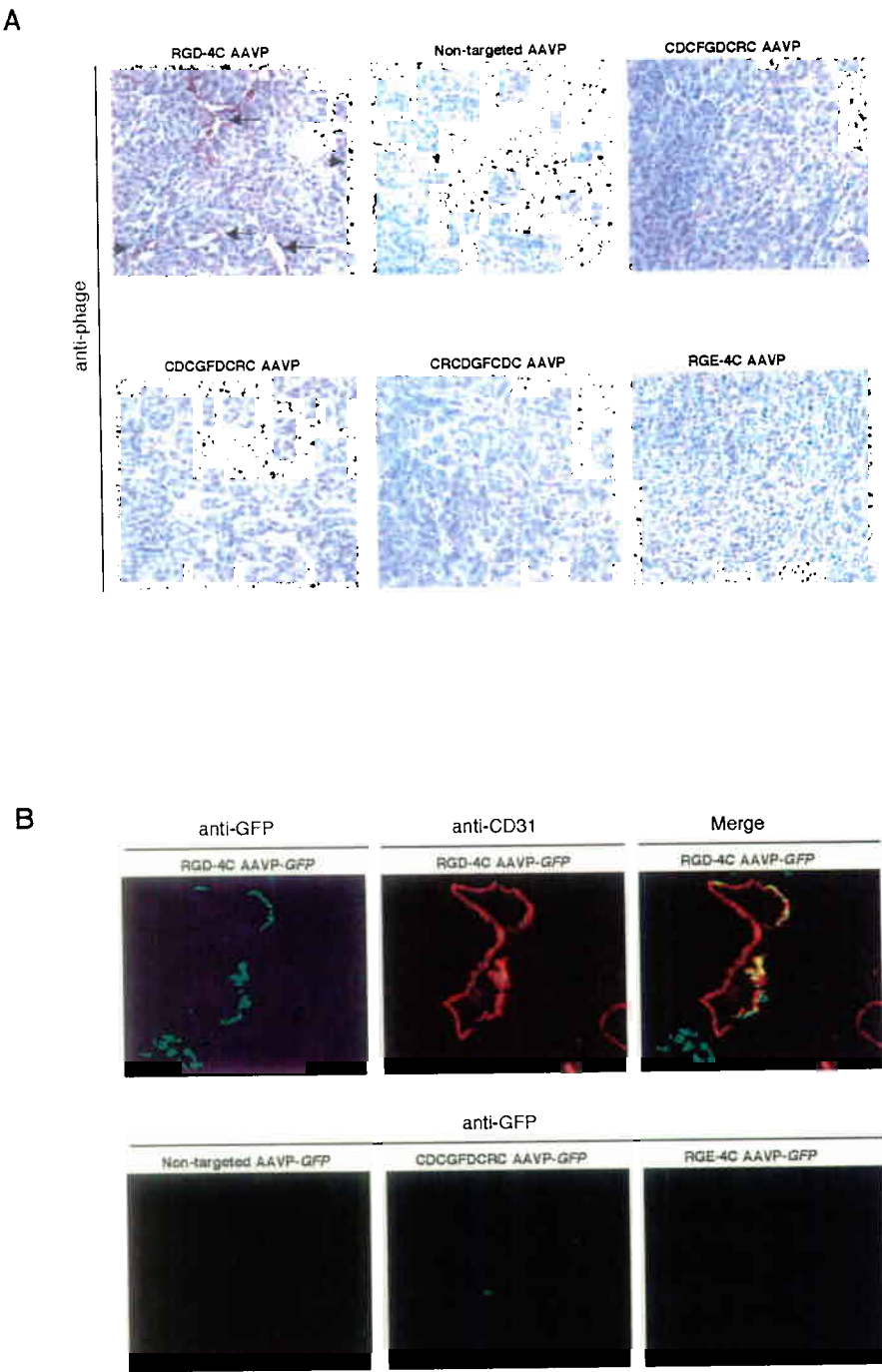


Figure 4

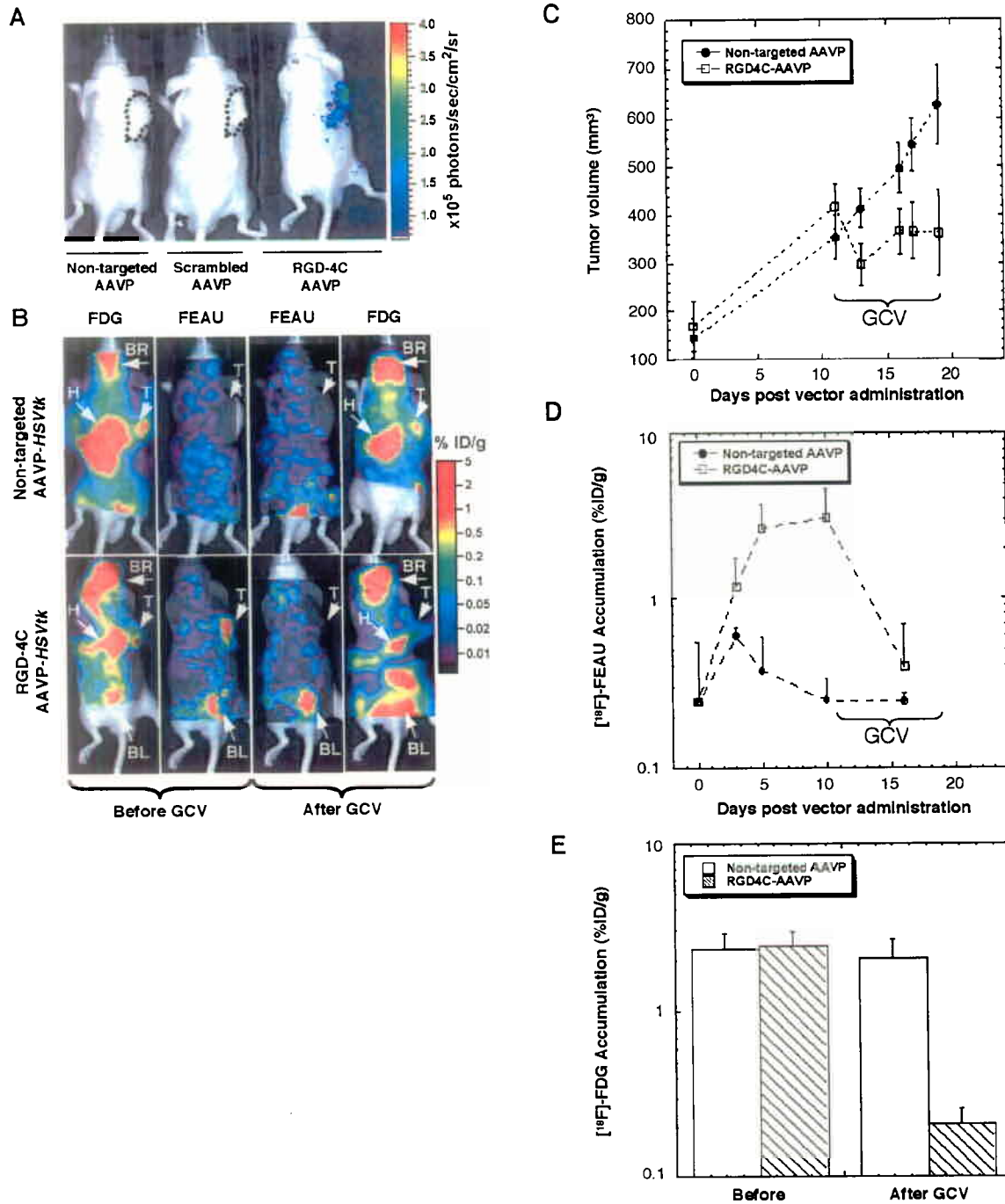


Figure 5

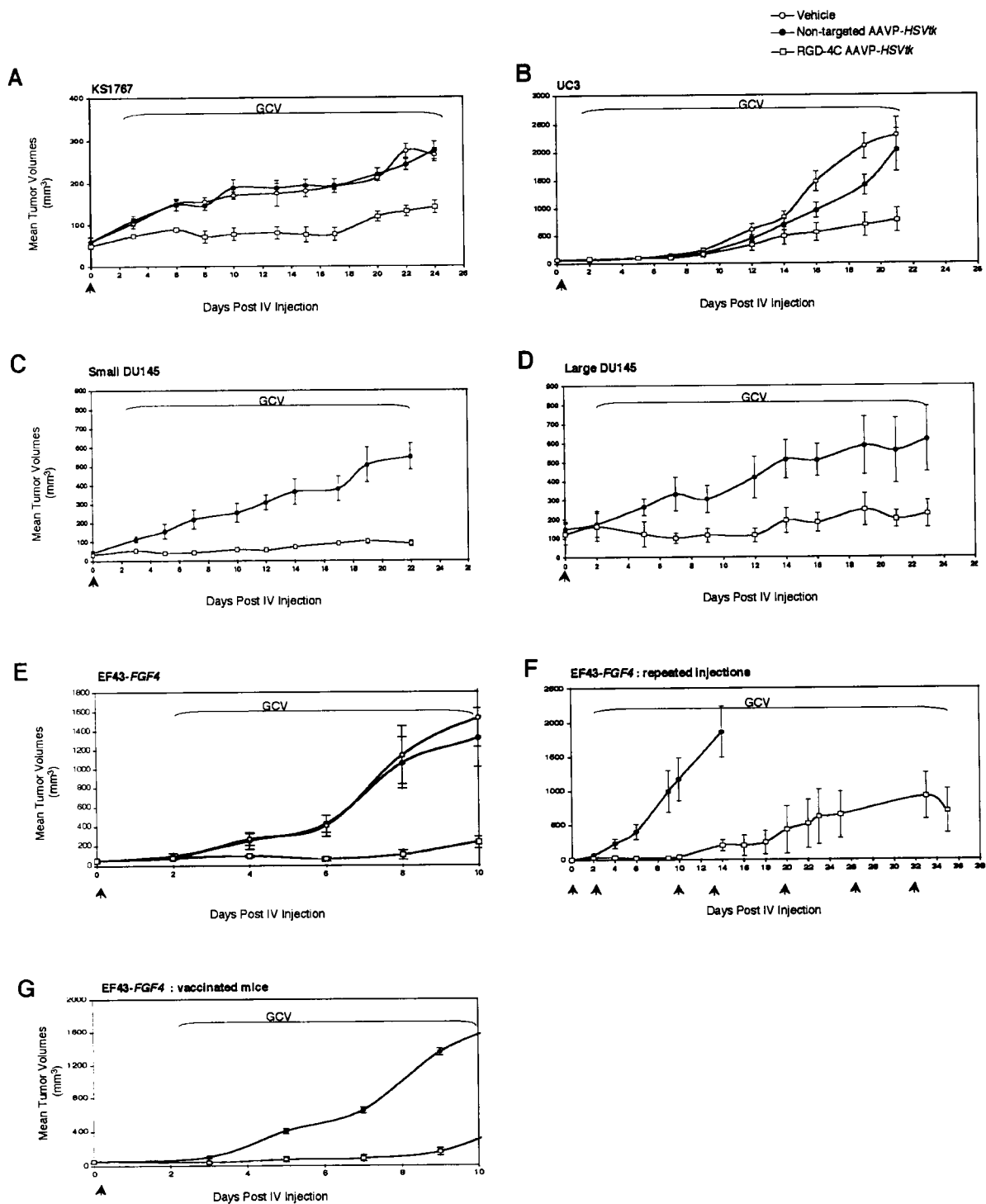
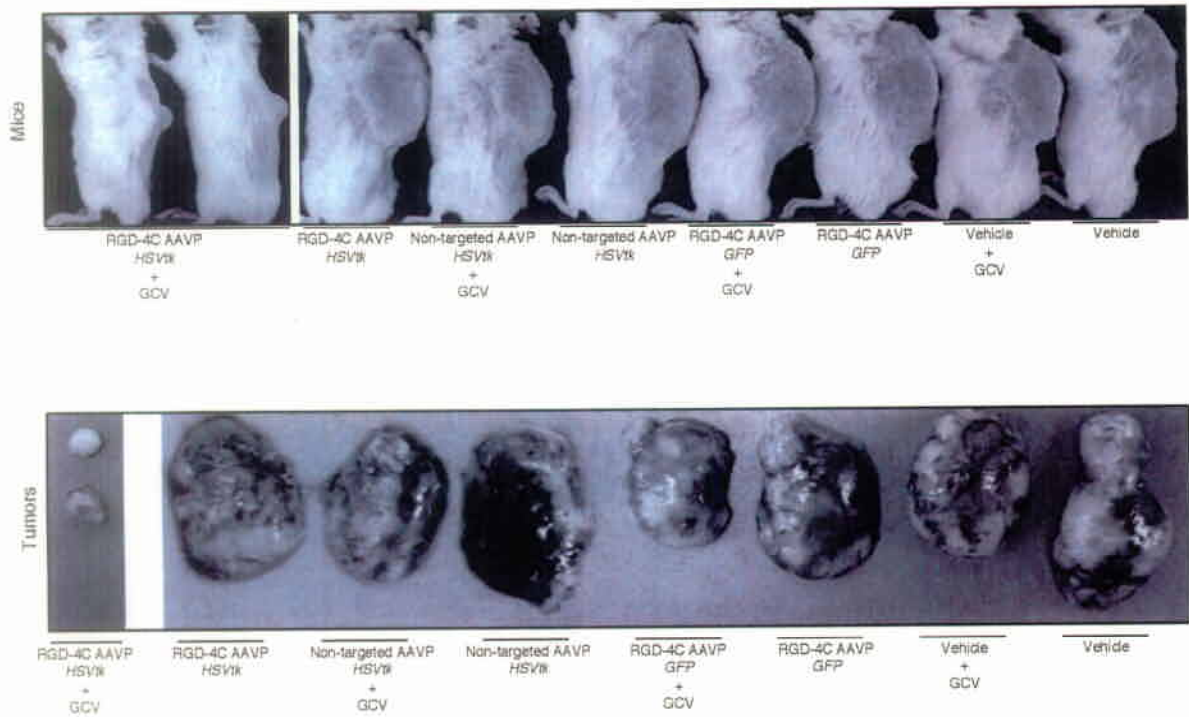




Figure 6

A



B

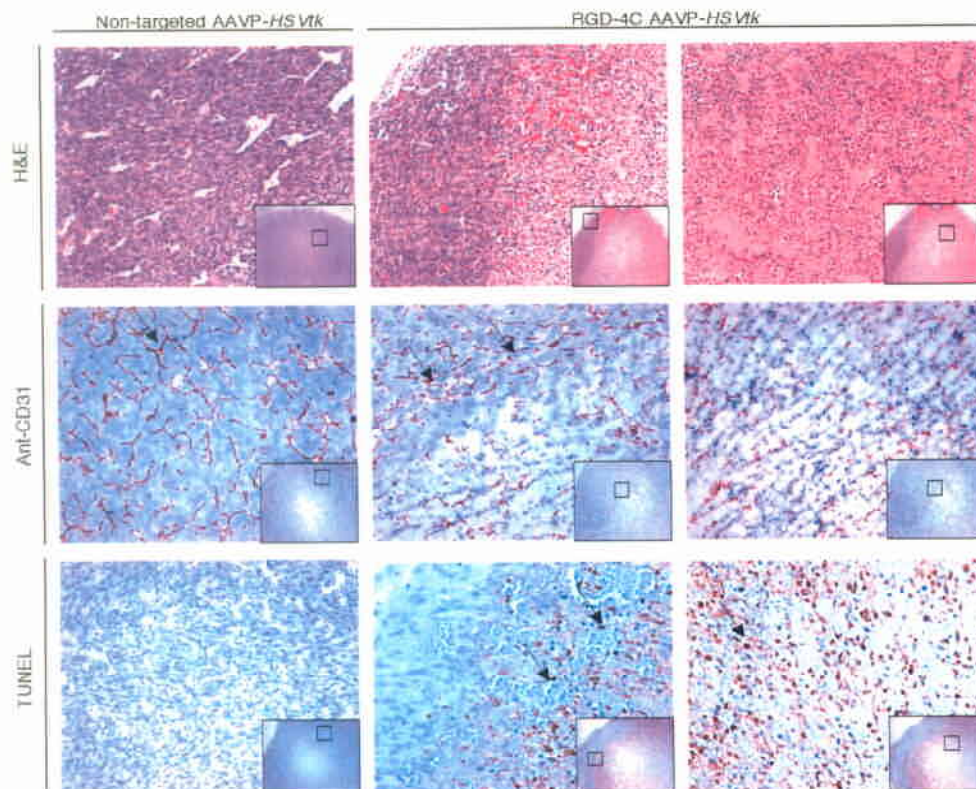
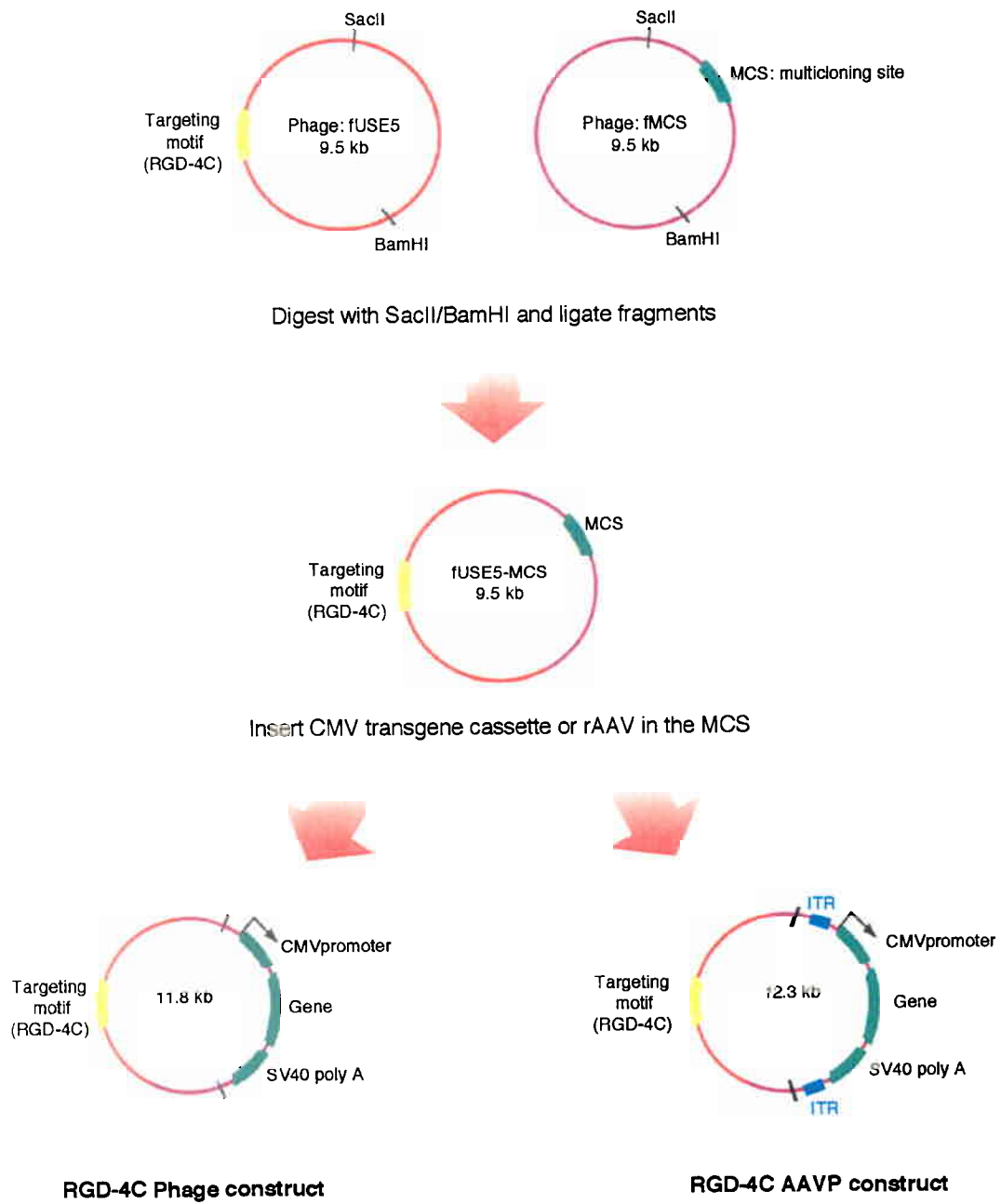




Figure S1



Hajitou et al., CELL In press

**Figure 1** displays the schematic diagrams and Southern blot analysis of the RGD-4C phage and AAVP-GFPneo constructs.

**Schematic Diagrams:**

- RGD-4C Phage-GFPneo (12.747 kb):** The phage genome (dashed line) is shown with the host cell genome (solid line). The phage genome contains the *gfp* gene (green box) and the *neo* gene (red box). The phage genome is flanked by *Sac*I and *Xba*I sites. The *gfp* gene is flanked by *Afl*II and *Xba*I sites. The *neo* gene is flanked by *Afl*II and *Xba*I sites.
- RGD-4C AAVP-GFPneo (13.152 kb):** The AAVP genome (dashed line) is shown with the host cell genome (solid line). The AAVP genome contains the *gfp* gene (green box) and the *neo* gene (red box). The AAVP genome is flanked by *Sac*I and *Xba*I sites. The *gfp* gene is flanked by *Afl*II and *Xba*I sites. The *neo* gene is flanked by *Afl*II and *Xba*I sites.

**Southern Blot Analysis:**

- Stu I:** Digestion of RGD-4C Phage-GFPneo and RGD-4C AAVP-GFPneo with *Stu*I. The phage genome is digested into fragments of approximately 12 kb and 8.0 kb. The AAVP genome is digested into fragments of approximately 13.152 kb and 8.0 kb.
- Xba I:** Digestion of RGD-4C Phage-GFPneo and RGD-4C AAVP-GFPneo with *Xba*I. The phage genome is digested into fragments of approximately 13.152 kb and 8.0 kb. The AAVP genome is digested into fragments of approximately 13.152 kb and 8.0 kb.
- Sac I-Mlu I:** Digestion of RGD-4C Phage-GFPneo and RGD-4C AAVP-GFPneo with *Sac*I and *Mlu*I. The phage genome is digested into fragments of approximately 5.374 kb and 4.969 kb. The AAVP genome is digested into fragments of approximately 5.374 kb and 4.969 kb.

The figure displays two schematic diagrams and corresponding gel electrophoresis results. The left schematic shows the RGD-4C phage-GFPneo vector with 5' and 3' junctions, a transgene cassette (H, T), and a 3' junction. The right schematic shows the RGD-4C AAVP-GFPneo chimera with 3' and 5' junctions, a transgene cassette (H, T), and a 3' junction. Below the diagrams are two gel electrophoresis images. The left gel shows the RGD-4C phage-GFPneo vector with lanes for M, Phage 1-9, Ultraviolet 200, Negative control, and Negative control. The right gel shows the RGD-4C AAVP-GFPneo chimera with lanes for M, AAVP 1-9, Ultraviolet 200, Negative control, and Negative control. Molecular weight markers are indicated on the left and right of the gels at 600 bp, 300 bp, and 100 bp.

[illegible]

Figure S3

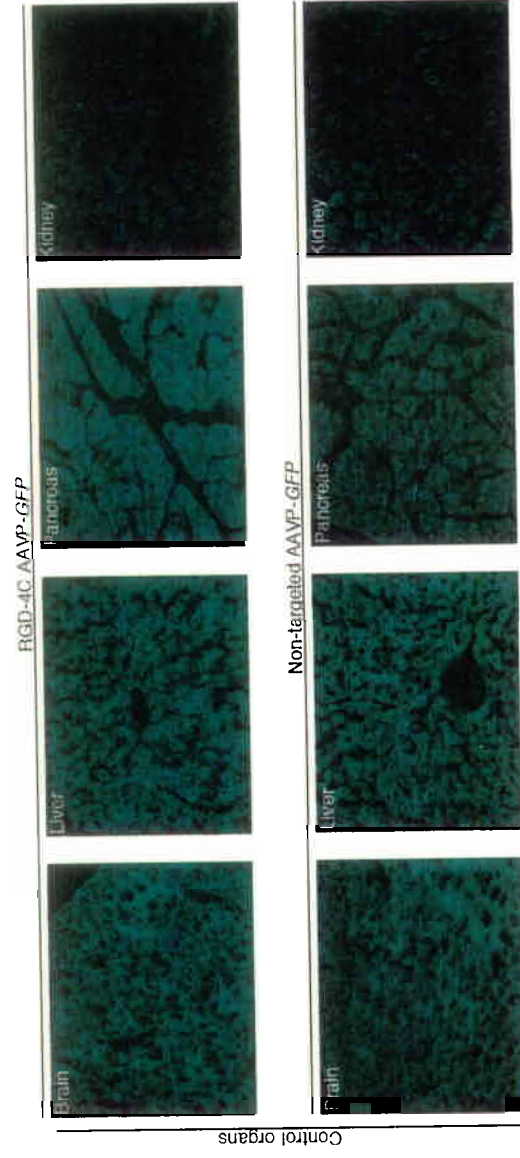


Figure S4

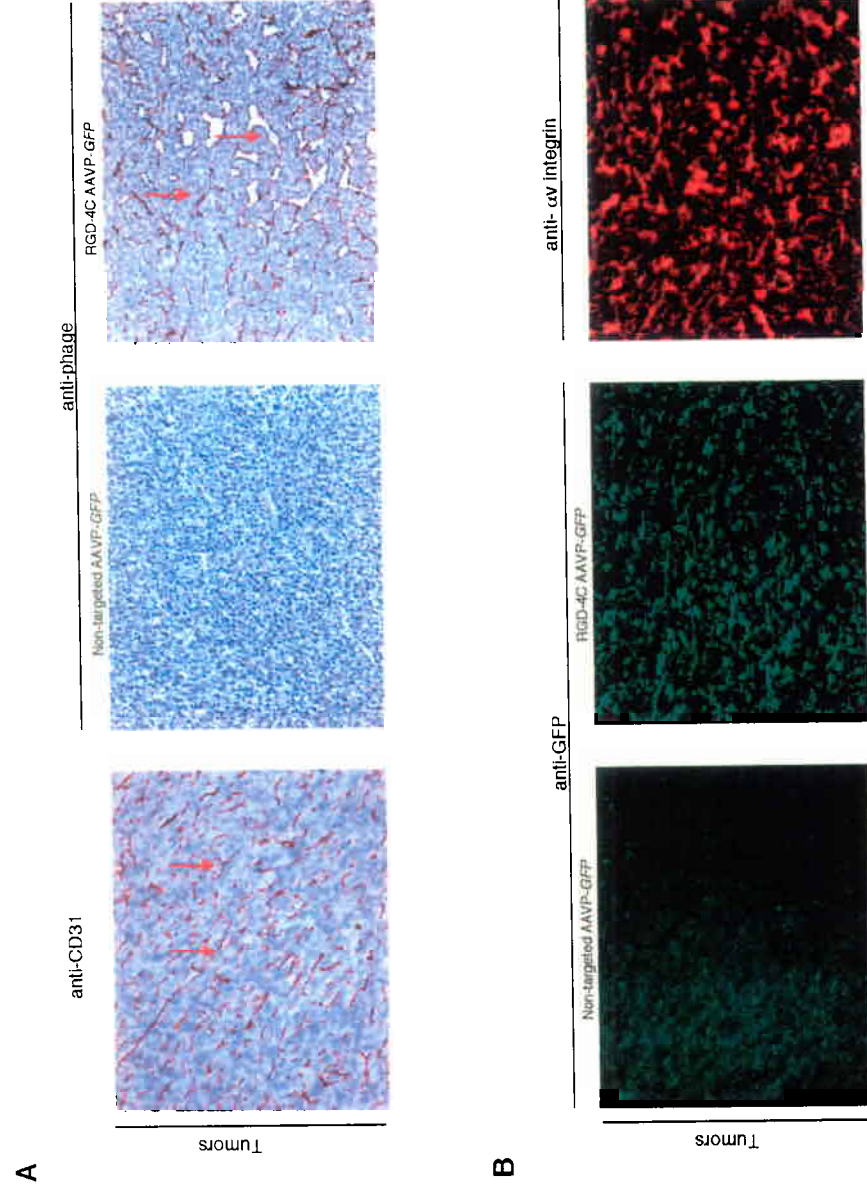
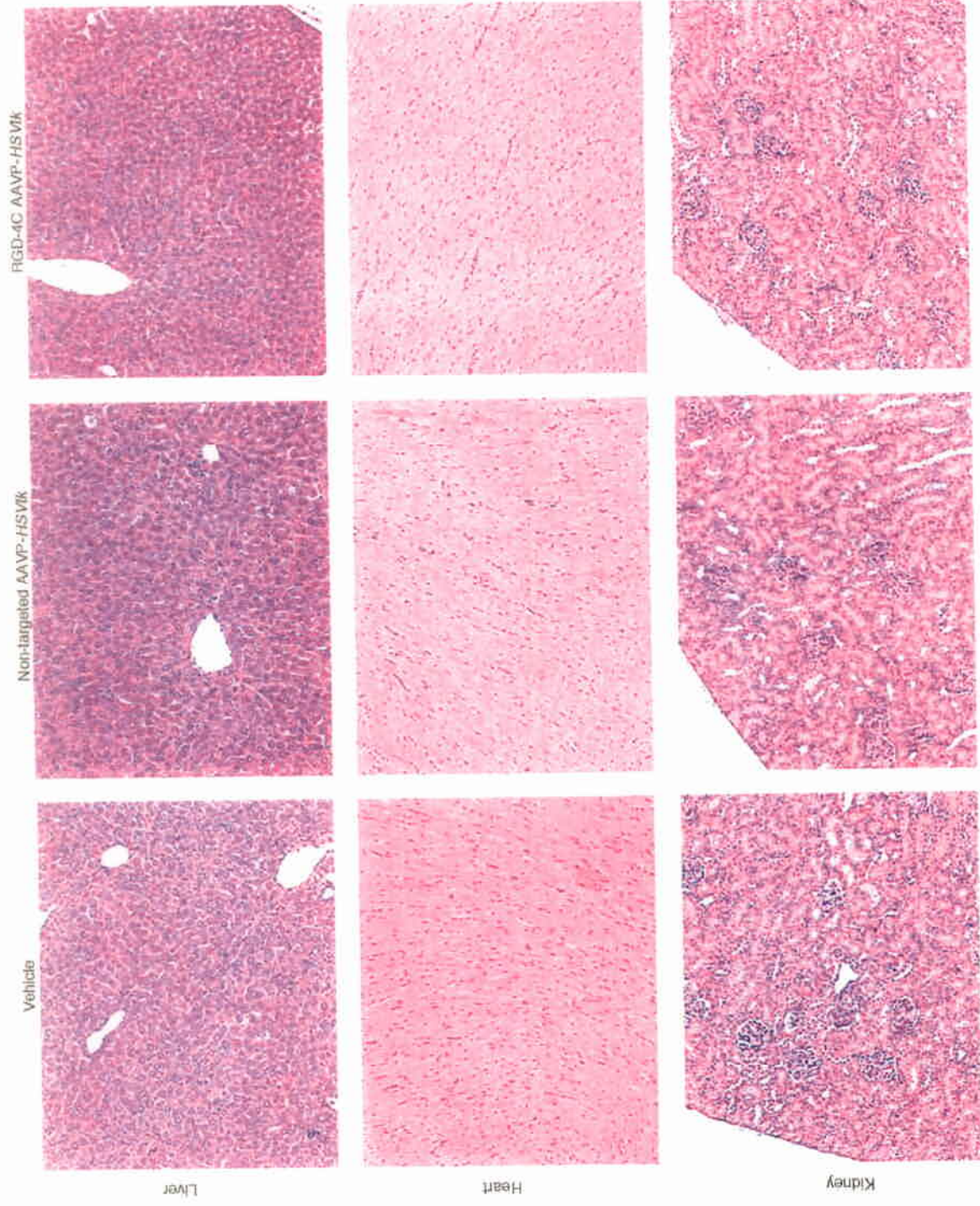




Figure S5



## Supplementary Figure Legends

Figure S1. Schematic Chart of the Construction of RGD-4C AAVP  
Cloning Strategy and Structure of the Resulting Vectors are Depicted.

Figure S2. Analysis of the DNA from RGD-4C AAVP-*GFPneo* or RGD-4C phage-*GFPneo* in 293 Transduced Clonal Cell Lines

(A) Southern blot of RGD-4C AAVP-*GFPneo* or RGD-4C phage-*GFPneo* are shown. Total cellular DNA from non-transduced 293 parental cells or individual stable cell clones transduced (#1-9 for each vector) was incubated with *StuI* (no restriction digest site within the vector DNA), *Xba-I* (single restriction digest site within the vector DNA), or *SacI-MluI*. Resulting DNA fragments were separated on 0.8% agarose gel, transferred to a nylon membrane and hybridized with a labeled neo probe as indicated. Digested vector plasmids were also used as controls.

(B) PCR analysis of concatemers of the transgene cassette in 293 clonal cell lines stably transduced with RGD-4C phage-*GFPneo* or RGD-4C AAVP-*GFPneo*. Non-transduced 293 parental cells served as a negative control; additional negative controls and a 100-bp molecular marker (Invitrogen) are also shown as indicated. Nested PCR with primers annealing close to the 5' and 3' end of the transgene cassette was performed to identify concatemeric forms in the DNAs corresponding to the RGD-4C AAVP and RGD-4C phage. Arrows indicate primers (H, head; T, tail). PCR-amplification products were detected in 2%

agarose gels and revealed concatemeric vector DNA exclusively in the cell clones transduced with AAVP.

(C) Sequencing results of different concatemeric forms in AAVP DNA (capital letters denote 3' end of transgene cassette, italic letters denote 5' end of transgene cassette), revealed Head-to-Tail concatemers with deleted ITRs.

Figure S3. Immunostaining of the Reporter Gene Expression GFP in Control Organs

Brain, liver, pancreas and kidney at day 7 after an intravenous dose ( $5 \times 10^{10}$  TU) of either RGD-4C AAVP-GFP or non-targeted AAVP-GFP into mice are shown.

Figure S4. Transduction of EF43-FGF4 Tumors in Immunocompetent Mice by The RGD-4C AAVP

(A) Immunohistochemical staining against AAVP after intravenous administration of RGD-4C AAVP (right panel) or non-targeted AAVP (middle panel) into immunocompetent BALB/c mice bearing EF43-FGF4 tumors. Constructs were allowed to circulate for 5 min, followed by perfusion and tissue recovery as described. A polyclonal antibody against phage was used for staining. Left panel shows tumor blood vessel staining by using an anti-CD31 antibody. Arrows point to tumor blood vessels.

(B) Immunofluorescence analysis of GFP expression in EF43-FGF4 tumors at 1 week after intravenous administration of non-targeted AAVP-GFP (left panel) or RGD-4C AAVP-GFP (middle panel) into mice bearing EF43-FGF4 tumors. Immunostaining against  $\alpha$ v-integrin in EF43-FGF4 tumors is also shown (right panel).



Figure S5. Histopathological Analysis of Control Organs

Liver, heart, and kidney from mice treated with non-targeted AAVP-*HSVtk*, RGD-4C AAVP-*HSVtk* vectors, or vehicle alone plus GCV maintenance are shown. No histological signs of toxicity were detected in these organs by H&E staining.

Table S1. Transgene Expression *In Vitro*

<i>Post-infection day #</i>	<i>0</i>	<i>5</i>	<i>10</i>	<i>15</i>	<i>20</i>	<i>30</i>	<i>35</i>	<i>40</i>	<i>45</i>	<i>50</i>	<i>55</i>	<i>60</i>
<i>RGD-4C phage</i>	-	++	+	-	-	-	-	-	-	-	-	-
<i>RGD-4C AAVP</i>	-	++	++	++	++	++	++	++	++	+	+	+

Two independent observers scored GFP expression semi-quantitatively in triplicate wells of 293 cells per time point.

Table S2. Fate of The Vector DNA In 293 Cell Clones Stably Transduced by RGD-4C AAVP-*GFPneo* or RGD-4C phage-*GFPneo*

RGD-4C phage or RGD-4C AAVP (denomination of stably transduced clones)	Contains integrated forms of construct	Contains episomal forms of construct	Contains concatemeric forms of transgene cassette	Transgene cassette preserved	Comments and interpretation
Phage 1	Yes	No	No	No	
Phage 2	Yes	Yes	No	Yes (episomal)	Episomal form of full-length phage vector
Phage 3	Yes	No	No	Yes	
Phage 4	Yes	No	No	No	
Phage 5	Yes	No	No	No	
Phage 6	Yes	Yes	No	Yes (episomal)	Episomal form of full-length phage vector
Phage 7	Yes	No	No	No	
Phage 8	Yes	No	No	No	
Phage 9	Yes	No	No	No	
AAVP 1	Yes	Yes	Yes	Yes	Non-concatemeric episomal form of full-length AAVP vector detected. Concatemeric integrated form with deleted <i>XhoI</i> site.
AAVP 2	Yes	No	Yes	Yes	Concatemeric form is head-to-tail with deleted ITRs at the junction site. ITRs flanking the concatemer and adjacent AAVP sequences are preserved.
AAVP 3	Yes	Yes	Yes	Yes	Non-concatemeric episomal form of full-length AAVP vector. At least one integrated form contains head-to-tail concatemers and ITRs flanking the concatemer as well as the adjacent AAVP sequences are preserved. At least one integrated form contains head-to-tail concatemers with deleted ITRs at the junction site.
AAVP 4	Yes	Yes	Yes	Yes	Non-concatemeric episomal form of full-length AAVP vector. At least one integrated form contains head-to-tail concatemers and ITRs flanking the concatemer as well as the adjacent AAVP sequences are preserved. At least one integrated form contains head-to-tail concatemers with deleted ITRs at the junction site.
AAVP 5	Yes	Yes	Yes	Yes	Non-concatemeric episomal form of full-length AAVP vector. At least one integrated form contains head-to-tail concatemers and ITRs flanking the concatemer as well as the adjacent AAVP sequences are preserved. At least one integrated form contains head-to-tail concatemers with deleted ITRs at the junction site.
AAVP 6	Yes	No	Yes	Yes	Concatemers are head-to-tail with deleted ITRs and <i>XhoI</i> sites. ITRs flanking the (concatemeric) transgene cassette as well as the adjacent AAVP sequences are preserved.
AAVP 7	Yes	No	Yes	Yes	Concatemers are head-to-tail with preserved ITRs. Additional concatemers with deleted ITRs.
AAVP 8	Yes	No	Yes	Yes	At least one integrated form contains head-to-tail concatemers and ITRs flanking the concatemer as well as the adjacent AAVP sequences are preserved. At least one integrated form contains head-to-tail concatemers with deleted ITRs at the junction site.
AAVP 9	Yes	Yes	Yes	Yes	Non-concatemeric episomal form of full-length AAVP vector. At least one integrated form contains head-to-tail concatemers and ITRs flanking the concatemer as well as the adjacent AAVP sequences are preserved. At least one integrated form contains head-to-tail concatemers with deleted ITRs at the junction site.

# Ligand-Directed Surface Profiling of Human Cancer Cells with Combinatorial Peptide Libraries

Mikhail G. Kolonin,<sup>1</sup> Laura Bover,<sup>1</sup> Jessica Sun,<sup>1</sup> Amado J. Zurita,<sup>1</sup> Kim-Anh Do,<sup>1</sup> Johanna Lahdenranta,<sup>1</sup> Marina Cardó-Vila,<sup>1</sup> Ricardo J. Giordano,<sup>1</sup> Diana E. Jaalouk,<sup>1</sup> Michael G. Ozawa,<sup>1</sup> Catherine A. Moya,<sup>1</sup> Glaucio R. Souza,<sup>1</sup> Fernanda I. Staquicini,<sup>1</sup> Akihiko Kunyiasu,<sup>1</sup> Dominic A. Scudiero,<sup>2</sup> Susan L. Holbeck,<sup>2</sup> Edward A. Sausville,<sup>2</sup> Wadih Arap,<sup>1</sup> and Renata Pasqualini<sup>1</sup>

<sup>1</sup>The University of Texas M.D. Anderson Cancer Center, Houston, Texas; and <sup>2</sup>Developmental Therapeutics Program, Division of Cancer Treatment and Diagnosis, National Cancer Institute, NIH, Bethesda, Maryland

## Abstract

A collection of 60 cell lines derived from human tumors (NCI-60) has been widely explored as a tool for anticancer drug discovery. Here, we profiled the cell surface of the NCI-60 by high-throughput screening of a phage-displayed random peptide library and classified the cell lines according to the binding selectivity of 26,031 recovered tripeptide motifs. By analyzing selected cell-homing peptide motifs and their NCI-60 recognition patterns, we established that some of these motifs (a) are similar to domains of human proteins known as ligands for tumor cell receptors and (b) segregate among the NCI-60 in a pattern correlating with expression profiles of the corresponding receptors. We biochemically validated some of the motifs as mimic peptides of native ligands for the epidermal growth factor receptor. Our results indicate that ligand-directed profiling of tumor cell lines can select functional peptides from combinatorial libraries based on the expression of tumor cell surface molecules, which in turn could be exploited as "druggable" receptors in specific types of cancer. (Cancer Res 2006; 66(1): 34-40)

## Introduction

The National Cancer Institute panel of human cancer cell lines from different histologic origins and grades (NCI-60) has been extensively used to screen compounds for anticancer activity (1, 2). The NCI-60 includes carcinomas of several origins (kidney, breast, colon, lung, prostate, and ovarian), tumors of the central nervous system, malignant melanomas, leukemias, and lymphomas. Gene expression determined by high-throughput microarrays has been used to survey the variation in abundance of thousands of distinct transcripts in the NCI-60; such data provided functional insights about the corresponding gene products in tumor cell transformation (2-4). This information-intensive genomic approach has yielded candidate diagnostic tumor markers to be validated at the protein level in prospective studies (4). Moreover, systematic proteomic studies based on two-dimensional PAGE (5) and protein microarrays (4) have also been implemented. Finally, in parallel

with the NCI-60 transcriptome and proteome initiatives, pharmacologic sensitivity of the cells to  $>10^5$  different chemical compounds has been registered (1, 2). Indeed, for some genes, correlation of expression data to drug sensitivity profiles has uncovered the mechanistic basis for the drug activity (3, 6-10). Thus, conventional genomic and proteomic approaches have identified several potential tumor markers and drug targets. However, despite such advances, correlation between drug activity and gene expression profiles has not as yet been established for most of the compounds tested (9, 11, 12). This suggests the likely existence of unknown factors and the need to develop alternative methodology to discover "druggable" molecular targets.

Over the past few years, it has been proposed that (a) characterization of molecular diversity at the tumor cell surface level (represented primarily by membrane-associated proteins that are often modified by lipids and carbohydrates) is required for the development of ligand-directed anticancer therapies, and that (b) peptides binding to surface receptors preferentially expressed on tumor cells may be used to ligand-direct therapeutics to sites of disease with potential for increased therapeutic windows (13, 14). It has become increasingly clear that selective cell surface features can be mapped by screening libraries of peptides (14-17). In fact, combinatorial peptide libraries displayed from pIII protein of an M13-derived phage have now been successfully screened on intact cells and *in vivo* (13-15). Peptide ligands selected from unbiased screens without any predetermined notions about the nature of the cellular receptor repertoire have been used for the subsequent identification of the corresponding target cell surface receptors (16-21). In addition, novel techniques, such as the biopanning and rapid analysis of selective interactive ligands (BRASIL), have enabled high-throughput phage library screening on cells (16). Here, we used the BRASIL method to systematically screen combinatorial libraries on tumor cells of the NCI-60 panel. Results of this feasibility study suggest that tumor cells can be grouped by profiles of their peptide ligands directed to differentially expressed cell surface receptors. Our data support the notion that many tumor cell surface-exposed receptors are expressed irrespective of tumor origin, thus suggesting they could be developed as broad tumor targets. Integration of ligand-directed surface profiling with other approaches related to the NCI-60 may uncover functional ligand-receptor pairs for the targeted drug delivery.

## Materials and Methods

**Combinatorial library screening on cells.** All the NCI-60 cell lines (1), except MDA-N (unavailable), were grown in RPMI 1640 supplemented with 5% fetal bovine serum (FBS) and 5 mmol/L L-glutamine. A phage display

Note: M.G. Kolonin and L. Bover contributed equally to the work.

Supplementary data for this article are available at Cancer Research Online (<http://cancerres.aacrjournals.org/>).

**Requests for reprints:** Renata Pasqualini or Wadih Arap, The University of Texas M.D. Anderson Cancer Center, 1515 Holcombe Boulevard, Houston, TX 77030. Phone: 713-792-2873; Fax: 713-745-2999; E-mail: [rpasqual@mdanderson.org](mailto:rpasqual@mdanderson.org); [warp@mdanderson.org](mailto:warp@mdanderson.org).

©2006 American Association for Cancer Research.

doi:10.1158/0008-5472.CAN-05-2748

random peptide library based on the vector fUSE5 displaying the insert CX<sub>7</sub>C was screened by using BRASIL as described (16). Exponentially growing cells were harvested with 0.5 mmol/L EDTA, 0.4 g/L KCl, 8 g/L NaCl, and 1 g/L dextrose, washed once with phosphate buffer saline (PBS), and resuspended in RPMI containing 1% bovine serum albumin (BSA) and 1 mmol/L HEPES. Cells (~ 10<sup>6</sup>) were incubated for 2 hours on ice with 10<sup>9</sup> transduction units of CX<sub>7</sub>C phage in 200-μL suspension, transferred to the top of a nonmiscible organic lower phase (dibutyl phthalate/cyclohexane, 9:1), and centrifuged at 10,000 × *g* for 10 minutes. The phage-bound cell pellet was incubated with 200 μL of K91 bacterial culture, and the bound phages were amplified and used in the following round. To prevent preferential isolation of peptides containing the RGD motif, which is selected on tissue-cultured cells due to expression of cell adhesion molecules binding to vitronectin, library screening was done in the presence of 1 mg/mL of the synthetic peptide RGD-4C (AnaSpec, San Diego, CA) in each round. After three rounds of selection, phage peptide-encoding inserts were sequenced as described (15, 17, 21).

**Hierarchical cluster analysis of peptide motif/cell line association.** We created an interactive sequence management database of all peptide sequences isolated in the screen. Calculation of tripeptide motif frequencies in CX<sub>7</sub>C peptides (in both directions) was done by using a character pattern recognition program based on SAS (version 8.1.2, SAS Institute, Cary, NC) and Perl (version 5.6.1) as described (17). To identify the most closely related tripeptides and cell lines, we generated clustered image maps (CIM) by using online software CIMminer available at <http://discover.nci.nih.gov/tools.jsp>. Data were centered (mean subtracted and divided by SD) on both cell lines and tripeptide motifs; correlation coefficient metric with average linkage algorithm was used as distance measurement. The tripeptide motif frequencies across the NCI-60 cell lines formed a two-dimensional data matrix that was used to correlate motif enrichment with groups of cell lines. To evaluate whether CIMminer algorithm is appropriate for clustering analysis of peptide frequency data, we devised a simulation test assuming that the frequencies of tripeptide motifs in a given data set follow an independent Poisson distribution. We simulated a random 3,280 × 59 data matrix of the dimension identical to that of tripeptide motif frequency data matrix (corresponding to the set of 3,280 tripeptides and 59 cell lines). These simulated data were centered the same way as the experimental data by transforming to mean of 0, variance of 1. For CIM in Fig. 1, tripeptides selected on all but one cell line of common origin (17) were used. Specificity of five tripeptides selectively overrepresented or underrepresented in lung tumor cell binding peptides for the 11 boxed cell lines (against the other 48 cell lines) was evaluated by using the R Package, version 2.0.0 (<http://www.r-project.org>) by performing two-sample *t* test (one tailed), as well as using Wilcoxon rank sum test (one tailed) and Fisher exact test (one tailed) as described (17).

**Identification of candidate targeted receptors.** To identify lead receptors targeted by tripeptide motifs, we screened the Molecular Target Database (<http://www.dtp.nci.nih.gov>) to identify proteins, expression levels of which in individual cell lines of the NCI-60 correlated with frequencies of individual tripeptides from Fig. 1 in the corresponding cell lines. We used the COMPARE software (<http://dtp.nci.nih.gov/docs/compare/compare.html>) to calculate pairwise Pearson correlations between tripeptide frequencies in cell lines and the protein expression patterns in the database. Minimum Pearson correlation coefficient of 0.2 served as cutoff for the selection of lead receptors, as it provided a reasonable number of candidate molecular targets for which NCI-60 expression profiles and tripeptide frequency distribution profiles correlated. To initially restrict the candidate targets analyzed to broad-specificity receptors, we included only putative cell surface molecules (Table 1), expression of which in the NCI-60 was found to correlate with the frequency profile of at least 25% of the tripeptides.

**Protein database screening for peptide motif similarity.** To identify natural prototype ligands of candidate receptors that are mimicked by selected peptides, we screened all 7-mer peptides selected in the screen by using online ClustalW software (<http://www.ebi.ac.uk/clustalw/>) to identify extended (four or longer amino acids) motifs shared between multiple peptides containing the broad-specificity tripeptides (Fig. 1). Nonredundant

databases of human proteins were searched by the BLAST software (<http://www.ncbi.nlm.nih.gov/BLAST/>) for proteins containing the cell-targeting 4-mers under the condition that at least the tripeptide part of the motif is identical to the part of the BLAST match.

**Validation of epidermal growth factor receptor as one of the peptide targets.** To isolate peptides binding to epidermal growth factor receptor (EGFR), phage clones selected on SKOV3 in rounds 2 and 3 of the screening were individually amplified and pooled, and 10<sup>9</sup> transduction units of the mixed phage were incubated overnight at 4°C with 10 μg of purified human EGFR (Sigma, St. Louis, MO), or BSA control immobilized on plastic. Unbound phages were extensively washed off with PBS, and then the bound phages were recovered by infecting host K91 *Escherichia coli* directly on the plate, and tetracycline-resistant clones were selected/quantified and sequenced. To identify EGFR ligand-matching motifs among phage-displayed SKOV3-binding peptides, custom-designed Perl 5.8.1-based software was used to run peptide sequences against biological EGFR ligand sequences. Each 7-mer peptide sequence was aligned in each orientation against the EGFR ligand sequences from the NH<sub>2</sub> to COOH terminus in one-amino-acid shifts. The peptide/protein similarity scores for each residue were calculated based on a BLOSUM62 matrix modified to identify peptide matches of at least three amino acids in any position being identical and one being similar to the corresponding amino acid positions in the EGFR ligands (Fig. 2A).

## Results

**Isolation of peptides binding to surface of the NCI-60 cancer cells.** As an initial attempt to profile cell surface of the tumor cell panel, we screened a large (2 × 10<sup>8</sup> unique sequences) cyclic random peptide library with the basic structure CX<sub>7</sub>C (C, cysteine; X, any residue) on every cell line of the NCI-60. Phage selection was done in the excess of a competing Arg-Gly-Asp (RGD) synthetic integrin-binding peptide (13) to minimize the recovery of RGD-containing peptides. This strategy was designed to facilitate the recovery of ligands binding to nonintegrin families of cell surface receptors because RGD tends to become dominant in the screening due to the high levels of integrin expression in adherent cells.<sup>3</sup> Preferential cell binding of specific cell-targeting peptides results in enrichment, defined by the increased recovery frequency of these peptide motifs in each subsequent round of the screen (14, 21). Thus, we set out to profile the expression of nonintegrin cell surface molecules among the cell lines of the NCI-60 according to the differential selection of motifs enriched in the screen.

**Hierarchical cluster analysis of peptides binding to the NCI-60 cells.** To analyze the spectrum of the peptides resulting from the screening and compare those among different cell lines of the panel, we adopted a combinatorial statistical approach based on the premise that three residue motifs (tripeptides) provide a sufficient structure for protein-peptide interactions in the context of phage display (17). For each NCI-60 cell line, we sequenced CX<sub>7</sub>C peptide-encoding DNA inserts from 96 phage clones recovered after three rounds of selection. We did a computer-assisted survey of all tripeptides within the library-derived sequences selected on each cell line by analyzing a database of 26,031 tripeptides contained within the 5,270 CX<sub>7</sub>C-encoded 7-mer peptides isolated (an average of eighty-nine 7-mer peptide sequences analyzed per each NCI-60 cell line). Thus, each cell line was assigned a unique set of tripeptides that was identified during the selection for cell surface binders, and the frequencies of each motif among all peptides for a given cell line were calculated.

<sup>3</sup> Unpublished observations.



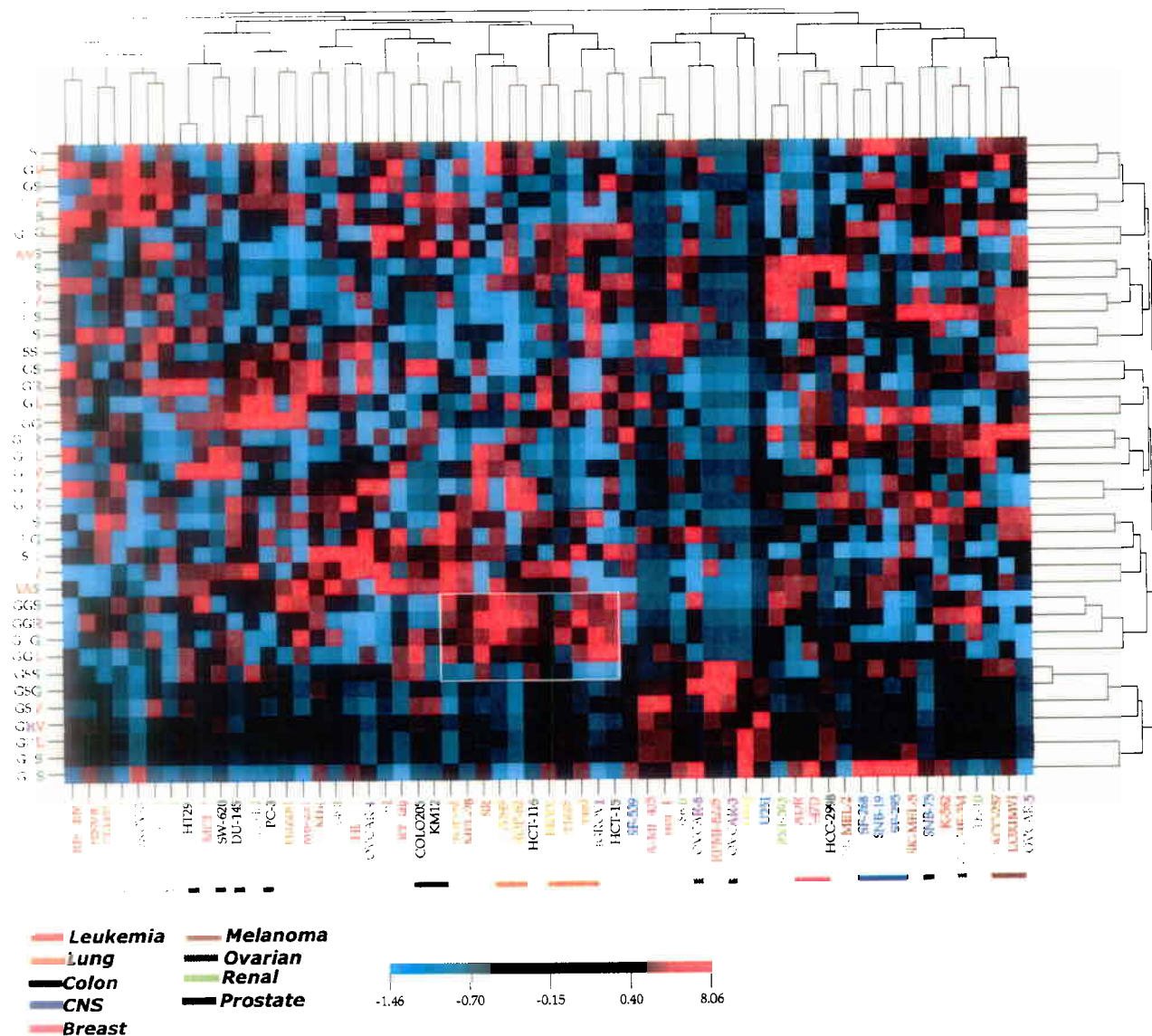


**Figure 1.** Selectivity of broad-specificity tripeptides for clusters of NCI-60 cell lines. Two-dimensional hierarchical clustering was applied to the frequencies of 38 tripeptides (rows) encountered in CX<sub>7</sub>C peptides selected on NCI-60 cell lines (columns). Tripeptides selected on all but one cell line of common origin were clustered based on their correlations with cell lines; cell lines were clustered based on their correlations with the tripeptides. Tripeptide frequencies were mean subtracted and average linkage clustered with correlation metric. Amino acid color code: red, hydrophobic; green, neutral and polar; purple, basic. The color in each CIM segment ranges from blue (negative correlation) to red (positive correlation), as indicated by the scale bar. Cell lines are color-coded based on previously defined histologic tumor origin (1, 2). Bars underneath dendrogram, clusters of cells of similar tumor tissue origin (one exception allowed). Boxed, cluster of lung cancer-derived cell lines and associated/dissociated tripeptides.

To classify cell lines according to their association with particular motifs, which might provide inference on the targeted surface molecules, we did a hierarchical clustering analysis of the 3,280 nonredundant tripeptides based on the frequency of association with the NCI-60 cell lines. For the construction of a CIM, we adapted a hierarchical clustering algorithm and a pseudo-color visualization matrix initially designed to address differential gene expression among the cells of the panel (3, 6–8). CIMMiner (2) was used for inference of the variation in peptide binding specificity across the cell lines by comparing relative frequencies of tripeptides found in 7-mer peptides binding to each cell (see Materials and Methods). Clustering of peptide motifs with similar

cell selectivity revealed that the peptide distribution of the combinatorial library within the NCI-60 set was nonrandom (Supplementary Fig. S1A). Computer simulations of the permuted data set show that the observed pattern could not be generated by random chance (Supplementary Fig. S1B), thus indicating that the discontinuous tripeptide frequency data is applicable for cluster analysis.

The selective spectra of peptide motifs interacting with the clustered cell lines suggest the existence of shared targeted surface receptor(s) expressed in these lines. In this study, we chose to focus on putative peptide-targeted receptors with broad cell line specificity, which would be more informative for an initial peptide

binding/receptor expression correlation analysis. We therefore excluded from the data set motifs selected only on a single or few cell lines. Instead, we focused on 38 tripeptides that showed a semiubiquitous distribution among the NCI-60 lines (Fig. 1). A CIM constructed according to the isolation frequency of these broader-specificity tripeptides from each cell line revealed several apparent

clusters of cell lines that displayed distinct profiles of association with certain classes of peptide motifs. For example, the majority of lung cancer-derived cell lines segregated as a separate group, suggesting that some of the receptors targeted may be conserved among cell lines derived from a common origin (Fig. 1). Thus, although we severely restricted our analysis by limiting it

**Table 1.** Candidate ligand-receptor interactions mimicked by NCI-60-binding tripeptides

Motif	Candidate peptide motif receptors		Candidate peptide-mimicked receptor ligands	
RLS	<b>ErbB2, ErbB4</b>	<b>FGF2,4</b>	<b>EGF-TM7</b>	
RGV				
RGS	<b>ErbB4</b>	<b>FGF2</b>	<b>EphA2,A3,A4,A6,B1</b>	<b>EGF-TM7, FGF-12b, FGF-5, NRG-beta</b>
RAV	<b>ErbB2</b>			<b>MEGF7, NGF-beta, NTF 5 alpha</b>
RAS		<b>TRKA</b>		<b>FGF-20, NRG-3</b>
GAG	<b>EGFR</b>	<b>FGF1,2,3</b>		<b>MEGF4, FGF6, NRG-beta</b>
AVS	<b>EGFR, ErbB2, ErbB4</b>	<b>FGF1</b>	<b>TRKB,C</b>	<b>EphA2,A3,A4,A7,B1,B2,B3,B5</b>
LLS				<b>TRK1</b>
LLR			<b>TRKA</b>	<b>amphiregulin</b>
LRV	<b>EGFR, ErbB2, ErbB4</b>	<b>FGF3</b>	<b>TRKA, B, C</b>	<b>EphA4</b>
LRS	<b>ErbB3</b>		<b>EphA2,A3,A7</b>	<b>FGF-12b, Eph-B3</b>
RVS	<b>EGFR, ErbB2, ErbB4</b>	<b>FGF1,2</b>	<b>TRKB</b>	<b>MEGF4, MEGF5, MEGF8, NRG-3, NGF-beta</b>
RSS		<b>FGF3</b>	<b>TRKA</b>	<b>MEGF10, amphiregulin</b>
AGS	<b>EGFR</b>		<b>EphA5</b>	<b>EGF-TM7, FGF-5, NRG-3</b>
AGR			<b>TRKA</b>	<b>MEGF6, brain NRG</b>
AQL	<b>EGFR, ErbB2, ErbB3</b>	<b>FGF1,3</b>		<b>MEGF2, MEGF4, FGF6, NTF 5, NTF-6</b>
AGG			<b>EphA5,A5,A6</b>	<b>MEGF12</b>
GVR	<b>EGFR, ErbB2, ErbB4</b>	<b>FGF1,2</b>	<b>EphA5</b>	<b>HB-EGF, Eph-B3</b>
GVL		<b>FGF1,2</b>	<b>EphA1</b>	<b>MEGF4, MEGF6, MEGF8, FGF-5, bFGF, brain NGF</b>
GAV			<b>EphA2,A3,A5,A6,B3</b>	<b>NGF2, Ephrin-B3</b>
GLV	<b>ErbB4</b>	<b>FGF4</b>	<b>EphA5</b>	<b>MEGF5, MEGF6, NGF-beta</b>
GLR	<b>ErbB4</b>			<b>EGF-TM7, betacellulin, NTF 3, Eph-B3</b>
LVS		<b>FGF1,4</b>	<b>EphA5,A6</b>	<b>MEGF5, EGFL5, FGF-12b, FGF-10, NRG-beta</b>
ARG	<b>ErbB2</b>	<b>FGF2,4</b>	<b>EphA1</b>	<b>EGFL5, FGF23, GDNF, Eph-B3</b>
ASL		<b>FGF1,2</b>		<b>FGF-12b, FGF23, NGF-beta, GDNF, NTF 6</b>
AAV			<b>TRKB</b>	<b>EGF-TM7, FGFR1</b>
AAS		<b>FGF1,2</b>	<b>EphA2,A3,A4,A7,B3,B5</b>	-
GGG			<b>TRKA</b>	-
GGR	<b>EGFR, ErbB2</b>	<b>FGF2</b>	<b>EphA5</b>	<b>Eph-B3, Eph-A4</b>
GLG	<b>ErbB2, ErbB3</b>	<b>FGF2,3,4</b>		<b>EGF-TM7, HB-EGF, FGF23, Ephrin-B3</b>
GGL	<b>ErbB2</b>		<b>EphA1,A6</b>	<b>heparin binding growth factor 3</b>
GSS	<b>EGFR, ErbB2</b>	<b>FGF3</b>	<b>TRKA,C</b>	<b>HB-EGF, MEGF5, EGFL5, NRG-3</b>
GSG	<b>EGFR</b>		<b>EphA5</b>	<b>MEGF5</b>
GSV	<b>EGFR, ErbB2, ErbB4</b>	<b>FGF4</b>	<b>TRKB</b>	-
GRV	<b>EGFR</b>		<b>EphA7,B2</b>	<b>MEGF5, NRG 3, Ephrin-B3</b>
GRL	<b>EGFR, ErbB2</b>			<b>MEGF8, EGF-TM7, FGF23, NTF4</b>
GPS	<b>EGFR, ErbB2, ErbB4</b>	<b>FGF3</b>	<b>EphA5,B1,B2,B4</b>	<b>betacellulin, EGFL5, NGF2, NTF5, EphB3, EphA4</b>
GVS	<b>EGFR</b>	<b>FGF4</b>	<b>EphA2,A3,A4,A7,B2,B5</b>	<b>MEGF5, EGFL5, EGF-like EMR3, SPGF</b>
			<b>TRKA</b>	<b>MEGF-1, MEGF5, NRG-3, NTF-6, NTF-5</b>

NOTE: Candidate peptide motif receptors are the human cell surface proteins (identified by COMPARE) expressed in profiles correlating with the selectivity of the corresponding tripeptides. Candidate peptide-mimicked receptor ligands are human proteins (identified by automated BLAST) that contained the corresponding tripeptides. Tripeptides in the column are ordered as in Fig. 1. Receptors of the same family and their corresponding candidate biological ligands identified based on tripeptide similarity are coded by the same color [EGFR, blue; FGFR, green; TRK receptor (NGFR), purple; ephrin receptor, red]. Tripeptides that both have a selectivity correlating with EGFR family receptor expression and are found within EGFR ligands (boldface). Tripeptides that were confirmed to reside within EGFR-binding SKOV3-selected peptides (Fig. 2; blue). See Supplementary Materials and Methods for Genbank accession nos. of BLAST-identified proteins.



to semiubiquitous tripeptides, clustering of some of them (predominantly with cell lines derived from the same tumor type) is consistent with their relative tissue specificity. To evaluate individual motifs for selectivity, we identified a distinct cluster of five tripeptides associated with lung tumor-derived cell lines (Fig. 1, boxed). We compared tripeptide frequencies for the 11 cell lines within this cluster with their frequencies for the rest of NCI-60 lines by using statistical tests (Fisher exact, Wilcoxon rank-sum, and *t* test). Consistently, we observed that motif GGS was isolated for the clustered lines significantly ( $P < 0.05$ ) more frequently than for the other NCI-60 cell lines (Supplementary Table S1).

Notably, the distribution of cell lines in the dendrogram (Fig. 1) was partially consistent with the reported association of cells derived from tumors with common tissue origin (3, 4). This suggests that some of the receptors, such as the one presumably recognized by the lung tumor-specific tripeptide GGS (Fig. 1; Supplementary Table S1), may be up-regulated only in certain cancer origins. However, the tumor cell phylogeny was recapitulated only to an extent; the majority of the observed clusters contained cell lines derived from unrelated tumor types (Fig. 1). The limited grouping of lines derived from tumors of common origin is perhaps not surprising: the relationship between different cell lines in our study is based on peptide binding to putative cell surface molecules, many of which may be tumor induced rather than characteristic of the tissue of origin. If so, our analysis of broad-specificity motif distribution may be well suitable for identification of specific surface molecules that are generally up-regulated by tumors and thus may constitute broad drug targets against cancer.

**Identification of candidate receptor targets for peptide motifs.** We next attempted to identify the targets for the 38 broad-specificity tripeptides, most of which presumably bind to receptors expressed by multiple NCI-60 cell lines. We used the NCI Molecular Targets Database that contains detailed information on the expression and activity of 1,218 human proteins measured by nonarray methods (22). By using the COMPARE algorithm (6), we correlated the selectivity profiles of the 38 tripeptide motifs with the expression profiles of the characterized molecular targets. We observed that several of the qualifying proteins, expression of which correlated with enrichment profiles of certain motifs, represented tyrosine kinase receptors, such as those for ligands belonging to families of EGFs, fibroblast growth factors (FGF), nerve growth factors (NGF), and ephrins (Table 1). When transferred to molecular target correlation data, the order of the 38-tripeptide motif set in the dendrogram (Fig. 1) revealed clusters of tripeptides for which cell line association profile correlated with expression profiles of EGF, FGF, NGF, or ephrin receptors (Table 1).

The peptide distribution-correlating tyrosine kinase receptors, belonging to EGFR, FGFR, NGFR, and ephrin receptor families (Table 1), are often up-regulated in many types of cancer (23). To determine if the cell-binding peptides may target these tyrosine kinases, we employed the notion that receptor-binding peptide motifs often mimic natural ligands for these receptors (16, 17, 19). Thus, we tested whether the selected motifs mimic ligands for the candidate tyrosine kinases by determining whether tripeptides listed in Table 1 are embedded into longer peptides that may be responsible for cell surface binding. We analyzed the CX<sub>2</sub>C phage inserts containing the 38 tripeptides by using the ClustalW software and compiled extended motifs containing the tripeptides shared among multiple peptides selected during the screen (data not shown). To identify candidate prototype human ligands, epitopes of which could be mimicked, we screened each of the

ClustalW-extended motifs against the nonredundant database of human proteins by using the BLAST software (National Center for Biotechnology Information). As a result of this analysis, we found the motifs containing 34 of 38 tripeptides (89%) to be identical or very similar to segments of proven or putative ligands for the tyrosine kinase receptors listed (Table 1).

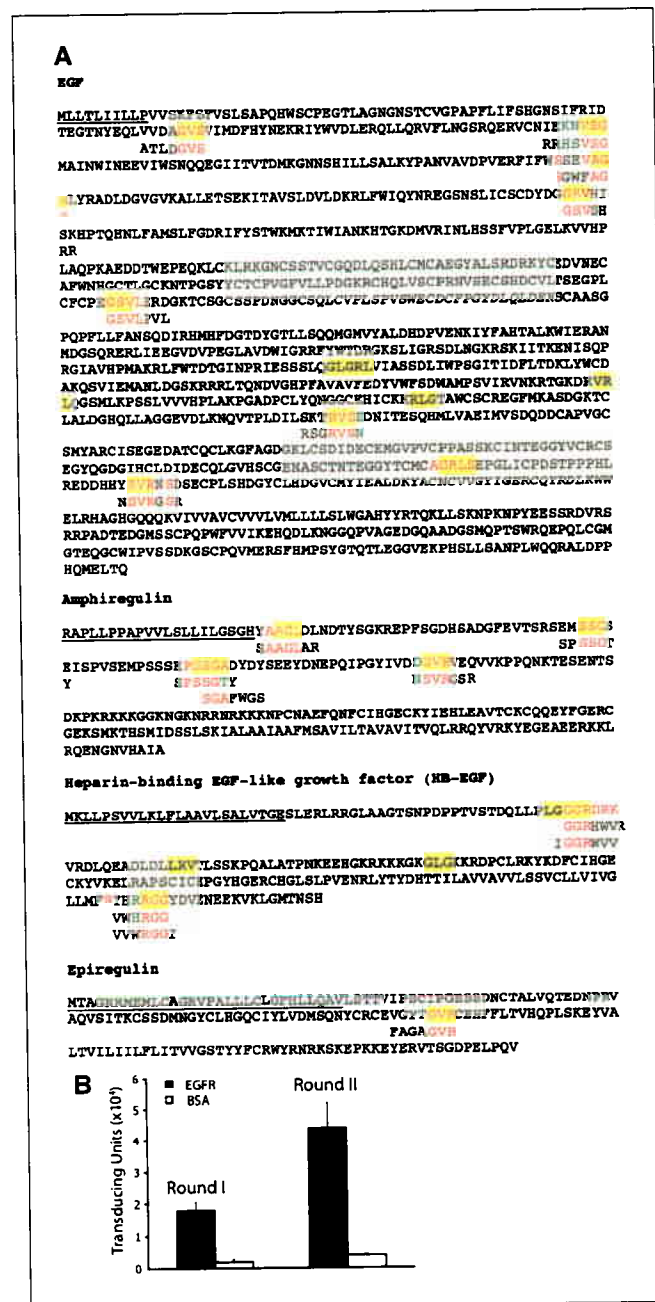


**Figure 2.** Identification of peptides mimicking EGFR ligands. **A**, EGFR-binding peptide sequences isolated from the SKOV3-selected phage pool were matched in each orientation to protein sequences of biological human EGFR ligands (leader peptide sequence underlined). Matches displayed are peptides with three or more amino acids being identical (red) and one or more being from the same class (green) as the correspondingly positioned protein amino acids. Tripeptides listed in Table 1 (yellow). **B**, isolation of peptides targeting EGFR. Binding of SKOV3-selected phage pool to immobilized EGFR compared with BSA in rounds 1 and 2 of biopanning of SKOV3-selected phage pool on immobilized human EGFR.

**Validation of EGFR as a targeted receptor.** To show that the approach taken can lead to actual targetable tumor cell surface proteins, we chose to test if the EGFR is bound by any of the tripeptide motifs distributed in the panel in a profile correlating with EGFR expression. Consistently, 24 of 38 tripeptides surveyed displayed NCI-60 cell line association pattern consistent with that of EGFR expression (Table 1). Of these tripeptides, 22 were isolated in the screens on ovarian cancer cell lines SKOV3 and OVCAR4 (data not shown). Because EGFR is well known to be associated with ovarian cancer (23), we deemed these cell lines to be likely expressors of targetable EGFR, which would account for the selection of EGFR ligand-mimicking motifs. To validate EGFR binding by the selected motifs, we screened the SKOV3-binding phage sublibrary (pooled clones recovered in rounds 2 and 3) on immobilized human EGFR. After two rounds of selection, we analyzed phage displaying the EGFR-binding peptides: the majority were comprised by different 7-mer peptides (Fig. 2A) that contained 17 of 22 SKOV3-selected tripeptide motifs distributed in the panel in a profile correlating with EGFR expression (Table 1). Phage displaying these peptides had specific affinity to EGFR, as determined by subjecting the same sublibrary to immobilized BSA control binding (Fig. 2B). Remarkably, computer-assisted analysis of sequences (Fig. 2A) revealed that 12 of the 7-mer EGFR-binding peptides contained amino acid motifs similar to those present in some of the biological EGFR ligands (23). These peptides, containing eight of the candidate tripeptides (RVS, AGS, AGL, GVR, GGR, GGL, GSV, and GVS), were found highly similar to fragments of EGF, amphiregulin, heparin-binding EGF-like growth factor, and epiregulin (Fig. 2A). Similarity search using the same algorithm on the same twelve 7-mers did not reveal any matches to two other EGFR ligands, transforming growth factor- $\alpha$  and  $\beta$ -cellulin, or randomly chosen control ligands of tyrosine kinase receptors from the three other candidate families listed in Table 1: ephrin A, NGF- $\beta$ , and FGF6 (data not shown). Taken together, these data suggest that at least some of the peptides selected on the NCI-60 cells target EGFR, whereas others may bind to different tyrosine kinases, possibly including those from TRK, ephrin, or FGF receptor families.

## Discussion

Expression profiles of the candidate receptor targets for peptides identified in the screen illustrate the concept that in cancer, at least some tumor-associated cell surface molecules seem up-regulated regardless of cancer tissue origin. As such, this is the case for the EGFR and other tyrosine kinases possibly targeted by peptide

ligands selected on the NCI-60 cell panel. This may also be the case for many other receptors with a role in tumorigenesis, expression profiles of which may not correlate with the overall proteomic profile of the original tumor tissue. In fact, these observations may account for the relatively limited success in correlating drug toxicity profiles with the genomic and/or proteomic profiles of the NCI-60 panel (12). On the other hand, some of the receptors, such as EphA5 presumably targeted by GGS tripeptide and its derivatives predominantly selective for lung tumor-derived cell lines (Fig. 1), seem to be at least partially specific for the progenitor cancer type.

The candidate ligand-receptor leads identified in this study can be characterized further for the development of targeted agents selective for tumors. Moreover, the peptides identified by the approach described here may map receptor interaction domains of biological (native) ligands. Similarity of peptides to the corresponding receptor-binding ligands has already been used for validation of the IL-11R $\alpha$  receptor as a target of an interleukin-11 mimic peptide homing to blood vessels in the prostate (17, 24). We and others have modeled the usage of peptides homing to receptors expressed by tumors (18) or nonmalignant tissues (19, 20) for directing the delivery of cytotoxics, proapoptotic peptides, metalloprotease inhibitors, cytokines, fluorophores, and genes (13, 14). Thus, our approach provides a straightforward way to identify drug-accessible tumor cell surface receptors and to discover peptide ligands that can serve as mimetic prototype drugs. Unlike genomic or proteomic-based approaches that rely on differential expression levels of transcripts or protein products, this discovery platform directly addresses functional protein-protein interactions at the level of physical binding. In contrast to protein array systems, it is possible to select binding peptides even if the ligand-receptor interaction is mediated by conformational (rather than linear) epitopes. In summary, ligand-directed screening of combinatorial libraries on tumor cell surfaces may lead to improved selection of functionally relevant peptides that can be developed for targeting "druggable" molecular targets.

## Acknowledgments

Received 8/3/2005; revised 10/12/2005; accepted 11/2/2005.

**Grant support:** NIH (R. Pasqualini, W. Arap, M.G. Kolonin, and K.-A. Do), SPORC Programs (Prostate Cancer and Leukemia, R. Pasqualini and W. Arap), Department of Defense (M.G. Kolonin) IMPACT (W. Ki Hong) and grant DAMD17-03-1-0638 (M.G. Kolonin), Lung Cancer Program (W. Ki Hong), A.J. Zurita was supported by a BEFI fellowship.

The costs of publication of this article were defrayed in part by the payment of page charges. This article must therefore be hereby marked *advertisement* in accordance with 18 U.S.C. Section 1734 solely to indicate this fact.

## References

- Monks A, Scudiero D, Skehan P, et al. Feasibility of a high-flux anticancer drug screen using a diverse panel of cultured human tumor cell lines. *J Natl Cancer Inst* 1991; 83:757-66.
- Weinstein JN, Myers TG, O'Connor PM, et al. An information-intensive approach to the molecular pharmacology of cancer. *Science* 1997;275:343-9.
- Scherf U, Ross DT, Waltham M, et al. A gene expression database for the molecular pharmacology of cancer. *Nat Genet* 2000;24:236-44.
- Nishizuka S, Charboneau L, Young L, et al. Proteomic profiling of the NCI-60 cancer cell lines using new high-density reverse-phase lysate microarrays. *Proc Natl Acad Sci U S A* 2003;100:14229-34.
- Myers TG, Anderson NL, Waltham M, et al. A protein expression database for the molecular pharmacology of cancer. *Electrophoresis* 1997;18:647-53.
- Zaharevitz DW, Holbeck SL, Bowerman C, Svetlik PA. COMPARE: a web accessible tool for investigating mechanisms of cell growth inhibition. *J Mol Graph Model* 2002;20:297-303.
- Blower PE, Yang C, Fligner MA, et al. Pharmacogenomic analysis: correlating molecular substructure classes with microarray gene expression data. *Pharmacogenomics J* 2002;2:259-71.
- Rabow AA, Shoemaker RH, Sausville EA, Covell DG. Mining the National Cancer Institute's tumor-screening database: identification of compounds with similar cellular activities. *J Med Chem* 2002; 45:818-40.
- Wallqvist A, Rabow AA, Shoemaker RH, Sausville EA, Covell DG. Establishing connections between microarray expression data and chemotherapeutic cancer pharmacology. *Mol Cancer Ther* 2002;1:311-20.
- Szakacs G, Annereau JP, Lababidi S, et al. Predicting drug sensitivity and resistance: profiling ABC transporter genes in cancer cells. *Cancer Cell* 2004;6:129-37.
- Brown JM. NCI's anticancer drug screening program may not be selecting for clinically active compounds. *Oncol Res* 1997;9:213-5.

12. Wallqvist A, Rabow AA, Shoemaker RH, Sausville EA, Covell DG. Linking the growth inhibition response from the National Cancer Institute's anticancer screen to gene expression levels and other molecular target data. *Bioinformatics* 2003;19:2212-24.
13. Arap W, Pasqualini R, Ruoslahti E. Cancer treatment by targeted drug delivery to tumor vasculature in a mouse model. *Science* 1998;279:377-80.
14. Kolonin MG, Pasqualini R, Arap W. Molecular addresses in blood vessels as targets for therapy. *Curr Opin Chem Biol* 2001;5:308-13.
15. Pasqualini R, Ruoslahti E. Organ targeting *in vivo* using phage display peptide libraries. *Nature* 1996;380:364-6.
16. Giordano RJ, Cardo-Vila M, Lahdenranta J, Pasqualini R, Arap W. Biopanning and rapid analysis of selective interactive ligands. *Nat Med* 2001;7:1249-53.
17. Arap W, Kolonin MG, Trepel M, et al. Steps toward mapping the human vasculature by phage display. *Nat Med* 2002;8:121-7.
18. Pasqualini R, Koivunen E, Kain R, et al. Aminopeptidase N is a receptor for tumor-homing peptides and a target for inhibiting angiogenesis. *Cancer Res* 2000;60:722-7.
19. Kolonin MG, Pasqualini R, Arap W. Teratogenicity induced by targeting a placental immunoglobulin transporter. *Proc Natl Acad Sci U S A* 2002;99:13055-60.
20. Kolonin MG, Saha PK, Chan L, Pasqualini R, Arap W. Reversal of obesity by targeted ablation of adipose tissue. *Nat Med* 2004;10:625-32.
21. Pasqualini R, Arap W, Rajotte D, Ruoslahti E. *In vivo* selection of phage-display libraries. In: Barbas C, Burton D, Silverman G, Scott J, editors. *Phage display: a laboratory manual*. New York (NY): Cold Spring Harbor Laboratory Press; 2001. p. 22.1-4.
22. Holbeck SL. Update on NCI *in vitro* drug screen utilities. *Eur J Cancer* 2004;40:785-93.
23. Vogelstein B, Kinzler KW. Cancer genes and the pathways they control. *Nat Med* 2004;10:789-99.
24. Zurita AJ, Troncoso P, Cardo-Vila M, et al. Combinatorial screenings in patients: the interleukin-11 receptor  $\alpha$  as a candidate target in the progression of human prostate cancer. *Cancer Res* 2004;64:435-9.

# **TGF- $\alpha$ and phosphorylated EGFR protein levels impact the survival of patients with stage I-III A Non Small Cell Lung Cancer**

*Erminia Massarelli, Xian Zhou, Natalie Ozburn, Marie Wislez, Benjamin N. Bekele, Jack A. Roth, Michael O'Reilly, Waun Ki Hong, John Kurie, Roy S. Herbst, Ignacio I. Wistuba*

In non-small cell lung cancer (NSCLC), HER family receptor signaling pathway abnormalities have been associated to pathogenesis, tumor prognosis and response to targeted therapy. However, there is controversial and limited information on the concurrent expression and clinical effect of HER ligands and receptors in large series of NSCLC. To better understand the correlations between HER ligands and receptors expression and their clinicopathological implications in NSCLC, we investigated the immunohistochemical (IHC) expression of HER ligands EGF, TGF- $\alpha$ , amphiregulin, and receptors EGFR, Her2/neu, p-EGFR (phosphorylated EGFR), p-Her3 (phosphorylated-Her3) in a series of NSCLCs placed in tissue microarrays (TMA). Correlations with clinicopathological characteristics and survival analyses were performed. In a subset of NSCLCs with adenocarcinoma histology, mutation status of *EGFR*, *KRAS*, *HER2* and *BRAF* genes was correlated with IHC expression.

Three hundred fifty-nine surgically resected tumors, 219 adenocarcinoma, 20 bronchioloalveolar carcinoma (BAC) and 120 squamous cell carcinoma, from patients with stage I-II-III A NSCLC were studied. A semi-quantitative analysis of nuclear, cytoplasmic and membranous localization expression was performed for each marker.

Different patterns of correlation between ligands and receptors IHC expression were identified. P-EGFR cytoplasmic and membranous overexpressions were found in cases TGF- $\alpha$  ( $p < 0.0001$ ,  $p = 0.01$ ) or amphiregulin ( $p < 0.0001$ ,  $p = 0.008$ ) positive and not in EGF-positive cases. Lower expression of EGFR and p-EGFR nuclear was found in never smokers ( $p = 0.01$ ,  $p = 0.001$ ) and in adenocarcinoma and BAC histologies ( $p < 0.0001$ ,  $p = 0.01$ ). Her2/neu was overexpressed in adenocarcinoma and BAC ( $p = 0.0005$ ). Moderate/high levels of cytoplasmic and membranous p-EGFR were found in stage II-III A cases ( $p = 0.001$ ,  $p = 0.03$ ). In the 14 (23.7%) EGFR-mutated cases, high levels of Her2/neu were present ( $p = 0.02$ ) and the frequency of mutations was higher in never smokers ( $p = 0.026$ ). The 10 cases (17.5%) with *KRAS* mutations showed low levels of Her2/neu and nuclear p-EGFR ( $p = 0.02$ ,  $p = 0.03$ ). With a median follow up of 3.4 years and a median recurrence-free survival of 4.7 years, independent of the age and stage, TGF- $\alpha$  overexpression demonstrated a favorable impact on recurrence-free ( $p = 0.003$ , RR=0.35, 95%CI 0.17, 0.70) and overall survival ( $p = 0.008$ , RR=0.32, 95%CI 0.14, 0.74). P-EGFR cytoplasmic overexpression resulted in reduced recurrence-free ( $p = 0.005$ , RR=2.17, 95%CI 1.25, 3.74) and overall survival ( $p = 0.001$ , RR=2.74, 95%CI 1.53, 4.94). In summary, TGF- $\alpha$  and p-EGFR overexpression have both been shown to have a prognostic role (the first positive and the second negative) in stage I-III A NSCLC as indicators of recurrence-free and overall survival. Grant Support: P50CA097007 and W81XWH0520027.

**WORDS: 2,458**

January 2006

Re: 2006 AACR Annual Meeting in Washington, DC

Temporary Abstract Number #3098

Title: TGF- $\alpha$  and phosphorylated EGFR protein levels impact the survival of patients with stage I-IIIa non small cell lung cancer

Dear Dr. Massarelli:

Your above-referenced abstract has been scheduled for oral presentation in a Minisymposium session at the 2006 AACR Annual Meeting in Washington, DC and will be published in the 2006 Proceedings of the American Association for Cancer Research. Presentation information pertaining to your abstract is below:

Session ID: Clinical Research 21

Session Date and Start Time:

Wednesday, April 5, 2006 12:00

PM

Permanent Abstract Number:

5729



### **Role of MDM2 in DNA repair**

Laura Paternoster, Anupama Munshi, Raymond E. Meyn.

Experimental Radiation Oncology, The University of Texas M.D. Anderson Cancer Center, Houston, TX 77030.

The p53 tumor suppressor protein plays a critical role in preventing tumorigenesis and the activation of p53 by stresses such as DNA damage or oncogene activation results in either cell cycle arrest or apoptotic cell death. MDM2, the *mdm2* gene product, is an E3 ligase that plays a central role in regulating p53 stability, targeting both p53 and itself for ubiquitination. p53 activates expression of MDM2, which keeps p53 levels low during normal growth and development, creating a feed-back auto-regulatory loop between p53 and MDM2. Amplification of *mdm2* or increased expression by unknown mechanisms occurs in many tumors that retain wild-type p53, leading to the hypothesis that overexpression of MDM2 is an important mechanism by which the cell inactivates p53 in the process of transformation. At the same time, some tumors contain both high levels of MDM2 and mutation in the p53 gene. The reasons for disrupting two components of the same pathway are unclear but suggest that MDM2 may have other p53-independent functions and the pathways that mediate these functions are unresolved. Recently, studies described a novel interaction of MDM2 with the DNA repair protein Nbs1. The binding between MDM2 and Nbs1 was direct and independent of p53 and occurred at Nbs1 nuclear foci following  $\gamma$ -irradiation. In light of these recent observations, we decided to investigate the possible involvement of MDM2 in DNA repair following  $\gamma$ -irradiation. We examined MDM2 nuclear localization following  $\gamma$ -irradiation in two non-small cell lung cancer (NSCLC) cell lines, A549 and H1299, the former expressing wild-type p53 and the latter being p53 null. Our results indicate that MDM2 localization in nuclear foci follows different kinetics in the two cell lines. In A549 cells, a relatively small number of foci were observed at 1 hour after irradiation, but these disappeared at 2 hours. Then, MDM2 foci reappeared at 4 hours and increased through 24 hours. This pattern while evident was not as dramatic in the H1299 cells which had a relatively high background in unirradiated cells. These new observations suggest that MDM2 can play a role in the DNA repair response which can be distinct from the DNA damage checkpoint response regulated by p53. The remaining question is what pathway signals MDM2's radiation response? In a preliminary analysis, we have shown that MDM2 is activated, at least partially, via the Raf-Raf-Mek-ERK signal transduction pathway. This new finding suggests that inhibitors of the Raf-Raf-Mek-ERK pathway may radiosensitize NSCLC cells by interfering with activation of MDM2. (Supported by DoD grant W81XWH-05-2-0027 01 IMPACT)

**Radiosensitization of human melanoma and NSCLC cells by sorafenib (BAY 43-9006), a multi-kinase inhibitor.** Anupama Munshi, Toshimitsu Tanaka, Marvette L. Hobbs, and Raymond E. Meyn. *The University of Texas M. D. Anderson Cancer Center, Houston, TX.*

The Ras/Raf signaling pathway is an important mediator of tumor cell proliferation and angiogenesis. Aberrant activation of this pathway as a result of activated Ras or mutant B-Raf is known to predict a malignant phenotype in solid tumors. Sorafenib (BAY 43-9006) is a potent inhibitor of Raf-1 (IC<sub>50</sub> 6 nM), and is also active against VEGFR-2 (IC<sub>50</sub> 90 nM), VEGFR-3 (IC<sub>50</sub> 20 nM), and PDGFR-β (IC<sub>50</sub> 57 nM). Sorafenib inhibits tumor cell proliferation and angiogenesis through blockade of these targets. Once-daily oral dosing of sorafenib (30 to 60 mg/kg) has demonstrated tumor growth inhibition in a range of xenograft tumors that express a mutation in K-Ras or B-Raf. Sorafenib has shown promise with evidence of tumor regression observed in multiple tumor types, including Renal cell carcinoma, melanoma, thyroid, sarcoma, and pancreas. Sorafenib has also been evaluated in a combination study with gemcitabine in patients with advanced pancreatic cancer and is currently in phase III clinical testing for the treatment of metastatic RCC and earlier phase studies for NSCLC, both as monotherapy and in combination with chemotherapy. However, no data exists on the use of sorafenib in combination with ionizing radiation, making a preclinical evaluation of this combination interesting. Therefore, in the present study, we report the effects of combined treatment with radiation and sorafenib on three human melanoma cell lines, A375, MeWo and WM793 and one NSCLC line, H1299. In clonogenic cell survival experiments, sorafenib had significant radiosensitizing effects. Cells were treated either with vehicle alone or with sorafenib (2μM for 24hrs for the A375 and MeWo; 10μM for 24hrs for the WM793 cells). Clonogenic cell survival assay showed that sorafenib enhanced tumor cell radiosensitivity with the survival factor at 2Gy (SF2) being reduced from 49% ± 0.5, 42.4% ± 0.97, and 37.7% ± 1.4 in vehicle treated to 25.2% ± 0.66, 22.5% ± 0.74, and 17.7% ± 1.74 in sorafenib-treated MeWo, A375 and WM793 cells respectively. Preliminary experiments indicate that the NSCLC cells are also radiosensitized. We examined potential mechanisms that may contribute to the enhanced radiation response induced by sorafenib. Radiation activated pERK1/2 and pAKT in these cell lines, however, this activation was suppressed by sorafenib correlating with its radiosensitizing effects. Overall, our results suggest that sorafenib synergistically interacts with radiation and enhances the radioresponse of human melanoma cells. Based on our results, sorafenib may mediate this effect via its ability to suppress ERK activation downstream of Ras/Raf activation. A detailed investigation of the mechanism is ongoing. The insight gained from the analyses of these molecular mechanisms will be very useful in future research examining the combination of agents such as sorafenib and ionizing radiation for the treatment of melanoma and NSCLC. (Supported by DoD grant W81XWH-05-2-0027 01 IMPACT).



# Activation of Akt and eIF4E Survival Pathways by Rapamycin-Mediated Mammalian Target of Rapamycin Inhibition

Shi-Yong Sun,<sup>1</sup> Laura M. Rosenberg,<sup>1</sup> Xuerong Wang,<sup>1</sup> Zhongmei Zhou,<sup>1</sup> Ping Yue,<sup>1</sup> Haian Fu,<sup>2</sup> and Fadlo R. Khuri<sup>1</sup>

<sup>1</sup>Department of Hematology and Oncology and Winship Cancer Institute and <sup>2</sup>Department of Pharmacology, Emory University School of Medicine, Atlanta, Georgia

## Abstract

The mammalian target of rapamycin (mTOR) has emerged as an important cancer therapeutic target. Rapamycin and its derivatives that specifically inhibit mTOR are now being actively evaluated in clinical trials. Recently, the inhibition of mTOR has been shown to reverse Akt-dependent prostate intraepithelial neoplasia. However, many cancer cells are resistant to rapamycin and its derivatives. The mechanism of this resistance remains a subject of major therapeutic significance. Here we report that the inhibition of mTOR by rapamycin triggers the activation of two survival signaling pathways that may contribute to drug resistance. Treatment of human lung cancer cells with rapamycin suppressed the phosphorylation of p70S6 kinase and 4E-BP1, indicating an inhibition of mTOR signaling. Paradoxically, rapamycin also concurrently increased the phosphorylation of both Akt and eIF4E. The rapamycin-induced phosphorylation of Akt and eIF4E was suppressed by the phosphatidylinositol-3 kinase (PI3K) inhibitor LY294002, suggesting the requirement of PI3K in this process. The activated Akt and eIF4E seem to attenuate rapamycin's growth-inhibitory effects, serving as a negative feedback mechanism. In support of this model, rapamycin combined with LY294002 exhibited enhanced inhibitory effects on the growth and colony formation of cancer cells. Thus, our study provides a mechanistic basis for enhancing mTOR-targeted cancer therapy by combining an mTOR inhibitor with a PI3K or Akt inhibitor. (Cancer Res 2005; 65(16): 7052-8)

## Introduction

The mammalian target of rapamycin (mTOR), a 289-kDa serine/threonine kinase, belongs to the phosphatidylinositol kinase-related kinase family. It plays a central role in regulating cell growth, proliferation, and survival, in part by regulation of translation initiation (1-3). In response to mitogen stimulation, mTOR regulates translation initiation through two distinct pathways: ribosomal p70 S6 kinase (p70S6K) and eukaryotic translation initiation factor 4E (eIF4E) binding proteins (4E-BPs). In one pathway, mTOR phosphorylates and activates p70S6K, which in turn phosphorylates the 40S ribosomal protein S6, leading to the enhancement of translation of mRNAs with a 5'-terminal oligopyrimidine, including mRNAs that encode for ribosomal proteins and

elongation factor-1. In another pathway, mTOR directly phosphorylates 4E-BP1, causing its dissociation from eIF4E, thereby increasing the availability of functional eIF4E, a rate-limiting component for cap-dependent translation. The free eIF4E then binds to eIF4G, promoting the assembly of the eIF4F initiation complex, which then leads to more efficient cap-dependent translation initiation, increasing the translation of mRNAs with long, highly structured 5'-untranslated regions, such as cyclin D1 and c-Myc (1-3).

The phosphatidylinositol-3 kinase (PI3K)/Akt signaling represents a major cell survival pathway. Its activation has long been associated with malignant transformation and apoptotic resistance (4). It has been well documented that mTOR functions downstream of the PI3K/Akt pathway and is phosphorylated (or activated) in response to stimuli that activate the PI3K/Akt pathway (1, 3). Normally, the phosphatase PTEN counters the PI3K activity and thus negatively regulates PI3K/Akt survival pathway. However, PTEN activity is frequently inactivated in many human tumor types through deletion, mutation, or silencing, leading to increased activation of Akt (4, 5). Additional mechanisms have also been found to induce the activation of the PI3K/Akt pathway, including oncogene (e.g., Ras) amplification and mutations, active mutations in the p110 and p85 subunits of PI3K, and Akt overexpression. Thus, mTOR signaling pathways are constitutively activated in many types of human cancer (1, 6). Recent studies have shown that the mutation of tuberous sclerosis complex and overexpression of Rheb that work downstream of Akt in regulating the mTOR signaling also occur in human cancers, contributing to mTOR activation (7). Moreover, eIF4E is overexpressed or amplified in multiple human cancers, which is often oncogenic (1, 6, 8). Therefore, mTOR signaling has emerged as an important and attractive therapeutic target for cancer therapy (1, 2). The potential applications of mTOR inhibitors for treating various types of cancer have been actively studied both preclinically and clinically. A recent animal study has shown that mTOR inhibition induces apoptosis of epithelial cells and reverses Akt-dependent prostate intraepithelial neoplasia (9). In the United States, several phase II or III trials are ongoing to test the effects of mTOR inhibitors on various cancers, including renal cell carcinoma, prostate, breast, pancreatic, and small cell lung cancers, recurrent brain tumors, recurrent mantle-cell lymphoma, and melanoma (1, 10).

The intrinsic sensitivity to mTOR inhibition by rapamycin among different cancer cell lines may vary by several orders of magnitude ranging from 1 to 5,000 nmol/L (IC<sub>50</sub>; ref. 11), indicating that some cancer cell lines are actually resistant to mTOR inhibition. Therefore, understanding the mechanisms by which cells become resistant to mTOR inhibitors may guide the development of successful mTOR-targeted cancer therapy. Using

Requests for reprints: Shi-Yong Sun, Winship Cancer Institute, Emory University School of Medicine, 1365-C Clifton Road, C3088, Atlanta, GA 30322. Phone: 404-778-2170; Fax: 404-778-5520; E-mail: shi-yong-sun@emoryhealthcare.org  
©2005 American Association for Cancer Research.  
doi:10.1158/0008-5472.CAN-05-0917

human non-small cell lung cancer (NSCLC) cells, here we report that mTOR inhibition by rapamycin induces activation of survival pathways involving increase of Akt and eIF4E phosphorylation. We show that prevention or disruption of the activation of Akt and eIF4E enhanced rapamycin-mediated growth inhibition, indicating that the induced activation of Akt and eIF4E survival pathways counteracts the mTOR inhibitor's effect on the growth of human cancer cells.

## Materials and Methods

**Reagents.** Rapamycin was purchased from LKT Laboratories, Inc. (St. Paul, MN). LY294002 and U0126 were purchased from LC Laboratories (Woburn, MA). PD98059 and SB203580 were purchased from Biomol (Plymouth Meeting, PA) and Calbiochem (San Diego, CA), respectively. These agents were dissolved in DMSO at a concentration of 10 or 20 mmol/L, and aliquots were stored at  $-80^{\circ}\text{C}$ . Stock solutions were diluted to the desired final concentrations with growth medium just before use. Rabbit polyclonal antibodies against Akt, mTOR, p70S6K, 4E-BP1, eIF4E, phospho-Akt (p-Akt, Ser<sup>473</sup>), phospho-mTOR (p-mTOR, Ser<sup>2448</sup>), phospho-GSK3 $\beta$  (p-GSK3 $\beta$ , Ser<sup>9</sup>), phospho-p70S6K (p-p70S6K, Thr<sup>389</sup>), phospho-4E-BP1 (p-4E-BP1, Ser<sup>65</sup>), phospho-eIF4E (p-eIF4E, Ser<sup>209</sup>), phospho-p44/p42 (p-p44/p42, Thr<sup>202</sup>/Tyr<sup>204</sup>), respectively, were purchased from Cell Signaling Technology, Inc. (Beverly, MA). Rabbit polyclonal anti-actin antibody was purchased from Sigma Chemical Co. (St. Louis, MO).

**Cell lines and cell culture.** Human NSCLC and other cancer cell lines used in this study were purchased from the American Type Culture Collection (Manassas, VA). They were grown in monolayer culture in RPMI 1640 supplemented with glutamine and 5% fetal bovine serum at  $37^{\circ}\text{C}$  in a humidified atmosphere consisting of 5%  $\text{CO}_2$  and 95% air.

**Growth inhibition assay.** Cells were seeded in 96-well cell culture plates and treated on the second day with rapamycin, LY294002, or rapamycin combined with LY294002. At the end of a 3-day treatment, cell number was estimated by the sulforhodamine B (SRB) assay as previously described (12). The percentage of growth inhibition was calculated by using the equation: % growth inhibition =  $(1 - A_t / A_c) \times 100$ , where  $A_t$  and  $A_c$  represent the absorbance in treated and control cultures, respectively.

**Colony formation assay.** Cells (single-cell suspension) were plated in 12-well plates at a density of 200 to 300 cells per well. On the second day, cells were treated with rapamycin, LY294002, or rapamycin plus LY294002. Every 3 days, the medium was replaced with fresh medium containing the corresponding agents. After a 10-day treatment, the medium was removed and cell colonies were stained with SRB dye as described (12). Pictures were then taken using a digital camera to record the result.

**Western blot analysis.** The procedures for preparation of whole cell protein lysates and for Western blotting were described previously (13). Whole cell protein lysates (50  $\mu\text{g}$ ) were electrophoresed through 7.5%, 10%, or 12% denaturing polyacrylamide slab gels and transferred to a Immobilon-P polyvinylidene difluoride membrane (Bio-Rad, Hercules, CA) by electroblotting. The blots were probed or reprobed with the primary antibodies and then antibody binding was detected using the SuperSignal West Pico Chemiluminescent Substrate (Pierce Biotechnology, Inc., Rockford, IL) according to the manufacturer's protocol.

## Results

**Inhibition of mammalian target of rapamycin signaling by rapamycin suppresses the growth of human non-small cell lung cancer cells.** To determine whether NSCLC cells were sensitive to mTOR inhibitors, we examined the effects of rapamycin on the growth of NSCLC cell lines representing adenocarcinoma, squamous cell carcinoma, and large cell carcinoma cells. As shown in Fig. 1, rapamycin at concentrations of  $\geq 1$  nmol/L was effective in inhibiting the growth of NSCLC cells, albeit with varying degrees. However, at concentrations ranging from 1 to

1,000 nmol/L, rapamycin did not seem to exhibit a dose-dependent growth-inhibitory effect. Rapamycin at concentrations  $< 1$  nmol/L dramatically decreased its efficacy against the growth of NSCLC cells. Interestingly, rapamycin at concentrations up to 1,000 nmol/L inhibited the growth of NSCLC cells only by 50% to 75%. Even when rapamycin's concentration was increased to 10  $\mu\text{mol/L}$ , its growth-inhibitory effects were not further increased (data not shown). These results suggest that certain portions of cells in the population are resistant to rapamycin or cancer cells have some resistant mechanisms to bypass growth inhibition caused by mTOR inhibitors. Under the microscope, cells exposed to rapamycin remained attached on dishes and had normal morphology in comparison with control cells, suggesting that rapamycin inhibits the growth of human NSCLC cells without apparently inducing cell death.

To determine whether the growth-inhibitory effects of rapamycin are due to impaired mTOR signaling, we examined the activation states of mTOR and the two downstream effectors of rapamycin-sensitive mTOR complex, p70S6K and 4E-BP1, in four representative NSCLC cell lines. Both mTOR and p70S6K were phosphorylated in these cell lines, whereas 4E-BP1 was phosphorylated in three (i.e., A549, H157, and H460) of the four cell lines (Fig. 2A). These results suggest that the mTOR signaling pathway is constitutively activated in human NSCLC cell lines. After treatment with rapamycin, the phosphorylation levels of p70S6K (p-p70S6K) and 4E-BP1 (p-4E-BP1) were drastically decreased although the levels of p-mTOR was not apparently altered (Fig. 2A), revealing a potent inhibitory effect of rapamycin on the mTOR signaling. Thus, it is likely that rapamycin inhibits the growth of NSCLC cells through a blockade of the mTOR signaling pathway.

**Inhibition of mammalian target of rapamycin by rapamycin increases the phosphorylation of Akt and eIF4E.** To evaluate the effects of rapamycin on the status of molecules proximal to the mTOR axis, we probed the phosphorylation states of Akt and eIF4E. Because Akt has been placed upstream of mTOR in many cell types, we speculated that rapamycin would not alter the phosphorylation levels of Akt (p-Akt). Unexpectedly, all of the

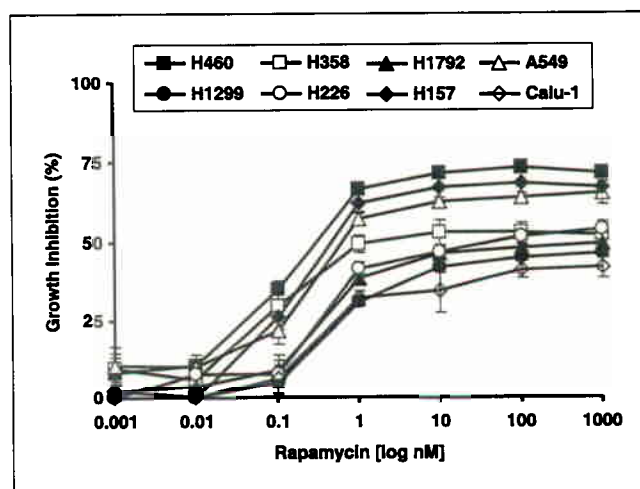


**Figure 1.** Effects of rapamycin on the growth of human NSCLC cells. The indicated cell lines were plated in 96-well plates and treated on the second day with the indicated concentrations of rapamycin. After 3 days, plates were subjected to determination of cell number using a SRB assay. Points, means of four replicate determinations; bars,  $\pm$ SD.

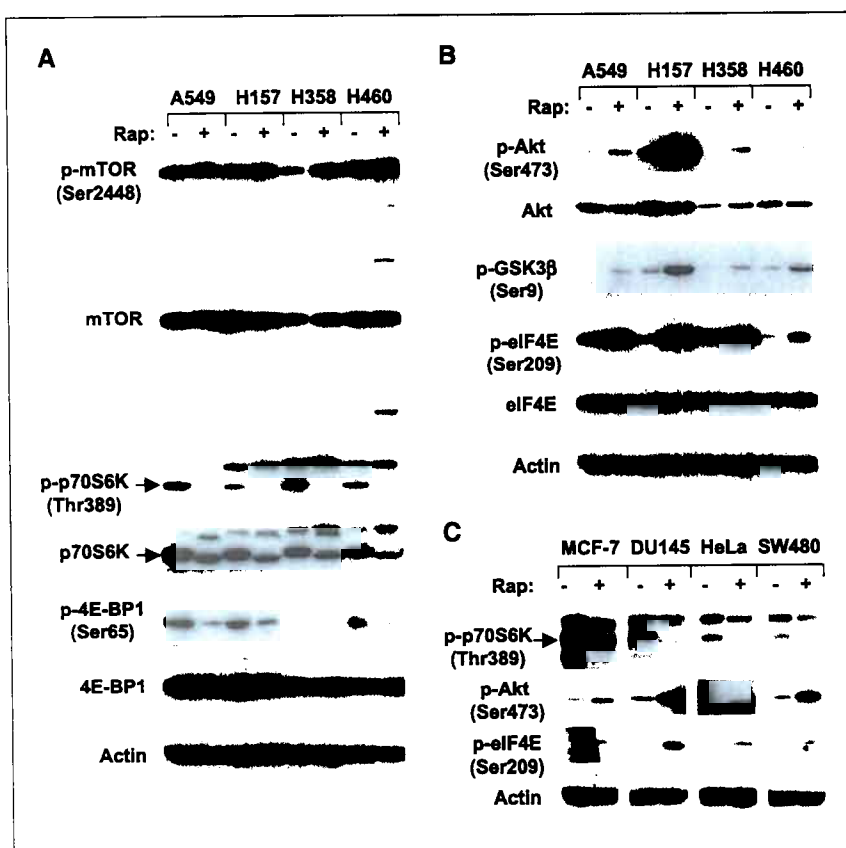


**Figure 2.** Rapamycin inhibits the mTOR signaling (A-C) and increases the phosphorylation of Akt and eIF4E (B and C) in human NSCLC (A-B) and other cancer (C) cell lines. The indicated cell lines were seeded in 10-cm-diameter cell culture dishes and treated on the second day with 100 nmol/L rapamycin for 24 hours (A and B) or 3 hours (C). The cells were then harvested for preparation of whole cell protein lysates and subsequent Western blot analysis.

tested cell lines exposed to rapamycin exhibited increased p-Akt at Ser<sup>473</sup>, indicative of an activated Akt in these cells (Fig. 2B). In support of this notion, in response to rapamycin treatment, GSK3 $\beta$ , a well-established physiologic substrate of Akt, is also phosphorylated in these cells at Ser<sup>9</sup>, a defined Akt phosphorylation site. These data suggest that rapamycin-induced mTOR inhibition results in the activation of the Akt survival pathway. In addition to Akt, the treatment of NSCLC cells with rapamycin also induced the phosphorylation of eIF4E (p-eIF4E), a molecule downstream of mTOR that is involved in promoting cell survival (8, 14). Phosphorylation of eIF4E may counteract the mTOR inhibition effect, leading to a decreased growth-inhibitory effect of rapamycin. Together, these results suggest that the inhibition of mTOR by rapamycin triggers a negative feedback mechanism by activating two survival pathways involving Akt and eIF4E. Such a mechanism may attenuate the rapamycin effects. This effect is not restricted to lung cancer cells. When a similar experiment was conducted in other cancer cell lines, we found that rapamycin also increased the levels of p-Akt and p-eIF4E whereas decreasing the levels of p-p70S6K (Fig. 2C), indicating that the increased phosphorylation of Akt and eIF4E by an mTOR inhibitor occurs commonly in cancer cells.

To correlate the dynamic changes in p-Akt and p-eIF4E with the inhibition of mTOR in response to rapamycin, we did a detailed time course analysis to examine rapamycin's effects on the alterations of p-p70S6K, p-4E-BP1, p-Akt, and p-eIF4E in two representative NSCLC cell lines. In both H157 and A549 cell lines, p-p70S6K and p-4E-BP1 levels decreased 3 hours after exposure to rapamycin; this decrease was sustained up to 24 hours. Concurrently, p-Akt and p-eIF4E levels increased soon after a 3-hour

exposure to rapamycin; this increase was still evident up to 24 hours after treatment (Fig. 3A). We also examined the effects of rapamycin on the expression levels of p70S6K, Akt, and eIF4E and found that rapamycin did not markedly alter their expression (Fig. 3A). To get more information on the dynamic changes of p-p70S6K, p-Akt, and p-eIF4E in response to rapamycin, we further shortened the exposure time to rapamycin. As shown in Fig. 3B, suppression of p-p70S6K and increase of p-Akt were detected 15 minutes after the cells were exposed to rapamycin. The increase of p-eIF4E was also detected 30 minutes (A549) and 60 minutes (H157) after rapamycin treatment. Collectively, it seems that the decrease of p-p70S6K and the increase of p-Akt are rapid and concurrent events in cells treated with rapamycin.

To further explore the relationship between the suppression of mTOR signaling and the increased phosphorylation of Akt and eIF4E, we examined p-p70S6K, p-Akt, and p-eIF4E in cells exposed to different concentrations of rapamycin ranging from 0.01 to 10 nmol/L. Rapamycin at 0.01 and 0.1 nmol/L failed to alter the phosphorylation levels of either protein. However, in cells treated with 1 or 10 nmol/L rapamycin, p-p70S6K levels decreased, accompanied with increases of both p-Akt and p-eIF4E levels (Fig. 3C). These findings indicate a close relationship between the suppression of mTOR signaling and the activation of Akt and eIF4E.

**Phosphatidylinositol 3-kinase is required for rapamycin-induced phosphorylation of Akt and eIF4E.** To understand the mechanism by which rapamycin induces Akt activation, we investigated the involvement of PI3K, an upstream regulator of Akt, in this process. PI3K catalyzes the production of the lipid second messenger phosphatidylinositol 3,4,5-trisphosphate (PIP3)

at the cell membrane. PIP3 in turn recruits other pleckstrin homology domain-containing proteins, in particular Akt, to the membrane, where Akt is activated by PDK1 and a Ser<sup>473</sup> kinase (4). If PI3K is involved in Akt activation induced by mTOR inhibition, the PI3K inhibitor LY294002 would block or suppress the Akt phosphorylation or activation by rapamycin. Therefore, we examined the effects of LY294002 on rapamycin-induced Akt activation and eIF4E phosphorylation. In the absence of LY294002, rapamycin at both 1 and 10 nmol/L increased p-Akt and p-GSK3 $\beta$  levels. In the presence of LY294002, rapamycin failed to increase Akt and GSK3 $\beta$  phosphorylation (Fig. 4A). These results suggest that rapamycin-induced Akt activation requires activated PI3K. Similarly, LY294002 also blocked the rapamycin-induced increase of eIF4E phosphorylation (Fig. 4A), suggesting that the rapamycin-induced increase of p-eIF4E is dependent on PI3K activation as well.

Both mitogen-activated protein kinase (MAPK) kinase (MEK)/extracellular signal-regulated kinase (ERK) and p38 MAPK are known to regulate eIF4E phosphorylation through Mnk1 (15, 16). To determine whether MEK/ERK or the p38 MAPK pathway was involved in the rapamycin-mediated increase of p-eIF4E, we analyzed the p-eIF4E levels in cells treated with rapamycin in the presence of various inhibitors. These inhibitors include the MEK inhibitors U0126 and PD98059, the p38 MAPK inhibitor SB203580, and the PI3K inhibitor LY294002. As shown in Fig. 4B, the presence of U0126, PD98059, or SB203580 neither affected the rapamycin-induced increase of p-eIF4E and p-Akt, nor the decrease of p-p70S6K by rapamycin. Rapamycin did not increase p-p44/p42 levels at the time point tested, whereas both U0126 and PD98059 decreased basal levels of p-p44/p42, indicating that they

indeed function to block MEK/ERK pathway. p38 MAPK levels were undetectable under the conditions tested (data not shown). These results suggest that either the MEK/ERK or the p38 MAPK pathway is unlikely involved in mediating the rapamycin-induced increase of p-eIF4E. As we have already shown, LY294002 did not block the rapamycin-mediated decrease of p-p70S6K but abrogated rapamycin-induced increases of both p-Akt and p-eIF4E. Thus, it seems that the rapamycin-induced increase of p-eIF4E is PI3K dependent but independent of the MEK/ERK and p38 MAPK pathway.

**Combination of rapamycin with LY294002 exhibits enhanced inhibitory effects on the growth and colony formation of non-small cell lung cancer cells.** It is well documented that Akt is a major survival kinase (4). Recently, eIF4E has also been shown to be a tumor survival factor (8, 14). Our data clearly show that suppression of mTOR by rapamycin activates Akt and eIF4E survival pathways. Thus, we speculated that PI3K/Akt and eIF4E activation would counteract mTOR inhibitors' anticancer effects. Because rapamycin-induced Akt activation requires its upstream regulator, PI3K, (Fig. 4A and B), blocking the PI3K/Akt survival pathway by LY294002 would be expected to enhance the rapamycin effect. Thus, we examined the effects of rapamycin combined with LY294002 on the growth of human NSCLC cells. As shown in Fig. 4C, the combination of rapamycin and LY294002 in a 3-day growth inhibition assay apparently exhibit growth-inhibitory effects that are greater than those caused by each single agent alone. For example, in H157 cells, rapamycin at 1 nmol/L inhibited cell growth by 30%, whereas LY294002 at 0.5, 1.0, 2.5, and 5.0  $\mu$ mol/L caused 4.6%, 3.2%, 11%, and 17.9% growth inhibition, respectively. However, their combinations led to growth inhibition by 46.5%,

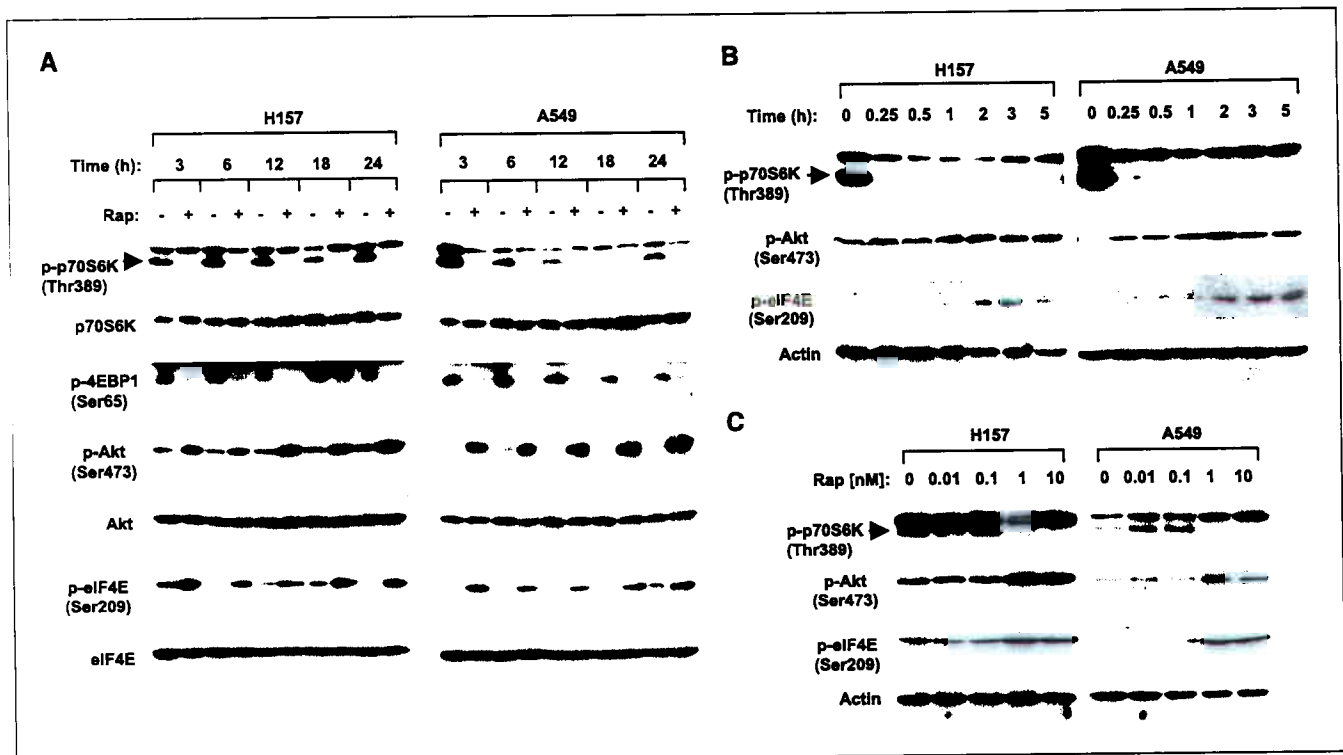


**Figure 3.** Increase of Akt and eIF4E phosphorylation by rapamycin is associated with suppression of the mTOR signaling in human NSCLC cells. The indicated cells lines were treated with 100 nmol/L rapamycin (*Rap*) for the given times (A and B) or with the indicated concentrations of rapamycin for 24 hours (C) and then subjected to preparation of whole cell protein lysates. The indicated proteins were detected by Western blot analysis.



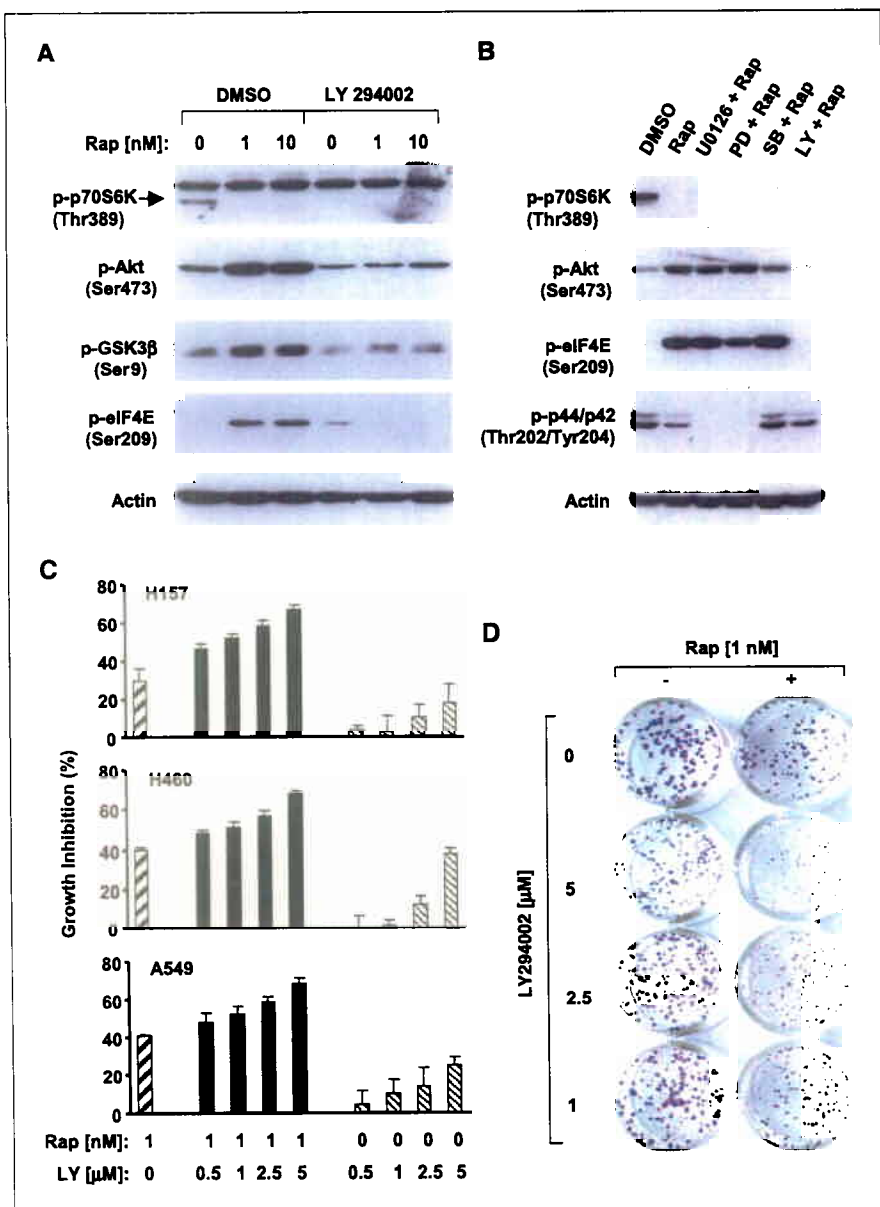


**Figure 4.** Involvement of PI3K in rapamycin-mediated increase of Akt and eIF4E phosphorylation (A and B) and enhancement of rapamycin-mediated growth inhibitor effects by LY294002 in NSCLC cells (C and D). **A**, H157 cells were pretreated with 5  $\mu\text{mol/L}$  LY294002 for 30 minutes and then cotreated with the indicated concentrations of rapamycin (Rap) for 3 hours. The cells were subjected to preparation of whole cell protein lysates for detection of the indicated proteins using Western blotting. **B**, H157 cells were pretreated with 20  $\mu\text{mol/L}$  U0126, PD98059 (PD), and SB203580 (SB), respectively, and 10  $\mu\text{mol/L}$  LY294002 (LY) for 30 minutes, and then cotreated with 10 nmol/L rapamycin. After 3 hours, the cells were subjected to preparation of whole cell protein lysates for detection of the indicated proteins using Western blot analysis. **C**, the individual cell lines, as indicated, were seeded in 96-well plates. On the second day, they were treated with the indicated concentrations of LY294002 alone, 1 nmol/L rapamycin alone, and their respective combinations. After 3 days, plates were subjected to determination of cell number using a SRB assay. Columns, means of four replicate determinations; bars,  $\pm$ SD. **D**, H460 cells at a density of  $\sim$ 250 cells per well were seeded in 12-well plates. On the second day, cells were treated with the indicated concentrations of LY294002 alone, 1 nmol/L rapamycin alone, and their respective combinations. The same treatments were repeated every 3 days. After 10 days, the plates were stained for the formation of cell colonies with SRB dye. The picture of the colonies was then taken using a digital camera.

52.2%, 58.9%, and 67.3%, respectively. These effects are apparently greater than the sum of the inhibitory effects caused by each agent alone, indicating a more than additive or synergistic effect. In the long-term colony formation assay, we obtained similar results as determined from the 3-day assay. LY294002 and rapamycin alone did not decrease the number of colonies, although they reduced the sizes of the colonies. The combination of the two agents not only decreased the size of colonies but also reduced the number of colonies (Fig. 4D), indicating that the combination causes a greater growth-inhibitory effect than that of each single agent. Taken together, these results indicate that the combination of rapamycin and LY294002 results in an augmented growth-inhibitory effect.

## Discussion

Using several human NSCLC cell lines, we have shown that rapamycin effectively inhibits cell growth to various degrees.

However, rapamycin failed to completely inhibit cell growth even when its concentration was increased up to 10  $\mu\text{mol/L}$ , suggesting that some cells remain resistant to mTOR inhibitors. Cell sensitivity to mTOR inhibitors has been linked to PTEN mutations or Akt activation (17–20). PTEN is a PIP3 phosphatase that negatively regulates the PI3K/Akt pathway. A recent animal study has shown that mTOR inhibition reverses Akt-dependent prostate intraepithelial neoplasia (9). It has been well documented that human NSCLCs have rare or low frequencies of PTEN mutations (21, 22). Among tested NSCLC cell lines, H157 is the only cell line with PTEN mutation (21). Compared with most NSCLC cell lines, which have very low or undetectable basal levels of p-Akt, H157 cells constitutively express high levels of p-Akt, as we have shown previously (23). However, H157 cells were not more sensitive than other cell lines, such as A549 and H460, to rapamycin. Therefore, the effect of PTEN mutations or Akt activation on rapamycin's effects in NSCLC cells is not clearly apparent in NSCLC cells.

Rapamycin at concentrations ( $\geq 1$  nmol/L) that exhibited growth inhibition rapidly and effectively suppressed the phosphorylation of p70S6K and 4E-BP1, indicating that rapamycin indeed blocks mTOR signaling. This blockage may well be the molecular basis for rapamycin to inhibit the growth of cancer cells. Unexpectedly, rapamycin rapidly induced the activation of Akt as shown by phosphorylation at Ser<sup>473</sup> and the phosphorylation of its substrate, GSK3 $\beta$ , whereas suppressing the phosphorylation of p70S6K and 4E-BP1. It seems that mTOR inhibition by rapamycin activates the Akt survival pathway. Even more surprisingly, cells treated with rapamycin within a concentration range that inhibits mTOR signaling increased eIF4E phosphorylation. To our knowledge, this is the first report to show that mTOR inhibition by rapamycin increases eIF4E phosphorylation.

Activation of Akt by mTOR inhibition was reported in *Drosophila* when studying the functional role of Rheb in regulation of p70S6K activity (24) and also in mammalian skeletal muscle cells, adipocytes, and fibroblasts when studying insulin signaling (25–27). Our study clearly shows that mTOR inhibition by rapamycin results in the activation of the Akt survival pathway in human NSCLC and other types of cancer cell lines. To the best of our knowledge, this is the first report to show mTOR inhibition-induced Akt activation in human cancer cells. Results from previous studies of insulin signaling suggest that the mTOR activation by insulin initiates a feedback inhibition of PI3K/Akt through p70S6K activation and its subsequent phosphorylation of insulin receptor substrate-1 (IRS-1). The phosphorylation of IRS-1 promotes IRS-1 degradation and reduces IRS-1 expression, leading to decreased activity of PI3K/Akt. Rapamycin suppresses p70S6K and thus relieves this negative feedback inhibition of Akt (28, 29). In our study, the presence of the PI3K inhibitor, LY294002, abrogated rapamycin-induced Akt activation (Akt and GSK3 $\beta$  phosphorylation), suggesting that PI3K activity is required for Akt activation by rapamycin. However, we currently do not know whether the Akt activation induced by rapamycin in human cancer cells is mediated by p70S6K suppression through the stabilization of IRS-1. It has been shown that there are two mTOR complexes in mammalian cells: the rapamycin-sensitive mTOR-raptor complex and the rapamycin-insensitive mTOR-riCTOR complex (30). A recent study has shown that the mTOR-riCTOR complex can directly phosphorylate Akt at Ser<sup>473</sup> (31). Reduction of mTOR expression using small interfering RNA decreased Akt phosphorylation (31). Our data seem to favor the model that rapamycin induces Akt phosphorylation in a PI3K-dependent mechanism. However, it remains possible that rapamycin may indirectly stimulate the mTOR-riCTOR kinase activity to phosphorylate Akt. Elucidation of these mechanisms requires further investigation.

eIF4E plays a critical role in the regulation of cap-dependent-protein translation and thus its activity is integral in determining global translation rates (32). Consistent with this role, eIF4E is required for cell cycle progression, exhibits antiapoptotic or survival activity, and when overexpressed, transforms cells (8, 14), largely due to its critical role in initiating translation of mRNAs that encode cell

cycle regulators or oncogenic proteins such as cyclin D1, ornithine decarboxylase, c-Myc, hypoxia-inducible factor 1 $\alpha$ , fibroblast growth factor, and vascular endothelial growth factor (1, 8, 24). Therefore, it is not surprising that elevated levels of eIF4E are found in a broad spectrum of transformed cells and human cancers, including lung cancers, and is often associated with aggressive, poorly differentiated tumors (1, 8). eIF4E is phosphorylated (usually at Ser<sup>209</sup>) in many systems in response to extracellular stimuli including growth factors, hormones, and mitogens (15, 16). Its phosphorylation increases its affinity for the cap and for mRNA and may also favor its entry into initiation complexes (15, 16, 33). Although mTOR inhibitors are expected to inhibit cap-dependent translation via activation of 4E-BP1 (i.e., promoting its dephosphorylation), we paradoxically found that cells treated with rapamycin exhibited increased eIF4E phosphorylation. Thus, it seems that rapamycin treatment generates conflicting signal to cap-dependent protein translation. Collectively, these findings suggest that rapamycin may promote cap-dependent protein translation, probably under certain conditions.

It has been documented that MEK/ERK and p38 MAPK signaling pathways activate eIF4E through Mnk1-mediated phosphorylation of eIF4E (15, 16). However, the MEK inhibitors U0126 and PD98059 or the p38 MAPK inhibitor SB203580 did not inhibit a rapamycin-induced elevation of p-eIF4E. Instead, LY294002 abolished the increase of p-eIF4E by rapamycin. Thus, it seems that the PI3K activity is required for mediating rapamycin-induced eIF4E phosphorylation. The investigation on the involvement of Mnk1 in rapamycin-induced eIF4E phosphorylation is ongoing.

Because Akt and eIF4E are often associated with cell survival and resistance to cancer therapy (4, 14), our findings imply that the activation of Akt and eIF4E through mTOR inhibition may counteract mTOR inhibitors' anticancer efficacy and confers resistance to mTOR-targeted cancer therapy. According to our results, Akt and eIF4E phosphorylation induced by rapamycin all occur downstream of PI3K. These findings may provide us the opportunity to interrupt or disrupt activation of the Akt and eIF4E survival pathways using a PI3K inhibitor or even an Akt inhibitor to enhance mTOR inhibitors' anticancer efficacy or mTOR-targeted cancer therapy. Our results indeed show that LY294002 in combination with rapamycin exhibits enhanced (synergistic) effects on the growth and colony formation of human NSCLC cells. Therefore, from a therapeutic point of view, our findings suggest a novel strategy to enhance mTOR-targeted cancer therapy through combining an mTOR inhibitor with an inhibitor of the PI3K/Akt pathway.

## Acknowledgments

Received 3/18/2005; revised 5/16/2005; accepted 6/16/2005.

**Grant support:** Winship Cancer Institute faculty start-up research fund (S.-Y. Sun), the Georgia Cancer Coalition Distinguished Cancer Scholar award (S.-Y. Sun and F.R. Khuri), Department of Defense IMPACT grant W81XWH-05-0027 (Project 5 to F.R. Khuri and S.-Y. Sun), and NIH R01 grant GM53165 (H. Fu).

The costs of publication of this article were defrayed in part by the payment of page charges. This article must therefore be hereby marked advertisement in accordance with 18 U.S.C. Section 1734 solely to indicate this fact.

## References

1. Bjornsti MA, Houghton PJ. The TOR pathway: a target for cancer therapy. *Nat Rev Cancer* 2004;4:335–48.
2. Sawyers CL. Will mTOR inhibitors make it as cancer drugs? *Cancer Cell* 2003;4:343–8.
3. Hay N, Sonenberg N. Upstream and downstream of mTOR. *Genes Dev* 2004;18:1926–45.
4. Vivanco I, Sawyers CL. The phosphatidylinositol 3-kinase AKT pathway in human cancer. *Nat Rev Cancer* 2002;2:489–501.
5. Sansal I, Sellers WR. The biology and clinical relevance of the PTEN tumor suppressor pathway. *J Clin Oncol* 2004;22:2954–63.
6. Bjornsti MA, Houghton PJ. Lost in translation: dysregulation of cap-dependent translation and cancer. *Cancer Cell* 2004;5:519–23.
7. Inoki K, Corradetti MN, Guan KL. Dysregulation of the

- TSC-mTOR pathway in human disease. *Nat Genet* 2005;37:19-24.
8. De Benedetti A, Graff JR. eIF-4E expression and its role in malignancies and metastases. *Oncogene* 2004;23:3189-99.
  9. Majumder PK, Febbo PG, Bikoff R, et al. mTOR inhibition reverses Akt-dependent prostate intraepithelial neoplasia through regulation of apoptotic and HIF-1-dependent pathways. *Nat Med* 2004;10:594-601.
  10. Rowinsky EK. Targeting the molecular target of rapamycin (mTOR). *Curr Opin Oncol* 2004;16:564-75.
  11. Huang S, Bjornsti MA, Houghton PJ. Rapamycins: mechanism of action and cellular resistance. *Cancer Biol Ther* 2003;2:222-32.
  12. Sun SY, Yue P, Dawson MI, et al. Differential effects of synthetic nuclear retinoid receptor-selective retinoids on the growth of human non-small cell lung carcinoma cells. *Cancer Res* 1997;57:4931-9.
  13. Sun SY, Yue P, Wu GS, et al. Mechanisms of apoptosis induced by the synthetic retinoid CD437 in human non-small cell lung carcinoma cells. *Oncogene* 1999;18:2357-65.
  14. Wendel HG, De Stanchina E, Fridman JS, et al. Survival signalling by Akt and eIF4E in oncogenesis and cancer therapy. *Nature* 2004;428:332-7.
  15. Raught B, Gingras AC. eIF4E activity is regulated at multiple levels. *Int J Biochem Cell Biol* 1999;31:43-57.
  16. Pyronnet S. Phosphorylation of the cap-binding protein eIF4E by the MAPK-activated protein kinase Mnk1. *Biochem Pharmacol* 2000;60:1237-43.
  17. Shi Y, Gera J, Hu L, et al. Enhanced sensitivity of multiple myeloma cells containing PTEN mutations to CCI-779. *Cancer Res* 2002;62:5027-34.
  18. Neshat MS, Mellinoff IK, Tran C, et al. Enhanced sensitivity of PTEN-deficient tumors to inhibition of FRAP/mTOR. *Proc Natl Acad Sci U S A* 2001;98:10314-9.
  19. Gera JF, Mellinoff IK, Shi Y, et al. AKT activity determines sensitivity to mammalian target of rapamycin (mTOR) inhibitors by regulating cyclin D1 and *c-myc* expression. *J Biol Chem* 2004;279:2737-46.
  20. Noh WC, Mondesire WH, Peng J, et al. Determinants of rapamycin sensitivity in breast cancer cells. *Clin Cancer Res* 2004;10:1013-23.
  21. Forgacs E, Biesterveld EJ, Sekido Y, et al. Mutation analysis of the PTEN/MMAC1 gene in lung cancer. *Oncogene* 1998;17:1557-65.
  22. Yokomizo A, Tindall DJ, Drabkin H, et al. PTEN/MMAC1 mutations identified in small cell, but not in non-small cell lung cancers. *Oncogene* 1998;17:475-9.
  23. Sun SY, Zhou Z, Wang R, Fu H, Khuri FR. The farnesyltransferase inhibitor Lonafarnib induces growth arrest or apoptosis of human lung cancer cells without downregulation of Akt. *Cancer Biol Ther* 2004;3:1092-8.
  24. Stocker H, Radimerski T, Schindelholtz B, et al. Rheb is an essential regulator of S6K in controlling cell growth in *Drosophila*. *Nat Cell Biol* 2003;5:559-65.
  25. Tremblay F, Marette A. Amino acid and insulin signaling via the mTOR/p70 S6 kinase pathway. A negative feedback mechanism leading to insulin resistance in skeletal muscle cells. *J Biol Chem* 2001;276:38052-60.
  26. Tremblay F, Gagnon A, Veilleux A, Sorisky A, Marette A. Activation of the mammalian target of rapamycin pathway acutely inhibits insulin signaling to Akt and glucose transport in 3T3-L1 and human adipocytes. *Endocrinology* 2005;146:1328-37.
  27. Harrington LS, Findlay GM, Gray A, et al. The TSC1-2 tumor suppressor controls insulin-PI3K signaling via regulation of IRS proteins. *J Cell Biol* 2004;166:213-23.
  28. Manning BD. Balancing Akt with S6K: implications for both metabolic diseases and tumorigenesis. *J Cell Biol* 2004;167:399-403.
  29. Harrington LS, Findlay GM, Lamb RF. Restraining PI3K: mTOR signalling goes back to the membrane. *Trends Biochem Sci* 2005;30:35-42.
  30. Sarbassov DD, Ali SM, Kim DH, et al. Rictor, a novel binding partner of mTOR, defines a rapamycin-insensitive and raptor-independent pathway that regulates the cytoskeleton. *Curr Biol* 2004;14:1296-302.
  31. Sarbassov DD, Guertin DA, Ali SM, Sabatini DM. Phosphorylation and regulation of Akt/PKB by the rictor-mTOR complex. *Science* 2005;307:1098-101.
  32. Richter JD, Sonenberg N. Regulation of cap-dependent translation by eIF4E inhibitory proteins. *Nature* 2005;433:477-80.
  33. Lachance PE, Miron M, Raught B, Sonenberg N, Lasko P. Phosphorylation of eukaryotic translation initiation factor 4E is critical for growth. *Mol Cell Biol* 2002;22:1656-63.



## **Analysis of *EGFR* Abnormalities in the Sequential Pathogenesis and Progression of Lung Adenocarcinoma.**

Ximing Tang, Marileila Varella-Garcia, Ana Carolina Xavier, Xiaoqing Bi, Natalie Ozburn, Waun Ki Hong, Ignacio I. Wistuba. Departments of Thoracic/Head and Neck Medical Oncology and Pathology, UT-MD Anderson Cancer Center, Houston, TX, and University of Colorado Cancer Center, Aurora, CO.

*EGFR* tyrosine kinase (TK) domain mutations, increased gene copy number and protein overexpression have been associated to lung cancer pathogenesis and correlated with response to *EGFR* TK inhibitors in lung adenocarcinoma. However, the sequence of these molecularly abnormal events in the pathogenesis and progression of lung adenocarcinoma is unknown. To elucidate this question, we performed a detailed mapping analysis correlating in the same tissue sites *EGFR* mutation, gene copy number and protein immunohistochemistry (IHC) expression in 94 formalin-fixed tissue sites comprising normal bronchial/bronchiolar epithelium (NBE; N=22), primary tumor (PT; N=43) and metastasis (MT; N=29) histologies obtained from 9 surgically resected *EGFR* mutant (exons 19 and 21) lung adenocarcinomas. *EGFR* mutation analysis was performed by PCR and direct sequencing from DNA extracted from precisely microdissected tissues. *EGFR* gene copy number analysis was performed using FISH, and high level of polysomy and gene amplification were considered as increased copy number. Semi-quantitative IHC expression analysis of cytoplasmic and cell membrane *EGFR* and phosphorylated *EGFR* (p-*EGFR*) was performed. *EGFR* mutation was found in 18% (4/22) NBE, 91% (39/43) PT and 86% (25/29) MT sites. Low genomic gain was found in 8 NBE sites (37%), but increased copy number was not detected. Of interest, the 4 *EGFR* mutant NBE sites exhibited normal gene copy number. No difference in the frequency of *EGFR* increased copy number was found comparing PT (39/43, 93%) and MT (25/29, 86%) sites. *EGFR* mutation frequency (89% vs. 41%;  $P<0.0000$ ) and mutant to wild-type ratio mean (1.04 vs. 0.49,  $P<0.0001$ ) in the sequencing chromatograms were significantly higher in tissue sites with increased copy number than areas with normal or low genomic gain. *EGFR* mutation heterogeneity, with two or more mutant genotypes in

the same tumor case, was found in 4 out of 9 (44%) PT cases, and this phenomenon was not observed in corresponding MTs. *EGFR* copy number heterogeneity was more frequent in PT than MT; however, significant copy number progression from PT to MT was not observed. Although no correlation was found between EGFR IHC and *EGFR* mutation or copy number status, significantly higher levels of EGFR and p-EGFR IHC expression were detected in mutant MT compared to PT sites ( $P= 0.005$  to  $<0.0001$ ). Our findings indicate that *EGFR* mutation precedes genomic gain in the sequential pathogenesis of lung adenocarcinoma. In tumor specimens, there was strong correlation between *EGFR* mutation and increased copy number. The heterogeneity of *EGFR* mutation and gene copy number in primary tumor, but not in metastasis, and the increased expression of total and p-EGFR IHC in metastasis sites are probably associated to tumor progression and could have clinical implications when these abnormalities are searched in small clinical specimens. Supported by grants W81XWH0410142 and W81XWH0520027.

January 2006

Re: 2006 AACR Annual Meeting in Washington, DC

Temporary Abstract Number #5233

Title: Cellular and Molecular Biology 3

Dear Dr. Tang:

Your above-referenced abstract has been scheduled for presentation in a Poster Session at the 2006 AACR Annual Meeting in Washington, DC and will be published in the 2006 Proceedings of the American Association for Cancer Research. Presentation information pertaining to your abstract is below:

Session ID: Cellular and Molecular Biology 3

Session Date and Start Time: Sunday, April 2, 2006 8:00 AM

Permanent Abstract Number: 69